UNCLASSIFIED

AD NUMBER

AD462060

NEW LIMITATION CHANGE

TO

Approved for public release, distribution unlimited

FROM

Distribution authorized to U.S. Gov't. agencies and their contractors; Administrative/Operational Use; 26 Feb 1965. Other requests shall be referred to Army Materiel Command, Alexandria, VA.

AUTHORITY

USAMC ltr, 2 Jul 1973

THIS PAGE IS UNCLASSIFIED

AD462060

ENGINEERING DESIGN HANDBOOK

BALLISTICS SERIES

INTERIOR BALLISTICS OF GUNS



REPRODUCED BY
NATIONAL TECHNICAL
INFORMATION SERVICE
U. S. DEPARTMENT OF COMMERCE
SPRINGFIELD, VA. 22161

Best Available Copy

HEADQUARTERS, U.S. ARMY MATERIEL COMMAND FEBRUARY 1965

HEADQUARTERS
UNITED STATES ARMY MATERIEL COMMAND
WASHINGTON, D.C. 20315

26 February 1965

AMCP 706-150, Interior Ballistics of Guns, forming part of the Ballistics Series of the Army Materiel Command Engineering Design Handbook Series, is published for the information and guidance of all concerned.

(AMCRD)

FOR THE COMMANDER:

SELWYN D. SMITH, JR.
Major General, USA
Chief of Staff

OFFICIAL:

STANLEY J. SAWICKI
Colonel, GS
Chief, Administrative Office

DISTRIBUTION: Special

PREFACE

The Engineering Design Handbook Series of the Army Materiel Command is a coordinated series of handbooks containing basic information and fundamental data useful in the design and development of Army materiel and systems. The handbooks are authoritative reference books of practical information and quantitative facts helpful in the design and development of Army materiel so that it will meet the tactical and the technical needs of the Armed Forces. Several of these handbooks give the theory and experimental data pertaining to interior, exterior and terminal ballistics. The present handbook deals with the interior ballistics of guns.

This handbook, *Interior Ballistics of Guns*, presents fundamental data, followed by development of the theory and practice of interior ballistics, with application to rifled, smooth-bore and recoilless guns. Included in the presentation are studies pertaining to heat transfer, temperature distribution and erosion, together with standard and experimental methods of measurements. Finally, ignition, flash and other special topics are explored.

This handbook has been prepared as an aid to scientists and engineers engaged in military research and development programs, and as a guide and ready reference for military and civilian personnel who have responsibility for the planning and interpretation of experiments and tests relating to the performance of military materiel during design, development and production.

The final text is the result of the joint writing efforts of R. N. Jones, H. P. Hitchcock and D. R. Villegas, of the staff of John I. Thompson and Company, for the Engineering Handbook Office of Duke University, prime contractor to the Army Research Office-Durham. Many valuable suggestions were made by the Interior Ballistics Laboratory and Development and Proof Services at Aberdeen Proving Ground, Picatinny Arsenal, Frankford Arsenal and Springfield Armory. During the preparation of this handbook Government establishments were visited for much of the material used and for helpful discussions with many technical personnel.

Elements of the U. S. Army Materiel Command having need for handbooks may submit requisitions or official requests directly to Publications and Reproduction Agency, Letterkenny Army Depot, Chambersburg, Pennsylvania 17201. Contractors should submit such requisitions or requests to their contracting officers.

Comments and suggestions on this handbook are welcome and should be addressed to Army Research Office-Durham, Box CM, Duke Station, Durham, North Carolina 27706.

TABLE OF CONTENTS—(continued)

CHAPTER 3

HEAT TRANSFER, TEMPERATURE DISTRIBUTION AND EROSION OF GUN TUBES

Paragraph		*Page*
	LIST OF SYMBOLS	3-1
3-1	Heat Transfer	3-2
3-1.1	General Discussion	3-2
3-1.2	Heat Transfer Coefficient	3-2
3-1.3	Calculation of the Rate of Heat Input	3-3
3-1.4	Nondimensional Heat Transfer Coefficient	3-5
3-2	Temperature Distribution	3-6
3-2.1	The Equations of Temperature Distribution in Reduced Variables	3-6
3-2.2	Heat Input	3-7
3-2.3	The "Thermal Analyzer"	3-7
3-2.4	Comparison With Experiment	3-8
3-3	Erosion	3-8
3-3.1	General Discussion	3-8
3-3.2	Estimation of the Erosion of Gun Tubes	3-9
3-3.3	Life of Gun Tubes	3-14
3-3.4	Erosion in Vents	3-14
	REFERENCES	3-21

CHAPTER 4

EXPERIMENTAL METHODS

	LIST OF SYMBOLS	4-1
4-1	Introduction	4-2
4-2	Pressure Measurements	4-2
4-2.1	General Principles	4-2
4-2.2	The Quartz Piezoelectric Gage	4-3
4-2.3	Strain Type Pressure Gages	4-5
4-2.4	Crusher Gage	4-8
4-3	Measurement of Muzzle Velocity	4-9
4-3.1	General Principles	4-9
4-3.2	Chronographs	4-10
4-3.3	Detecting Devices	4-12
4-3.4	The Calculation of the Muzzle Velocity	4-12
4-4	Travel-Time Measurements	4-14
4-4.1	Barrel Contacts	4-14
4-4.2	Microwave Interferometer	4-14
4-4.3	Measurement of Projectile Travel Near the Start of Motion	4-17
4-5	In-Bore Velocity and Acceleration Measurement	4-17
4-5.1	Differentiation of the Travel-Time Data	4-17
4-5.2	The Measurement of Velocity	4-18
4-5.3	The Measurement of Acceleration	4-19
4-6	The Measurement of Base Pressure	4-20

TABLE OF CONTENTS—(continued)

Paragraph		*Page*
4-7	The Measurement of Bore Friction	4-21
4-8	The Measurement of Barrel Erosion	4-22
4-8.1	General	4-22
4-8.2	The Star Gage	4-22
4-8.3	The Pullover Gage	4-22
4-8.4	The Automatic Recording Bore Gage	4-23
4-9	Barrel Temperature Measurements	4-23
4-9.1	Thermocouples	4-23
4-9.2	Resistance Type Temperature Measuring Gages	4-25
4-10	Motion of the Propellant During Burning	4-26
4-11	Rotating Mirror Camera	4-28
	REFERENCES	4-32

CHAPTER 5

SPECIAL TOPICS

	LIST OF SYMBOLS	5-1
5-1	The Hydrodynamic Problems of Interior Ballistics	5-2
5-1.1	Pressure Distribution and Kinetic Energy of the Propellant Gases	5-2
5-1.2	The Emptying of the Gun	5-4
5-2	Ignition of Propellants	5-7
5-2.1	General Discussion	5-7
5-2.2	Laboratory Investigations of Ignition	5-7
5-2.3	Theories of Ignition	5-8
5-2.4	Ignition in Guns	5-10
5-2.5	Ignition Systems for Guns	5-12
5-3	Flash and Smoke	5-12
5-3.1	Flash	5-12
5-3.2	Flash Suppression	5-16
	REFERENCES	5-18

LIST OF ILLUSTRATIONS

Fig. No.	*Title*	*Page*
1-1	Recoil Gun System	1-3
1-2	Recoilless Gun System	1-4
1-3	Pressure-Travel and Velocity-Travel Curves	1-5
1-4	Pressure-Travel Relationship	1-6
1-5	Effects of Grain Configuration on Pressure-Travel Curves	1-7
1-6	Effects of Independently Varying Grain Size	1-7
1-7	Typical Shapes of Propellant Grains	1-8
1-8	Sizes of Some Typical Grains	1-8
1-9	Web Thickness and Route of Burning Progress through a Progressively Burning Grain	1-9
1-10	Relative Areas of Burning As a Function of Percent of Individual Grain Consumed for Several Typical Grain Shapes	1-9
2-1	Theoretical Pressure-Time Curve for 105mm Howitzer Using Taylor's Theory	2-23
2-2	Result of the Analysis of a Firing Record for a 105mm Howitzer Round (Measured Values of Pressure and Displacement. Velocity and Acceleration Determined by Numerical Differentiation of Displacement.)	2-30
2-3	Engraving Force for a Typical 105mm Howitzer Round	2-31
2-4	Charge Burned versus Time for 37mm Gun	2-33
2-5	Linear Burning Rate versus Pressure for 105mm Howitzer, M1 Propellant	2-34
3-1	Observed Radial Wear per Round at the Commencement of Rifling versus Calculated Heat Input per cm^2 per Round	3-10
3-2	Change in Vertical Land Diameter at 0.1 Inch from Commencement of Rifling versus Number of Rounds in the 8-Inch Gun, M1	3-12
3-3	Bore Enlargement at Origin versus Equivalent Service Rounds. 16-inch/45 Caliber Guns Marks 6 and 8	3-13
3-4	The General Shape of Vent Erosion versus Charge	3-15
3-5	Early Design of Erosion Test Vent	3-15
3-6	Final Design of 0.50-Inch Erosion Test Vent. (Vents With Different Diameters Are Obtained by Adding a Constant Increment to the Numbers Shown.)	3-16
3-7	Weight Loss versus Round Number	3-16
3-8	Diameter Increase versus Number of Rounds	3-17
3-9	Weight Loss versus Number of Rounds	3-18
3-10	Weight Loss and Diameter Increase versus Number of Rounds	3-19
3-11	Dependence of Erosion on Initial Wall Temperature	3-20
4-1	Quartz Piezoelectric Pressure Gage	4-3
4-2	Diagram of Recording System for Piezoelectric Pressure Gage	4-4
4-3	Typical Pressure-Time Records from Quartz Piezoelectric Gage (155mm Gun)	4-4
4-4	Dead Weight Apparatus for Calibration of Pressure Gages	4-5
4-5	The C-AN Strain Type Pressure Gage Using a Wire-Wrapped Ferrule	4-6

LIST OF ILLUSTRATIONS—(continued)

Fig. No.	*Title*	*Page*
4-6	An Improved Strain Type Pressure Gage Using Cemented Foil Strain Patches to Permit the Use of a Smaller Ferrule to Reduce Dimensions of the Gage	4-7
4-7	Internal Strain Type Pressure Gage Mounted in Cartridge Case to Measure Breech Pressure	4-7
4-8	The Hat Gage Mounted in Cartridge Case to Measure Breech Pressure	4-8
4-9	Typical Input Circuit of Strain Type Pressure Gages	4-8
4-10	Frequency Response Curves for Different Types of Pressure Gages When Subjected to a Stepwise Pressure Signal in a High Pressure Shock Tube	4-9
4-11	Cross Section of Internal Copper Crusher Pressure Gage Using Cylindrical Copper Crusher	4-10
4-12	Photograph of a Drum Camera Chronograph Mounted in Range Recording Room	4-11
4-13	Drum Camera Chronograph Record of Signal from Velocity Coils	4-12
4-14	Lumiline Screens in Use in an Indoor Range	4-13
4-15	Typical Microwave Interferometer Record of Projectile Travel versus Time (Caliber .50)	4-15
4-16	Block Diagram of the Microwave Interferometer for Measuring Projectile Travel versus Time	4-15
4-17	Typical Travel-Time Record at Start of Travel Using Back-Lighted Slits in Cutoff Tube (Caliber .50), Back-Lighting Intermittent, 10^5 Exposures per Second	4-16
4-18	Foil Contactor Assembly for Measuring Travel During the Engraving Process, 105mm Howitzer	4-17
4-19	Consolidated Plot of the Data and Results for the First Four Inches of Travel in the 105mm Howitzer	4-18
4-20	Diagram of Quartz Piezoelectric Acceleration Gage Assembled in the Projectile	4-19
4-21	Diagram of the Variable Capacitance Acceleration Gage	4-19
4-22	Diagram of Quartz Piezoelectric Base Pressure Gage Mounted in the Projectile	4-20
4-23	Variable Capacitance Base Pressure Gage Diagram of Parts and Assembly	4-21
4-24	Record Produced by the Automatic-Recording Bore Gage. Three Complete Scans in Both Directions to Test Repeatability.	4-21
4-25	Diagram of One Model of the Automatic-Recording Bore Gage	4-22
4-26	Diagram of Bore Surface Thermocouple and Housing, BRL Model	4-22
4-27	Block Diagram of Apparatus for Observing Motion During Firing of a Radioactive Source Imbedded Initially in a Propellant Grain	4-23
4-28	Photograph of Apparatus for the Study of Propellant Motion During Firing Using Radioactive Tracer Technique. 37mm Gun With Four Scintillation Counters on Each Side of the Barrel	4-24
4-29	Calibration Curves Showing Radioactive Source Position versus Time	4-25
4-30	Typical Record of Source Position and Pressure versus Time	4-26

LIST OF ILLUSTRATIONS—(continued)

Fig. No.	*Title*	*Page*
4-31	Consolidated Plot of Observations Showing Correlation of Radioactive Source and Projectile Positions versus Time	4-27
4-32	Consolidated Plot of Radioactive Source and Projectile Motion Compared With Gas Motion As Predicted by the Lagrange Approximation	4-27
4-33	Distance Traveled by Radioactive Source As a Function of Initial Position Compared With the Displacement of the Gas Given by the Lagrange Approximation	4-28
4-34	Velocity Attained by Radioactive Source As a Function of Initial Position Compared With the Velocity of the Gas Given by the Lagrange Approximation	4-29
4-35	Schematic Diagrams of the BRL Rotating Mirror Camera	4-30
4-36	Photograph of BRL Four-Surface Rotating Mirror Camera for Recording Interior Ballistic Trajectories (Cover Removed)	4-31
5-1	Graph of c_1 As a Function of ϵ and n	5-5
5-2	Contour Map of Lines of Constant c_1	5-6
5-3	Reduced Surface Temperature, U, versus Logarithm of Reduced Time, τ	5-11
5-4	Muzzle Flash from 57mm Gun	5-13
5-5	Still Photograph of Caliber .30 Rifle With Shortened Barrel Fired in Air and Nitrogen	5-14
5-6	Primary Flash and Muzzle Glow from 37mm Gun	5-15

LIST OF CHARTS

Chart No.	*Title*	*Pag*
2-1	Pressure Ratio	2-1
2-2a, 2-2b, 2-2c	Interior Ballistics Trajectories	2-
2-3	Time, Pressure and Travel Functions	2-
2-4	Chart for Interior Ballistic Calculations by the Scheme of Strittmater	2-
2-5	Velocity at $U_m/U_0 = 5$ and $P_m = 60$ kpsi As a Function of C/W (Small Arms)	2-
2-6	Relative Velocity Normalized to Unity at an Expansion Ratio of 5 As a Function of Expansion Ratio (Small Arms)	2-
2-7	Velocity Relative to the Velocity at a Peak Pressure of 60 kpsi As a Function of Peak Pressure (Small Arms)	2
2-8	Relative Pressure As a Function of Expansion Ratio	2
2-9	Ratio of Nozzle Pressure to Reservoir Pressure	2

LIST OF TABLES

Table No.	*Title*	*P*
1-1	Calculated Thermochemical Values for Standard Propellants (Including Residual Volatiles)	1
2-1	Differential Coefficients for Artillery Weapons	2
2-2	Values of η, β, η_1 and β_1 for Standard Weapons	2
2-3	Thrust Coefficient, C_T	2
3-1	Heat Transfer Function, $f(\tau)$, for Guns During Burning	
3-2	Heat Transfer Function, $f(\tau)$, for Guns After All Burnt for $\tau_b = 24$ and 28	
3-3	Heat Transfer Integral, I	
3-4	Wear of Guns	
5-1, 5-2, 5-3, 5-4	Tables for the Pidduck-Kent Solution	
5-5	Approximate Range of Values of the Variables and Parameters Used in Hicks' Thermal Theory of Ignition	
5-6	Interior Ballistic Data for 8-inch Howitzer Firing HE Projectile M106	

CHAPTER 1

LIST OF SYMBOLS

B	Burning rate coefficient	n	Number of moles of gas per unit weight of propellant gas
C	Mass of propelling charge		
C_v	Specific heat of propellant gas at constant volume	P	Pressure
		R	Molar gas constant
$\bar{C}_v$	Average specific heat of propellant gas at constant volume	S	Area of burning surface of propelling charge
		S_0	Initial surface area of propelling charge
c	Mass of propellant burned	T	Temperature of propellant gas
D	Outer diameter of propellant grain	T_0	Adiabatic flame temperature of propellant
d	Diameter of the perforations of propellant grain	t	Time
		U_g	Volume of the propellant gas
E	Specific energy or potential of solid propellant	u	Travel of projectile
F	Force of propellant	V	Velocity
f	Fraction of web burned through	w	Web thickness
I	Internal energy of propellant gas	α	Burning rate pressure exponent
K	Energy expended by propellant gas in doing work and heating tube	γ	Factor analogous to the ratio of specific heats at constant pressure and volume
M	Mass of projectile	η	Specific covolume of propellant gas
N	Number of grains in the charge	ρ	Specific mass of the propellant

CHAPTER 1

DISCUSSION OF THE PROBLEM

1-1 INTRODUCTION

The imparting of high velocities to projectiles requires tremendous force. The source of the energy which supplies these forces must be readily manufactured, easy to transport, and capable of being safely applied. At various times, proposals have been made for utilization of energy provided by means other than explosives, such as compressed air, electromagnetic force, and centrifugal force. Thus far, however, no results have been attained from any of these sources which approach those realized from chemical explosives.

Interior ballistics of guns (that branch of ballistics dealing with motion imparted to a projectile by a gun) comprises a study of a chemical energy source, a working substance, and the accessory apparatus for controlling the release of energy and for directing the activity of the working substance. Of allied interest is the mechanical functioning of guns and accessories. General information on the types of guns and their construction and functions is given in Reference 1. References applicable to each chapter of this Handbook are given at the end of the chapter.

Since unnecessary weight is an unjustified logistical extravagance, weapons are designed to operate under greater extremes of temperature and pressure than are usually encountered in the use of nonmilitary engines. Because the time cycle involved is quite small, there is not sufficient time for the consummation of slow processes such as heat transfer. Consequently, it is necessary that the chemical energy source also furnish the gaseous products which in themselves constitute the working substance. This energy source may be a solid propellant, as in most guns, or a liquid fuel and oxidizer source, such as is sometimes used in rocket propulsion.

Propellants are studied from several aspects. Thermodynamic properties indicate the release of as much energy per unit weight as may be consistent with other demands. Studies of the mechanism of decomposition indicate the effects of uncontrollable parameters such as ambient temperature. Dynamics of the gases are necessarily a subject of investigation because the kinetic energy of the propelling gases is an important part of the total energy of the process. The study of motion of a projectile inside the gun tube is not a matter of simply applying Newton's laws to the motion of the projectile regarded as a point mass, but a complicated study of the rate at which the high temperature gas is evolved from the propellant; the motion of the gas so produced; and the effect of this gas on the motion of the projectile itself. The passage of the projectile stresses the tube mechanically and subjects the interior of the barrel to siding friction. The passage of high temperature gases, in addition to the high pressures generated, heats the barrel to the extent that chemical interaction with the metal itself occurs.

Interior ballistics is defined as the branch of applied mechanics which deals with the motion and behavior characteristics of projectiles while under the influence of the gases produced by the propellant. As an applied science it is still much of an art and largely empirical. The phenomena with which it deals are explicable in terms of well established physical and chemical principles. Unfortunately, the phenomena are complex and related in subtle and obscure ways so that considerable experience and judgment are necessary in the application of the principles if trustworthy theoretical results are to be derived. There occur in the formulation of the theory quantities which are difficult to determine by independent measurement because their proper values for particular cases depend in obscure ways on the particular circumstances of the case considered. They have the nature of empirical correction factors whose values can frequently be estimated only from the results of numerous examples involving comparison of the theory used with the records of actual firings. The beginner is, therefore, forewarned to be on his guard. All theoretical results should be as firmly backed up by comparison with actual firings as is possible. In this sense the theory serves as a means of interpolation between, or extrapolation from, existing designs.

The subject of interior ballistics of guns has been investigated through more than 200 years, starting with the invention of the ballistic pendulum in 1743.

A very extensive literature has been built up, and many excellent texts are available. For general background, the texts prepared by Corner[2] and Hunt[3] are recommended. More specific treatments have been made by Bennett[1] and Taylor and Yagi[5]. A consolidated NDRC report, written by Curtiss and Wrench[6], covers the work done during World War II. A general treatment of the problem with applications to guns is given in Reference 7.

1-2 GUNS

1-2.1 Definition

The term *gun* in this handbook, unless otherwise indicated, may be taken in its general sense, that is, a projectile-throwing device consisting essentially of a projectile-guiding tube, with an incorporate or connected reaction chamber in which the chemical energy of a propellant is rapidly converted into heat and the hot gases produced expand to expel the projectile at a high velocity.

1-2.2 Classification

For convenience of discussion guns are classified according to their salient features, functions, modes of operation, etc.[1] The boundaries of these classifications are not always clearly defined, and the classifications and nomenclature are often traditional. The classifications are useful, however, and are in common use. The principal one is based roughly on size and portability and classifies guns as small arms and artillery. Small arms are in general less than 30mm in caliber and are usually portable by foot soldiers. Artillery consists of the larger weapons usually mounted on carriages and moved by other than human power. Small arms are more variable in design and function. They include such weapons as rifles, machine guns, pistols, etc. Artillery weapons include guns (specific), howitzers and mortars. Guns (specific) include those firing usually at lower elevation and higher velocity, and howitzers include those which operate in general in a lower velocity range. The latter can be fired at high angles and use zoned charges, that is, charges which are loaded in separate increments and can be varied within limits by the gunner. Mortars operate at high angles like howitzers but operate at still lower velocities and are generally loaded from the muzzle. They are simple in design and can be broken down and transported by foot soldiers.

1-2.3 Action Inside the Gun

A gun is essentially a heat engine. Its action resembles the power stroke of an automobile engine with the expansion of hot gases driving the projectile instead of a piston (Figure 1-1). When the charge is ignited, gases are evolved from the surface of each grain of propellant, and the pressure in the chamber increases rapidly. Resistance to initial motion of the projectile is great and relatively high chamber pressures are attained before much motion of the projectile takes place. In the solution of the interior ballistics problem, fictitious starting pressures are assumed, which work well in practice.

The chamber volume is increased by the movement of the projectile, which has the effect of decreasing the pressure; however, the rate of burning of the charge increases. The net effect is a rapid increase in the propellant pressure until the point of maximum pressure is reached. This occurs at a relatively short distance from the origin of rifling. Beyond that point, pressure drops and, at the muzzle, reaches a value considerably less than maximum pressure, probably of the order of 10% to 30% thereof, depending upon the weapon design and the propellant. This muzzle pressure continues to act on the projectile for a short distance beyond the muzzle. Thus, the projectile continues to accelerate beyond the muzzle.

A special form of this method of propulsion is represented by the recoilless system (Figure 1-2). Here recoil forces are countered by the discharge of gases through a nozzle at the breech. The rate of discharge of gases can be controlled by controlling propellant burning, thus permitting a balance of the momentum of the gun-propellant gas-projectile

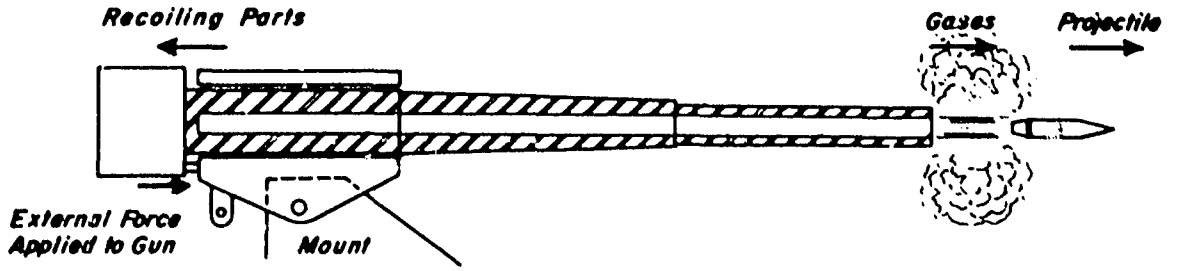


FIGURE 1-1. *Recoil Gun System.*

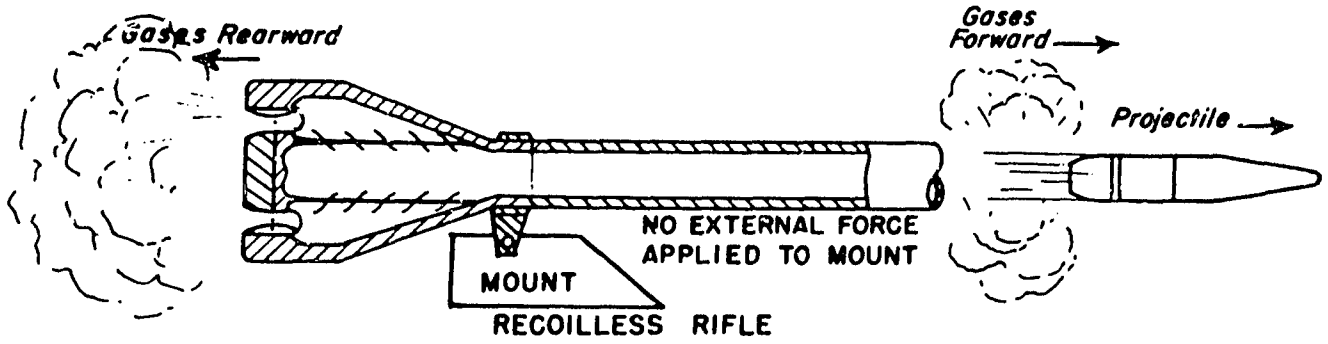


FIGURE 1-2. *Recoilless Gun System.*

system. The interior ballistic problem here is not only one of combustion but of balancing the orifice diameter against thrust required to maintain a mean recoil velocity of the weapon at zero. The propellant weight in this case exceeds that for a comparable recoil gun by a factor of 2 to 3. The pressure-travel curve is designed for minimum muzzle velocity consistent with satisfactory exterior ballistic performance, thus permitting the use of a thin gun tube which is necessary to maintain the characteristic light weight of this weapon. The subject of recoilless weapons and other leaking guns is covered more fully in Chapter 2 of this handbook.

1-3 PROJECTILES

Projectiles, like guns, exist in a great variety of designs, depending upon the intended use. Since most of the design characteristics do not affect the interior ballistics, we shall consider only a few. The most important of these factors is the mass of the projectile. This must always be taken into account in the formulation of interior ballistics theory, as it has a major effect on acceleration and velocity of the projectile, as well as on the propellant pressure at all points.

Another very important characteristic is the design of the rotating band on those projectiles which are to be spin stabilized. The band is slightly larger than the tube diameter and must be swaged to the tube diameter and engraved by the rifling. The result of this process is a high initial resistance to motion of the projectile, which means that the gases must build up a relatively large starting pressure before the projectile has moved appreciably. This has an important effect on the interior ballistics, particularly on the maximum pressure reached and the time at which it occurs. This variable is largely eliminated in recoilless weapons in which the rotating band of the projectile is preengraved to fit the rifling. It is also eliminated in smooth bore weapons which fire fin-stabilized projectiles. Here an important factor is the amount of clearance between the projectile and the tube, as this determines the leakage of gas around the projectile. The principal weapon having this problem is the mortar. Here, with muzzle loading, the clearance must be sufficient to permit the escape of air so that the projectile will slide down the bore and strike the firing pin with the impact energy required to initiate the primer.

Only one other characteristic of the projectile need be mentioned and that is the axial moment of inertia for spin-stabilized projectiles. And here the effect on interior ballistics is quite small, as the energy of rotation normally represents only a fractional percent of the energy of translation of the projectile.

1-4 DISTRIBUTION OF ENERGY

As an indication of the relative magnitude of the factors involved in utilizing the energy developed by the burning of the propellant in a medium caliber recoil gun, the following possible distribution is given:

Energy Absorbed	*% of Total*
Translation of projectile	32.0
Frictional work on projectile (Due to engraving of rotating bands and wall friction)	2.0
Translation of propellant gases	3.0
Heat loss to gun and projectile	20.0
Sensible and latent heat losses in propellant gases	42.0
Rotation of projectile and translation of recoiling parts (each about 0.1% and residuals in approximations total)	1.0
Propellant potential, E	100.00

Distribution of the available energy of the propellant charge is discussed in Chapter 2, as basic to the solution of the interior ballistics problem.

1-5 PRESSURE-TRAVEL CURVES

In order that the projectile may acquire the designated muzzle velocity, and that the pressures

developed to accomplish this do not damage the weapon, all tubes are designed in accordance with a desirable pressure-travel curve for the proposed weapon.[8]

The pressure-travel curves (Figure 1-3) indicate the pressure (or force if pressure is multiplied by the cross-sectional area of the bore) existing at the base of the projectile at any point of its motion. Hence, the area under any of the curves represents the work done on the projectile per unit cross-sectional area, by the expanding gases.

If the areas under curves A and B are equal, then the work performed in each of these cases will be equal, and the muzzle velocities produced by each of these propellants will be the same, since

$$WORK = KE = \tfrac{1}{2}MV^2$$

The fact that curve A exceeds the permissible pressure curve cannot be tolerated.

Should it be desired to increase the muzzle velocity of a projectile, the work performed, or the area under some new curve, must be greater than the area under a curve giving a lower muzzle velocity. Such an increase in velocity is indicated by curve C whose maximum pressure is equal to that of curve B, but whose area is greater than that under B. It appears that the ideal pressure-travel curve would be one which would coincide with the curve of permissible pressure; however, if it were possible to design a propellant capable of producing such a result, many objectionable occurrences would take place. In addition to producing excessive erosion (a factor which would materially decrease the accuracy life of the gun), brilliant flashes and non-uniform velocities due to high muzzle pressure would result. Moreover, the chamber would have to be materially increased and this would affect the weight and hence the mobility of the gun. As a result of experience, the velocity prescribed for a particular gun is always somewhat below the maximum which it is possible to obtain; and the propellant grain most suitable for producing this result is the one which will give the prescribed velocity uniformly from round-to-round without exceeding the permissible pressure at any point in the bore.

1-6 CONTROL OF INTERIOR BALLISTIC PERFORMANCE

Consideration of the desired relationships between gas pressure and projectile velocity necessary to meet the demands imposed for the achievement of desired ballistic performance has been discussed in a general sense; however, it remains a fundamental problem of interior ballistics to determine and evaluate the influence of all variables of the problem. The solution may be based on theoretical analysis, established empirical relationships, or detailed, meticulous experimentation.

The variables basic to the problem include the following:

a. Variation in chemical composition of the propellant.

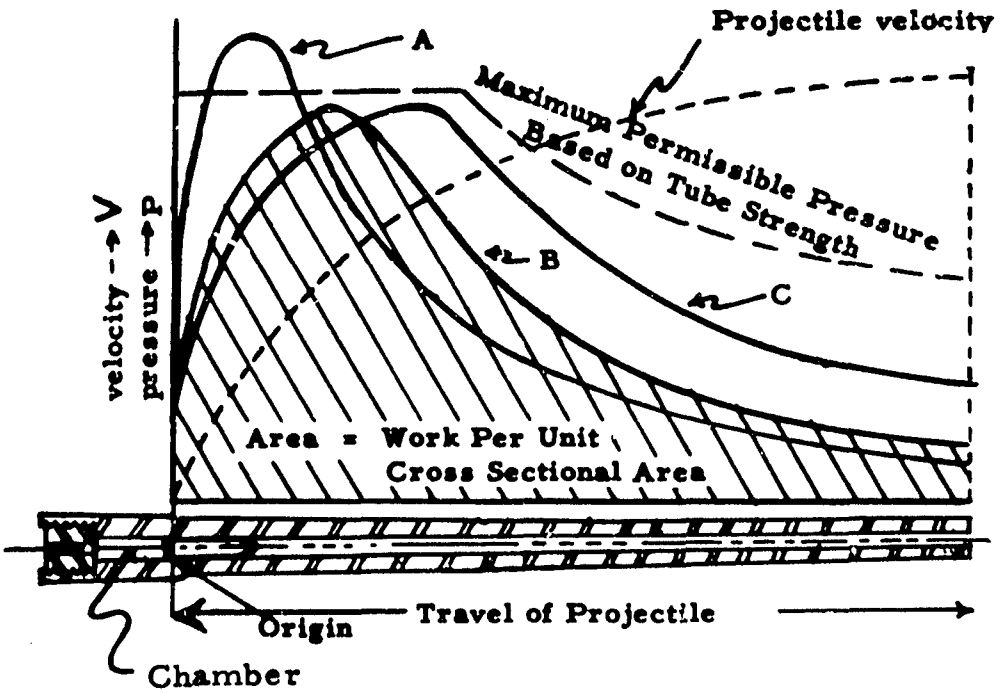


FIGURE 1-3. *Pressure-Travel (Solid Lines) and Velocity-Travel (Dotted Line) Curves.*

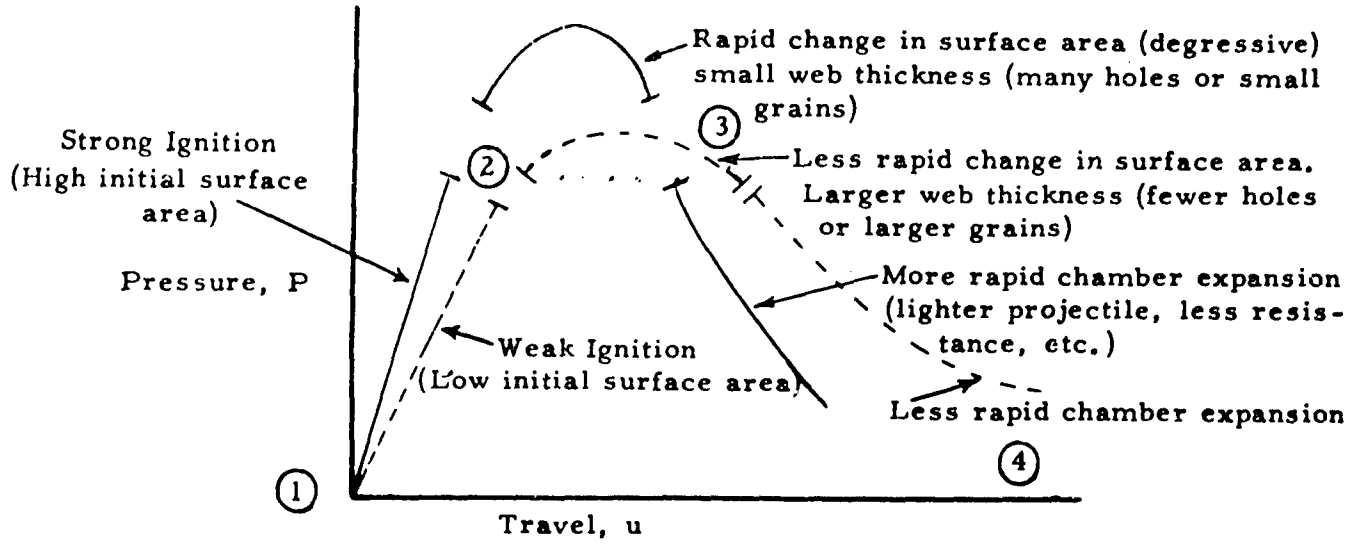


FIGURE 1-4. *Pressure-Travel Relationship.*

b. Variations in rate of reaction.
c. Variations in ignition characteristics.
d. Variation in grain geometry (surface factors).
e. Variation in charge weight (density of loading).
f. Environmental factors.

1-7 EFFECTS OF PROPELLANT GRAIN CHARACTERISTICS

Assuming proper ignition of all propellant grains, the characteristic shaping of pressure-travel or pressure-time relationships for the gun system is dependent on such variables as grain composition (quickness), grain size, grain configuration, and density of loading. Although in a final design all factors may be involved, it is of basic importance to note first the independent effects of such variables.

Propellant compositions (single-base, double-base, nitroguanidine, etc.) and definitions of configurations (degressive, neutral and progressive burning propellants) are discussed in subsequent paragraphs of this chapter. Performance of gun systems is usually demonstrated using pressure (P)-travel (u) coordinates, although pressure-time relationships are often used in experimental investigations.

In each case discussed in this paragraph, initial burning rates are directly related to area exposed for the total number of grains per charge; hence, it is difficult to consider the influence of single factors without making allowance for the total area initially exposed to kindling temperatures. For any pressure-travel curve, the shape of the curve is affected by the variables shown in Figure 1-4. For a given pressure-travel curve (Figure 1-4) the slope of the curve in the region (1) to (2) is dictated by ignition characteristics and total area initially exposed to burning. The region (3) to (4) will be governed primarily by the grain configuration. The methods of manufacturing propellants and determining and maintaining the desired configuration of the propellant grains are covered in References 7 and 9.

1-7.1 Grain Configuration

Exposed burning area as a function of "percent grain consumed" (Figure 1-10) offers a key to the effects of configuration on pressure-travel relationships. As indicated in Figure 1-5, changing configuration to a more progressive burning design (employing grains of the same initial surface area, composition, and total charge weight) results in lowered peak pressures (with peak pressure occurring later in the cycle) and in higher muzzle pressure when compared with degressive grains. For identical charge weight, areas under the curve are approximately equal. In order to meet requirements for equal initial surface areas for the total charge, the degressive grains must be the smallest of the designs considered.

1-7.2 Grain Size

For a fixed weight of charge of similar composition and configuration, shaping of pressure-travel relationships may be accomplished by varying the initial area exposed to burning by varying grain size. Similar effects illustrated in Figure 1-5 result as grain size is increased (Figure 1-6).

Similarly, comparative results of independently varying composition (quickness) or web thickness (a combination of size and configuration parameters) can be demonstrated. In adapting such relationships

to specific gun systems, a compromise of their characteristics must be utilized. Hand and shoulder weapons require pressure-travel relationships that minimize muzzle blast at the expense of reaching high peak pressures and, characteristically, utilize "quick", degressive, small-grained propellant design. High peak pressures, avoided in larger guns because of design problems of the gun tubes, are minimized by propellant designs based on "slow," progressive or neutral burning configurations of large size.

1-7.3 Density of Loading

The various types of guns, with different calibers and lengths, and each with its own muzzle velocity requirement, present special problems for the propellant designer. The lengths of travel of the projectile in the bore and, consequently, the times of its travel, differ greatly. In addition, the volume of the chamber and the weight of the projectile introduce elements which must enter into the selection of a propellant for a gun.

Since muzzle energy is directly dependent on the amount of charge burned, it becomes necessary to consider feasible means for increasing the total amount of energy made available to perform useful work done on the projectile. It is possible, by choosing increasingly large charges of slow propellants, to obtain increased velocity without exceeding the maximum allowable pressure. Efficiency will be correspondingly lowered; hence, it is not advantageous to fire slow propellant in a gun not designed for it. Irregularity in muzzle velocity is closely associated with overall efficiency. If the burning rate is lowered enough, unburned propellant is expelled in varying amounts, increasing irregularity, muzzle blast, and flash. With slower propellants, the point of maximum pressure occurs later, thus demanding stronger, and therefore heavier, construction over the length of the tube. Conversely, increasing the weight of charge of propellant of given quickness increases the maximum

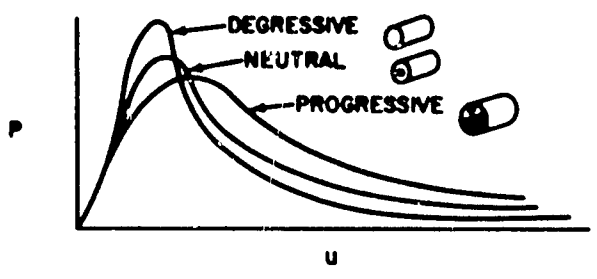


FIGURE 1-5. *Effects of Grain Configuration on Pressure-Travel Curves. (Charge weight is equal in each case.)*

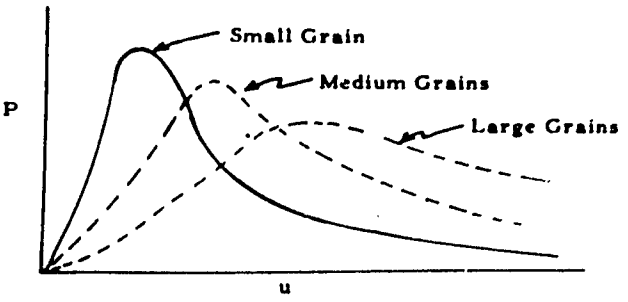


FIGURE 1-6. *Effects of Independently Varying Grain Size. (Charge weight is equal in each case.)*

pressure attained and causes it to occur sooner in the travel of the projectile.

1-8 BLACK POWDER*

Black powder, once the only available propellant, is no longer used for that purpose. It is still of interest because of other military uses. It is manufactured as small, shiny black grains. The ingredients are usually finely pulverized potassium or sodium nitrate, charcoal, and sulfur which are incorporated into an intimate mechanical mixture. The charge is pressed into a cake and pressed or extruded to the desired grain size and shape. The grains are glazed with graphite to prevent caking and accumulation of static electricity. The potassium or sodium nitrate (about 75%) acts as an oxidizing agent, while charcoal (about 15%) and sulfur (about 10%) are combustibles. Sulfur also lowers the ignition temperature of the mixture from 340°C to 300°C.

Black powder is no longer considered suitable as a propellant because of its many objectionable features and because of the development of newer propellants in which the undesirable qualities have been overcome or improved. It is difficult to control accurately the burning speed of black powder. Consequently, the range of a projectile propelled by it may vary. Black powder is too easily ignited, being extremely sensitive to heat and friction, and therefore, must be handled very carefully. It is hygroscopic, which requires that sealing precautions be taken to retain stability. Its strength is relatively low and the large amount of solid residue which it leaves makes smoke reduction difficult. Flash reduction is also a problem with black powder.

Black powder, in its several grades, is still used for the following military purposes:

a. Propellant igniters in artillery ammunition.
b. Delay elements in fuzes.

* Additional information on black powder will be found in Reference 9.

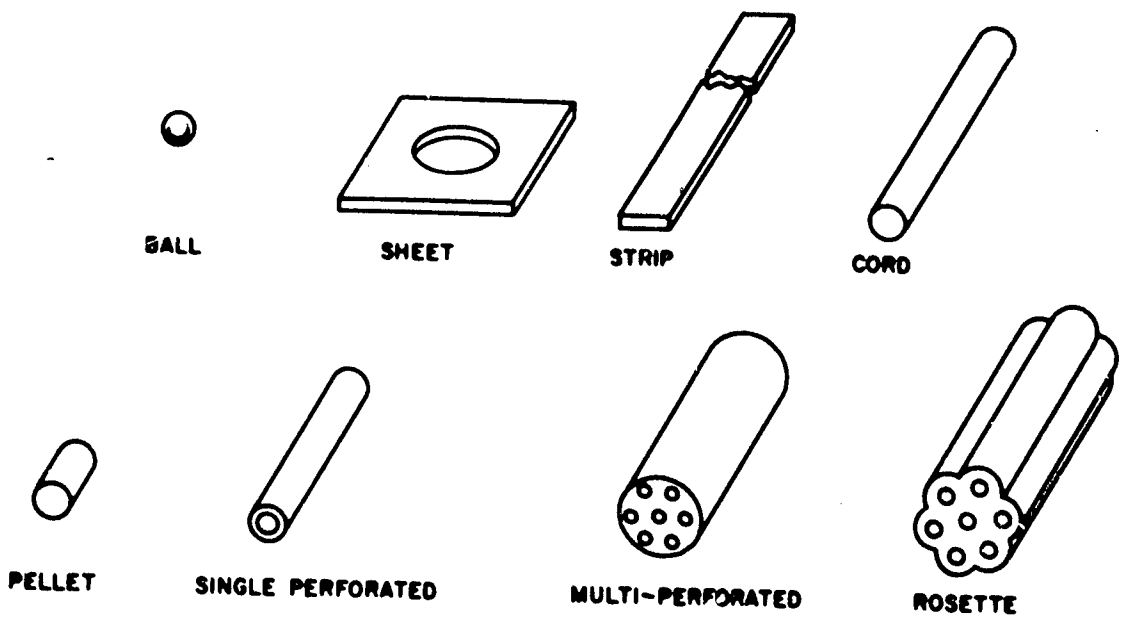


FIGURE 1-7. *Typical Shapes of Propellant Grains.*

c. Saluting and blank charges.
d. Spotting charges for practice ammunition.
e. Safety fuse (burning rate, 1 ft in 30–40 seconds).
f. Quickmatch (burning rate, 9-120 ft per second).

1-9 GUN PROPELLANTS*

1-9.1 Present Gun Propellants

Present gun propellants are forms of nitrocellulose explosives with various organic and inorganic additives. They may be divided by composition into classes of which two, the single-base and double-base, are the most common. Both classes are manufactured in quantity in a variety of shapes including flakes, strips, sheets, pellets, or perforated cylindrical grains (Figure 1-7). The cylindrical grains are made in various diameters and lengths, depending on the size of the gun. Figure 1-8 shows, to approximately $\frac{2}{3}$ full size, grains for various calibers of guns. The grains for a caliber .30 cartridge are 0.032 inch in diameter and 0.085 inch long, while those for a 16-inch round are 0.947 inch in diameter and $2\frac{7}{16}$ inches long. The perforations shown in Figure 1-7 are for the purpose of controlling the rate of gas liberation as well as burning time.

* Additional information on gun propellants will be found in Reference 9.

1-9.2 Burning Time

The burning time can be controlled by the following means:

a. The size and shape of the grains including the number of perforations (Figure 1-7).

b. The web thickness or amount of solid propellant between burning surfaces; the thicker the web, the longer the burning time (Figure 1-9).

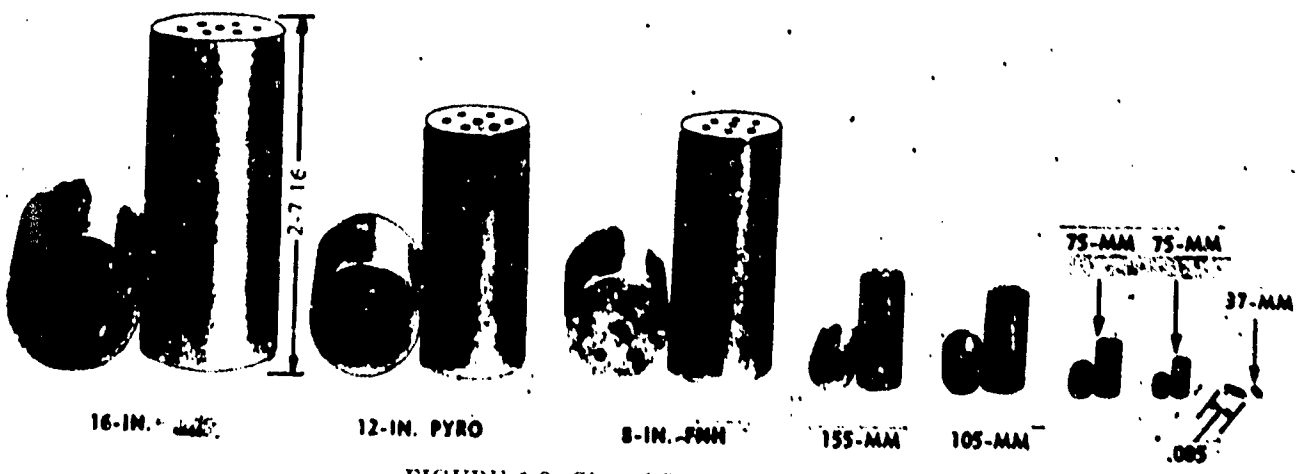


FIGURE 1-8. *Sizes of Some Typical Grains.*

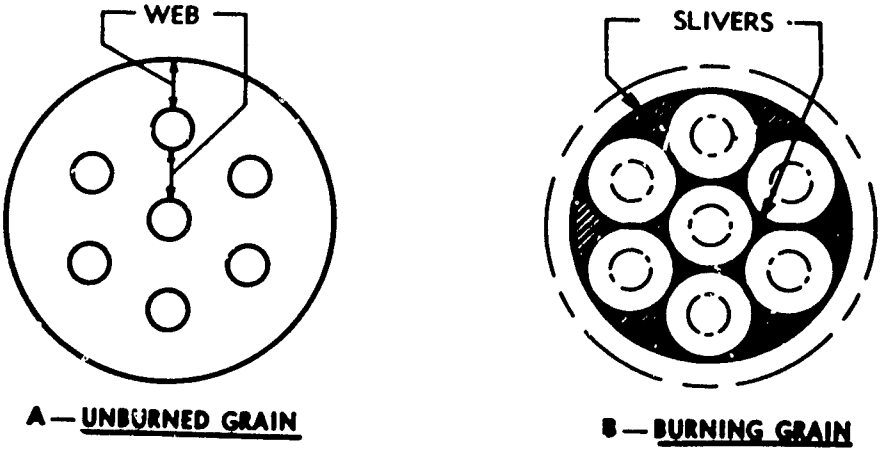


FIGURE 1-9. *Web Thickness and Route of Burning Progress through a Progressively Burning Grain.*

c. The quickness or rate of burning of the propellant.

d. The percentages of volatile materials, inert materials, and moisture present. A 1% change in volatiles in a low volatile content propellant may cause as much as a 10% change in burning rate.

1-9.3 Burning Action

Unconfined smokeless propellant burns with little ash or smoke. When confined, its rate of burning increases with temperature and pressure. In order not to exceed the permissible chamber pressure of the weapon, the time of burning of the propellant is controlled. At constant pressure the time of burning is proportional to the amount of exposed propellant surface. Therefore, a propellant charge is made up of accurately sized grains of specified shape.

Since the grains burn only on exposed surfaces, the rate of gas evolution for a given propellant will depend upon the area of the burning surface. For a given weight of propellant the initial burning surface will depend upon the form and dimensions of the grains. As burning continues, the rate of combustion and of pressure variation will depend upon how the area of surface changes, that is, upon the rate of area increase or decrease. Figure 1-10 shows, for typical grain configurations, the relation between percent of grain consumed and area of burning surface.

The rapidity with which a propellant will burn depends upon the chemical composition, pressure, and area exposed to burning. The quickness of a propellant is a relative term only, expressing its rate of burning compared with others. A quick propellant will burn more rapidly and produce a higher pressure in a given gun than a slow one. Propellants of fixed weight, chemical composition, and grain geometry may be made quicker by decreasing size, thus increasing burning area.

1-9.4 Degressive Burning

The total surface of a propellant grain changes with burning, and on cord and strip forms the surface area of the grain decreases. The burning action of these grains is classified as degressive.

1-9.5 Neutral Burning

As a single-perforated grain burns, the outer surface decreases and the inner surface increases. The result of the two actions is that the net burning surface remains approximately the same. The burning of this type of grain is known as neutral.

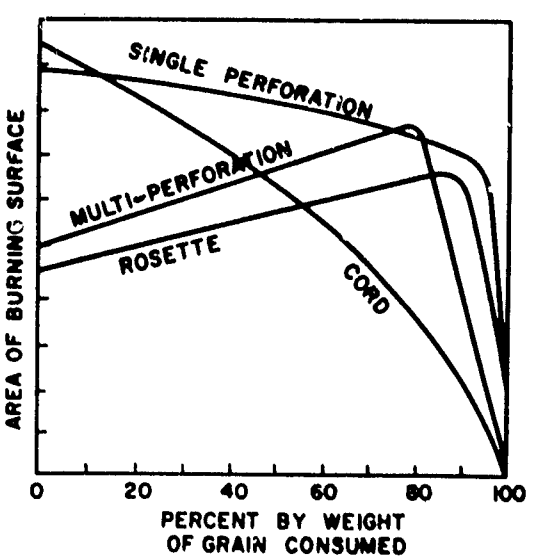


FIGURE 1-10. *Relative Areas of Burning As a Function of Percent of Individual Grain Consumed, for Several Typical Grain Shapes.*

1-9.6 Progressive Burning

When the multiperforated grain burns, the total surface area increases since the perforated grain burns from the inside and outside at the same time. This type of burning is called progressive (Figure 1-9). When a multiperforated grain is not completely consumed, as may be the case when a reduced charge is used, portions of the grain remain in the form of slivers and may be ejected as such from the weapon. The rosette grain (Figure 1-7) was designed to reduce the formation of slivers.

1-9.7 Single-Base Propellants

Single-base propellants are essentially gelatinized nitrocellulose to which various organic substances are added either to produce improved qualities or for special purposes. Single-base propellants are amber, brown, or black in color, depending on the additives present.

Single-base propellant is rather insensitive. In fact, it is difficult to ignite, requiring a powerful primer and additionally, in large ammunition, a black powder igniter. It ignites at 315°C. In the open, single-base propellant burns very much like celluloid. Seemingly, this explosive is very safe but the fact should not be overlooked that, although it is used as a low explosive, it is an organic nitrate and may detonate if burned in large quantities. It may also detonate sympathetically from the detonation of other explosives, although in actual practice this rarely occurs. Single-base propellant is more powerful than black powder, giving off 1000 calories and 900 cubic centimeters of gas per gram, compared with 700 calories and 300 cubic centimeters per gram of black powder. It has a burning speed of 0.1 to 18 centimeters per second at pressures up to 60,000 pounds per square inch.

Single-base propellant is unstable and decomposes in hot moist storage. It is hygroscopic, although not as hygroscopic as black powder. Nitrocellulose in the presence of moisture hydrolizes to free acid, which takes the form of oxides of nitrogen. These oxides accelerate the decomposition, building up heat to an ignition temperature, and spontaneous combustion may result. Addition of a chemical stabilizer brings the stability to acceptable limits.

To summarize, the characteristics of single-base propellants are:

a. Controlled burning. The burning time of single-base propellants can be controlled to a point where the maximum propelling effect is obtained.

b. Sensitivity. Ignition is difficult, and the propellant is reasonably safe.

c. Stability. The propellant is unstable, but this can be controlled to within acceptable limits by the addition of stabilizers.

d. Residue. There is some residue and smoke.

e. Manufacture. This is complicated but safe. Raw materials are plentiful.

f. Erosive action. Single-base propellant erodes the bore, but not quite as much as black powder. Its isochoric adiabatic flame temperature is 2400°K to 3000°K.

g. Flash. This is caused by hot gases which ignite when they come into contact with oxygen at the muzzle. It can be controlled by adding cooling materials to the propellant.

Single-base propellant can be produced in a form lacking most of the objectionable features.

The propellant grains for small arms are usually glazed with graphite to facilitate machine loading and to prevent the accumulation of static electricity, and thus present a black, polished appearance. Since the grains are small, they ignite more readily and burn more freely than cannon propellant. When moisture is present or abnormal temperatures prevail, they are subject to more rapid deterioration than the larger grains.

1-9.8 Double-Base Propellants

This form of propellant is essentially a combination of nitroglycerin and nitrocellulose with certain additives to give special properties. The nitroglycerin increases the potential and reduces hygroscopicity, the latter improving the stability. The color of the grains is gray-green to black, and the forms are the same as for single-base propellant.

Double-base propellant is more sensitive than single-base propellant, igniting at 150°C to 160°C. It detonates more readily than single-base propellant and can be made to yield a higher potential and liberate more heat, but produce a smaller volume of gas. The burning rate, generally faster than that of single-base propellant, can be controlled similarly.

The characteristics of double-base propellants are, in summary:

a. Controlled burning. Burning can be controlled, as with single-base propellants.

b. Sensitivity. This is greater than for single-base propellant, slightly increasing hazard.

c. Stability. Double-base propellants can be made stable by the addition of stabilizing ingredients.

d. Residue. Since there is not so much inert material, there is little solid residue. Smoke can be controlled.

e. Manufacture. Not as safe as single-base pro-

pellant due to presence of nitroglycerin. Raw materials are readily available.

f. Erosive action. High temperature and heat of explosion from the higher potential double-base propellants cause more erosion than results from use of single-base propellants.

g. Flash. As in the case with single-base propellants, flash can be controlled to a certain extent by the use of additives. The presence of nitroglycerin accentuates the tendency to flash by increasing the flame temperature.

Double-base propellants have limited use in artillery weapons and in small arms in the U. S. They are widely used in mortars, where erosion is not an important factor. However, they are used as the standard propellants in most other countries. The U. S. Army and Navy both evaluated single-base and double-base propellants in guns prior to World War I and decided in favor of the former due to their lesser erosive effect.

1-9.9 Nitroguanidine (Triple-Base) Propellants

A propellant containing nitroguanidine in addition to nitroglycerin and nitrocellulose as principal ingredients is commonly referred to as a triple-base propellant. This type of propellant was developed in Great Britain during World War II as a result of research directed toward obtaining a propellant with desirable properties such as cool burning, low erosion, and flashlessness, without decrease in stability or potential. The British have designated their nitroguanidine propellant as Cordite N. The nitroguanidine propellant, designated M-15, developed by the United States, represents an interim solution for selected rounds of ammunition where the flash or obscuration problem is critical and where its special properties are particularly needed.

The M-15 propellant has a ballistic potential comparable to single-base propellants currently in use but with a lower erosive effect and less tendency to flash.

1-9.10 Solvent Emulsion Propellant (Ball Powder)

A radically different manufacturing process uses a volatile solvent to form propellant in small grains of spherical shape, designated Ball Powder.* The sizes of the grains are appropriate for use in small arms. The propellant is produced by dissolving wet nitrocellulose in a solvent (ethyl acetate) with additives. When a protective colloid is added and the solution is agitated, small globules are formed. When the volatile solvent is removed by evaporation the globules solidify, and when coated, dried, and graphited, become balls or spheres, A wide variety of double-base and single-base compositions may be produced by this technique. Because of the economy and speed with which this powder can be manufactured, this propellant has promise in future applications not limited to small arms.

* Trademark of Olin Mathieson Chemical Corporation. Reference 9 contains additional information.

1-9.11 Characteristics of Standard Propellants

The compositions of some of the standard and experimental (M and T designations, respectively) propellants, and some of the thermodynamic and calorific values of them are given in Table 1-1. The practice, as illustrated therein, of specifying certain additives, coatings and residues as percentages of the total of the principal constituents, resulting in over 100% total contents, is standard in the explosives field.

1-9.12 The Rate of Burning

Since the burning of a propellant occurs only on the exposed surfaces, the smallest dimensions between the exposed surfaces become the critical dimensions, as it determines in general when the propellant will be completely consumed. This critical dimension is called the web. As was explained in discussion of the progressive, multiperforated grain, burning through of the web is followed, in this case, by burning of the slivers. A corrected form of multiperforated grain is the rosette, illustrated in Figure 1-7. With the exception of multiperforated grains, all forms of propellant grains are completely consumed when the web is burned through.

In the multiperforated grains, having seven symmetrically located perforations, Figure 1-9, the web may be calculated from the formula

$$w = 0.25(D - 3d) \qquad (1\text{-}1)$$

where

w = web thickness
D = outside diameter of the grain
d = diameter of the perforations.

Experimental measurements show that the rate of burning of a propellant is primarily dependent on the pressure under which the reaction proceeds and this dependence may be expressed approximately by the pressure to some power.

The mass rate at which gas is produced may then be expressed as

$$\frac{dc}{dt} = \rho S B P^{n} \qquad (1\text{-}2)$$

where

e is the mass of propellant burned
t the time
P the pressure
B the burning rate coefficient
α the burning rate pressure exponent
ρ the specific mass of the propellant
S the area of the burning surface

The dependence of the burning surface area on the remaining web as the charge is consumed can be calculated from the geometry of the grain by assuming that this geometry does not change during burning, i.e., that the linear burning rate is the same at all points on the burning surface. For propellant in thin sheets, the area of the edges is negligible and the surface is constant during burning. For single perforated cylinders, if S_0 is the initial surface and f the fraction of the web burned through

$$S = S_0 - 2\pi N f w(D_0 + d_0) \qquad (1\text{-}3)$$

where N is the number of grains in the charge. The second term on the right arises from the combined effect of the change in the area of the end surfaces and the reduction in length of the grain. Otherwise, the decrease in the outer diameter is compensated by the increase in the inner diameter. If the second term can be neglected, the burning surface is constant. For single perforated grains of the usual proportions, the neglect of this second term gives a surface area, at burnout of the charge, which is approximately ten percent too high. That is, the charge is actually somewhat degressive. For seven perforated grains, the charge is progressive until the web is burned through; after which it is degressive.

A relation such as Equation 1-3, which takes account of the effect on the rate of gas evolution of the changing burning surface area, is called the form function of the granulation. This function is simple for sheets, cords and long single perforated grains or tubes. For seven perforated grains, it is complex, especially after splintering. For the simple shapes it is expressed as a polynomial in the remaining web, but for seven perforated grains it is often given in tabular form. Formulas for the surfaces for complex shapes are given in Reference 10. For other formulations of the form function see References 2, 3 and 6.

In practice the difference in the interior ballistics for single and multiple perforated grains is not as great as theory indicates. In calculating the surfaces from the geometry, the assumption is made that the ignition is simultaneous over all surfaces. This is never the case in practice. For the seven perforated charges the degressive burning of the slivers remaining after the web is burned through tends to reduce the progressive character of the early burning. Also the burning rate is influenced not only by the pressure but also by the flow of the gas over the grain and within the perforations. The shape of the grains is not exactly maintained during burning. Except, therefore, for highly degressive grains such as cords, the assumption of a constant burning surface is adequate.

With this assumption, the burning surface of the charge may be calculated by the formula

$$S = \frac{2C}{\rho w} \qquad (1\text{-}4)$$

where

C is the mass of charge

In practice, the rate at which gas is evolved depends on the detailed conditions under which the charge is burned. A standard method for determining burning rates is to burn the charge in a closed chamber at constant volume and measure simultaneously the pressure and its time derivative. Then, if the relation between e and P is known, a value for the burning rate coefficient, B, can be derived by the use of Equations 1-2 and 1-4. The coefficient, B, so determined, is also called the closed chamber burning rate coefficient, and it is used mainly for comparative purposes and for standardizing propellant lots. The details of the method are given in References 3 and 7.

The closed chamber burning rate coefficient rarely yields good agreement with observation if used in interior ballistic calculations for guns. The conditions in the gun are very different, and the burning rate coefficient must be determined by adjustment to the results of actual firings. By observing the results of numerous firings when fitted to a given formulation of the theory, the user can estimate a burning rate coefficient for a particular case which then can be adjusted to the actual case in question.

The burning rate pressure index, α, varies for different propellants, but the latest experiments indicate that it lies between 0.8 and 0.9. A figure as low as $\frac{1}{2}$ has been used by some authors, and frequently it is assumed to be equal to unity. In the latter case, the solution of the equations of the theory can be given analytically, otherwise this is not possible and numerical methods must be used. With the development of high speed computing

TABLE 1-1 CALCULATED THERMOCHEMICAL

VALUES FOR STANDARD PROPELLANTS

(INCLUDING RESIDUAL VOLATILES)

(Located in the back of this handbook)

nachines, this is not the disadvantage it once was.

The value of α may be determined from closed chamber measurements. The methods are described n Reference 3.

1-9.13 Energy of Propellants

The propellant gas is a complex mixture of several gases and for the mixture to have the same properties of independence of energy from density) all changes n equilibrium which occur must be equivoluminar nd independent of the density. This in effect estricts the theory to "cool" propellants,* that is, o those for which the temperature is not high nough to produce significant dissociation of the nain constituents of the gas mixture. To the approxmation of the assumed equation of state, each ropellant formulation has a definite explosion temerature. Thus, the decomposition of a unit mass f propellant always liberates the same amount of nergy which then heats the product gases to the ame temperature independent of the density. For nost propellants, the most important equilibrium s the water gas equilibrium and since this equilibium is equimolar, the assumed equation of state s sufficiently accurate for use in the interior ballistic heory of guns. The use of a more accurate equation f state would greatly complicate the theory and ;ould not be justified in view of other simplifying ssumptions and approximations which are always art of any formulation of the theory. In treating he thermochemistry of propellants, however, a more ccurate equation of state must be used. Extended reatments of the thermochemistry of propellants re given in References 1 and 5.

It is standard practice in the formulation of nterior ballistic theory to assume an equation of tate of the simple covolume type. This is an equaion of state of the Van der Waals type with the *a*" term omitted but not the "*b*" term and is nown as the Abel equation of state. For a gas beying such an equation of state, the internal nergy depends only on the temperature and not n the density. The Abel equation is expressed as

$$P(V - \eta) = nRT \qquad (1\text{-}5)$$

n interior ballistics it is usually written in terms f a unit weight of gas, so that V and η have dimenions volume per unit weight and n is the number f moles per unit weight. Many authors also define ? as the gas constant per unit weight so that n does not appear explicitly in the equation. R so defined is not constant unless n is also.

If T_0 is the adiabatic flame temperature, the energy released by the decomposition of unit weight of propellant, called the "force" of the propellant, although it has the dimensions of energy per unit weight, i.e., length, is defined by

$$F = nRT_0 \qquad (1\text{-}6)$$

The force can be determined experimentally by burning a charge of propellant in a closed chamber (i.e., at constant volume) and measuring the maximum pressure produced and using Equation 1-5, along with suitable cooling corrections. To do this requires a knowledge of η which can be determined simultaneously by firing a series of charges of different masses and measuring the corresponding maximum pressures.

Table 1-1 includes values of the force for a number of standard and experimental gun propellants. Force and other thermodynamic parameters of propellants can be calculated theoretically if the necessary thermochemical data are available. Results of extended calculations of this sort are given in Reference 11. The subject is also covered briefly in Reference 9.

During the operation of the gun, the gas is produced at temperature, T_0, and falls to a lower temperature, T, due to the loss of heat to the tube and the performance of work during the expansion. The change in internal energy per unit mass of gas can be expressed as $\bar{C}_v(T_0 - T)$ where $\bar{C}_v$ is an average value of the specific heat of the gas at constant volume averaged over the temperature range, $(T_0 - T)$. This energy is used in heating the gun and in imparting kinetic energy to the projectile, the gas, and moving parts of the weapon. The quantity $\bar{C}_v T_0$ is called the specific energy or potential of the propellant.

It is assumed in interior ballistics that the average specific heat at constant volume, $\bar{C}_v$, bears the same relation to ρ, the gas constant, as the specific heat at constant volume for a perfect gas does, so that it may be stated $nR = \bar{C}_v(\gamma - 1)$. However, γ is not now the actual ratio of specific heats, but is analogous to it, its value being adjusted for best fit to the theory used. In effect, $\bar{C}_v$ is replaced by $nR/\gamma - 1$. Then, from Equation 1-6, if E denotes the potential, $\bar{C}_v T_0$

$$E = \frac{F}{\gamma - 1} \qquad (1\text{-}7)$$

E represents effectively the total energy available

* "Cool" propellants may be defined roughly as those or which the uncooled explosion temperature is not greater han 3000° K.

Preceding page blank

from unit mass of propellant. It is equal approximately to the internal energy of unit mass of the propellant gas at the adiabatic flame temperature, T_0, which is given by $\int_0^{T_0} C_v\, dT$.

The equation of state of the gas in the gun is written as

$$P(U_v - c\eta) = cnRT \tag{1-8}$$

where c is the mass of propellant burned, equal to the mass of gas, and U_v is the actual volume of the gas. Actually the pressure is not uniform throughout the mass of gas, nor is the temperature, so both P and T are unknown average values consistent with the equation as written, and P, U_v, c and T are rapidly varying functions of the time. η and n are also variable, but less so, so that average values can be used.

If it is assumed that the internal energy, I, of the gas can be represented by $c\bar{C}_v T$ with sufficient accuracy, then

$$I = \frac{P(U_v - c\eta)}{\gamma - 1} \tag{1-9}$$

and the general energy equation of interior ballistics can be written

$$\frac{cF}{\gamma - 1} = \frac{P(U_v - c\eta)}{\gamma - 1} + K \tag{1-10}$$

where K is the energy expended by the gas in the doing of work and in heat conducted to the gun.

REFERENCES

1. AMCP 706-250, Engineering Design Handbook, *Guns—General.*
2. J. Corner, *Theory of the Interior Ballistics of Guns*, John Wiley & Sons, N. Y., 1950.
3. F. R. W. Hunt, *Internal Ballistics*, Philosophical Library, Inc., N. Y., 1951.
4. A. A. Bennett, *Tables for Interior Ballistics*, War Dept. Document No. 2039, 1921. Revision and expansion directed by H. P. Hitchcock, BRL Report No. 993, 1956 and BRL Technical Note No. 1298, 1960.
5. W. C. Taylor and F. Yagi, *A Method for Computing Interior Ballistic Trajectories in Guns for Charges of Arbitrarily Varying Burning Surface*, BRL Report No. 1125, 1961.
6. C. F. Curtiss and J. W. Wrench, Jr., *Interior Ballistics, A Consolidation and Revision of Previous Reports*, Interior Ballistics I to VII, National Defense Research Committee Report No. A-397, DDC Document No. ATI 24855.
7. AMCP 706-247, Engineering Design Handbook, *Design for Projection.*
8. AMCP 706-252, Engineering Design Handbook, *Gun Tubes.*
9. AMCP 706-175, Engineering Design Handbook, *Solid Propellants, Part One.*
10. Jerome M. Frankle and Jones R. Hudson, *Propellant Surface Area Calculations for Interior Ballistic Systems*, BRL Memorandum Report No. 1187, 1959.
11. Paul G. Baer and Kenneth R. Bryson, *Tables of Computed Thermodynamic Properties of Military Gun Propellants*, BRL Memorandum Report No. 1338, 1961.

CHAPTER 2

LIST OF SYMBOLS

A	Area of the cross section of the bore, in^2
A	Area of the cross section of a nozzle, in^2
A_l	Leakage area, in^2
a	Acceleration, in/sec^2
a	Throat area of nozzle, in^2
a_0	Sonic velocity in gas, in/sec
B	Burning rate coefficient, $in/sec\text{-}P^n$
B	Momentum index, dimensionless
C	Weight of the propellant, lb
C_0	Weight of propellant for ideal rifle, lb
C_T	Thrust coefficient, dimensionless
c	Weight of propellant burnt, lb
c_v	Specific heat at constant volume, in-lb/12 slugs-°K
d	Caliber of the gun, diameter of the projectile body, in
E	Specific energy of the propellant, in-lb/lb
E_0	Standard specific energy of the propellant, in-lb/lb
e	Ballistic efficiency, dimensionless
F	Specific force of the solid propellant, in-lb/lb
F_e	Engraving force, lb
F_T	Thrust force, lb
f	Similarity factor, dimensionless
f	Momentum factor, dimensionless
f	Heat loss ratio, dimensionless
g	Gravitational acceleration, in/sec^2
I	Internal energy of the gas, in-lb
I_x	Axial moment of inertia of the projectile, $lb\text{-}in\text{-}sec^2$
K	Work done by the gas, in-lb
k	Axial radius of gyration of the projectile, in
k	Leakage factor, dimensionless
ℓ	Reduced chamber length, dimensionless
M	Effective mass of the projectile, 12 slugs
M_1	Modified effective mass of the projectile, 12 slugs
m	Log. 10 (approximately 2.3026)
m	Momentum of gun, lb-sec
N	Angular velocity of the projectile, rad/sec
N	Proportion of the propellant that is in a recoilless rifle in gaseous form, dimensionless
n	Lead of rifling, dimensionless
P	Space average pressure, lb/in^2
p	P/π, dimensionless
$\bar{p}$	Reduced pressure, dimensionless
Q	Heat loss, in-lb
q	Quickness (Bennett), dimensionless
q	Rate of flow, $lb/in^2\text{-}sec$
q_1	Empirical quickness factor, $(in^3/lb)^{\frac{1}{2}}$
R	Weight of gun and recoiling parts, lb
R	Gas constant, in-lb/lb-°K
r	Linear rate of regression, in/sec
r	Ratio of actual to tabular velocity, dimensionless
r	Ballistic parameter, dimensionless
r_1	Empirical velocity factor, $(lb/in^3)^{\frac{1}{2}}$
S	Surface area of the grains, in^2
s	Space ratio (expansion), dimensionless
T	Energy of the fraction of the charge burned, in-lb
T	Temperature, °K
T'	Ratio of the gas temperature at any time after burnt to the mean value during burning, dimensionless
T_0	Adiabatic flame temperature, °K
t	Time, sec
$\bar{t}$	Reduced time, dimensionless
$\bar{t}$	Dimensionless time
U	Free volume, in^3
U	Volume from nozzle throat to base of projectile in recoilless rifles, in^3
U_{ch}	Chamber volume, in^3
U_g	Volume of the propellant gas, in^3
u	Specific volume of the solid propellant, in^3/lb
u_g	Specific volume of the gas, in^3/lb
u_w	Specific volume of water: 27.68 in^3/lb
V	Velocity of the projectile, in/sec
V_1	Leakage velocity coefficient, in/sec
V_r	Velocity of the recoiling parts of the gun and carriage, in/sec
V_s	Sonic velocity in air, in/sec
$\bar{V}$	Dimensionless projectile velocity
$\bar{V}$	Average projectile velocity after burnt, in/sec
v	Velocity of gas, in/sec
W	Weight of the projectile, lb
W_e	Effective projectile weight (Strittmater), lb
W'	Effective projectile weight, lb (Mayer and Hart; and Bennett)
w	Web thickness, in
X	Travel of the projectile, in
X	Axial coordinate of the projectile, in

X Dimensionless travel

x Volume expansion ratio: V_m/V_0, dimensionless

η Ratio of muzzle pressure to peak pressure: P_m/P_p, dimensionless

ε Piezometric efficiency, dimensionless

α Burning rate exponent (assumed = 0.8)

α Differential coefficient: $(C\partial V_m)/(V_m\partial C)$, dimensionless

α_0 Escape speed of gas, in/sec

α_1 Differential coefficient: $(C\partial P_p)/(P_p\partial C)$, dimensionless

β Burning rate coefficient (linear law), in/lb-sec

β Differential coefficient: $(V_{ch}\partial V_m)/(V_m\partial V_{ch})$, dimensionless

β_1 Differential coefficient: $(V_{ch}\partial P_p)/(P_p\partial V_{ch})$, dimensionless

γ Ratio of specific heats of the gas (assumed effective value: 1.30)

γ Differential coefficient: $(X_m\partial V_m)/(V_m\partial X_m)$, dimensionless

$\bar{\gamma}$ Ratio of specific heats of the gas, adjusted to take account of loss of heat to the gun, dimensionless

Δ Density of loading, specific gravity of loading, dimensionless

δ Differential coefficient: $(\Delta\partial V_m)/(V_m\partial\Delta)$, dimensionless

δ Pidduck-Kent constant, dimensionless

δ_1 Differential coefficient: $(\Delta\partial P_p)/(P_p\partial\Delta)$, dimensionless

ϵ Interior ballistic parameter, in-lb

ζ Interior ballistic parameter: $\psi aw/\beta C\lambda^{\frac{1}{2}}$, dimensionless

η Specific covolume of the gas, in^3/lb

η Differential coefficient: $(W\partial V_m)/(V_m\partial W)$, dimensionless

η_1 Differential coefficient: $(W\partial P_p)/(P_p\partial W)$, dimensionless

θ Factor accounting for rotational energy and frictional resistance (assumed value: 0.05)

κ Fraction of total energy available to projectile: Katsanis factor, dimensionless

κ Differential coefficient $(w\partial V_m)/(V_m\partial w)$, dimensionless

κ_1 Differential coefficient: $(w\partial P_p)/(P_p\partial w)$, dimensionless

λ Differential coefficient: $(E\partial V_m)/(V_m\partial E)$, dimensionless

λ_1 Differential coefficient: $(E\partial P_p)/(P_p\partial E)$, dimensionless

$\mu(\omega)$ Pressure function, dimensionless

μ Ratio of throat area to bore area: A_t/A, dimensionless

$\nu(\omega)$ Travel function, dimensionless

ξ Dependent variable: $\omega/(dK/dT)$, dimensionless

π Pressure factor, lb/in^2

ρ Specific weight of propellant, lb/in^3

σ Ballistic parameter: $F\rho SB/A(\gamma - 1)$, dimensionless

$\tau(\omega)$ Time function, dimensionless

τ Time unit, sec

ϕ Independent variable: log (T/E), dimensionless

ϕ Proportion of the propellant burned, dimensionless

ψ Ballistic parameter, function λ, dimensionless

ω Dependent variable $(K/T)^{\frac{1}{2}}$, dimensionless

Subscripts

0 Initial value: when $t = 0$

1 Characteristic of fast propellant in dual granulation charge

2 Characteristic of slow propellant in dual granulation charge

a Of atmosphere

b At end of burning: "burnt" value

c Chamber value: at breech

e At nozzle exit

i Either 1 or 2

m Muzzle value: when base of projectile is at muzzle

n Nozzle opening

p At peak or theoretical maximum

r In reservoir

r Space maximum at any instant

s At base of projectile

t Tabulated value (Bennett)

t At nozzle throat

CHAPTER 2

THEORY AND PRACTICE OF INTERIOR BALLISTICS

2-1 INTRODUCTION

There are numerous systems of interior ballistics. Different ballisticians have formulated the theory in various ways. Their systems, if they are not purely empirical, do not differ essentially since they are treatments of the same thermodynamical and mechanical phenomenon. They differ in the simplifying assumptions made, that is, mainly in degree of complexity and sophistication of treatment and in the details of the mathematical procedures. For many practical problems, very simple formulations are adequate and these are much used. However, with the widespread and increasing availability of high speed automatic computers the more complicated formulations can be used without too much expenditure of time and effort.

There are five general equations which are used in the formulations of interior ballistic theory. They are: (1) the equation of state of the propellant gases; (2) the equation of energy; (3) the equation of motion; (4) the burning rate equation; and (5) the equation of the form function. The first two of these are related, as the first is involved in the formulation of the second; therefore, only four equations are basic to any particular formulation of the theory.

The form of the equation of state of the propellant gases generally used in interior ballistics has been discussed in Chapter 1 and is given in Equation 1-8. The equation has been shown, by experience, to be sufficiently accurate for the purpose.

The equation of energy has also been discussed in Chapter 1 and its form is given in Equation 1-10. The equation of energy is a statement of how the energy released by the combustion of the propellant is distributed during the operation of the gun.

The equation of motion is the formulation of Newton's second law as applicable to the interior ballistic problem. It relates the forces due to the gas pressure to the acceleration of the projectile.

The burning rate equation takes account of the rate at which new gas is being generated in the gun by the combustion of the charge. This rate is assumed to be a function only of the pressure, under which the combustion takes place, and the area of the reacting surface. The form of the equation used here is given in Equation 1-2.

If the reacting surface is not constant, it is necessary to introduce the form function to account for the effect of the changing burning surface on the rate of generation of gas in the gun. Except for very degressive granulations, the assumption of constant burning surface is generally sufficiently accurate and this assumption is made in the explicit treatments which follow.

2-2 STATEMENT OF THE EQUATIONS

2-2.1 The Energy Equation

There is presented here first the formulation due to Taylor[1]. The fundamental units used in the Taylor system are the inch, pound (weight) and second. This makes mass a derived unit with dimensions weight over gravitational acceleration. With the length unit the inch, the unit of mass is equal to 12 slugs.

The energy equation may be stated simply as

$$T = K + I \tag{2-1}$$

where

- T is the energy released by the amount of charge which has been burned
- K the work done by the gas, plus energy lost by heating the barrel
- I the internal energy of the gas

By Equation 1-10

$$T = \frac{cF}{\gamma - 1} \tag{2-2}$$

where F is now defined as the energy per unit weight of propellant (specific force) and by Equation 1-9

$$I = \frac{P(U_g - c\eta)}{\gamma - 1} \tag{2-3}$$

where U_g is the volume occupied by the gas. K, the work done by the propellant gas, consists of several parts.

a. The principal part is the translational kinetic

energy of the projectile, equal to $WV^2/2g$ where W is the weight of the projectile, V its velocity and g the gravitational acceleration.

b. Treating the gases and unburned propellant as a fluid consisting of the gases and burning solid grains thoroughly mixed, and supposing the tube to be cylindrical (that is, neglecting chambrage), an approximation of Lagrange in which the density of the fluid is assumed independent of position may be used for ordinary velocities. Then the velocity of this fluid increases linearly from 0 at the breech to V at the base of the projectile; the average velocity is $V/2$, and the mean square velocity is $V^2/3$. Hence, the kinetic energy of the unburned propellant and the gas is $CV^2/6g$, where C is the weight of the propellant charge.

c. The projectile, propellant, and recoiling parts of the gun and carriage may be considered a system whose initial momentum is zero and remains so providing there is no recoil mechanism or shoulder of the user to prevent free recoil. Under this assumption, if R is the weight of the recoiling parts and $-V_r$ their velocity, the momentum equation is

$$\frac{1}{g}(WV + CV/2 - RV_r) = 0 \qquad (2\text{-}4)$$

whence

$$V_r = \frac{(W + C/2)V}{R} \qquad (2\text{-}5)$$

Therefore, in free recoil, the kinetic energy of the recoiling parts is

$$\frac{(W + C/2)^2V^2}{2gR} \qquad (2\text{-}5a)$$

For standard weapons, the ratio $(W + C/2)/R$ is of the order of 0.02. The energy of recoil is, therefore, a very small fraction of K. The recoil velocity is much less than that given by Equation 2-5; as the energy is absorbed in cannon by the recoil mechanism. In nonautomatic small arms fire the energy is transferred to the body of the man firing the weapon. The energy of recoil can be neglected without serious effect.

d. The rotational kinetic energy of the projectile is

$$\frac{I_xN^2}{2} \qquad (2\text{-}6)$$

where

I_x is the axial moment of inertia and
N is the angular velocity.

The axial moment of inertia may be expressed as

$$I_x = k^2\frac{W}{g} \qquad (2\text{-}6a)$$

where

k is the axial radius of gyration

The angular velocity is

$$N = 2\pi V/nd \qquad (2\text{-}7)$$

where

n is the lead or twist of rifling in calibers, that is, the number of calibers in which the land makes one complete turn and

d is the caliber

By substitution, it is found that

$$\frac{I_xN^2}{2} = \left(\frac{2\pi k}{nd}\right)^2\frac{WV^2}{2g} \qquad (2\text{-}8)$$

For most guns, n is between 18 and 32 calibers, say 25. For a solid cylinder, $(k/d)^2$ is 0.125; but for high explosive projectiles, it is about 0.14. Therefore, the factor $(2\pi k/nd)^2$ is approximately 0.01.

e. The work done against the frictional resistance to the motion of the projectile, including the engraving of the rotating band, is equal to a small proportion of the translational kinetic energy, say

$$\frac{\theta_1WV^2}{2g}$$

If θ_1 is taken to be constant, this is equivalent to assuming that the resistance is proportional to the pressure. The value of θ_1 is usually of the order of 0.04.

f. The heat transferred from the hot gas to the gun is denoted by Q. Adding the contributions *a.* to *f.*

$$K = \frac{WV^2}{2g} + \frac{CV^2}{6g} + \frac{(W + C/2)^2V^2}{2gR} + \left(\frac{2\pi k}{nd}\right)^2\frac{WV^2}{2g} + \frac{\theta_1WV^2}{2g} + Q \qquad (2\text{-}9)$$

Equation 2-9 is complicated but can be simplified in the following manner. Drop the third term on the right as negligible, and let

$$\theta = (2\pi k/nd)^2 + \theta_1 \qquad (2\text{-}10)$$

In the calculations, θ will be taken equal to 0.05. Also, let an "effective" mass be defined as

$$M = \frac{(1 + \theta)W + C/3}{g} \qquad (2\text{-}11)$$

Then, if Q is neglected or accounted for in some other manner, K takes the simple form

$$K = \frac{MV^2}{2} \tag{2-12}$$

It is customary to take account of the heat loss Q by adjusting the value of γ upward so that the estimated total available energy of the gas is reduced. The effect of the heat loss is to reduce the kinetic energy produced by the gas and has an effect similar to an increase in the effective mass. Assuming that the effect can be taken account of by simply increasing the effective mass by a constant factor,

$$Q = f\frac{MV^2}{2} \tag{2-13}$$

Then, omitting the covolume term for simplicity

$$\frac{1}{\gamma - 1}(eF - PU_g) = \frac{MV^2}{2}(1 + f),$$

and if $\bar{\gamma}$ is the adjusted value of γ

$$\frac{1}{\bar{\gamma} - 1}(eF - PU_g) = \frac{MV^2}{2}$$

so that

$$\frac{\bar{\gamma} - 1}{\gamma - 1} = 1 + f \tag{2-14}$$

In practice f is about 0.15 but may be considerably larger than this especially in small arms. To take account of heat loss then, one simply substitutes the value of $\bar{\gamma}$ for γ wherever the latter occurs. Taylor assumed an adjusted value of γ equal to 1.30. In what follows it will be assumed that γ has been adjusted so that, in the subsequent text, γ represents the adjusted value, unless the heat loss, Q, occurs explicitly in the equation. For more detailed discussion of the heat loss problem, see References 2 and 6, also Corner[3], page 141.

The internal energy of the propellant gas is then expressed as

$$I = \frac{P(U_g - c\eta)}{\gamma - 1} = \frac{PU}{\gamma - 1} \tag{2-15}$$

where

- P is an average pressure consistent with the equation of state and
- U_g the volume occupied by the gas

The complete expression for the free volume is

$$U = AX + U_{ch} - Cu + cu - c\eta \tag{2-16}$$

where

- A is the area of the cross section of the bore
- X the travel of the projectile
- U_{ch} the chamber volume
- u the specific volume of the solid propellant and
- η the specific covolume of the gas.

Initially $X = 0$, the free volume is then

$$U_0 = U_{ch} - Cu + c_0(u - \eta) \tag{2-17}$$

where c_0 is the weight of the small amount of charge burned before start of projectile motion. Substituting U from Eq. 2-16 in Eq. 2-15 the equation for the internal energy of the gas is

$$I = \frac{P}{\gamma - 1}[AX + U_{ch} - Cu + c(u - \eta)] \tag{2-18}$$

The specific volume of the propellant (u) is about 17.5 in^3/lb. The specific covolume (η) (the volume apparently occupied by the molecules in a unit weight of gas) is approximately 27.7 in^3/lb. The specific covolume of the gas is thus about 1.5 times the specific volume of the solid propellant. It is assumed here that they are equal, $\eta = u$ for the sake of simplicity. This assumption is often made in interior ballistics, but its validity becomes questionable for high ratios of charge to chamber volume.

With this assumption, Equation 2-17 becomes

$$U_0 = U_{ch} - Cu \tag{2-17a}$$

and from Eqs. 2-16 and 2-18

$$U = U_0 + AX \tag{2-16a}$$

$$I = \frac{P}{\gamma - 1}(AX + U_{ch} - Cu) \tag{2-18a}$$

Substituting from Equations 2-2, 2-12 and 2-18a in Equation 2-1 the energy equation becomes

$$\frac{Fc}{\gamma - 1} = \frac{MV^2}{2} + \frac{P}{\gamma - 1}(AX + U_{ch} - Cu) \tag{2-19}$$

2-2.2 The Equation of Motion

The equation of motion expresses the relation between the acceleration of the projectile and the pressure on its base, P_s. Since the unburned propellant and the gas are being accelerated along with the projectile and there is also friction at the bore surface, there is a pressure gradient in the gas. The result is that the average pressure, P, occurring in Equation 2-19 is not the same as the base pressure, P_s. Furthermore, it is customary to measure the pressure in a gun at a location at or near the breech. To solve the equations theoretically and to express

the result in terms of the measured pressure, P_c, some assumption must be made concerning the relations between the different pressures. An assumption commonly used is that

$$P_c : P : P_s = 1 + \frac{C}{2(1+\theta)W} : 1 + \frac{C}{3(1+\theta)W} : 1 \tag{2-20}$$

This relation is an approximation based on a special solution of the Lagrange problem which is discussed more fully in Chapter 5. Its use is restricted to artillery weapons firing at moderate velocities. When applied to treatments of high velocity weapons or to small arms, it yields poor results. Using Equations 2-11 and 2-20

$$P_s = \frac{(1+\theta)W}{(1+\theta)W + C/3} P = \frac{(1+\theta)W}{Mg} P \tag{2-21}$$

If the friction of the bore surface is neglected, the equation of motion of the projectile is

$$AP_s = \frac{(1+\theta)W}{g} \frac{dV}{dt} \tag{2-22}$$

Substituting Eq. 2-21 in Eq. 2-22, gives

$$AP = M \frac{dV}{dt} \tag{2-23}$$

which expresses the equation of motion in terms of the average pressure and the effective mass, M, given by Equation 2-11.

Since

$$V = \frac{dX}{dt} \tag{2-24}$$

the equation of motion may be written

$$AP = MV \frac{dV}{dX} \tag{2-25}$$

2-2.3 The Burning Rate Equation

The burning has been described in Chapter 1. The area of the burning surface, which is here assumed constant, may be calculated by the formula

$$S = \frac{2C}{\rho w} \tag{2-26}$$

where

S is the surface area of the propellant grains
w the web thickness and
ρ the specific weight of the propellant, that is, the weight per unit volume.

The rate of regression of the surface is assumed to be uniform over the entire surface. Propellant gas is evolved at a rate

$$\frac{dc}{dt} = \rho SBP^{\alpha} \tag{2-27}$$

where

B is the burning rate coefficient and
α is the burning rate pressure exponent, which is here assumed to be 0.8.

B should be determined for each type of propellant under actual conditions of use; that is, by adjusting its value for best fit of the theory to actual firing records. B is frequently determined from closed chamber measurements but these values usually yield poor results when used in gun calculations because the conditions in the gun are very different from those in the closed chamber. The closed chamber values are, however, of great value in determining relative burning rates of different types and lots of propellant.

2-2.4 Elimination of Variables

The preceding equations involve about a dozen variables. By straightforward manipulation, they can be reduced to three equations involving only four variables: K, P, X and T. T will be treated as the independent variable. Differentiating Equation 2-12, gives

$$dK = MV\,dV \tag{2-28}$$

By substitution in Eq. 2-25.

$$dK = AP\,dX \tag{2-29}$$

Since $A\,dX = dU$ by differentiation of Eq. 2-16a

$$dK = P\,dU \tag{2-30}$$

Finally, since $dX = V\,dt$ by definition

$$dK = APV\,dt \tag{2-31}$$

The right members of these four equations are all equal. Furthermore, by differentiating Eq. 2-1,

$$dT = dK + dI \tag{2-32}$$

Now, by Eqs. 2-2 and 2-31,

$$\frac{dK}{dT} = \frac{APV\,dt}{F\,dc/(\gamma - 1)} \tag{2-33}$$

which, by Eq. 2-27, may be expressed

$$\frac{dK}{dT} = \frac{(\gamma - 1)APV}{F\rho SBP^{\alpha}} \tag{2-34}$$

Defining a constant

$$\sigma = \frac{F\rho SB}{A(\gamma - 1)} \tag{2-35}$$

and substituting Eq. 2-12, Equation 2-34 becomes

$$\frac{dK}{dT} = \sqrt{\frac{2K}{M}}\frac{P^{1-\alpha}}{\sigma} \tag{2-36}$$

Combining Eqs. 2-32 and 2-36

$$1 = \sqrt{\frac{2K}{M}}\frac{P^{1-\alpha}}{\sigma} + \frac{dI}{dT} \tag{2-37}$$

Substituting Eq. 2-30 in the differential of Eq. 2-15 gives

$$dI = \frac{dK}{\gamma - 1} + \frac{U\,dP}{\gamma - 1} \tag{2-38}$$

Combining the last three equations yields

$$\gamma - 1 = \gamma\sqrt{\frac{2K}{M}}\frac{P^{1-\alpha}}{\sigma} + \frac{U\,dP}{dT} \tag{2-39}$$

Eliminating I from Eqs. 2-1 and 2-15

$$U = \frac{(T - K)(\gamma - 1)}{P} \tag{2-40}$$

Substituting this in Eq. 2-39 and rearranging produces

$$\frac{dP}{dT} = \frac{P}{(\gamma - 1)(T - K)}\left[\gamma - 1 - \gamma\sqrt{\frac{2K}{M}}\frac{P^{1-\alpha}}{\sigma}\right] \tag{2-41}$$

Eliminating U from Eqs. 2-16a and 2-40 gives

$$U_0 + AX = \frac{(T - K)(\gamma - 1)}{P} \tag{2-42}$$

Equations 2-36 and 2-41 form a system of two first order differential equations in K and P with T as independent variable, and Eq. 2-42 relates X to these variables.

2-3 SOLUTION OF THE EQUATIONS

2-3.1 Reduction to Normal Form

Let the system of equations that was just derived be rewritten:

$$\frac{dK}{dT} = \sqrt{\frac{2K}{M}}\frac{P^{1-\alpha}}{\sigma} \tag{2-36}$$

$$\frac{dP}{dT} = \frac{P}{(\gamma - 1)(T - K)}\left[\gamma - 1 - \gamma\sqrt{\frac{2K}{M}}\frac{P^{1-\alpha}}{\sigma}\right] \tag{2-41}$$

$$U_0 + AX = \frac{(T - K)(\gamma - 1)}{P} \tag{2-42}$$

In order to obtain solutions which are compatible with observed results, initial conditions must be imposed that represent gun conditions as closely as feasible. The resistance to the motion of the projectile during the engraving of the rotating band is much greater than it is at any later stage. Closer agreement between computed and observed results is frequently obtained at small cost in added complexity by imposing an added resistance corresponding to engraving resistance, which prevents the projectile from moving until the pressure reaches a certain value, P_0, called the starting pressure. This has already been taken into account in that a resistance proportional to pressure varies somewhat like a combination of engraving resistance and later bore friction, being large in the early stage and small later.

The initial conditions are then

$$V = 0, \quad K = 0, \quad P = P_0, \quad X = 0,$$

$$T = T_0 = \frac{U_0 P_0}{\gamma - 1}, \quad U = U_0 \tag{2-43}$$

where

U_0 is the initial free volume as given by Equation 2-17a namely,

$U_0 = U_{ch} - Cu$ and T_0 (the adiabatic flame temperature) is derived from Equation 2-43.

In order to facilitate the solution of this system by machine methods, three new variables, ϕ, ω and ξ are defined by the following relations:

$$T = \epsilon 10^{\phi} \tag{2-44}$$

$$\omega = \sqrt{K/T} \tag{2-45}$$

$$\frac{\omega}{\xi} = \frac{dK}{dT} \tag{2-46}$$

where ϵ is a constant to be defined later (Eq. 2-61) and ϕ is the new independent variable.

In accordance with these definitions,

$$\frac{d\omega}{d\phi} = \frac{m}{2}\left(\frac{1}{\xi} - \omega\right) \tag{2-47}$$

where m = log. 10 (approximately 2.3026).

Eliminating dK/dT from Eqs. 2-36 and 2-46, and differentiating logarithmically, produces

$$\frac{d\omega}{\omega} - \frac{d\xi}{\xi} = (1 - \alpha)\frac{dP}{P} + \frac{1}{2}\frac{dK}{K} \tag{2-48}$$

Using Eqs. 2-41 and 2-45, this may be expressed

$$-\frac{d\xi}{\xi} = \frac{dT}{T}\left\{\frac{1}{2} + \frac{1-\alpha}{1-\omega^2}\left[1 - \frac{\gamma}{\gamma-1}\sqrt{\frac{2K}{M}}\frac{P^{1-\alpha}}{\sigma}\right]\right\} \tag{2-49}$$

Finally, using Eqs. 2-36, 2-46 and 2-44, this becomes

$$\frac{1}{m\xi}\frac{d\xi}{d\phi} = -\left\{\frac{1}{2} + \frac{1-\alpha}{1-\omega^2}\left[1 - \frac{\gamma}{\gamma-1}\frac{\omega}{\xi}\right]\right\} \tag{2-50}$$

From Eqs. 2-46, 2-36 and 2-45, there results

$$\frac{1}{\xi} = \frac{1}{\omega}\frac{dK}{dT} = \frac{P^{1-\alpha}}{\omega\sigma}\sqrt{\frac{2K}{M}} = \sqrt{\frac{2K}{M}}\frac{P^{1-\alpha}}{\sigma}\sqrt{\frac{T}{K}} \tag{2-51}$$

Let $T \to T_0$ and $\xi \to \xi_0$ when $\omega \to 0$; then $P \to P_0$ and

$$\xi_0 = \sqrt{\frac{M}{2}}\frac{\sigma}{P_0^{1-\alpha}\sqrt{T_0}} \tag{2-52}$$

Substituting T_0 from Eq. 2-43, this becomes

$$\xi_0 = \sqrt{\frac{M}{2}}\frac{\sigma\sqrt{\gamma-1}}{P_0^{1-\alpha}\sqrt{U_0P_0}} \tag{2-53}$$

Since, by definition,

$$\sigma = \frac{F\rho SB}{A(\gamma-1)}$$

this may be written

$$\xi_0 = \frac{1}{\sqrt{2(\gamma-1)}}\frac{\rho SBF}{A}\sqrt{\frac{M}{U_0}}\left[\frac{1}{P_0}\right]^{(3-2\alpha)/2} \tag{2-54}$$

Let

$$\Pi = \left[\frac{\rho SBF}{A}\sqrt{\frac{M}{U_0}}\right]^{2/(3-2\alpha)} \tag{2-55}$$

and substitute in Eq. 2-54,

$$\xi_0 = \frac{1}{\sqrt{2(\gamma-1)}}\left[\frac{\Pi}{P_0}\right]^{(3-2\alpha)/2} \tag{2-56}$$

Next define

$$p = \frac{P}{\Pi}, \quad \text{so that} \quad p_0 = \frac{P_0}{\Pi} \tag{2-57}$$

and let

$$\phi_0 = \log p_0 = \log\frac{P_0}{\Pi} \tag{2-58}$$

From Eqs. 2-44 and 2-43,

$$T_0 = \epsilon 10^{\phi_0} = \frac{U_0P_0}{\gamma-1} \tag{2-59}$$

This gives

$$\phi_0 = \log\frac{U_0P_0}{\epsilon(\gamma-1)} \tag{2-60}$$

Identifying this with Eq. 2-58, produces, from Eq. 2-55

$$\epsilon = \frac{\Pi U_0}{\gamma-1} = \frac{U_0}{\gamma-1}\left[\frac{\rho SFB}{A}\sqrt{\frac{M}{U_0}}\right]^{2/(3-2\alpha)} \tag{2-61}$$

or, from Eq. 2-35

$$\epsilon = U_0^{(2-2\alpha)/(3-2\alpha)}M^{1/(3-2\alpha)}(\gamma-1)^{(2\alpha-1)/(3-2\alpha)}\sigma^{2/(3-2\alpha)} \tag{2-62}$$

Also from Eqs. 2-56 and 2-58 it follows that

$$\log\xi_0 = -\tfrac{1}{2}\log 2(\gamma-1) - \frac{3-2\alpha}{2}\phi_0 \tag{2-63}$$

Thus the system of Equations 2-36, 2-41 and 2-42 has been changed into the normal form

$$\frac{d\omega}{d\phi} = \frac{m}{2}\left(\frac{1}{\xi} - \omega\right) \tag{2-47}$$

$$-\frac{d\xi}{d\phi} = m\xi\left\{\frac{1}{2} + \frac{1-\alpha}{1-\omega^2}\left[1 - \frac{\gamma}{\gamma-1}\frac{\omega}{\xi}\right]\right\} \tag{2-50}$$

$$\log\xi_0 = -\tfrac{1}{2}\log 2(\gamma-1) - \frac{3-2\alpha}{2}\phi_0 \tag{2-63}$$

Here, the independent variable is

$$\phi = \log(T/\epsilon) \tag{2-44a}$$

where ϵ is defined by Eq. 2-61, and the dependent variables are

$$\omega = \sqrt{K/T} \tag{2-45}$$

$$\xi = \omega\frac{dT}{dK} \tag{2-46}$$

The numerical solution of the normal form and its use in computing trajectory data will be discussed next. After that, some simple methods of estimating trajectory data will be given, and the effects of variations in the parameters will be explained.

2-3.2 Numerical Integration of the Normal Form

The system of equations in normal form represents a one-parameter family of trajectories. The parameter is the initial value ϕ_0 of the independent variable ϕ. This system has been integrated numerically by computer for values of ϕ_0 ranging from -2.5 to $+1.8$. It was observed that the set of curves for ϕ_0 less than -2.5 tends asymptotically to the solution for the case of zero starting pressure, which may be called the "limiting trajectory". From the solutions working charts have been constructed.

2-3.3 Interior Ballistic Trajectories During Burning

The principal problem of interior ballistic theory is to determine the pressure history and the travel of the projectile in the gun. To obtain this information, the pressure, P, and the velocity, V, as functions of the time, t, or travel, X, are needed, and also X as a function of t. This may be obtained from the trajectories, which are conveniently divided into two phases: (1) during burning and (2) after burning. The first phase will now be considered.

From Equation 2-12, the work done by the gas is expressed as

$$K = \frac{MV^2}{2}$$

Combining this with the definitions in Eqs. 2-44 and 2-45, yields

$$V/\omega = \sqrt{2\epsilon/M}\,10^{\phi/2} \tag{2-64}$$

From Eqs. 2-36, 2-46 and 2-12,

$$\frac{V}{\omega} = \frac{\sigma}{\xi P^{1-\alpha}} \tag{2-65}$$

Equating the right members and simplifying gives

$$P^{1-\alpha} = \frac{\sigma}{\xi}\sqrt{\frac{M}{2\epsilon}}\,10^{-\phi/2} \tag{2-66}$$

If the values of P are calculated for a fixed $\phi = \phi_0$ trajectory, the point at which the peak pressure, P_p, occurs can be located. By taking values from all the trajectories, P_p can be obtained as a function of the normal variables ω and ξ.

In Equation 2-40 the free volume was expressed as

$$U = \frac{(T - K)(\gamma - 1)}{P}$$

Substituting the values of T, K and P from Equations 2-44, 2-45 and 2-66 makes

$$U = \frac{(1 - \omega^2)(\gamma - 1)\epsilon 10^{\phi}}{\left[\frac{\sigma}{\xi}\sqrt{\frac{M}{2\epsilon}}\,10^{-\phi/2}\right]^{1/(1-\alpha)}} \tag{2-67}$$

As can be seen from Equation 2-16a,

$$X = \frac{U - U_0}{A}$$

Hence,

$$X = \frac{(1-\omega^2)\epsilon^{(3-2\alpha)/(2-2\alpha)}10^{(3-2\alpha)/(2-2\alpha)\phi}(\gamma - 1)}{A\left[\frac{\sigma}{\xi}\sqrt{\frac{M}{2}}\right]^{1/(1-\alpha)}} - \frac{U_0}{A} \tag{2-68}$$

For $\alpha = 0.8$ and $\gamma = 1.30$, this becomes

$$X = \frac{1.6968(1 - \omega^2)\epsilon^{3.5}10^{3.5\phi}\xi^5}{A\sigma^5 M^{2.5}} - \frac{U_0}{A} \tag{2-68a}$$

Equations 2-64 and 2-68 give V and X as functions of ϕ. These quantities can be obtained by routine calculation. However, the computation of pressure and time can be facilitated by the use of a reduced pressure and a reduced time.

2-3.4 Reduced Variables

The reduced pressure, $\tilde{p}$, is defined by the formula

$$\tilde{p} = (\xi 10^{\phi/2})^{1/(1-\alpha)} \tag{2-69}$$

Then Eq. 2-66 becomes

$$P = \frac{\left[\sigma\sqrt{M/2\epsilon}\right]^{1/(1-\alpha)}}{\tilde{p}} \tag{2-70}$$

or, using the definitions of σ and ϵ, Equations 2-35 and 2-61

$$P = \frac{2^{1/[2(\alpha-1)]}(\gamma - 1)^{(1-2\alpha)/[2(1-\alpha)]}\epsilon}{U_0\tilde{p}} \tag{2-71}$$

For $\alpha = 0.8$ and $\gamma = 1.30$, Equations 2-69 and 2-71 become

$$\tilde{p} = (\xi 10^{\phi/2})^5 \tag{2-69a}$$

and

$$P = 1.076\,\frac{\epsilon}{U_0\tilde{p}} \tag{2-71a}$$

By Equation 2-2 the released energy is

$$T = \frac{cF}{\gamma - 1}$$

and by Equation 2-27 the rate of burning is

$$\frac{dc}{dt} = \rho SBP^{\alpha}$$

Substituting the derivative of T from Equation 2-2 and using the definition of σ from Equation 2-35 leads to

$$dT = A\sigma P^{\alpha}\,dt \tag{2-72}$$

By differentiation of Equation 2-44

$$dT = m\epsilon 10^{\phi}\,d\phi \tag{2-73}$$

where $m = \log_e 10$

Equating the right members gives

$$dt = \frac{m\epsilon 10^{\phi}}{AP^{\alpha}\sigma}\,d\phi \tag{2-74}$$

The reduced time is defined by the formula

$$\bar{t} = \int_{\phi_0}^{\phi} \xi^{\alpha/(1-\alpha)} 10^{(2-\alpha)/[2(1-\alpha)]\phi}\, d\phi \qquad (2\text{-}75)$$

Then, with the help of Eq. 2-66 the integral of Eq. 2-74 may be expressed

$$t = \frac{m}{A}\left[\frac{2}{M}\right]^{\alpha/[2(1-\alpha)]} \frac{\epsilon^{(2-\alpha)/[2(1-\alpha)]}}{\sigma^{1/1-\alpha}}\, \bar{t} \qquad (2\text{-}76)$$

For $\alpha = 0.8$,

$$\bar{t} = \int_{\phi_0}^{\phi} 10^{3\phi}\xi^{4}\, d\phi \qquad (2\text{-}75a)$$

$$t = \frac{4\epsilon^3 m}{A\sigma^5 M^2}\, \bar{t} \qquad (2\text{-}76a)$$

2-3.5 Pressure Ratio Chart

The ratio of initial pressure, P_0, to peak pressure, P_p, as a function of

$$p_0 = \frac{P_0}{\Pi}$$

where Π is defined by Equation 2-55 is shown in Chart 2-1. This chart permits a determination of P_p, the theoretical maximum pressure, to be expected for any choice of starting pressure for any given gun, propellant and projectile system.

2-3.6 Interior Ballistic Trajectory Charts

On Charts 2-2a, -2b and -2c several sets of curves give data from the interior ballistic trajectories. The abscissa is ω and the ordinate is log ξ.

ϕ_0-trajectories are solid curves, starting with the labeled values of ϕ and showing the coordinates along each trajectory. (Chart 2-2a)

ϕ-curves are dashed curves joining the points of constant ϕ on all trajectories. The value of ϕ on each of these curves is the labeled value. (Chart 2-2a)

P_p-curve crosses all trajectories at the points where the pressure is a maximum. (Chart 2-2a)

$\bar{t}$-curves join points of constant reduced time on each trajectory, and are so labeled. (Chart 2-2b)

$\bar{p}$-curves join points of constant reduced pressure on each trajectory. They are labeled with the values of log $\bar{p}$. (Chart 2-2c)

The charts reproduced here are for illustration purposes only. For use in calculations they should be reproduced on a much larger scale.

The use of the trajectory charts is as follows. Estimate a starting pressure, which depends on the gun and projectile. Bennett[4] assumed a value of 2500 psi for his tables, but it may be anywhere from 1000 to 5000 psi. Compute U_0, M, S, σ and ϵ from Equations 2-17a, 2-11, 2-26, 2-35 and 2-62, respectively. Setting $\gamma = 1.30$ and $\alpha = 0.8$ the latter two equations become

$$\sigma = \frac{\rho SBF}{0.3A} \qquad (2\text{-}35a)$$

and

$$\epsilon = [0.027 U_0^2 M^3 \sigma^{10}]^{1/7} \qquad (2\text{-}62a)$$

Then compute

$$\phi_0 = \log \frac{U_0 P_0}{0.3\epsilon} \qquad (2\text{-}60a)$$

This identifies the ϕ_0 trajectory (the set of values of ω, ξ and ϕ along the solid line from $\phi = \phi_0$ on Chart 2-2a) which is applicable until the end of burning. If "burnt" values are denoted by the subscript b, ϕ becomes

$$\phi_b = \log \frac{FC}{0.3\epsilon} \qquad (2\text{-}77)$$

The intersection of the ϕ-curve for $\phi = \phi_b$ (dotted line on Chart 2-2a) and the ϕ_0-trajectory indicates the point on the trajectory at which the charge was all burned, that is the point $(\omega_b, \xi_b, \phi_b)$.

The intersections of the $\bar{p}$-curves and the $\bar{t}$-curves with the ϕ_0-trajectory give the values of the reduced pressure and reduced time. (To do this using the three Charts 2-2a, 2-2b and 2-2c requires that the ϕ_0 trajectory be transposed from Chart 2-2a to Chart 2-2b for $\bar{t}$, and to Chart 2-2c for $\bar{p}$.) (The three charts have been combined into one so that this transposition is not necessary. The combined chart however, is complicated and hard to read unless made very large. A combined chart was produced on a large scale at Ballistic Research Laboratories and copies can be obtained. A reduced copy is published in Reference 1.) Then the pressure and time can be computed by Equations 2-71a and 2-76a. In particular, the "burnt" values, $\bar{p}_b$ and $\bar{t}_b$, can be found. Also, the peak pressure, P_p, can be calculated from $\bar{p}_p$, which is the value of $\bar{p}$ at the intersection of the P_p-curve (Chart 2-2a) and the ϕ_0-trajectory. P_p is the theoretical peak pressure which is not necessarily the same as the actual maximum pressure. It will be the same only if the charge does not burn out before P_p is reached, that is, the time to reach the theoretical peak pressure must be less than the time to burnt. If this is not the case, the actual maximum pressure is the pressure at burnt, P_b.

After ϕ_b has been calculated from Eq. 2-77, ω_b has been obtained from Chart 2-2a, and P_b has been computed, the free volume, U_b, the travel, X_b and the velocity, V_b, at "burnt" can be calculated by

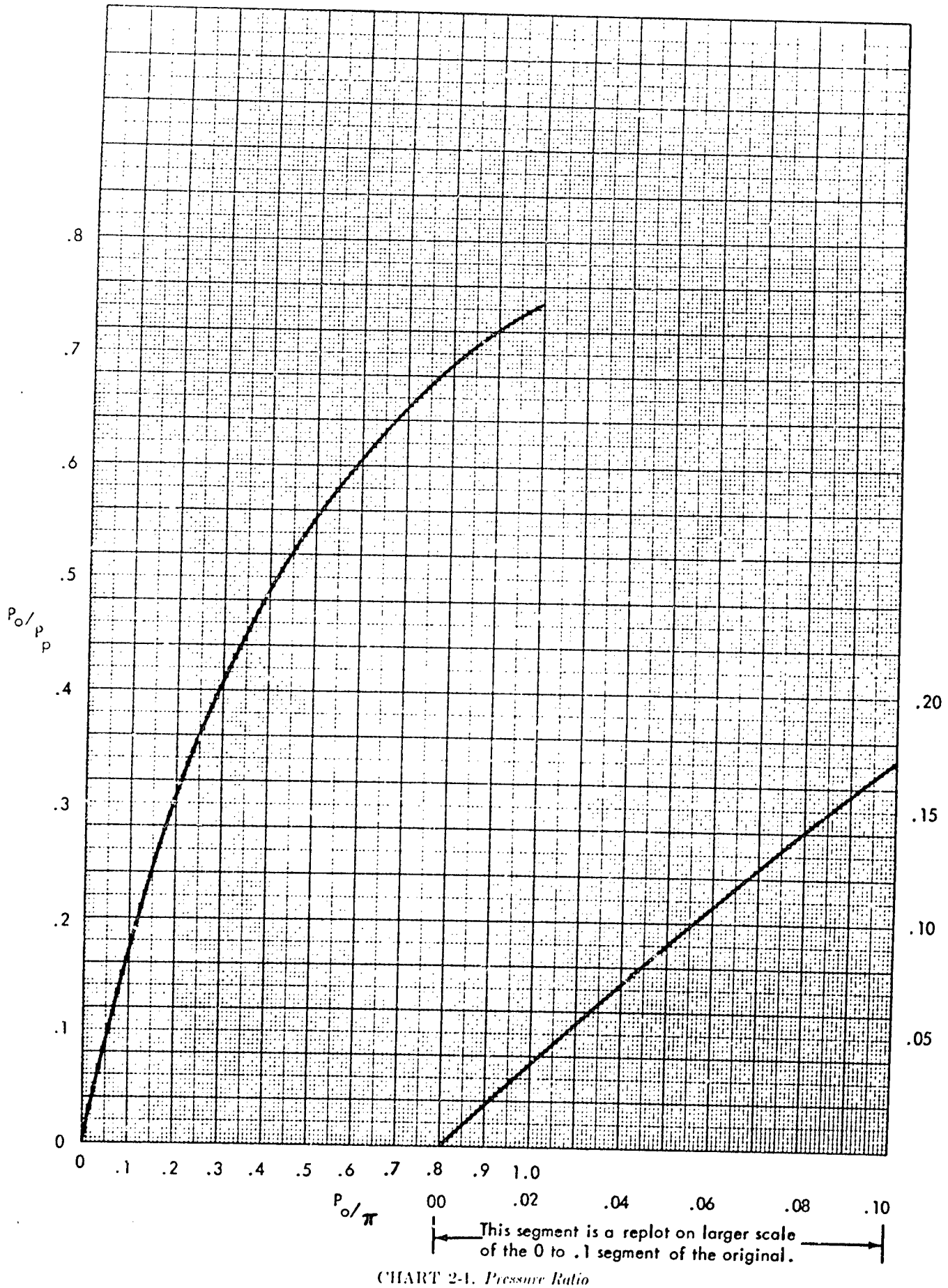


CHART 2-1. *Pressure Ratio*

CHART 2-2a. INTERIOR BALLISTICS
TRAJECTORIES

(Located in the back of this handbook)

CHART 2-2b. INTERIOR BALLISTICS
TRAJECTORIES

(Located in the back of this handbook)

Preceding page blank

CHART 2-2c. INTERIOR BALLISTICS
TRAJECTORIES

(Located in the back of this handbook)

Preceding page blank

the formulas

$$U_b = \frac{(1 - \omega_b^2)FC}{P_b} \tag{2-78}$$

$$X_b = \frac{U_b - U_0}{A} \tag{2-79}$$

$$V_b = \omega_b \sqrt{\frac{2\epsilon}{M}}\, 10^{\epsilon/2} \tag{2-80}$$

2-3.7 Conditions After Burnt

After all the propellant is burned, $c = C$. With this substitution, Equation 2-2 shows that the released energy is

$$T = \frac{FC}{\gamma - 1} = \text{constant} \tag{2-81}$$

As before, the work done by the gas is, Equation 2-12

$$K = \frac{MV^2}{2}$$

and the internal energy is, Equation 2-15

$$I = \frac{PU}{\gamma - 1}$$

Hence, the energy equation may be expressed

$$FC = PU + \frac{\gamma - 1}{2} MV^2 \tag{2-82}$$

Taking differentials produces,

$$0 = P\,dU + U\,dP + (\gamma - 1)MV\,dV \tag{2-83}$$

By Equations 2-28 and 2-30

$$MV\,dV = P\,dU \tag{2-84}$$

so that

$$\frac{dP}{P} = -\gamma \frac{dU}{U} \tag{2-85}$$

Integrating with P_b and U_b as initial values, yields

$$PU^\gamma = P_b U_b^\gamma \tag{2-86}$$

Since the right member is a constant, the expansion is adiabatic; actually, the value of γ is adjusted to account for the loss of heat.

From Equations 2-40 and 2-45, the energy equation may also be expressed

$$PU = (\gamma - 1)(1 - \omega^2)T \tag{2-87a}$$

At burnt,

$$P_b U_b = (\gamma - 1)(1 - \omega_b^2)T_b \tag{2-87b}$$

But after burnt, $T = T_b$, so that

$$\frac{1 - \omega^2}{1 - \omega_b^2} = \frac{PU}{P_b U_b} \tag{2-88}$$

Then, by Eq. 2-86

$$\frac{1 - \omega^2}{1 - \omega_b^2} = \left[\frac{U}{U_b}\right]^{1-\gamma} \tag{2-89}$$

Hence

$$U = \frac{U_b}{(1 - \omega_b^2)^{1/(1-\gamma)}} [1 - \omega^2]^{1/(1-\gamma)} \tag{2-90}$$

Substituting Eqs. 2-90 and 2-81 in Eq. 2-87a, gives

$$P = [1 - \omega_b^2]^{1/(1-\gamma)} \frac{FC}{U_b} [1 - \omega^2]^{\gamma/(\gamma-1)} \tag{2-91}$$

By Eqs. 2-82 and 2-86,

$$V^2 = \frac{2}{(\gamma - 1)M} (FC - P_b U_b^\gamma U^{1-\gamma}) \tag{2-92}$$

Using Eqs. 2-81, 2-87b and 2-90, produces

$$V = \sqrt{\frac{2FC}{(\gamma - 1)M}}\, \omega \tag{2-93}$$

The travel is, from Equation 2-16a

$$X = \frac{U - U_0}{A}$$

From Equation 2-23

$$dt = \frac{M}{AP}\, dV$$

With t_b and V_b as initial values, the integral of this is

$$t = t_b + \frac{M}{A} \int_{V_b}^{V} \frac{dV}{P} \tag{2-94}$$

Substituting Eqs. 2-91 and 2-93 in Eq. 2-94, gives

$$t = t_b + \frac{U_b}{A} \sqrt{\frac{2M}{(\gamma - 1)FC}} [1 - \omega_b^2]^{1/(\gamma-1)} \cdot \int_{\omega_b}^{\omega} \frac{d\omega}{[1 - \omega^2]^{\gamma/(\gamma-1)}} \tag{2-95}$$

2-3.8 Time, Pressure and Travel Functions

To facilitate the determination of time, pressure and travel after burnt, Chart 2-3 has curves of the following functions of ω:

$$\tau(\omega) = \int_0^{\omega} (1 - \omega^2)^{-13/3}\, d\omega \tag{2-96}$$

$$\mu(\omega) = (1 - \omega^2)^{13/3} \tag{2-97}$$

$$\nu(\omega) = (1 - \omega^2)^{-10/3} \tag{2-98}$$

Using these functions with $\gamma = 1.30$, Equations 2-95, 2-91 and 2-90 may be expressed

$$t = t_b + \frac{U_b}{A\nu(\omega_b)} \sqrt{\frac{2M}{0.3FC}} [\tau(\omega) - \tau(\omega_b)] \tag{2-99}$$

$$P = \frac{FC\nu(\omega_b)}{U_b} \mu(\omega) \tag{2-100}$$

$$U = \frac{U_b}{\nu(\omega_b)} \nu(\omega) \tag{2-101}$$

Then X can be calculated by Eq. 2-16a and V by Eq. 2-93, with $\gamma = 1.30$.

Preceding page blank

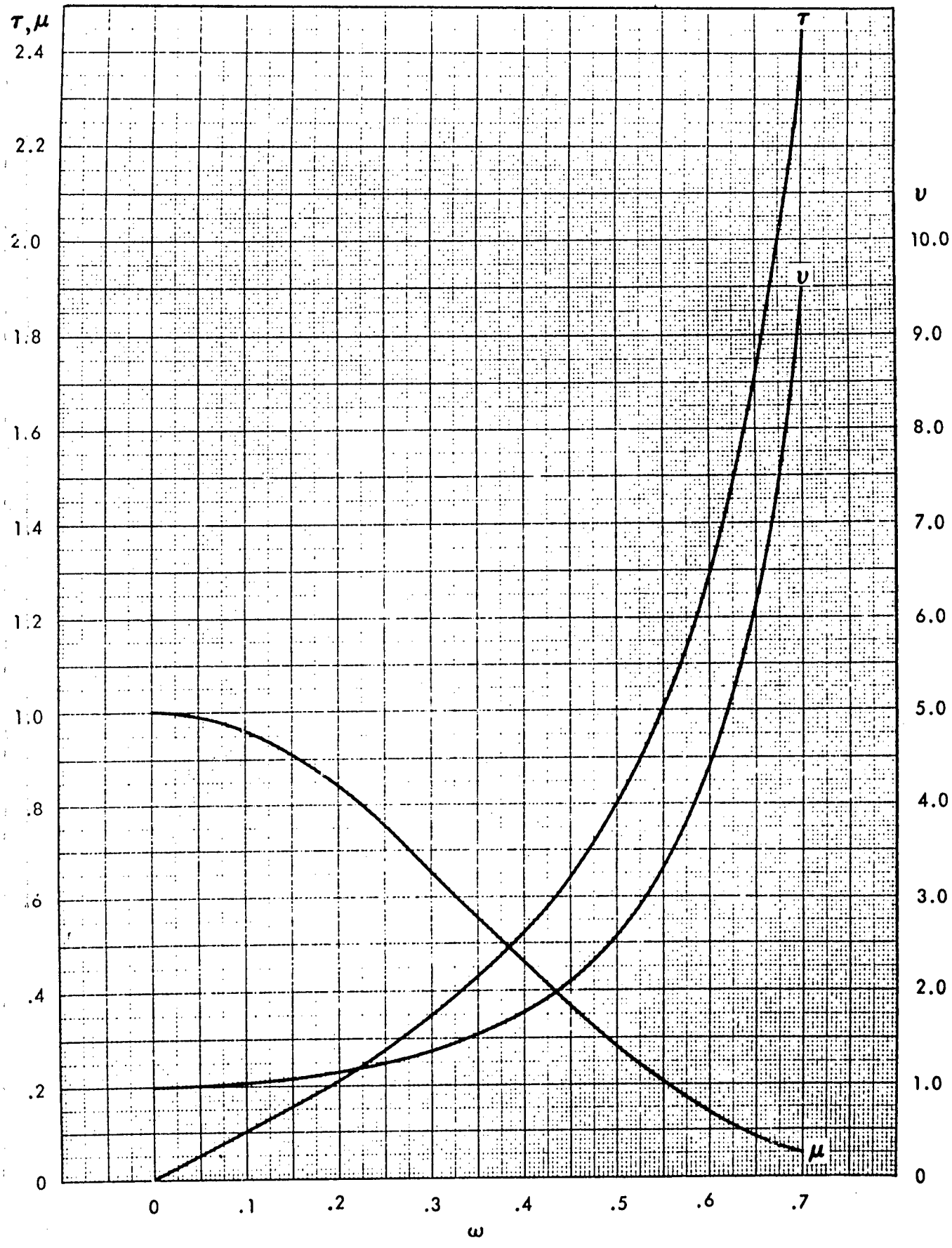


CHART 2-3. *Time, Pressure and Travel Functions*

These equations apply from the position at burnt, denoted by the subscript, b, to the muzzle, denoted by the subscript, m. If X_m is known, V_m can be found,

$$V_m = V_0 + AX_m \qquad (2\text{-}102)$$

and then

$$\nu(\omega_m) = \frac{V_m}{V_b}\nu(\omega_b) \qquad (2\text{-}103)$$

then ω_m can be determined from the chart.

Finally, t_m, P_m and V_m can be calculated as explained above. In practice V_m is divided by 12 to obtain the muzzle velocity in feet per second.

2-3.9 Examples

a. Determine the maximum pressure; the time, pressure and travel at burnt; and the time, pressure and velocity at the muzzle for the 105mm Howitzer M4, firing the High Explosive Projectile M1, propelled by 10 ounces of multiperforated propellant M1 lot _____*.

* A "lot" of propellant, is the product of one set of manufacturing operations such that its characteristics are essentially uniform, or a combination of such products obtained by blending so that the grains are thoroughly mixed and statistical uniformity among charges may be expected, even though slight variations exist among individual grains. The manufacturer furnishes the characteristics of each lot.

Characteristic	Symbol	Value	Unit	Remarks
Area of bore	A	13.4	in^2	Given
Chamber volume	V_{ch}	153.8	in^3	Given
Travel (to muzzle)	X_m	80.4	in	Given
Weight of projectile	W	33.0	lb	Given
Starting pressure	P_0	4000	psi	Given
Weight of propellant	C	0.625	lb	Given
Burning rate coefficient	B	0.0011	$\frac{\text{in/sec}}{(\text{psi})^{0.8}}$	Given
Force of propellant	F	3.73×10^6	in-lb/lb	Given
Specific weight†	ρ	0.0571	lb/in^3	Given
Web thickness	w	0.0140	in	Given
Friction factor	θ	0.05		Given
Adjusted ratio of specific heats	$\bar{\gamma}$	1.30		Given
Burning surface	S	1564	in^2	Eq. 2-26
Initial free volume	V_0	142.9	in^3	Eq. 2-17a
Effective mass	M	0.0903	12 slugs	Eq. 2-11
Constant	σ	9.115×10^4		Eq. 2-35
Constant	ϵ	5.384×10^6		Eq. 2-62a
ϕ_0-trajectory	ϕ_0	−0.451		Eq. 2-60a
ϕ-curve	ϕ_b	0.160		Eq. 2-77
Abscissa of intersection	ω_b	0.323		Chart 2-2a
Ordinate of intersection	$\log \xi_b$	0.056		Chart 2-2a
Reduced time curve	$\bar{t}_b$	1.87		Chart 2-2b
Reduced pressure curve	$\log \bar{p}_b$	0.670		Chart 2-2c
Reduced peak pressure curve	$\log \bar{p}_p$	0.660		Charts 2-2a, -2c
Maximum pressure	P_p	8870	psi	Eq. 2-71a
Pressure at burnt	P_b	8665	psi	Eq. 2-71a
Time at burnt	t_b	3.91×10^{-3}	sec	Eq. 2-76a
Free volume at burnt	V_b	240.9	in^3	Eq. 2-78
Travel at burnt	X_b	7.31	in	Eq. 2-79
Free volume at muzzle	V_m	1220	in^3	Eq. 2-102
Travel function	$\nu(\omega_b)$	1.435		Chart 2-3
Travel function	$\nu(\omega_m)$	7.27		Eq. 2-103
Abscissa	ω_m	0.670		Chart 2-3
Time function	$\tau(\omega_m)$	1.970		Chart 2-3
Time function	$\tau(\omega_b)$	0.380		Chart 2-3
Pressure function	$\mu(\omega_m)$	0.075		Chart 2-3
Time at muzzle	t_m	14.02×10^{-3}	sec	Eq. 2-99
Pressure at muzzle	P_m	1040	psi	Eq. 2-100
Velocity at muzzle	V_m	8789	in/sec	Eq. 2-93
Velocity at muzzle	V_m	732	ft/sec	Eq. 2-93

† The manufacturer customarily gives the specific gravity of the propellant. To obtain the specific weight in pounds per cubic inch, this must be divided by the specific volume of water, which is 27.68 in^3/lb.

If desired, the foregoing process can be repeated for selected values of ϕ less than ϕ_b, and selected values of ω between ω_b and ω_m. Interpolated values of time, pressure, travel and velocity corresponding to the selected points can then be determined from which pressure-time, pressure-travel and velocity-travel curves can be drawn. Figure 2-1 is the pressure-time curve for the preceding example.

b. Determine the weight of the same lot of propellant that will give a maximum pressure of 10,000 psi in the same gun, firing the same projectile as in the first example (par. 2-3.9*a*), and compute the resulting muzzle velocity.

For this example, some of the formulas need revision. First, equate the right members of Equations 2-58 and 2-60, and obtain

$$\epsilon = \frac{U_0 P_0}{0.3 p_0} \qquad (2\text{-}104)$$

Also, Equation 2-62a may be expressed

$$\sigma = \left[\frac{\epsilon^7}{0.027 U_0^2 M^5}\right]^{1/10} \qquad (2\text{-}105)$$

Finally, combining Equations 2-26 and 2-35 yields

$$C' = \frac{0.15 w A}{FB}\,\sigma \qquad (2\text{-}106)$$

Since $P_0 = 4{,}000$ psi, $P_0/P_p = 0.400$. Entering Chart 2-1 with this ratio, find $p_0 = 0.2935$.

Now, a trial and error method should be used. Using an estimated value of C, compute U_0 and M as in the first example then calculate ϵ, σ and C' by the formulas above. If the two values of C are not the same, use the calculated C as the second estimate, and repeat the calculations. If necessary, repeat again. When both values agree, this gives the desired maximum pressure; the muzzle velocity can then be found as in the first example.

Since 0.625 pound of propellant gave a maximum pressure of 8,870 psi, C' must be greater in the present problem. Paragraph 2-9 will explain how this increase can be estimated; however, for the present, a charge of 0.800 pound will be assumed.

The following tables give the results of the computations.

Thus, a charge of 0.709 pound will give a maximum pressure of 10,000 psi and a muzzle velocity of 780 fps.

c. Determine the weight and web thickness of a charge of M1 propellant that will give a maximum pressure of 15,000 psi and a muzzle velocity of 1000 fps in the same gun, firing the same projectile as in the preceding examples.

C' (est)	0.800	0.704	0.709
U_0	139.8	141.5	141.5
M	0.09047	0.09036	0.09039
ϵ	6.351×10^6	6.428×10^6	6.424×10^6
σ	1.027×10^5	1.034×10^5	1.033×10^5
C' (calc.)	0.704	0.709	0.709

ϕ_0	−0.532
ϕ_b	0.137
ω_b	0.319
log p_0	0.69
P_b	9080
U_b	238.0

U_m	1220
$\nu(\omega_b)$	1.43
$\nu(\omega_m)$	7.33
ω_m	0.670
$V_m/_{12}$	780

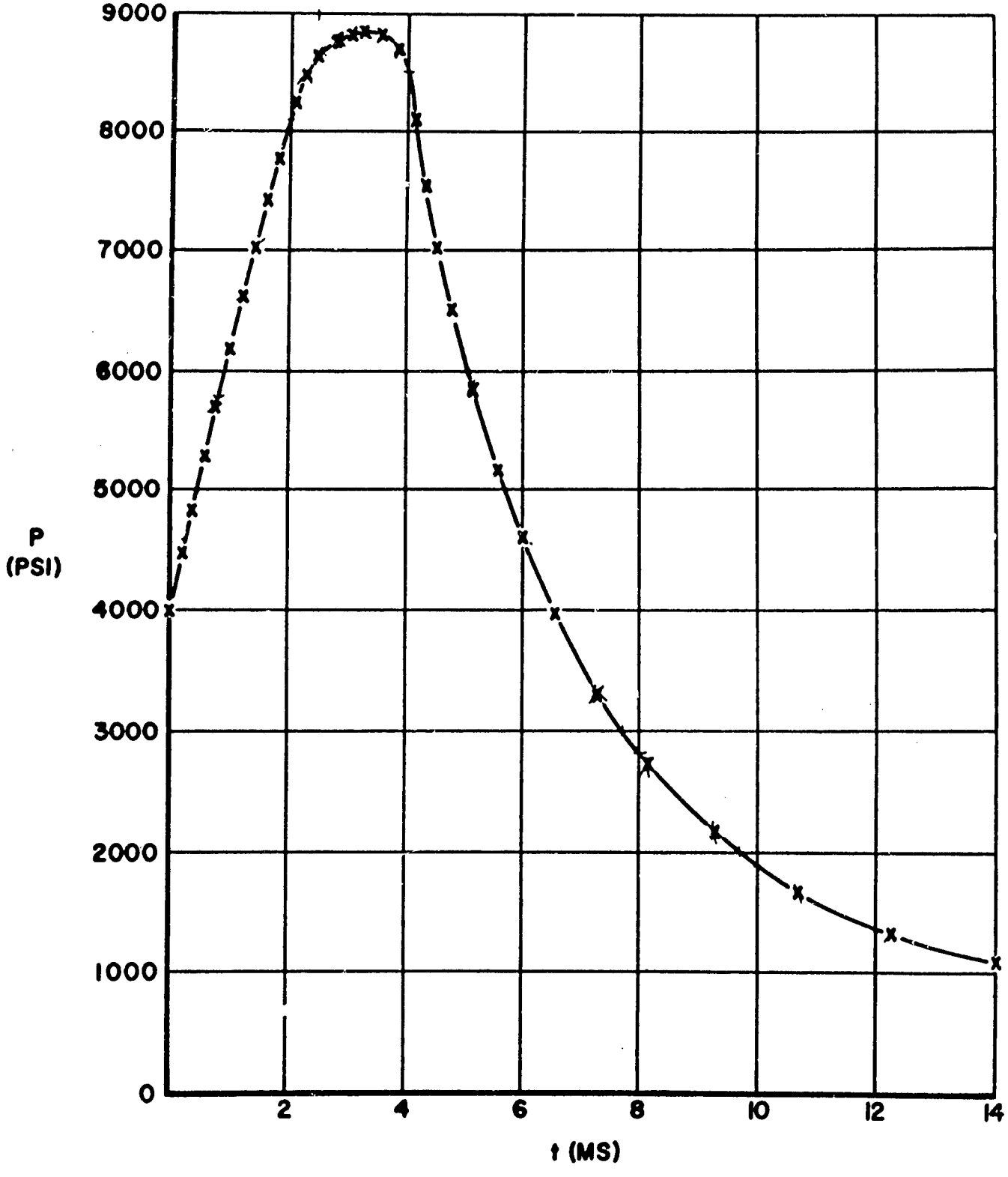


FIGURE 2-1. *Theoretical Pressure-Time Curve for 105mm Howitzer Using Taylor's Theory.*

Solving Equation 2-106 for w gives

$$w = \frac{FBC}{0.15A\sigma} \qquad (2\text{-}106a)$$

Entering Chart 2-1 with the ratio $P_0/P_p = 0.2667$, find $p_0 = 0.170$.

Assume a series of values of C; calculate ϵ, σ and w by Equations 2-104, 2-105 and 2-106a; and compute the muzzle velocity as in the first example. The value of C that will produce a muzzle velocity of 1000 fps and the corresponding web thickness can then be found by interpolation. The results of such a calculation are tabulated below.

Charge, lb	Web thickness, in	Muzzle Velocity, fps
1.000	.0137	927
1.100	.0152	969
1.200	.0167	1004
1.188*	.0165*	1000

* Interpolated.

d. When the HE Projectile M1 was propelled by 1 pound of propellant M1 with a web thickness of 0.0140 inch in the 105mm Howitzer M4, a maximum pressure of 14,200 pounds per square inch and a muzzle velocity of 920 feet per second were observed. Adjust the values of the factor θ and the burning rate coefficient, B, so that the calculated results will agree with the observed ones.

With the known values of P_0 and P_p, Chart 2-1 can be used to find p_0. With this value of p_0, ϵ can be computed by Equation 2-104. Then ω_b and $\log \tilde{p}_b$ can be found with the help of Chart 2-2c, and ω_m with the help of Chart 2-3. With the known value of V_m, the adjusted value of M can be computed by the formula

$$M = \frac{\omega_m^2 FC}{0.15 V_m^2} \qquad (2\text{-}107)$$

Solving Equation 2-11 for θ, gives

$$\theta = \frac{Mg - C/3}{W} - 1 \qquad (2\text{-}11b)$$

Using the adjusted values of ϵ and M, σ can be calculated by Equation 2-105. Finally, solving Equation 2-106 for B, yields

$$B = \frac{0.15Aw\sigma}{FC} \qquad (2\text{-}106b)$$

Thus the factor θ, which accounts for rotational energy and frictional resistance, is 0.062 instead of the assumed value 0.050; the burning rate coefficient, B, is 0.00106, which is practically the same as the closed chamber value, 0.00110.

The results of these computations are given below.

Symbol	Value	Remarks
A	13.4	Given
U_{ch}	153.8	Given
X_m	80.4	Given
W	33.0	Given
P_0	4000	Given
C	1.00	Given
F	3.73×10^6	Given
ρ	0.0571	Given
w	0.0140	Given
P_p	14,200	Given
V_m	11,040	Given
P_0/P_p	0.2817	
p_0	0.183	Chart 2-1
ϕ_0	−0.738	Eq. 2-58
U_0	136.3	Eq. 2-17a
ϵ	9.93×10^6	Eq. 2-104
ϕ_b	0.0975	Eq. 2-77
ω_b	0.320	Chart 2-2a
$\log \xi_b$	0.102	Chart 2-2a
$\log \tilde{p}_b$	0.747	Chart 2-2c
$\log \tilde{p}_p$	0.737	Charts 2-2a, -2c
P_p	14,360	Eq. 2-71a
P_b	14,040	Eq. 2-71a
U_b	239	Eq. 2-78
U_m	1214	Eq. 2-102
$\nu(\omega_b)$	1.42	Chart 2-3
$\nu(\omega_m)$	7.21	Eq. 2-103
ω_m	0.670	Chart 2-3
M	0.0916	Eq. 2-107
θ	0.062	Eq. 2-11b
σ	1.402×10^5	Eq. 2-105
B	0.00106	Eq. 2-106b

2-3.10 Dual Granulation Charges

In some guns, especially howitzers and mortars, two or more charges are used so as to obtain various muzzle velocities and thus vary the angle of fall. The lowest velocity is obtained with a base charge; and the higher velocities, by adding increments.

The same velocity can be obtained with different types of propellant or different web thicknesses by adjusting the weight of charge. A charge with a faster burning rate or a smaller web thickness will produce a higher pressure along the first part of the travel, and therefore a higher maximum pressure, and a lower pressure along the latter part of the travel, including the muzzle. It has been found that the round-to-round dispersion in muzzle velocity for a given charge is large when the max-

imum pressure is very low. Therefore, it is desirable to use a fast propellant for the low velocities. However, the use of such a fast propellant at the high velocities is likely to make the maximum pressure exceed the pressure that the gun can stand without damage.

This difficulty could be solved by using fast propellant throughout for the low charges and slow propellant throughout for the high charges. However, it is more feasible to use fast propellant for the base charge and low increments, and slow propellant for the additional increments. For howitzers, it is customary to use small, single-perforated grains for the low charges and add increment charges of large, multiperforated grains for the high charges. More than two granulations could be used, but this is not customary.

The fundamental theory is the same for dual granulation as for single granulation, but some of the equations have to be modified to make them applicable to dual granulation. It is here assumed that both kinds of propellant are ignited at the same time, but the faster propellant is burnt sooner than the slower propellant.

The subscript 1 will be used to refer to the characteristics of the fast propellant, or to the trajectory during the simultaneous burning of both propellants. The subscript 2 will be used to refer to the characteristics of the slow propellant, or to the trajectory during the burning of the slow propellant alone. The subscript i will denote either 1 or 2.

The characteristics of the gun and projectile are the same as before: the area of the cross section of the bore, A; the chamber volume, U_{ch}; the travel, X (X_m at the muzzle); weight of the projectile, W; and starting pressure, P_0. The characteristics of the propellants are: the burning rate coefficient, B_i; the force, F_i; the specific weight, ρ_i; and the web thickness, w_i.

Obviously, the total charge is

$$C = C_1 + C_2 \tag{2-108}$$

The surface area of the grains may be calculated by the formula

$$S_i = 2C_i/\rho_i w_i \tag{2-109}$$

The initial free volume is

$$U_0 = U_{ch} - \left(\frac{C_1}{\rho_1} + \frac{C_2}{\rho_2}\right) \tag{2-110}$$

As before,

$$M = \frac{1.05W + C/3}{386}$$

While both propellants are burning, the constants

$$\sigma_1 = \frac{(F\rho SB)_1 + (F\rho SB)_2}{0.3A} \tag{2-111a}$$

and

$$\epsilon_1 = (0.027U_0^2M^5\sigma_1^{10})^{1/7} \tag{2-112a}$$

The trajectory starts at

$$\phi_{a1} = \log \frac{P_0U_0}{0.3\epsilon_1} \tag{2-113}$$

At the burnt position of the fast propellant,

$$\phi_{1b} = \log \frac{F_1C_1[1 + (F\rho SB)_2/(F\rho SB)_1]}{0.3\epsilon_1} \tag{2-114a}$$

On Chart 2-2a, at the intersection of the ϕ_{a1}-trajectory and the ϕ_{1b}-curve, the coordinates ω_{1b} and $\log \xi_{1b}$ are found.

While only the slow propellant is burning,

$$\sigma_2 = \frac{(F\rho SB)_2}{0.3A} \tag{2-111b}$$

The second phase starts at the coordinates ω_{1b} and $\log \xi_{2a}$; and

$$\log \xi_{2a} = \log (\xi_{1b}\sigma_2/\sigma_1) \tag{2-115}$$

On Chart 2-2a, the ϕ_{a2}-trajectory and the ϕ_{2a}-curve that cross this point are found. Then, since the weight of burnt propellant and the pressure are the same at the beginning of the second phase as at the end of the first phase,

$$\epsilon_2 = \epsilon_1(10^{\phi_{1b}}/10^{\phi_{2a}}) \tag{2-112b}$$

At the burnt position of the slow propellant,

$$\phi_{2b} = \log \frac{F_1C_1 + F_2C_2}{0.3\epsilon_2} \tag{2-114b}$$

On Charts 2-2a, -2c at the intersection of the ϕ_{a2}-trajectory and the ϕ_{2b}-curve, ω_{2b} and $\log \bar{p}_{2b}$ are found. At all burnt, then, the pressure is

$$P_{2b} = \frac{1.076\epsilon_2}{U_0\bar{p}_{2b}} \tag{2-116a}$$

and the free volume is

$$U_{2b} = \frac{(1 - \omega_{2b}^2)(F_1C_1 + F_2C_2)}{P_{2b}} \tag{2-117}$$

If the reduced peak pressure curve crosses the used part of either the ϕ_{a1}-trajectory or the ϕ_{a2}-trajectory, the intersection indicates the value of $\bar{p}_{ip}$. Then, the maximum pressure can be calculated by the formula

$$P_p = \frac{1.076\epsilon_i}{U_0\bar{p}_{ip}} \tag{2-116b}$$

If the p_p-curve does not cross either trajectory, P_{2b} is the actual peak pressure.

At the muzzle, the free volume is

$$U_m = AX_m + U_0 \tag{2-102}$$

After finding $\nu(\omega_{2b})$ from Chart 2-3, compute

$$\nu(\omega_m) = \frac{U_m}{U_{2b}} \nu(\omega_{2b}) \qquad (2\text{-}118)$$

and find ω_m from the chart. Then the velocity at the muzzle is

$$V_m = \sqrt{\frac{2(F_1C_1 + F_2C_2)}{0.3M}}\,\omega_m \qquad (2\text{-}119)$$

The modifications of the formulas for time, pressure, velocity, and travel at arbitrary values of ω are obvious; they will not be given here.

2-3.11 Example for Dual Granulation Charges

Determine the maximum pressure and muzzle velocity for the 105mm Howitzer M4, firing the HE Projectile M1, propelled by 2 ounces of single-perforated propellant M8 lot _____ and 8 ounces of multiperforated propellant M1 lot _____.

Characteristic	Symbol	Value	Unit	Remarks
Area of bore	A	13.4	in²	Given
Chamber volume	U_{ch}	153.8	in³	Given
Travel (to muzzle)	X_m	80.4	in	Given
Weight of projectile	W	33.0	lb	Given
Starting pressure	P_0	4000	psi	Given
Charge: M8	C_1	0.125	lb	Given
M1	C_2	0.500	lb	Given
Total	C	0.625	lb	Eq. 2-108
Burning rate coefficient	B_1	0.0025	$\frac{\text{in/sec}}{(\text{psi})^{0.8}}$	Given
	B_2	0.0011		Given
Force	F_1	4.60×10^6	in-lb/lb	Given
	F_2	3.73×10^6	in-lb/lb	Given
Specific weight	ρ_1	0.0571	lb/in³	Given
	ρ_2	0.0571	lb/in³	Given
Web thickness	w_1	0.0040	in	Given
	w_2	0.0140	in	Given
Burning Surface	S_1	1095	in²	Eq. 2-109
	S_2	1251	in²	Eq. 2-109
Initial free volume	U_0	142.9	in³	Eq. 2-110
Effective mass	M	0.00031	12 slugs	Eq. 2-11a
Constant	σ_1	$2\,518 \times 10^5$		Eq. 2-111a
Constant	ϵ_1	2.209×10^7		Eq. 2-112a
ϕ_{a1}-trajectory	ϕ_{a1}	−1.081		Eq. 2-113
ϕ_{1b}-curve	ϕ_{1b}	−0.930		Eq. 2-114a
Abscissa	ω_{1b}	0.023		Chart 2-2a
Ordinate	$\log \xi_{1b}$	0.782		Chart 2-2a
Constant	σ_2	7.291×10^4		Eq. 2-111b
Ordinate	$\log \xi_{2a}$	0.244		Eq. 2-115
ϕ_{a2}-trajectory	ϕ_{a2}	−0.225		Chart 2-2a
ϕ_{2a}-curve	ϕ_{2a}	−0.190		Chart 2-2a
Constant	ϵ_2	4.184×10^6		Eq. 2-112b
ϕ_{2b}-curve	ϕ_{2b}	0.299		Eq. 2-114b
Abscissa	ω_{2b}	0.366		Chart 2-2a
Reduced Pressure	$\log \bar{p}_{2b}$	0.616		Chart 2-2c
Reduced peak pressure	$\log \bar{p}_{2p}$	0.567		Charts 2-2a, -2c
Maximum pressure	P_p	8540	psi	Eq. 2-116b
Pressure at burnt	P_{2b}	7630	psi	Eq. 2-116a
Free volume at burnt	U_{2b}	277	in³	Eq. 2-117
Free volume at muzzle	U_m	1220	in³	Eq. 2-102
Travel function	$\nu(\omega_{2b})$	1.00		Chart 2-3
Travel function	$\nu(\omega_m)$	7.05		Eq. 2-118
Abscissa	ω_m	0.665		Chart 2-3
Velocity at muzzle	V_m	8924	in/sec	Eq. 2-119
Velocity at muzzle	V_m	744	ft/sec	Eq. 2-119

2-4 THE HIRSCHFELDER SYSTEM

In the Hirschfelder System it is assumed that the burning rate is linearly proportional to the pressure, that is, $\alpha = 1$. With this assumption the equations are solvable analytically. Hirschfelder does not assume $\eta = u$ nor that the burning surface is constant. If the burning surface is not constant a fourth equation, the form function equation, is introduced into the system of equations to be solved simultaneously. The form of this equation depends on the shape of the grains and in effect takes account of the change in the burning surface as the web burns away. The system also assumes a starting pressure taken as the pressure produced when one percent of the charge has been consumed. This can be obtained from closed chamber data since until the projectile moves the burning is at constant volume. The Hirschfelder System is covered completely and in detail in Reference 6 of Chapter 1 (Report No. 1) and is presented together with charts and working tables for use in gun design problems. There is also included a discussion of the thermodynamic properties of propellants.

2-5 "SIMPLE" INTERIOR BALLISTIC SYSTEMS

2-5.1 General

By neglecting all, or most, secondary effects which are difficult to evaluate, such as heat and friction losses and starting pressures, and by making all or most of the usual simplifying assumptions, a very simple analytical treatment can be given. Examples of this are the British RD-38 System (Cf. Corner[3]) and the Mayer and Hart System[5]. These systems result in simple analytic formulas for the variables and, if the adjustable parameters are adequately evaluated by numerous comparisons with firing records, can yield results valid to a few percent for standard guns, especially for the larger calibers. They are also useful in that the interrelations between the more important parameters are more obvious than in the more involved systems, so that they allow a more direct feeling for the interrelations to develop.

2-5.2 The Mayer and Hart System

The Mayer and Hart System employs the following simplifying assumptions:

(1) the starting pressure and engraving pressure are zero, that is, the projectile starts to move as soon as the propellant begins to burn;
(2) the covolume of the gas is equal to the original charge volume, that is, $\eta = u$;
(3) the burning rate is linearly proportional to the pressure, that is, $\alpha = 1$;
(4) the burning surface is constant throughout the burning;
(5) all terms in the kinetic energy expression are negligible except those for the kinetic energy of the gas and the projectile; and
(6) energy losses due to friction and heating are also negligible.

Assumptions (5) and (6) do not affect the form of the theory, since the neglected energies are taken account of in practice by adjusting the values of the weight of the projectile and the specific heat ratio, γ, to some effective values. Consistent with the practice of other interior ballistics methods, the kinetic energy of the propellant gas is accounted for by adding one-third of the charge weight to the projectile weight, producing an adjusted projectile weight, W', equal to projectile weight plus $C/3$. The symbol W' will be used in the remainder of this discussion for the adjusted weight. The value of γ may be adjusted according to the judgment or experience of the user. In the preceding method, according to Taylor, an adjusted value of γ of 1.30 is assumed. This value may not be valid in the Mayer and Hart method, because of assumption in the latter method of linear proportionality of the burning rate to the pressure.

In the following, the original notation of Mayer and Hart has been changed to conform to that exhibited in the List of Symbols at the beginning of Chapter 2. Mayer and Hart also introduced numerical factors in their formulas to adjust for the units used. These have been omitted, leaving it to the user to express the quantities in a consistent set of units.

The three fundamental equations are then

$$\frac{dc}{dt} = \frac{2CBP}{w} \tag{2-120}$$

$$PU = cF - (\gamma - 1)\frac{W'}{2g}V^2 \tag{2-121}$$

and

$$\frac{W'}{g}\frac{dV}{dt} = PA \tag{2-122}$$

Mayer and Hart define two ballistic parameters having the dimensions of pressure

$$P_n = \left(\frac{2BCF}{Aw}\right)^2\left(\frac{W'}{gU_0}\right) \tag{2-123}$$

and

$$P_e = \frac{CF}{U_0} \tag{2-124}$$

where U_0 is the initial free volume, equal to the chamber volume minus the volume of the charge. P_e is the pressure which would be developed in the chamber if there were no motion of the projectile. If it is assumed that the pressures occurring in Equations 2-120 and 2-121 are the same, that is, that the pressure drop in the gas can be neglected

$$P\left(\frac{U}{U_0}\right) = P_e\left(\frac{c}{C}\right)\left[1 - \frac{\gamma - 1}{2}\left(\frac{P_e}{P_B}\right)\left(\frac{c}{C}\right)\right] \tag{2-125}$$

and also

$$\frac{U}{U_0} = \left[1 - \frac{\gamma - 1}{2}\left(\frac{P_e}{P_B}\right)\left(\frac{c}{C}\right)\right]^{-2/(\gamma-1)} \tag{2-126}$$

$$\frac{c}{C} = \left[\frac{2P_B}{P_e}(\gamma - 1)\right]\left[1 - \left(\frac{U}{U_0}\right)^{-(\gamma-1)/2}\right] \tag{2-127}$$

which state the relations between the fraction of the charge burned and the expansion ratio. Since $U = U_0 + AX$, Equation 2-126 yields also the relation between the fraction of charge burned and the travel.

By Eqs. 2-125 and 2-127

$$P = \frac{2PB}{\gamma - 1}\left(\frac{U}{U_0}\right)^{-\gamma}\left[\left(\frac{U}{U_0}\right)^{(\gamma-1)/2} - 1\right] \tag{2-128}$$

The pressure is, theoretically, a maximum when

$$\frac{U}{U_0} = \left[\frac{2\gamma}{\gamma + 1}\right]^{2/(\gamma-1)} \tag{2-129}$$

and

$$\frac{c}{C} = \frac{P_B}{\gamma P_e} \tag{2-130}$$

and has the theoretical value

$$P_{max} = P_B[(\gamma + 1)^{(\gamma+1)}\gamma^{-2\gamma}2^{-(\gamma+1)}]^{1/(\gamma-1)} \tag{2-131}$$

This value will be reached only if $P_B/P_e \geqq \gamma$, that is, if the theoretical maximum pressure is reached before the charge is all burned. Otherwise P_{max} occurs when c/C is equal to unity and the maximum pressure is then the pressure at burnt.

The energy of the projectile up to burnout is given by

$$\frac{W'V^2}{2g} = \frac{2P_BU_0}{(\gamma - 1)^2}\left[1 - \left(\frac{U}{U_0}\right)^{-(\gamma-1)/2}\right]^2 \tag{2-132}$$

The conditions at burnt can be obtained by setting $c/C = 1$ in Eq. 2-126 to derive U at burnt, and substituting U at burnt in Eqs. 2-128 and 2-132 to derive P and V at burnt. The travel at burnt is derived from $U = U_0 + AX$.

The corresponding values at burnout are

$$U_b = U_0\left[1 - \tfrac{1}{2}(\gamma - 1)\left(\frac{P_e}{P_b}\right)\right]^{-2/(\gamma-1)} \tag{2-132a}$$

$$P_b = P_e\left[1 - \tfrac{1}{2}(\gamma - 1)\frac{P_e}{P_b}\right]^{(\gamma+1)/(\gamma-1)} \tag{2-132b}$$

$$V_b = P_e\left(\frac{U_0g}{W'P_B}\right)^{1/2} \tag{2-132c}$$

$$X_b = \frac{U_b - U_0}{A} \tag{2-132d}$$

After burnout the gas expands adiabatically so that, when the projectile is at the muzzle, the pressure is given by $(U_b/U_m)^\gamma P_b$. The pressure when the projectile is at the muzzle is therefore given from Equations 2-132a and 2-132b by

$$P_m = P_e\left(\frac{U_0}{U_m}\right)^\gamma\left[1 - \tfrac{1}{2}(\gamma - 1)\frac{P_e}{P_B}\right]^{-1} \tag{2-133}$$

The muzzle energy is given by

$$\frac{W'}{2g}V_m^2 = \frac{CF}{\gamma - 1}\left\{1 - \left(\frac{U_0}{U_m}\right)^{\gamma-1}\left[1 - \tfrac{1}{2}(\gamma - 1)\frac{P_e}{P_B}\right]^{-1}\right\} \tag{2-134}$$

2-6 THE EFFICIENCY OF A GUN-AMMUNITION SYSTEM

There are two "efficiencies" commonly used to estimate the effectiveness of a given gun-propellant system in imparting energy to a projectile. These are thermodynamic or ballistic efficiency and the piezometric efficiency.

The former is defined as the ratio of the translational energy of the projectile at the muzzle to the total energy of the charge as defined by Equation 2-2, that is

$$\text{Thermodynamic Efficiency} = \frac{(\gamma - 1)WV_m^2}{2CFg} \tag{2-135}$$

The piezometric efficiency is defined as the ratio of the mean base pressure, which acting during the travel to the muzzle, would produce the muzzle velocity, to the maximum pressure. It is related to the flatness of the pressure-travel relation. A high piezometric efficiency means a higher muzzle pressure and the projectile position at burnt further toward the muzzle. This will result in increased muzzle blast and greater round to round variation in muzzle velocity.

A high ballistic efficiency results when the charge is completely burned as early as possible in the projectile travel. Thus a high thermodynamic or ballistic efficiency corresponds to a low piezometric efficiency.

2-7 COMPARISON WITH EXPERIMENT

2-7.1 General Considerations

Whatever system of interior ballistics one makes use of, when faced with a practical problem in the analysis of interior ballistic measurements or in the design of a gun, one must assign values to certain of the parameters occurring in the theory which cannot be determined by independent means. The most important of these parameters is the burning rate coefficient which will occur in any formulation of the theory. Others are the heat loss ratio which determines the adjusted value of γ, the starting pressure, and the burning rate pressure exponent. Proper values of these parameters must be determined by adjustment to fit the theory to records of actual gun firings. To match the theory to observation by simultaneous adjustment of all such uncertain parameters would be very tedious, and, in view of the simplifying assumptions made in the formulation of the theory, unwarranted. One must make a judgment as to the most uncertain parameters and those to which the solution is most sensitive and assign approximate values to the least important ones and adjust the others for best fit." By a process of trial and error one arrives at the best set of values to fit the theory to the experimental data. It is often possible to estimate approximate or limiting values of certain parameters theoretically or by independent measurements. For example, the thermodynamic value of γ can be calculated and the effective value will be greater than this. The heat loss could be calculated approximately by the method of Chapter 3. Relative values of the burning rate constant can be determined for different propellants from closed chamber measurement.

If one has to deal with guns of unconventional design such as the so called light gas guns or other guns operating outside the usual range of pressure and velocity a greater dependence on theory becomes necessary. A major difficulty in treating high performance guns such as modern tank guns is the proper treatment of the pressure gradient in the gas. This problem is discussed in some detail in Chapter 5.

2-7.2 Experimental Evaluation of the Parameters

a. General Procedures. The interior ballistic quantities that can be measured with modern instrumentation are described in Chapter 4. To try to furnish data on all of these would not be warranted except possibly for firings carried out in connection with research in the subject. Usually the data supplied will be much less extensive and complete. This will influence the complexity of the theory used to analyze the data and the procedures followed. If all that is available are crusher gage values of the peak pressure and the muzzle velocity a very simple theory such as that of Mayer and Hart may be adequate.

For a more detailed analysis of the interior ballistic trajectories, the firing records will furnish breech pressure and projectile travel as functions of the time. The records will be provided with a common time scale and fiducial marks to adjust the time scales to a common zero time (see Chapter 4). These records are read by means of an optical comparator capable of measuring both horizontal and vertical displacements on the record. Usually the travel-time data are derived from an interferometer record which furnishes values of the time for equal intervals of distance. By interpolation, these data are converted to intervals of distance for equally spaced intervals of time so that one finally has the breech pressure and projectile travel presented on a common time scale. The travel data is then differentiated twice to provide values of the velocity and acceleration of the projectile also as functions of the time. This will require considerable smoothing and other mathematical manipulation. For details and references to the mathematical literature underlying the process see Reference 7.

To reduce the data in this manner and to make comparisons with the theoretical formulas in detail for many records, is a very time consuming process. To analyze the records from a single firing may take two or more man weeks if carried out with desk calculators. Where the necessary automatic record-measuring and computing equipment is available, the procedures can be automated and coded for high speed computers so that the data from a gun

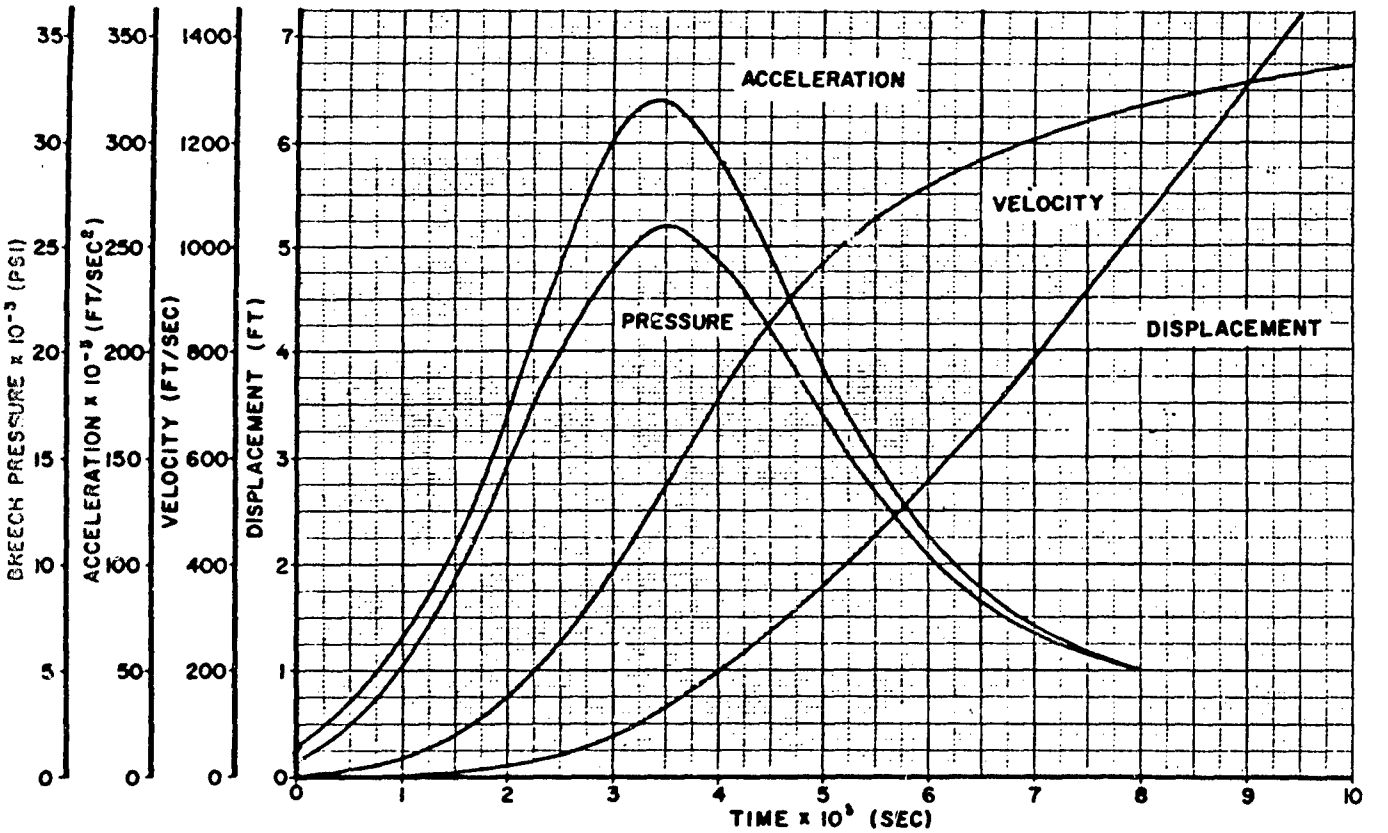


FIGURE 2-2. *Result of the Analysis of a Firing Record for a 105mm Howitzer Round (Measured Values of Pressure and Displacement. Velocity and Acceleration Determined by Numerical Differentiation of Displacement)*

firing can be processed in a matter of hours.[7] A plot of the result of such a record analysis, for a typical case, is shown in Figure 2-2.

b. The Conditions in the Early Stages of Burning; the Starting Pressure. From such a record, the pressure at the actual start of motion can be read directly. From the record shown, it is about 750 psi. It should be emphasized, however, that the time of start of motion is difficult to determine accurately because it is difficult to determine from the record just where the displacement actually begins. This would be true even if the graph were precisely determined. Error of reading and reduction will increase the uncertainty.

The "starting pressure" used in the formulation of interior ballistic theories is a quantity quite different from the actual pressure at the start of motion. Immediately after the projectile starts to move, the rotating band engages the rifling and a large resisting force is developed. After engraving, the resisting force drops rapidly to a much lower value. One might expect this to show as an irregularity in the graph of the acceleration in Figure 2-2. It does not do so because the resolution of the apparatus and the data reduction procedures are not sufficient to show it. This is usually the case unless special methods are used to study the motion during engraving. A description of one such method is given in paragraph 4-4.3.

If the acceleration is adequately determined, the effective pressure, P_e, on the base of the projectile, that is the difference between the actual base pressure and the pressure necessary to balance the forces of engraving and friction, can be determined from the relation

$$P_e = \frac{Wa}{Ag} \qquad (2\text{-}136)$$

If a measurement of the base pressure, P_b, is available or if it can be calculated by the use of a formula such as Equation 2-20, an estimate of the engraving and frictional force can be calculated from the difference $P_bA - P_eA$. A graph of this force for a typical 105mm Howitzer round is shown in Figure 2-3. The observed maximum force of about 45000 pounds, divided by the nominal bore area of 13.4 square inches gives a starting pressure of 3350 pounds per square inch. This compares reasonably well with the value indicated on Figure 2-1 of 4000 psi.

In assigning starting pressures some average value of the engraving force should determine the assigned value. The engraving force will evidently be quite variable from round to round. It will be sensitive to manufacturing tolerances in the size of the rotating band, how closely the band fits the projectile and possibly in the thickness of the projectile wall.

When comparing their theories with experiment, most authors assign a starting pressure in an arbitrary manner. It is hardly possible to do it in any other way. The experimental values of engraving forces can serve only to set some limits on it. In the Hirschfelder system, for example, the starting pressure is assumed to be the pressure existing when one percent of the charge has been consumed. Since the projectile has presumably not moved up to this time, the starting pressure is that which would be produced in a closed chamber under similar loading conditions.

c. The Rate of Charge Consumption. The amount of propellant burned up to any specified time can be determined from the energy balance equation. This equation, as developed in paragraph 2-2.1, can be written as

$$\frac{cF}{\gamma - 1} = \frac{P[AX + U_{ch} - Cu - c(\eta - u)]}{\gamma - 1} + \frac{MV^2}{2} + Q \qquad (2\text{-}137)$$

where γ is the calculated thermodynamic ratio of specific heats and P is the average pressure consistent with the equation of state. Q is mainly heat loss to the tube, but may contain other losses not taken care of by the definition of the effective mass, M.

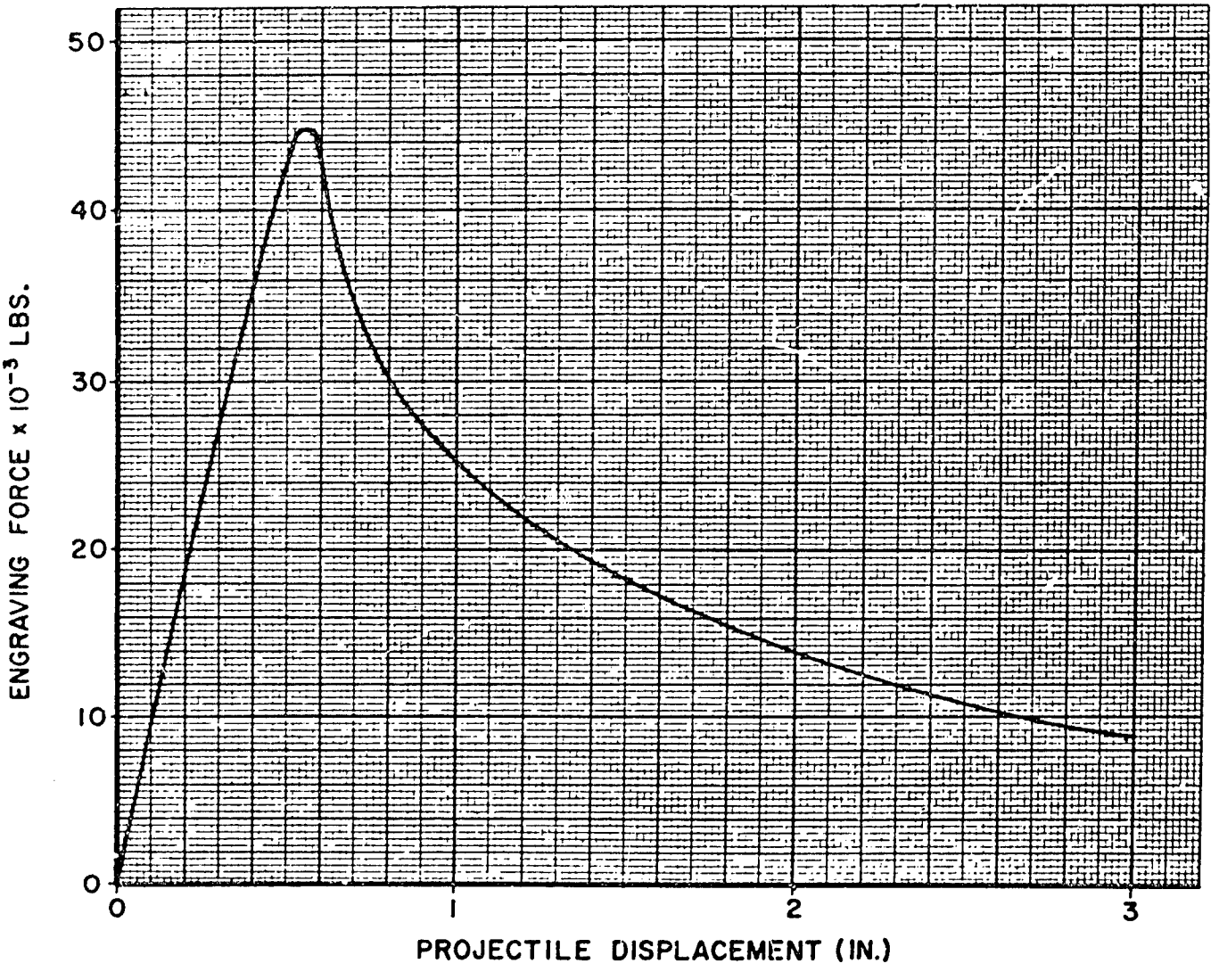


FIGURE 2-3. *Engraving Force for a Typical 105mm Howitzer Round*

P can be converted to breech pressure by the use of the Pidduck-Kent solution for the pressure ratios determined from paragraph 5-1.1 or by the use of Equation 2-20 for the case of low velocity weapons. The value of the effective mass, M, may also be determined more accurately by the use of the Pidduck-Kent solution for the kinetic energy of the unburned propellant and the gas.

Assuming that P is correctly related to the breech pressure and that M is determined with sufficient accuracy, c can be determined from Equation 2-137 provided some knowledge of the value of Q is available.

Q is often neglected entirely because of the difficulty of incorporating it in the analysis. This may lead to error, as the heat loss can be a considerable fraction of the available energy, especially in smaller weapons or when hot propellants are used. The use of a nominal value of from 5 to 20 percent of $MV^2/2$ should improve the analysis; the lower value to be used for standard cannon, and the upper range for high velocity guns and small arms.

Allowing for Q in this manner and substituting measured values of P, X and V in Equation 2-137 c can be calculated for specified values of t and a graph of c against t plotted. This graph should approach a limit when $c = C$ since the charge does not burn out discontinuously, as the charge is not ignited simultaneously over its entire surface and the burning rate is not the same everywhere. The burning surface, and therefore dc/dt go to zero at burnout. This may not be obvious on the graph depending on the shape of the grains and the effectiveness of the ignition as well as the time resolution of the data.

Because of errors in the values of P and in the assigned value of Q, c will not, in general, equal C when dc/dt becomes equal to zero. Since it should do so a further adjustment must be made in P or Q or both to bring it about. As Q is a correction term its value does not affect the adjustment as strongly as does that of P and since the formulas for the pressure ratios are admittedly uncertain the adjustment should be brought about mainly by changes in the values of P.

After burnout, the right-hand side of Equation 2-137 should remain constant, equal to $CF/\gamma - 1$. As V and X increase, P declines, as the gas continues to do work and lose heat to the barrel. The graph for c should, therefore, remain at the value C. This can be brought about by continuing to make the necessary adjustments in P.

In the interval before burnt, P can be adjusted using the same ratio of P to P_a (the adjusted value of P) as was necessary to make c equal to C at burnt. This is in accord with the usual formulas which state that the pressure ratios are constant during burning. This, however, is hardly possible at the start of motion where the ratio ought to be equal to unity. A procedure which has been used in practice is to adjust the ratio linearly with time from its experimental value at burnt to unity at the start of motion. A graph of c versus t constructed in this way, for a 37mm gun firing, is shown in Figure 2-4.

Once the graph of c versus t has been constructed in this way an experimental value of the time to burnt can be read off immediately and experimental values of the travel and velocity at burnt will be known from the associated values of X and V.

The graph can also be differentiated and the rate of charge consumption determined as a function of time. The surface area, S, of the burning grains can be calculated from the geometry of the grains[8] and the linear burning rate, r, at any specified time determined from the relation

$$r = \frac{1}{\rho S}\frac{dc}{dt} \qquad (2\text{-}138)$$

Since the pressure, P, at the same instant is also known, a graph of the linear rate of burning versus P can be constructed. In general this graph will not be a straight line when plotted on a log-log scale indicating that the burning rate dependence on the pressure cannot be represented by a simple power relation. This is to be expected because the burning in the gun takes place at different pressures in different parts of the tube and the average burning rate will depend on the pressure distribution and also on how the unburned propellant is distributed. The rate at any time during the burning depends also on factors other than the pressure, such as the velocity of the gas. The graph, however, can be used to estimate an effective value of the pressure exponent. A graph of linear burning rate versus pressure contructed in this way for the 105mm Howitzer is shown in Figure 2-5. The closed chamber burning rate for the same propellant is also shown. Above about 1700 psi the pressure exponent for the gun burning rate is lower than that for the closed chamber and below 1700 psi the exponent for the gun is considerably larger than for the closed chamber. It is also considerably greater than unity. There is no theoretical reason why this should not be possible.

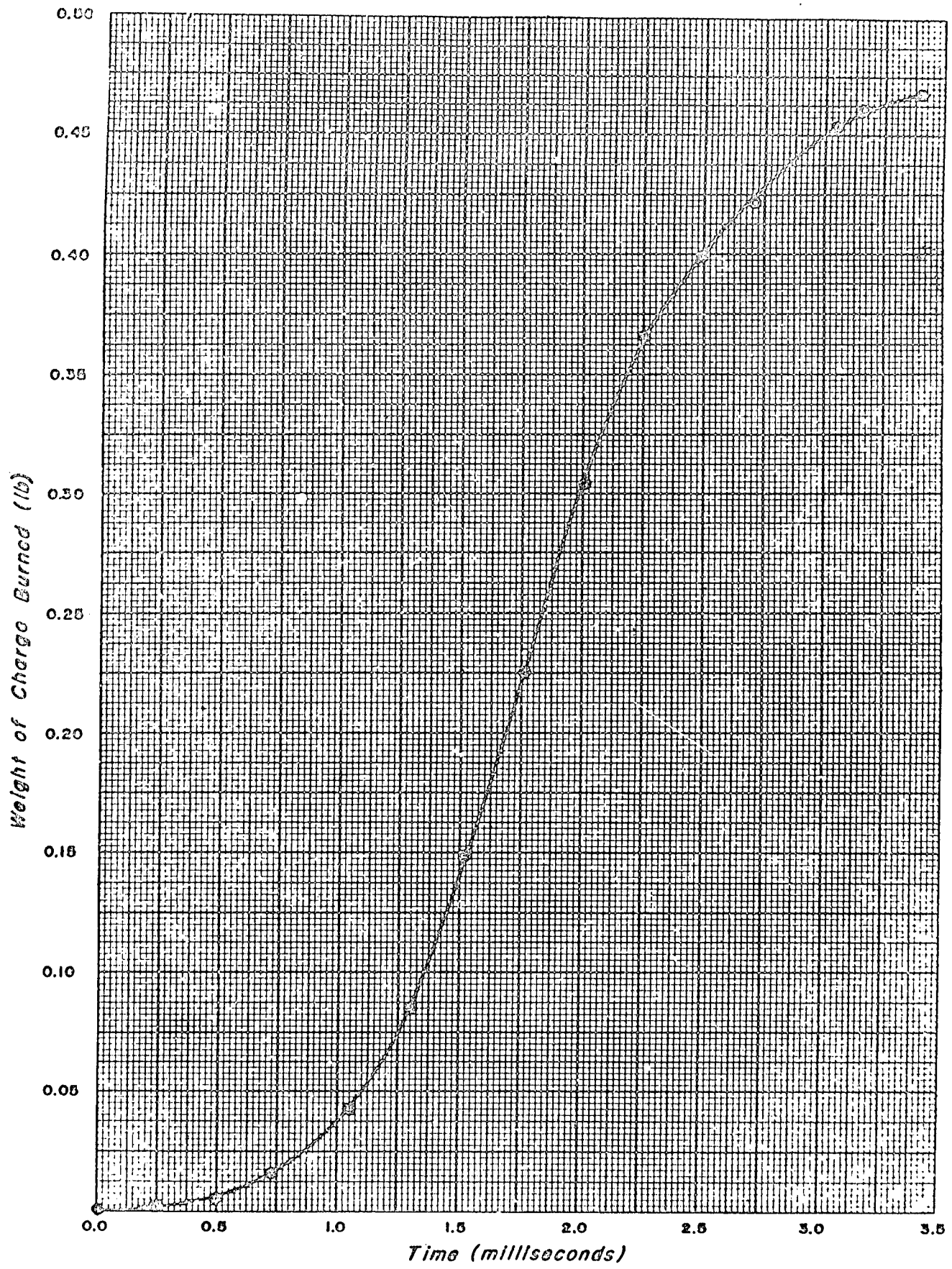


FIGURE 2-1. *Charge Burned Versus Time for 57mm Gun*

theory such as that of Mayer and Hart and that their specification does not involve a knowledge of unknown quantities such as starting pressures or burning rates. Charts or nomograms are then constructed showing the relation between the chosen parameters. The charts or nomograms are adjusted to their final form by fitting to numerous firing records. In solving a practical problem the given data will permit the evaluation of certain of the parameters and from the charts or nomograms the proper values of the others can be read off. The parameters are known functions of the desired variables such as maximum pressure and muzzle velocity so that the latter can be determined once the proper values of the parameters are known.

Such a scheme is that published by Strittmater[11] which is presented in a single working chart (Chart 2-4). The theory used is that of Mayer and Hart supplemented by a further assumption that bore friction is proportional to chamber pressure. This assumption is used to improve the agreement between the chart and experiment by adjusting the effective projectile weight.

The resulting effective weight is defined as

TABLE 2-2. VALUES OF η, β, η_1, AND β_1 FOR STANDARD WEAPONS

Weapon, Gun	Projectile			Propellant				Zone	Vel, fps	Crusher Press, psi	Coefficient			
											Velocity		Pressure	
	Model	Type	Wt, lb	Lot	Type	Web, in	Wt				η	β	η_1	β_1
76mm M1	M42A1	HE	12.80	60105-S	MP, M6	.0365	55.72 oz		2700	37100	−.31	−.21	.65	−1.17
	M62A1	APC-T	15.40	17636-R	MP, M6	.0419	61.17 oz		2600	42300	−.35	−.22	.69	−1.18
76mm M32	M352	HE	15.00	60105-S	MP, M6	.0365	55.01 oz		2400	28400	−.38	−.19	.69	− .82
	M339	AP-T	14.50	63848	MP, M17	.0565	85.40 oz		3200	44800	−.30	−.21	.66	−1.18
90mm M1	M71	HE	23.40	17665	MP, M6	.0496	115.13 oz		2700	36600	−.30	−.22	.68	−1.01
90mm M36, M41	M71E1	HE-T	23.40	63439	MP, M1	.0340	85.38 oz		2400	35800	−.39	−.21	.67	− .90
	T91	HE-T	18.00	38740-S	MP, M1	.0267	72.46 oz		2400	26500	−.38	−.21	.66	− .78
	M318A1	AP-T	24.10	38714-S	MP, M17	.0784	141.58 oz		3000	44000	−.24	−.23	.65	−1.22
120mm M1	M73	HE	50.00	38470-S	MP, M6	.0674	23.38 lb		3100	37200	−.30	−.24	.66	− .97
120mm M58	M356	HE	50.40	38723-R	SP, M15	.0344	12.24 lb		2500	38500	−.39	−.21	.57	− .82
	M358	AP-T	50.85	33879-S	MP, M17	.1140	29.43 lb		3500	44800	−.23	−.25	.62	−1.21
155mm M2	M101	HE	95.00	30348-S	MP, M6	.0559	20.68 lb Reduced		2100	17300	−.35	−.21	.64	− .69
							30.86 Full		2800	38600	−.37	−.24	.67	− .90
8 in M1	M103	HE	240	16697-S	MP, M6	.0839	80.89 lb Reduced		2600	29300	−.31	−.25	.66	− .80
					M10 Charge		92.27 lb Normal		2850	37600	−.42	−.26	.88	− .86
				8501-S	MP, M6	.0691	53.00 lb Reduced		2100	18700	−.34	−.22	.64	− .66
					M9 Charge		74.50 lb Normal		2600	33500	−.34	−.25	.66	− .78
280mm T131	M124	HE	600	39370 60580	MP, M6	.0688 .100	52.83 lb	1	1380	8800	−.39		.60	
							90.15 lb	2	1780	15400	−.39		.60	
							118.70 lb	3	2100	22000	−.39		.64	
							156.92 lb	4	2500	33400	−.38		.65	

2-8 SIMILARITY AND SCALING

When the solution of the equations for a theory of interior ballistics is attained, the solutions for particular cases are found to be characterized by certain ballistic parameters which are combinations of the quantities specifying the details of the gun and charge. What these parameters are and their form will depend on the way the theory is formulated. If the characteristics of two gun-ammunition systems lead to the same numerical values for the ballistic parameters, the theoretical solutions for both will have the same form and the actual solutions can be transformed one into the other by simple changes of scale.

If now one starts from a standard gun-ammunition system which has been well studied experimentally so that the gun-ammunition parameters occurring in the theory are properly adjusted to match the theory to experiment and numerical values of the ballistic parameters are known, the similarity can be used to predict the trajectories for scaled models of the standard gun system.

It follows also that in tabulating solutions the extent of the tables can be much reduced by tabulating solutions for only certain values of the ballistic parameters. Solutions for other values can then be obtained by interpolation. The tables can be converted also into graphs or nomographs from which

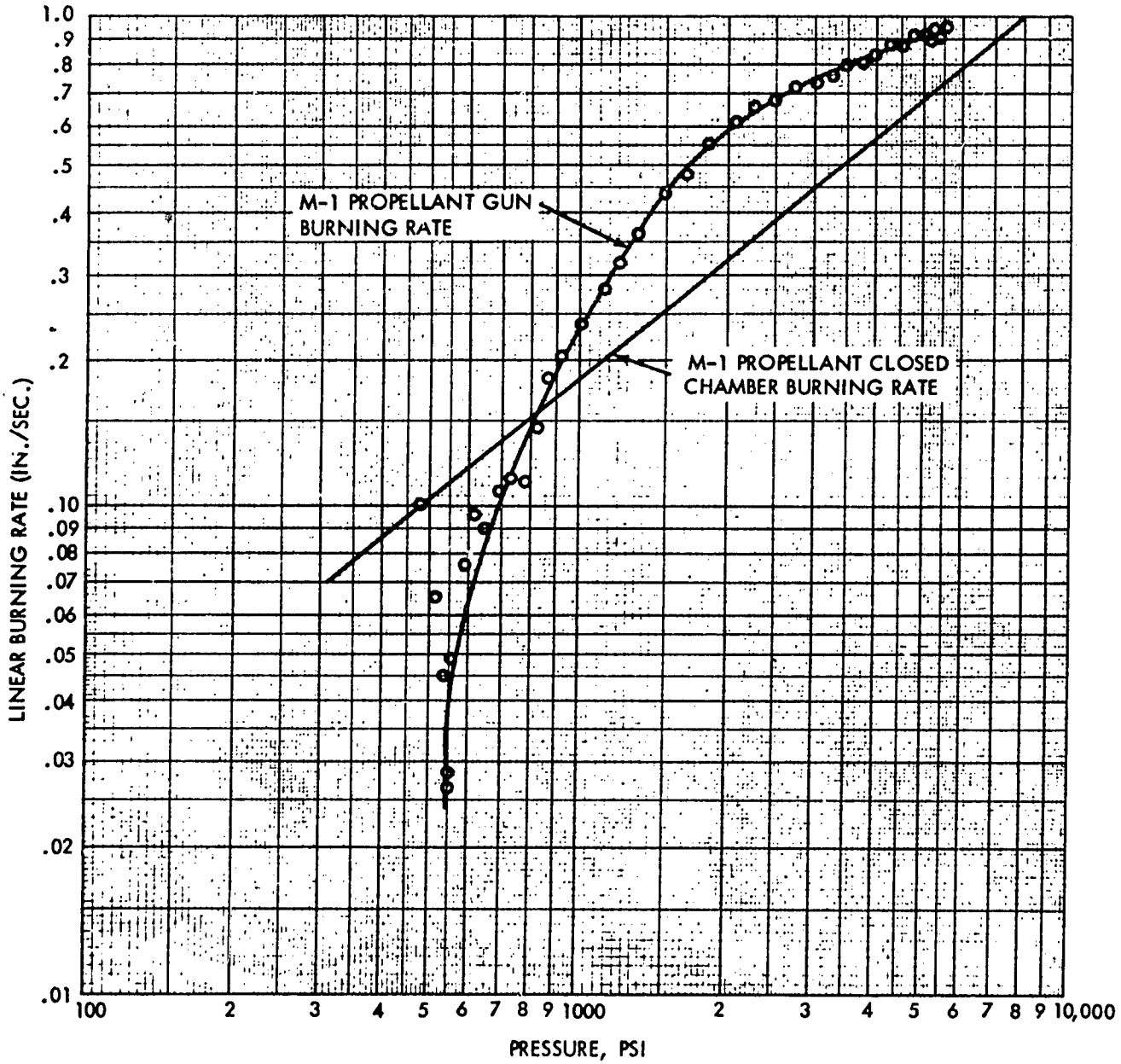


FIGURE 2-5. *Linear Burning Rate versus Pressure for 105mm Howitzer, M1 Propellant*

TABLE 2-2. (Continued)

Weapon, Howitzer	Projectile			Propellant				Zone	Vel, fps	Crusher Press, psi	Coefficient			
											Velocity		Pressure	
	Model	Type	Wt, lb	Lot	Type	Web, in	Wt				η	β	η_1	β_1
105mm M2A1	M1	HE	33.00	61080 61180	SP, MP, M1	.0143 .0262	8.55 oz 9.98 oz 12.51 oz 16.31 oz 22.08 oz 30.85 oz 45.24 oz	1 2 3 4 5 6 7	650 710 780 875 1020 1225 1550	6600 8200 9000 11000 14300 19800 31000	−.48 −.48 −.48 −.44 −.43 −.42 −.40	−.18 −.17 −.18 −.14 −.15 −.16 −.18	.62 .62 .62 .57 .64 .66 .69	− .67 − .67 − .69 − .58 − .60 − .69 − .85
155mm M1A1	M107	HE	95.00	65460-S M4A1 Charge 3742-S M3 Charge	MP, M1 SP, M1	.0331 .0165	4.16 lb 5.32 lb 7.05 lb 9.82 lb 13.19 lb 1.95 lb 2.44 lb 3.09 lb 3.98 lb 5.50 lb	3 4 5 6 7 1 2 3 4 5	880 1020 1220 1520 1850 680 770 880 1020 1220	5500 7000 10200 17500 31000 4800 6200 8400 12000 18900	−.33 −.33 −.34 −.37 −.38 −.46 −.46 −.46 −.46 −.45	−.11 −.15 −.17 −.20 −.23 −.12 −.13 −.14 −.18 −.20	.50 .55 .60 .64 .67 .62 .62 .62 .62 .61	− .46 − .49 − .58 − .69 − .84 − .48 − .50 − .51 − .57 − .73
8 in M2	M106	HE	200.00	8295-S M1 Charge 10567-S M2 Charge	SP, M1 MP, M1	.9161 .0414	5.33 lb 6.28 lb 7.52 lb 9.54 lb 13.16 lb 16.62 lb 21.84 lb 28.05 lb	1 2 3 4 5 5 6 7	820 900 1000 1150 1380 1380 1640 1950	7600 9600 12400 17100 27000 12900 19800 32000	−.43 −.44 −.44 −.44 −.45 −.23 −.26 −.29	−.12 −.13 −.15 −.15 −.16 −.13 −.16 −.18	.58 .60 .62 .60 .56 .60 .66 .68	− .47 − .49 − .55 − .65 − .84 − .70 − .85 − .99
240mm M1	M114	HE	360.00	63310	MP, M6	.0719	43.64 lb 54.01 lb 66.59 lb 79.75 lb	1 2 3 4	1500 1740 2020 2300	10400 15100 22900 34000	−.30 −.31 −.34 −.35	−.16 −.18 −.21 −.22	.60 .64 .66 .70	− .63 − .65 − .79 − .89

$$W_e = W + 5 \times 10^5\, dX_m/V_m^2 \qquad (2\text{-}160)$$

The parameters are presented on Chart 2-4. They are in reduced form and are the following:

- e thermodynamic efficiency
- z piezometric efficiency
- x volume expansion ratio
- r energy ratio
- y pressure ratio

They are defined by the following equations

$$e = \frac{(\gamma - 1)(W_e + C/3)V_m^2}{2gFC} \qquad (2\text{-}161)$$

$$z = \frac{(W_e + C/3)V_m^2}{2g\bar{P}_p U_m} \qquad (2\text{-}162)$$

$$x = \frac{U_m}{U_0} \qquad (2\text{-}163)$$

$$r = \frac{FC}{\bar{P}_p U_0} \qquad (2\text{-}164)$$

$$y = \frac{P_m}{\bar{P}_p} \qquad (2\text{-}165)$$

Equation 2-162 is in accord with the definition in paragraph 2-6, when V_m is defined as the product of the bore area multiplied by the projectile travel

different solutions can be obtained with little auxilliary computation.

As an example, the effect of increasing all linear dimensions of a gun-ammunition system will be investigated using Bennett's theory and tables.[4] The ballistic parameters and the scaling factors of Bennett's theory are the quantities q, Δ, r, and ℓ as defined below, and to take account of changes in propellant type a standard specific energy, E_0, is used equal to 1.5×10^6 in-lb/lb. The effective projectile weight is taken as

$$W' = W + C/3 \tag{2-139}$$

and weight ratio is defined as

$$e = \frac{W + C/2}{R} \tag{2-140}$$

where R is the weight of gun and recoiling parts. The quickness, q, is then defined as

$$q = q_1 \frac{(E/E_0)^{7/6} U_{ch}^{1/2} (W')^{1/2}}{wA(1 + e)} \tag{2-141}$$

where q_1, which depends on the type, temperature and moisture content of the propellant, is determined empirically.

Δ, the density of loading, is defined by

$$\Delta = U_w C / U_{ch} \tag{2-142}$$

where U_w is the specific volume of water. Δ, so defined, is actually a specific gravity of loading and is dimensionless. It is numerically equal to density of loading in grams per cubic centimeter. The projectile travel, X, is given in terms of the expansion, s, as defined by

$$s = 1 + (A/U_{ch})X \tag{2-143}$$

Three of Bennett's tables tabulate values of pressure, P_t, velocity, V_t, and time, t_t, as functions of q, Δ and s. The actual values of P, V and t are related to the tabulated values by the following relations

$$P = (E/E_0)P_t \tag{2-144}$$

so that if the propellant is not changed the actual pressure is the tabulated one.

$$V = rV_t \tag{2-145}$$

where $r = r_1(E/E_0)^{\frac{1}{2}}(U_{ch}/W')^{\frac{1}{2}}$ and r_1 is again a factor to be determined empirically.

$$t = (\ell/r)t_t \tag{2-146}$$

where

$$\ell = \frac{U_{ch}}{A(1 + e)} \tag{2-147}$$

Now consider the effects of changing all linear dimensions of the gun-ammunition system by a factor, f. The composition of the propellant will not be changed so that E is not changed but the web and other dimensions of the propellant will change by a factor, f. A will change by f^2. U_{ch}, R, W and C will all change by f^3.

It follows from Equations 2-141 and 2-142 that q and Δ remain unchanged so that the tabulated values of pressure, velocity and time remain unchanged for the same value of the expansion, s. The actual value of the pressure is the tabulated value and since r is also unchanged the velocity is the same for the same expansion. The displacement, X, will be changed according to Eq. 2-143, the second term on the right being divided by f. Since ℓ is changed by a factor, f, the time scale will be multiplied by f so that it will take f times as long to reach the same expansion.

2-9 EFFECTS OF CHANGES IN THE PARAMETERS

To be considered chiefly are the effects on muzzle velocity, V_m and maximum pressure, P_p, due to changes in C, U_{ch}, X_m, W, w and E. A change in C and/or U_{ch} may be expressed as a change in Δ. Equations 2-26 and 2-27 show that the effects of a change in B is equal to the same proportional change in w, but in the opposite sense; that is, a 10 percent increase in B produces the same effect as a 10 percent decrease in w.

The effects are usually expressed as differential coefficients, which are defined by the formulas (*See*: List of Symbols)

$$\frac{dV_m}{V_m} = \alpha \frac{\partial C}{C} + \beta \frac{\partial U_{ch}}{U_{ch}} + \gamma \frac{\partial X_m}{X_m} + \eta \frac{\partial W}{W} + \kappa \frac{\partial w}{w} + \lambda \frac{\partial E}{E} \tag{2-148}$$

$$\delta = \frac{\Delta \partial V_m}{V_m \partial \Delta} \tag{2-149}$$

$$\frac{dP_p}{P_p} = \alpha_1 \frac{\partial C}{C} + \beta_1 \frac{\partial U_{ch}}{U_{ch}} + \eta_1 \frac{\partial W}{W} + \kappa_1 \frac{\partial w}{w} + \lambda_1 \frac{\partial E}{E} \tag{2-150}$$

$$\delta_1 = \frac{\Delta \partial P_p}{P_p \partial \Delta} \tag{2-151}$$

These differential coefficients may be determined either experimentally or theoretically by changing one of the parameters at a time. In testing a new lot of propellant or a new projectile, it is customary

TABLE 2-1. DIFFERENTIAL COEFFICIENTS FOR ARTILLERY WEAPONS

Propellant Composition	No. of Values Considered	Caliber of Weapons Considered		Velocity Coefficients α	β	γ	η	κ	λ	Pressure Coefficients α_1	β_1	η_1	κ_1	λ_1
M1 Single-Base	39	37mm-8-inch	Mean	.57	−.17	.21	−.36	−.26	.82	1.42	− .79	.62	−1.29	2.50
			Max	.66	−.26	.33	−.47	−.59	1.19	1.83	−1.62	.78	−1.58	2.84
			Min	.47	−.05	.13	−.20	−.06	.57	.88	− .39	.47	− .96	2.12
M6 Single-Base	36	57mm-240mm	Mean	.62	−.21	.21	−.32	−.30	.85	1.79	− .98	.67	−1.51	2.76
			Max	.72	−.27	.30	−.42	−.69	1.30	2.02	−1.28	.88	−1.64	2.91
			Min	.52	−.15	.13	−.15	−.16	.69	1.23	−.55	.60	−1.29	2.51
M2 Double-Base	11	37mm-90mm	Mean	.59	−.18	.21	−.35	−.29	.84	1.61	− .91	.63	−1.37	2.60
			Max	.66	−.23	.25	−.48	−.55	1.14	1.88	−1.22	.67	−1.48	2.73
			Min	.53	−.07	.18	−.20	−.10	.62	1.25	− .63	.60	−1.22	2.42
M17 Triple-Base	9	76mm-120mm	Mean	.67	−.23	.23	−.24	−.44	1.00	2.04	−1.19	.61	−1.48	2.73
			Max	.73	−.28	.27	−.29	−.60	1.10	2.33	−1.40	.68	−1.51	2.76
			Min	.64	−.20	.19	−.16	−.36	.92	1.64	− .90	.39	−1.35	2.58

to use a series of charges of increasing weight, plot the observed values of muzzle velocity and maximum pressure, and draw smooth curves to fit the points. Although this is done primarily to determine the charge that will give the required muzzle velocity and to see whether the maximum pressure exceeds that for which the gun was designed, the curves also indicate the effects of changes in weight of charge. The effects of a change in projectile weight can be determined by comparative firings of projectiles of the same model but different weight.

Taylor's charts have not yet been used to calculate the differential coefficients. The coefficients for single perforated grains have been computed by means of Röggla's charts,[9] averaging the effects of a 10 percent increase and a 10 percent decrease in each parameter. The coefficients for multiperforated grains have been computed by means of Bennett's tables, averaging the effects of one tabular interval increase and decrease in η, Δ and s to find $-\kappa$, δ, γ, $-\kappa_1$ and δ_1, then calculating the other coefficients by the formulas[10],

$$\alpha = D_1(-\kappa) + \delta - C/6W' \qquad (2\text{-}152)$$

where

$$D_1 = \frac{C}{6W'} - \frac{C}{2R'}$$

$$W' = W + C/3$$

$$R' = R + W + C/2$$

$$\beta = 0.5(-\kappa) - \delta - \gamma + 0.5 \qquad (2\text{-}153)$$

$$\eta = D_2(-\kappa) - W/2W' \qquad (2\text{-}154)$$

where

$$D_2 = \frac{W}{2W'} - \frac{W}{R'}$$

$$\gamma = \tfrac{7}{8}(-\kappa) + 0.5 \qquad (2\text{-}155)$$

$$\alpha_1 = D_1(-\kappa_1) + \delta_1 \qquad (2\text{-}156)$$

$$\beta_1 = 0.5(-\kappa_1) - \delta_1 \qquad (2\text{-}157)$$

$$\eta_1 = D_2(-\kappa_1) \qquad (2\text{-}158)$$

$$\lambda_1 = \tfrac{7}{8}(-\kappa_1) + 1 \qquad (2\text{-}159)$$

Table 2-1 gives the average values of the differential coefficients for artillery weapons. Table 2-2 gives the values of η, β, η_1 and β_1 for standard weapons.

Following are some estimated values for recoilless rifles:

$$\alpha = 1.0$$

$$\eta = -0.65$$

$$\alpha_1 = 2.4$$

$$\eta_1 = 0.62$$

2-10 SIMPLE GRAPHICAL METHODS

Numerous schemes have been devised by interior ballisticians for making rapid approximate calculations of certain interior ballistic variables especially of maximum pressure and muzzle velocity. These schemes are formulated in terms of a set of parameters chosen so that their form and interrelations can be determined by the use of some simplified

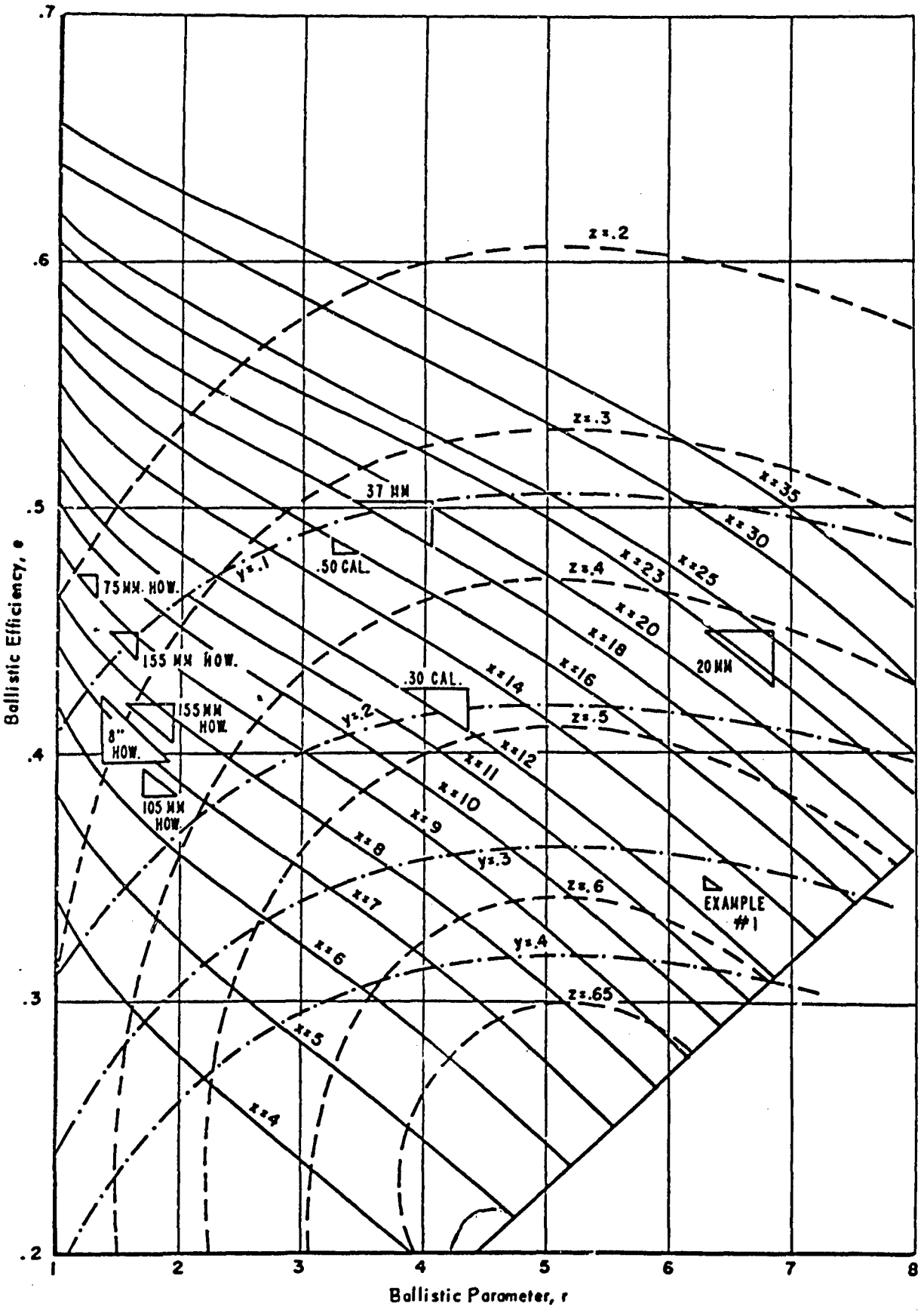


CHART 2-4. *Chart for Interior Ballistic Calculations by the Scheme of Stritimater*

to the muzzle and $\bar{P}_p$ is defined as the space mean pressure at the time of maximum pressure. The latter may also be called the space mean peak pressure.

With Equation 2-166 substituted in Eqs. 2-161 and 2-162 using the numerical values 1.30 and 386 for γ and g, the ballistic and piezometric efficiencies may be expressed

$$e = 3.89 \times 10^{-4} \frac{(W + C/3)V_m^2 + 5 \times 10^5 dX_m}{FC} \tag{2-161a}$$

$$z = \frac{(W + C/3)V_m^2 + 5 \times 10^5 dX_m}{772\bar{P}_p U_m} \tag{2-162a}$$

Solving the former for V_m^2 gives

$$V_m^2 = \frac{2574FCe - 5 \times 10^5 dX_m}{W + C/3} \tag{2-166}$$

If the maximum breech pressure, P_{cp}, is given, the space mean peak pressure, $\bar{P}_p$, is calculated by the formula

$$\bar{P}_p = \frac{W + C/3}{W + C/2} P_{cp} \tag{2-167}$$

The initial free volume is defined by Equation 2-17a as

$$U_0 = U_{ch} - Cu$$

The free volume at the muzzle is defined by Equation 2-102 as

$$U_m = U_0 + AX_m$$

Theoretically, if any two of the reduced parameters are known, the other three can be evaluated by means of the chart.

The use of the chart will be illustrated by an example. The data were taken from the firing record for a caliber .30 gun, firing a 150.5-grain bullet, propelled by 50 grains of a certain lot of propellant. The characteristics of the gun and charge are:

Characteristic	Symbol	Value	Unit	Remarks
Propellant weight	C	0.00714	lb	Given
Specific force	F	4.023×10^6	in-lb/lb	Given
Specific volume	u	17.5	in³/lb	Given
Chamber volume	U_{ch}	0.258	in³	Given
Area of bore	A	0.0735	in²	Given
Bore diameter	d	0.30	in	Given
Travel to muzzle	X_m	21.79	in	Given
Projectile weight	W	0.0215	lb	Given

To calculate at least two of the parameters one also needs to know either the muzzle velocity or the space mean peak pressure. One or both of these will normally be specified in any gun design problem. In the present example the maximum breech pressure will be assumed to be given and equal to the measured value 35,890 lb/in², so that the space mean peak pressure can be calculated by Equation 2-167.

Now suppose the following are calculated:

Characteristic	Symbol	Value	Unit	Remarks
Initial free volume	U_0	0.133	in³	Eq. 2-17a
Muzzle free volume	U_m	1.735	in³	Eq. 2-102
Space mean peak pressure	$\bar{P}_p$	34,180	lb/in²	Eq. 2-167
Volume expansion ratio	x	13.05		Eq. 2-163
Ballistic parameter	r	6.32		Eq. 2-164

Then from Chart 2-4 e, z and y can be read as:

Ballistic efficiency, $e = 0.352$
Piezometric efficiency, $z = 0.566$
Pressure ratio, $y = 0.316$

from which muzzle pressure is calculated as 10,800 lb in², and the muzzle velocity as 2,572 feet per second. The observed value of the muzzle velocity was 2,565 feet per second for the firing used.

If the theory represented by the chart were exact, the lines representing the five different parameters for any gun-ammunition system would all intersect at a point. When experimental values for the quantities defining the parameters are substituted in the corresponding equations the lines so determined do not cross at a single point but form a polygon. If the experimental values are not subject to serious error, the dimensions of this polygon are a measure of the discrepancies involved in using the chart. The triangles shown on the chart are the result of using experimental values (inserted into Equations 2-161, 2-163 and 2-164), to determine e, x and r for the weapons indicated. For the example, the predicted value of e, using the values for x and r in the preceding table, is 0.352 which the triangle indicates is too high by about 0.006; the amount corresponding to the height of the triangle.

A set of nomograms constructed by similar methods, for the rapid determination of muzzle velocities for artillery weapons has been constructed by Kravitz. These are published in usable form with instructions for their use in Reference 12.

2-11 EMPIRICAL METHODS

For many practical problems of gun design, theory is used as a guide to the selection of a set of dimensionless parameters in terms of which the scheme to be used is formulated and to define the chosen parameters in terms of the interior ballistic variables themselves. If then sufficient firing data are available from a group of weapons, not too dissimilar from each other, fitted graphs or charts can be prepared connecting pertinent variables with the chosen ballistic parameters which will vary for different members of the reference group. The most commonly used parameters are propellant weight per unit projectile weight, expansion ratio and density of loading. From such a set of graphs the parameters and ballistic variables of a new but similar weapon system can be determined by simple interpolation. Such a set of graphs, prepared at Frankford Arsenal for use in small arms design, are presented on Charts 2-5, 2-6, 2-7 and 2-8. These normalized graphs were obtained by reducing experimental data from firing eleven different small arms weapon systems. Least squares curves were drawn to give the best fit to the data. They are used to relate maximum pressure, propellant weight, projectile weight, expansion ratio, muzzle velocity and chamber pressure at a given projectile travel.

Example: Given the Cartridge, Caliber .30, Ball M2 data as follows:

Projectile weight	- 150 grains
Propellant weight	- 49.9 grains
Bore area	- 0.0732 in^2
Case volume	- 0.25 in^3
Bullet travel	- 21.9 in
Maximum pressure	- 51.2 kpsi

Find the muzzle velocity.
Calculation:

$$\frac{C}{W} = \frac{49.9}{150} = 0.333$$

$$\frac{V_m}{V_0} = \frac{0.0732 \times 21.9 + 0.25}{0.25} = 7.41$$

$$V = V_{3.60} \times \frac{V_s}{V_3} \times \frac{V_m}{V_{60}}$$

$$= 2610 \times 1.106 \times 0.981 = 2832 \text{ ft/sec}$$

where: 2610 is read from Chart 2-5, 1.106 is read from Chart 2-6 and 0.981 is read from Chart 2-7.

For comparison, the muzzle velocity was actually recorded as 2832 ft/sec.

It should be noted that these graphs work well for a nearly optimum selection of propellant and primer. In order to select the best propellant for a given system, use is made of the relation:

$$web \propto \frac{WV_b}{A}$$

where W and A have the usual meanings and V_b is the projectile velocity at all burnt. This generally occurs in small arms systems at an expansion ratio of about 3.5. For purposes of estimation, the velocity at burnout may be replaced by muzzle velocity, and a new system compared to an existing well performing one.

2-12 THE ATTAINMENT OF HIGHER VELOCITIES

2-12.1 General

In many tactical situations great advantage is derived from the use of guns with higher muzzle velocities. The use of such guns means shorter time of flight to the target and a flatter trajectory thus improving the probability of hitting the target, especially a moving one. Against an armored target such as a tank, high velocity is necessary to penetrate the armor with a projectile depending on striking energy for penetration. The using services therefore demand higher velocity guns.

2-12.2 The Optimum Gun

a. If the geometry of the gun, the mass and geometry of the projectile, the propellant to be used and the maximum pressure are specified, the density of loading is varied there is a density of loading for which the muzzle velocity is a maximum. To avoid exceeding the maximum pressure one must vary the web, increasing the web as the density of loading is increased. Increasing the web will cause the travel of the projectile at burnout to shift toward the muzzle and perhaps increase the variation of the muzzle velocity. The thermodynamic efficiency will also decrease because the muzzle pressure and temperature will be higher, as the gas formed late in the cycle does less work on the projectile. As stated previously, the piezometric efficiency will increase.

b. If the total volume of the gun, the density of loading and the maximum pressure are fixed, and the expansion ratio is varied by changing the chamber volume, the muzzle velocity will attain a maximum value for a certain chamber volume, that is, for a certain charge.

c. When these two conditions are simultaneously

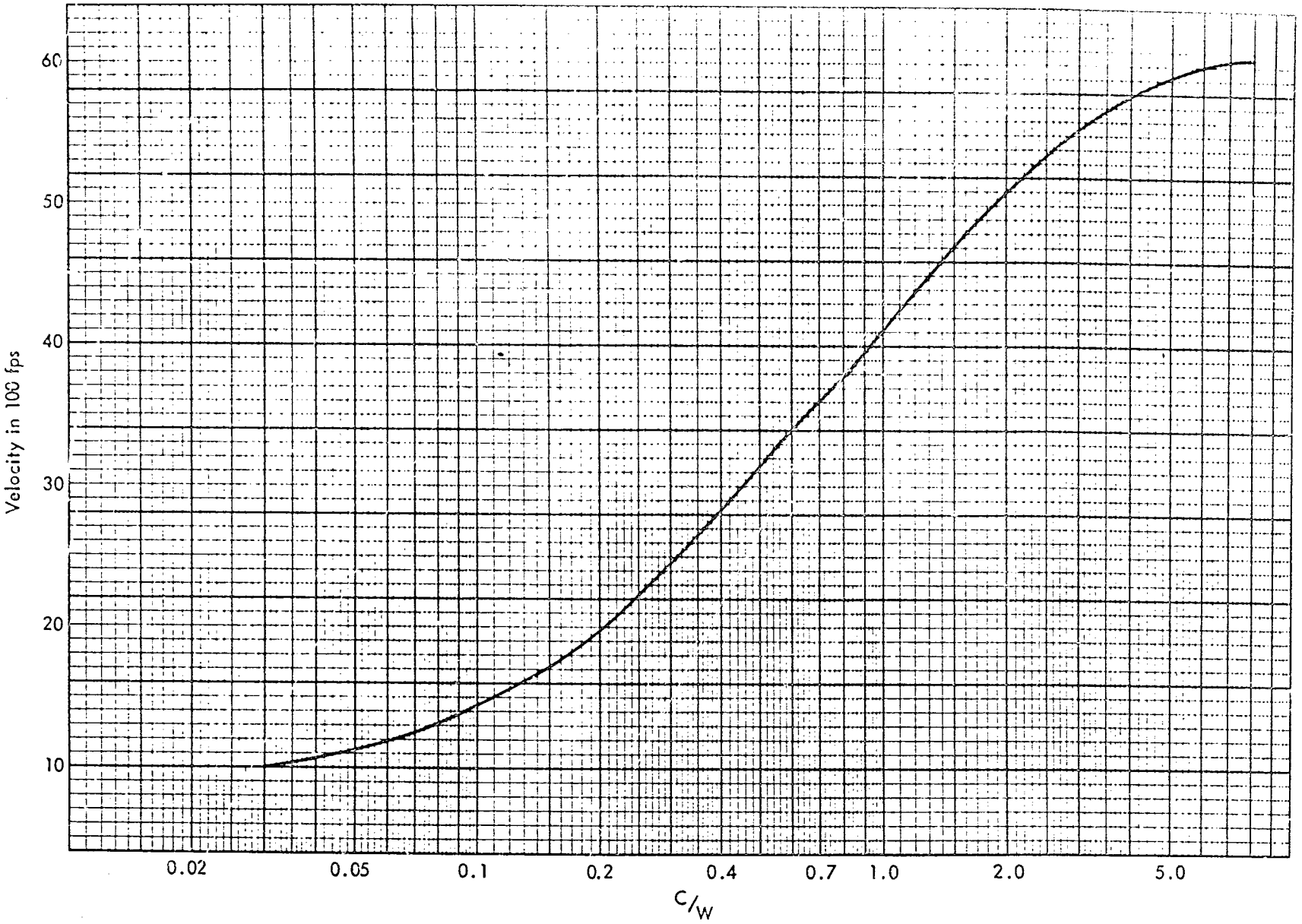


CHART 2-5. *Velocity at $U_m/U_0 = 5$ and $P_m = 60$ kpsi as a Function of C/W (Small Arms)*

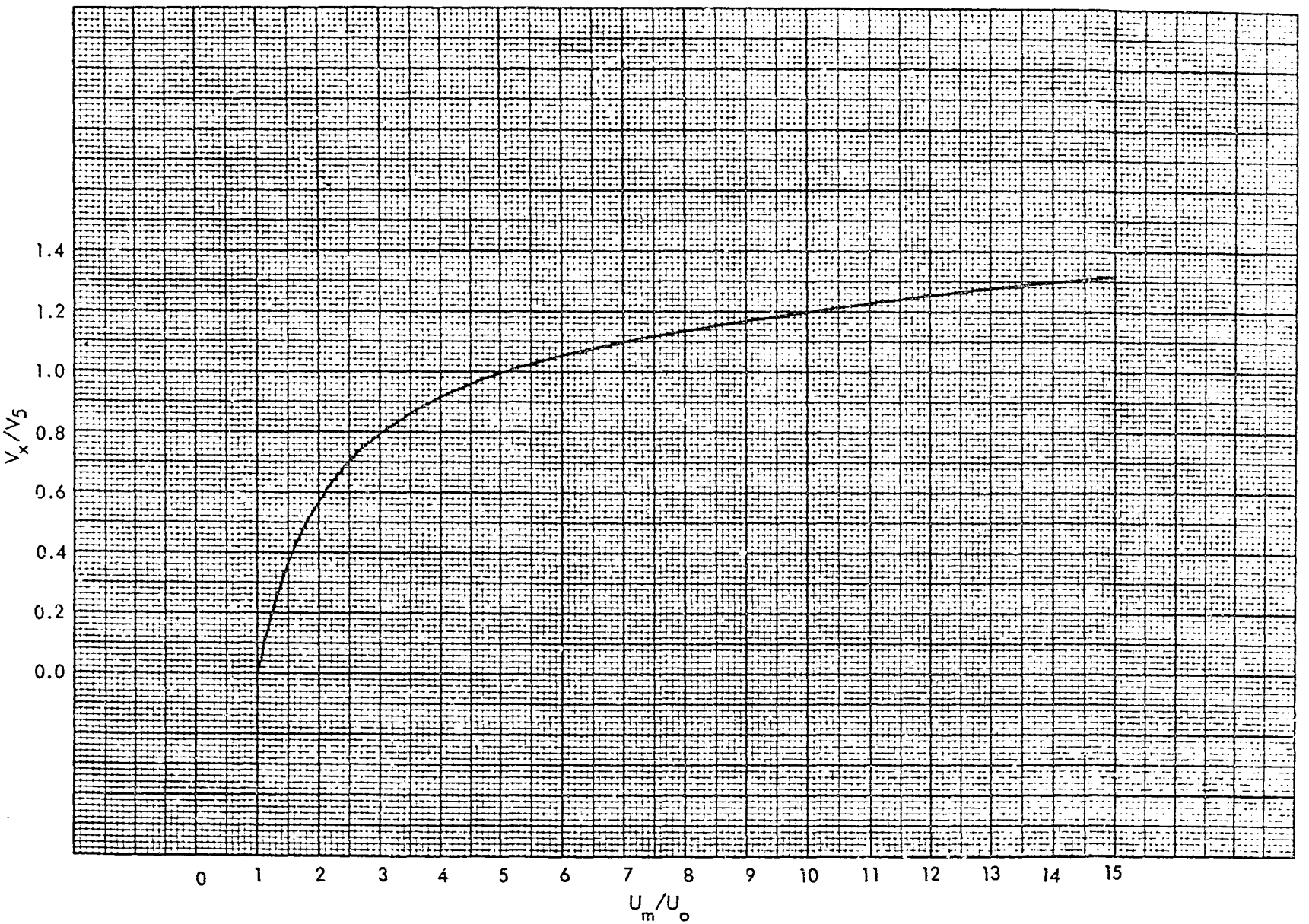


CHART 2-6. *Relative Velocity Normalized to Unity at an Expansion Ratio of 5 as a Function of Expansion Ratio (Small Arms)*

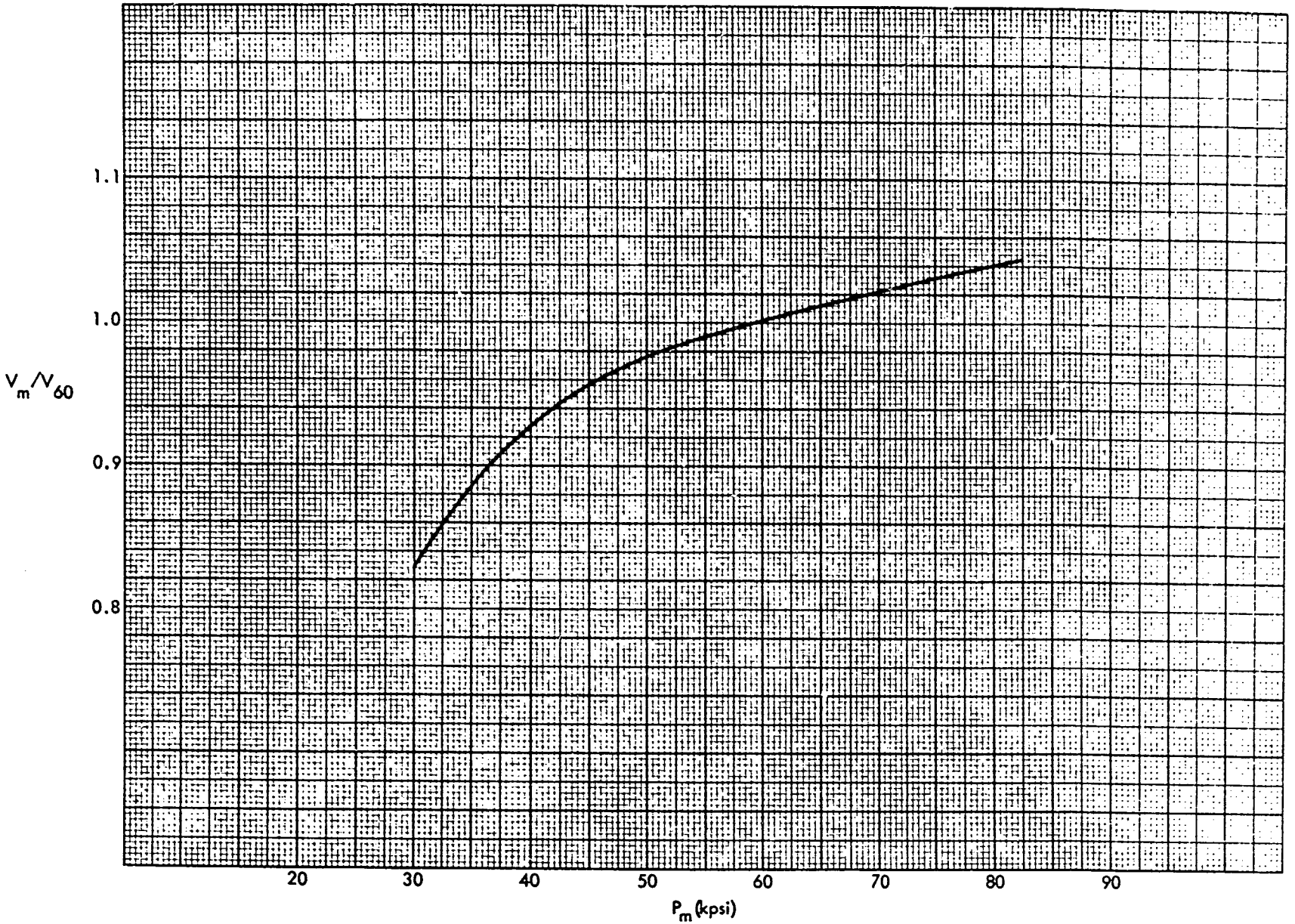


CHART 2-7. *Velocity Relative to the Velocity at a Peak Pressure of 60 kpsi as a Function of Peak Pressure (Small Arms)*

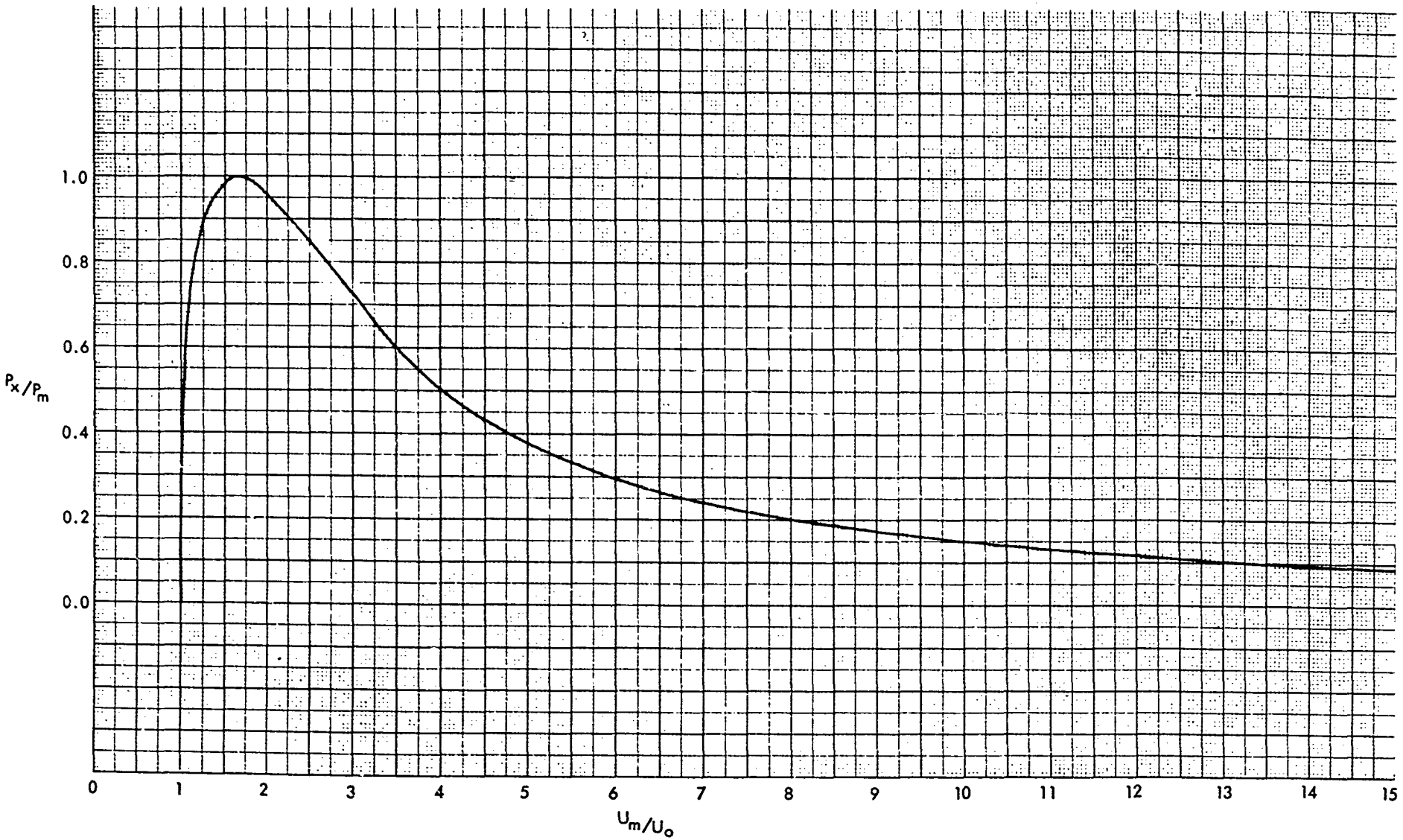


CHART 2-8. *Relative Pressure as a Function of Expansion Ratio*

satisfied, for a gun of specified total volume and maximum pressure, the gun should give the maximum muzzle velocity which can be imparted to the projectile with the propellant used. That is, the gun is operating at its maximum efficiency.

To satisfy these conditions may require a gun having unsatisfactory muzzle velocity regularity or other characteristics that would prohibit its use in practice. Few standard gun systems are optimum in the theoretical sense but employ compromises among the many factors involved.

2-12.3 The Conventional Procedure to Attain Higher Velocities

In order to increase muzzle velocity the available energy must be increased. This involves using a larger charge of hotter propellant with a lower value of γ. The larger charge at optimum density of loading requires a larger chamber. If the expansion ratio is to be near optimum a larger tube volume is required for the gun. In general, the length of the gun must be limited for practical reasons, so that the increased volume must often be attained by increasing the tube diameter. The muzzle velocity for a given projectile travel can be increased further by increasing the permitted operating pressure of the gun by using a stronger tube. Then a smaller web can be used for the optimum density of loading. This will permit the travel at burnt to be smaller and increase the efficiency. To attain higher velocities, therefore, by conventional means, one must use a larger gun operating at higher pressure.

The optimum solution for a specified operating pressure may be such that the caliber of the gun required to give the muzzle velocity wanted is larger than the diameter of the projectile. This means that the projectile must be provided with some type of sleeve, called a sabot, to fit properly in the bore. The sabot forms an integral part of the projectile while in the bore but is designed to be discarded immediately after exit. From an interior ballistic point of view the sabot permits the use of a larger bore which, for a given pressure, increases the force on the projectile and hence the acceleration, so that a higher velocity is reached for the same travel. The extra mass of the sabot is useless and must be kept to a minimum. Design of the sabot is, therefore, a very important feature.

The increase in the operating pressure of the gun is limited by the yield strength of the steel available and also by weight considerations which limit the wall thicknesses which can be used. The strength of the barrel cannot be increased indefinitely by increasing the wall thickness. There is a limiting ratio of inside to outside diameter of the tube beyond which no increase in the tube strength results. Tubes can be made stronger however, by special fabrication methods.[13] The operating pressure will also be limited by the design of the projectile and sabot which may not be able to withstand the resulting base pressures and set back forces due to the larger accelerations. The development of modern high strength steels have made it possible to design gun tubes to withstand higher pressures and the operating pressures of high velocity guns are being constantly increased with a consequent increase in muzzle velocity.

The use of hot propellants is limited by the rapid increase in erosion of the tube that accompanies increase in the temperature of the propellant gas. Since high pressure and velocity also increase the erosion high velocity guns usually have relatively short lives. Special methods for reducing erosion have been developed, however, so that the erosion problem is not as serious as it once was.

2-12.4 Unconventional High Velocity Guns

Several unconventional schemes have been proposed to attain higher muzzle velocities from guns. None of these, however, shows much promise of resulting in a practical field weapon and only one has been much developed as a laboratory device. Two such schemes that have been seriously considered are incorporated in the so called traveling charge gun and the light gas gun. They are both designed to circumvent the limitation imposed on the attainment of high velocity by the pressure gradient which must exist in the gas during expansion and to reduce the amount of kinetic energy in the gas. The more rapidly this expansion must take place the greater will be the drop in pressure between the breech and the projectile base. This limits the acceleration that can be produced and hence the velocity attained in a given travel.

a. The Traveling Charge Gun. The traveling charge gun attempts to surmount this difficulty by having the charge attached to and move with the projectile and burn at the rear surface at such a rate as to form gas just fast enough to maintain a constant pressure in the gas column. The gas then is at rest up to exit of the projectile and a larger fraction of the available energy is transferred to the projectile. Although this ideal situation cannot be realized in practice, some increase in gun efficiency could possibly be attained by partial application of the principle. The main difficulties encountered

in attempts to apply the principle are designing propellants with sufficiently high burning rates and arranging the charge so that the burning rate is sufficiently controllable over the burning period. Even if the difficulties could be overcome, poor muzzle velocity uniformity probably would result. Laboratory studies of the travelling charge principle are described in Reference 14 and work on the development of rapidly burning charges in References 15 and 16.

b. The Light Gas Gun. The light gas gun is so designed that the expanding gas which does work on the projectile has a low molecular weight and a high value of γ. This assures that for a given projectile velocity the fraction of the energy appearing as kinetic energy of the gas is reduced. The pressure gradients in the gas will also be reduced because these depend on the velocity at which rarefaction waves can propagate in the gas; that is, on the velocity of sound in the gas. If the projectile had zero mass, the gas would expand freely. There is a limit to the free rate of expansion determined by what is called the escape speed of the gas given by the relation

$$a_e = \frac{2a_0}{\gamma - 1} \tag{2-168}$$

where a_e is the escape speed and a_0 is the velocity of sound. For a perfect gas a_0 is given by

$$a_0 = (\gamma g R T)^{1/2} \tag{2-169}$$

Since a large escape speed means a reduced pressure gradient for a given expansion rate, the working gas of a gun should have a low molecular weight and a high value of γ. The working gas most often used in light gas guns is helium for which $M = 4$ and $\gamma = \frac{5}{3}$.

Light gas guns have undergone much development as laboratory devices for launching small projectiles of various shapes to be used in experiments on high velocity impact and for launching models for the study of the aerodynamics of projectiles at very high velocities. These developments are continuing and a number of schemes have been proposed and studied. The most successful have been the combustion heated light gas gun[17] and the piston compressor type in which the light gas is heated adiabatically by compression with a propellant driven piston[18].

2-12.5 Extension of Interior Ballistic Theory to High Velocity Weapons

The formulations of the theory of interior ballistics so far presented are limited in their usefulness if applied to very high velocity guns mainly because they lack an adequate incorporation into the theory of the hydrodynamics of the propellant gas. The use of unrealistic expressions for the pressure ratios is one of the chief factors which limit their usefulness when extended to guns with muzzle velocities above about 3000 feet per second (Cf. par. 5-1.1). The development of light gas guns particularly has demanded an extension of interior ballistic theory to permit its application to high velocity weapons[19]. A general discussion of the pressure ratios and their dependence on projectile velocity and chamber geometry is given in Reference 10 of Chapter 5.

2-13 THE HIGH-LOW PRESSURE GUN

Under some circumstances it may be desirable to fire a projectile from a standard gun at much lower than the standard velocity. This means that the gun must operate at a much reduced pressure. The pressure may be so low that it becomes difficult to ignite the charge effectively and the charge may not burn with sufficient uniformity from round to round. To circumvent this difficulty and maintain a high pressure in the chamber and a lower pressure in the bore, a plate pierced by one or more nozzles or holes can be interposed between the chamber and the bore, that is, at the mouth of the cartridge case. The area of the nozzles is adjusted to maintain adequate pressure in the chamber to assure stable ignition and burning and also to provide sufficient mass flow of gas through the nozzles to adjust the pressure in the bore to the required limits. Such a gun is called a high-low pressure gun. A theory of the high-low pressure guns is given in Reference 3. The theory of the burning in the high pressure chamber of such a gun is given by Vinti and Kravitz.[20]

An application of the high-low pressure principle appears in the design of mortar cartridges where part of the charge is ignited and burned inside a perforated chamber. The principle could also have application in special low pressure cartridge actuated thrusters and ejectors such as are used to eject apparatus from aircraft and rockets[21]

2-14 RECOILLESS RIFLES[13]

2-14.1 Theory of Efflux of Gas Through Nozzles[3, 26, 27]

1. Introduction. In order to eliminate the need for heavy recoil mechanisms, some guns are built with a nozzle in the breech, so that part of the propellant gas can flow backward and counterbalance the momentum of the projectile and the

part of the propellant that moves forward. Such guns are called recoilless guns or recoilless rifles.

The theory of efflux of gas through nozzles will first be discussed in simple form and then applied to the interior ballistics of recoilless rifles. This presentation is essentially that developed by Corner[3].

It is assumed that the gas originates in a large reservoir; that the cross-sectional area of the nozzle decreases to a minimum, called the throat; and then the area increases to the exit, where the gas flows into the atmosphere. It is also assumed that the condition of the gas is a function of the coordinate X, measured along the axis of the nozzle, and is uniform across each normal cross section; that loss of heat to the walls, turbulence, and surface resistance can be neglected; and that the fluid does not separate from the walls. The assumption that the reservoir is large means that the conditions in the reservoir do not change appreciably in the time required for an element of the gas to pass through the nozzle; the flow is then said to be quasi-steady; that is, it is assumed that the equations for steady flow apply at each instant of time and may be applied to the non-steady flow in the recoilless rifle. It is also assumed that the nozzle is so designed and that the flow conditions are such that the gas undergoes a continuous expansion through the nozzle so that the velocity of the gas increases steadily and the pressure falls steadily between the reservoir and the exit of the nozzle. This will occur if the reservoir pressure is always considerably higher than the pressure at the exit and if the flow entering the nozzle is subsonic and becomes sonic at the throat of the nozzle. Except at the beginning and possibly the end of the firing cycle of a recoilless gun the pressures and temperatures of the gas are such as to satisfy these conditions.

2. Theory. As stated the following equations are strictly true only for a steady state, but they are approximately true for slowly varying flow. The expansion is adiabatic. The effects of the covolume of the gas are neglected, they amount to only a few percent theoretically, and can be compensated for by using empirical coefficients. The discussion, therefore, is for perfect gases and for adiabatic flow. The fundamental units are as before the inch, pound (weight), second.

The rate of gas flow, q (weight per second), at any section of area, A, is a constant and is given by

$$q = A\rho v = A_t\rho_t v_t \qquad (2\text{-}170)$$

where ρ is the weight of the gas per unit volume and v its velocity. Since the expansion is adiabatic,

$$P\rho^{-\gamma} = P_t\rho_t^{-\gamma} = P_r\rho_r^{-\gamma} \qquad (2\text{-}171)$$

The subscripts r and t refer to conditions in the reservoir and at the throat, respectively. The equation of state of a perfect gas is

$$P/\rho = RT \qquad (2\text{-}172)$$

where R is in inch-pounds per pound weight per degree. The equation of energy may be expressed as

$$\frac{\gamma R(T_r - T)}{\gamma - 1} = \frac{v^2}{2g} \qquad (2\text{-}173)$$

Since

$$\left(\frac{dA}{dx}\right)_t = 0 \qquad (2\text{-}174)$$

by logarithmic differentiation of Equation 2-170

$$\left(\frac{1}{\rho}\frac{d\rho}{dx}\right)_t + \left(\frac{dv}{v\,dx}\right)_t = 0 \qquad (2\text{-}175)$$

From Equations 2-171, 2-172 and 2-175 it can be shown that

$$\frac{T_t}{T_r} = \frac{2}{\gamma + 1} \qquad (2\text{-}176)$$

$$\frac{P_t}{P_r} = \left[\frac{2}{\gamma + 1}\right]^{\gamma/(\gamma-1)} \qquad (2\text{-}177)$$

$$\frac{\rho_t}{\rho_r} = \left[\frac{2}{\gamma + 1}\right]^{1/(\gamma-1)} \qquad (2\text{-}178)$$

and from Equations 2-173 and 2-176

$$v_t^2 = \frac{2\gamma g R T_r}{\gamma + 1} \qquad (2\text{-}179)$$

Let

$$\psi = \gamma^{1/2}\left[\frac{2}{\gamma + 1}\right]^{(\gamma+1)/[2(\gamma-1)]} \qquad (2\text{-}180)$$

Then the rate of flow may be expressed

$$q = \psi\rho_r A_t(gRT_r)^{1/2} \qquad (2\text{-}181)$$

or

$$q = \psi P_r A_t(RT_r)^{-1/2} g^{1/2} \qquad (2\text{-}182)$$

For most propellants, γ is approximately 1.25, and, according to Equation 2-180, ψ is close to 0.66. Actually, the covolume correction and other variations from standard conditions bring the empirical value of ψ a few percent below the theoretical value.

For $\gamma = 1.25$, Equations 2-178 and 2-179 show that the specific weight and velocity at the throat are

$$\rho_t = 0.62\rho_r, \qquad v_t = 1.05(gRT_r)^{1/2}$$

The pressure at any expansion ratio, A_t/A, may be found from the relation

$$\left[\frac{P}{P_r}\right]^{2/\gamma} - \left[\frac{P}{P_r}\right]^{(\gamma+1)/\gamma} = \frac{\gamma-1}{2}\left[\frac{2}{\gamma+1}\right]^{(\gamma+1)/(\gamma-1)}\left[\frac{A_t}{A}\right]^2 \quad (2\text{-}183)$$

For $\gamma = 1.25$, this may be expressed

$$(P/P_r)^{1.6} - (P/P_r)^{1.8} = 0.04335(A_t/A)^2 \quad (2\text{-}183a)$$

The pressure ratios that satisfy Equation 2-183a may be read from Chart 2-9. If desired, the temperature may be found from the relation

$$\left[\frac{T}{T_r}\right]^{2/(\gamma-1)} - \left[\frac{T}{T_r}\right]^{(\gamma+1)/(\gamma-1)} = \frac{\gamma-1}{2}\left[\frac{2}{\gamma+1}\right]^{(\gamma+1)/(\gamma-1)}\left[\frac{A_t}{A}\right]^2 \quad (2\text{-}184)$$

The corresponding gas velocity is given by

$$v^2 = \frac{2\gamma}{\gamma-1} gRT_r[1 - (P/P_r)^{(\gamma-1)/\gamma}] \quad (2\text{-}185)$$

The ratio

$$\left[\frac{v}{v_t}\right]^2 = \frac{\gamma+1}{\gamma-1}\left[1 - \frac{2}{\gamma+1}\left(\frac{A_t v_t}{A_r}\right)^{\gamma-1}\right] \quad (2\text{-}186)$$

can be solved numerically by successive approximations.

3. Thrust. The thrust on the nozzle is the sum of the rate of change of momentum and the force exerted by the excess pressure at the exit:

$$F_T = \frac{q}{g} v_e + A_e(P_e - P_a) \quad (2\text{-}187)$$

In applications to recoilless rifles, the atmospheric pressure, P_a, is negligible compared to the exit pressure, P_e.

The thrust coefficient, C_T, is defined as the ratio

$$C_T = \frac{F_T}{A_t P_r} \quad (2\text{-}188)$$

If there were no expansion, the exit would be at the throat, and the thrust would be

$$(F_T)_t = \frac{q}{g} v_t + A_t P_t \quad (2\text{-}187a)$$

By substituting Equations 2-177, 2-179 and 2-182 in Eq. 2-187a, it is found that the thrust coefficient for this case is

$$(C_T)_t = (\gamma+1)\left[\frac{2}{\gamma+1}\right]^{\gamma/(\gamma-1)} \quad (2\text{-}189)$$

For

$$\gamma = 1.25, \quad (C_T)_t = 1.248 \quad (2\text{-}189a)$$

This formula can be used only if the throat area is small compared to the cross section of the reservoir; for, if the system were a pipe of uniform section, closed at one end, the momentum term in Equation 2-187a would vanish, and $(C_T)_t$ would be equal to 1.

In the usual case of an expanding nozzle, the formula for the thrust coefficient becomes

$$C_T = \left[\frac{2}{\gamma+1}\right]^{\gamma/(\gamma-1)}\left[\gamma\left(\frac{v_e}{v_t}\right) + \left(\frac{A_t}{A_r}\right)^{\gamma-1}\left(\frac{v_t}{v_r}\right)^{\gamma}\right] \quad (2\text{-}190)$$

which can be solved with the help of Equation 2-186. Table 2-3 gives the values of C_T as a function of γ and A_r/A_t. Linear interpolation can be used in this table. The effect of covolume on thrust is small and in the foregoing discussion it has been entirely neglected.

TABLE 2-3. THRUST COEFFICIENT, C_T*

A_r/A_t	$\gamma = 1.20$	$\gamma = 1.30$
1.0	1.242	1.255
1.2	1.318	1.327
1.4	1.369	1.374
1.6	1.408	1.409
1.8	1.439	1.438
2.0	1.466	1.461
2.5	1.516	1.505
3.0	1.554	1.537
3.5	1.583	1.562
4.0	1.607	1.582
5	1.644	1.612
6	1.673	1.635
8	1.713	1.667
10	1.742	1.689

* Table 2-3 has been reprinted in part from J. Corner, *Theory of the Interior Ballistics of Guns*, Copyright 1950, with permission from John Wiley and Sons, Inc.

2-14.2 Application to Recoilless Rifles

1. Assumptions. It is assumed that no unburned propellant is lost through the nozzle, and that the flow out of the gun can be represented by the equations for quasi-steady flow through nozzles, which have been derived in paragraph 2-14.1, beginning instantaneously with a nozzle-start pressure. The nozzle or cartridge case is originally sealed with a rupture closure which ruptures at the nozzle start pressure. It is also assumed that the burning law is

$$\frac{dc}{dt} = \rho SBP^n \quad (2\text{-}191)$$

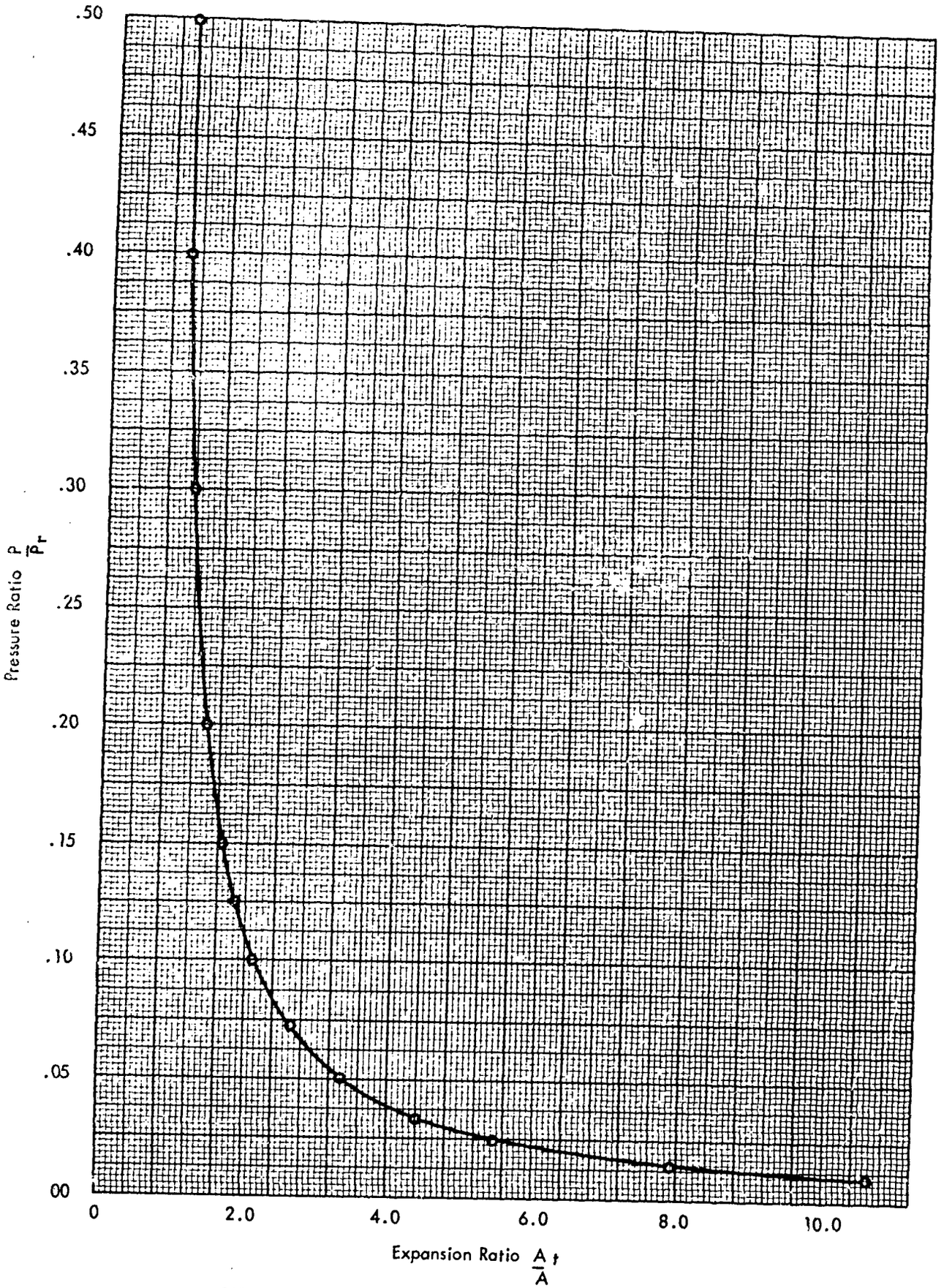


CHART 2-9. *Ratio of Nozzle Pressure to Reservoir Pressure*

but the surface of the grains is not necessarily constant.

2. Equations of Motion. The equation of state for unit weight of the uncooled products of explosion is expressed as

$$P(u_g - \eta) = RT_0 \qquad (2\text{-}192)$$

The specific force is

$$F = RT_0 \qquad (2\text{-}193)$$

The relations connecting the space mean pressure, P, the breech pressure, P_0, and the projectile pressure, P_s, discussed in paragraph 2-2.2, are affected by the flow through the nozzle, because this changes the velocity distribution. At any instant, there is a maximum pressure at some place in the gun; this is identified with the "reservoir pressure", P_r. The propellant weight, C, must here be replaced by kCN, where N is the proportion of the charge that has burned but remains in the gun, and k is an empirical factor (taken as a constant, although it actually varies during the motion of the projectile). When there is no backward flow, $k = 1$; but with backward flow, k is appreciably less than 1. The pressure relations now become (Cf. Equation 2-20)

$$P = \frac{(1 + \theta)W}{(1 + \theta)W + kCN/6} P_r \qquad (2\text{-}194)$$

$$P_s = \frac{(1 + \theta)W}{(1 + \theta)W + kCN/2} P_r \qquad (2\text{-}195)$$

On the basis of Equation 2-195, the modified effective mass of the projectile is (Cf. Equation 2-11)

$$M_1 = \frac{(1 + \theta)W + kCN/2}{g} \qquad (2\text{-}196)$$

The specific volume of the gas, u_g, is assumed to be uniform along the gun. Then the volume occupied by the gas in the gun is

$$CNu_g = U_{ch} + AX - Cu + cu \qquad (2\text{-}197)$$

From Equation 2-194, the equation of state at the reservoir temperature, T_r, may be written

$$P_r(u_g - \eta) = RT_r\left[1 + \frac{kCN}{6(1 + \theta)W}\right] \qquad (2\text{-}198)$$

Multiplying by CN and substituting Eq. 2-197 makes this

$$P_r(U_{ch} + AX - Cu + cu - CN\eta) = CNRT_r\left[1 + \frac{kCN}{6(1 + \theta)W}\right] \qquad (2\text{-}199)$$

During burning, this equation may be approximated by

$$P_r(U_{ch} + AX - Cu) = CNRT_r\left[1 + \frac{kCN}{6(1 + \theta)W}\right] \qquad (2\text{-}199a)$$

After burning, this approximation is inadequate, and Equation 2-199 must be used.

The equations of motion of the projectile are now

$$AP_r = M_1 \frac{dV}{dt}, \qquad V = \frac{dX}{dt} \qquad (2\text{-}200)$$

with M_1 defined by Equation 2-196.

3. Nozzle Flow and Energy. In order to solve these equations, M_1, which involves CN (weight of gas remaining in the gun), must be evaluated. If $C\phi$ denotes the weight of propellant burned, the rate of flow through the nozzle is

$$q = C\frac{d\phi}{dt} - C\frac{dN}{dt} \qquad (2\text{-}201)$$

Substituting Eq. 2-182 in Eq. 2-201

$$C\frac{dN}{dt} = C\frac{d\phi}{dt} - \psi g^{1/2} P_r A_t (RT_r)^{-1/2} \qquad (2\text{-}202)$$

So the reservoir temperature, T_r, must be determined. To do this, divide the temperature differential into three parts:

$$dT_r = dT_1 + dT_2 + dT_3 \qquad (2\text{-}203)$$

First, in providing the kinetic energy, $AP_r dX$, the gas loses temperature by the amount

$$dT_1 = -\frac{gAP_r}{CNc_r} dX \qquad (2\text{-}204)$$

where c_r is the specific heat at constant volume, that is, energy per unit mass per degree. But

$$c_r = \frac{gR}{\gamma - 1} \qquad (2\text{-}205)$$

so

$$dT_1 = -\frac{(\gamma - 1)AP_r}{CNR} dX \qquad (2\text{-}206)$$

Second, if E is the specific internal energy, the gas acquires energy at the rate

$$CE(T_0)\, d\phi = CE(T_r)\, d\phi + \frac{CNc_r}{g} dT_2 \qquad (2\text{-}207)$$

If c_r is constant from T_r to T_0,

$$dT_2 = \frac{T_0 - T_r}{N} d\phi \qquad (2\text{-}208)$$

Third, since the gas that escapes through the nozzle at the rate, q, expands adiabatically

$$\frac{dT_3}{T_r} = \frac{(\gamma - 1)\, d\rho}{\rho} \tag{2-209}$$

neglecting the covolume. Also

$$\frac{d\rho}{\rho} = \frac{dN - d\phi}{N} \tag{2-210}$$

Hence

$$dT_3 = (\gamma - 1)\frac{dN - d\phi}{N} T_r \tag{2-211}$$

Adding Equations 2-206, 2-208 and 2-211, multiplying by N, and substituting in Eq. 2-203 gives

$$N dT_r = -(\gamma - 1)\frac{AP_r}{CR} dX + (T_0 - T_r)\, d\phi + (\gamma - 1)T_r(dN - d\phi) \tag{2-212}$$

Since

$$d(NT_r) = N\, dT_r + T_r\, dN \tag{2-213}$$

Equations 2-202 and 2-212 yield

$$\frac{d(NT_r)}{dt} = -(\bar{\gamma} - 1)\frac{AP_r}{CR}\frac{dX}{dt} + T_0\frac{d\phi}{dt} - \frac{\gamma\psi A_t P_r}{CR}(gRT)^{1/2} \tag{2-214}$$

where $\bar{\gamma}$ denotes the ratio of specific heats adjusted to take account of the loss of heat to the gun, as explained in paragraph 2-2.1.*f*.

In terms of ϕ and P_r, Equation 2-191 may be expressed

$$\frac{d\phi}{dt} = \frac{\rho S B P_r^a}{C} \tag{2-191a}$$

The differential Equations 2-200, 2-202, 2-214 and 2-191a can be solved numerically with the help of Equations 2-196 and 2-199 or 2-199a. Before P_r is high enough to open the nozzle, $A_t = 0$. Before it is high enough to start the projectile, $X = 0$. Before the propellant is all burned, ϕ is less than 1, and Equation 2-199a may be used; after it is all burned, $\phi = 1$ and Equation 2-199 must be used.

4. Recoil Momentum. While the projectile is moving in the bore, there is a force, AP_r, tending to move the rifle backward. While the gas is flowing through the nozzle, there is a thrust, F_T, tending to move the rifle forward. Their difference is the rate of change of momentum:

$$\frac{dm}{dt} = AP_r - F_T \tag{2-215}$$

if $AP_r > F_T$ the momentum, m, is positive to the rear. Using the definition of the thrust coefficient, C_T (Eq. 2-188), and letting

$$\mu = A_t/A \tag{2-216}$$

Equation 2-215 may be written

$$\frac{dm}{dt} = (1 - \mu C_T)AP_r \tag{2-217}$$

Note that A denotes the cross-sectional area of the bore, not the nozzle.

If the nozzle flow starts at the same time as the projectile begins to move, it is theoretically possible to find a throat area that makes the resultant force vanish at all times, including the post-ejection period. The rifle would then be truly recoilless. However, this condition is difficult to achieve. Furthermore, if the nozzle start time, t_n, is different from the projectile start time, t_s, it is theoretically impossible. Therefore, there is no alternative but to make the total integrated momentum zero. Since the force acts for only a short time, the rifle will recoil only a short distance and return to its original position.

Before the projectile is ejected, at time, t_m, the pressure, P_r, is evaluated in solving the interior ballistic equations. Thereafter, according to Hugoniot's theory of efflux of gases from a reservoir

$$P_r = \frac{CN_m RT_m}{U_m}\left[1 + \frac{t - t_m}{\tau}\right]^{-2\gamma/(\gamma-1)} \tag{2-218}$$

where

$$\tau = \frac{2}{\gamma - 1}\left(\frac{U_m}{A + A_t}\right)\left[\frac{1}{\gamma g RT_m}\left(\frac{\gamma + 1}{2}\right)^{(\gamma+1)/(\gamma-1)}\right]^{1/2} \tag{2-219}$$

By integrating Equation 2-217 it is found that the momentum at projectile ejection is

$$m_m = A\int_{t_s}^{t_m} P_r\, dt - \mu C_T A\int_{t_n}^{t_m} P_r\, dt \tag{2-220}$$

Similarly, by substituting Equation 2-218 in Eq. 2-217, the additional momentum after projectile ejection is found

$$\Delta m = (1 - \mu C_T)A\frac{CN_m RT_m}{U_m}\left(\frac{\gamma - 1}{\gamma + 1}\right)\tau \tag{2-221}$$

Approximately, if γ is about 1.25

$$\Delta m = 1.34\frac{1 - \mu C_T}{1 + \mu} CN_m\left(\frac{RT_m}{g}\right)^{1/2} \tag{2-221a}$$

The total momentum, then, is

$$m = m_m + \Delta m \qquad (2\text{-}222)$$

It is theoretically possible to determine a ratio, μ, of throat area to bore area that will make $m = 0$.

5. Ballistic Efficiency. The ballistic efficiency of a conventional weapon is defined as the ratio of the linear kinetic energy of the projectile at the muzzle to the energy of the solid propellant

$$e = \frac{WV_m^2}{2gCE} \qquad (2\text{-}223)$$

The specific energy of the propellant E, defined as $F/\gamma - 1$, is discussed in paragraph 1-8.13. The modification of the projectile weight, considered in paragraph 2-2.1, is neglected here.

In a recoilless rifle, part of the energy is used in preventing recoil. Katsanis has proposed a new definition of its ballistic efficiency[22]

$$e = C_0/C \qquad (2\text{-}224)$$

where C_0 is the propellant weight for an ideal recoilless rifle. If C_e is the weight of propellant gas that leaves the nozzle, the total energy for the ideal recoilless rifle is

$$C_0E = \frac{C_ev_e^2}{2g} + \frac{WV_m^2}{2g} \qquad (2\text{-}225)$$

where v_e is an effective exit velocity. If κ is the fraction of the total energy available to the projectile,

$$\kappa C_0E = \frac{WV_m^2}{2g} \qquad (2\text{-}226)$$

Then the weight of the propellant gas that balances the recoil in the ideal rifle is

$$C_e = (1 - \kappa)C_0 = C_0 - \frac{WV_m^2}{2gE} \qquad (2\text{-}227)$$

The actual recoilless rifle may have a small momentum, which is designated fWV_m/g. The factor, f, is positive if the rifle moves backward; negative if it moves forward. Then the momentum equation is

$$C_ev_e + fWV_m = WV_m \qquad (2\text{-}228)$$

The exit velocity is then

$$v_e = \frac{(1 - f)WV_m}{C_e} \qquad (2\text{-}229)$$

Squaring and multiplying by $C_e/2g$ with the help of Equation 2-227 produces

$$\frac{C_ev_e^2}{2g} = \frac{(1 - f)^2EW^2V_m^2}{2gC_0E - WV_m^2} \qquad (2\text{-}230)$$

Substituting this in Equation 2-225 and rearranging yields

$$C_0 = \frac{WV_m^2}{2gE}\left[1 + \frac{(1 - f)^2W}{C_0 - WV_m^2/2gE}\right] \qquad (2\text{-}231)$$

Solving as a quadratic equation in C_0 gives, as the positive solution

$$C_0 = \frac{WV_m^2}{2gE}\left[1 + \sqrt{(1 - f)^2 2gE/V_m^2}\right] \qquad (2\text{-}232)$$

Therefore, according to the definition, Eq. 2-224, the ballistic efficiency of a recoilless rifle is

$$e = \frac{WV_m^2}{2gCE}\left[1 + \sqrt{(1 - f)^2 2gE/V_m^2}\right] \qquad (2\text{-}233)$$

The ballistic efficiences of the 57mm M18, 75mm M20, 105mm M27, and 106mm M40 Rifles, firing High Explosive, High Explosive Antitank and White Phosphorus Projectiles, vary from 0.44 to 0.54.

2-14.3 Graphical Methods for Recoilless Rifles

To avoid the large amount of computation necessary if a general theory such as that given above is used in the design of conventional recoilless guns, Katsanis has developed a simplified semiempirical treatment and presented it in the form of graphs and nomograms that can be used to determine the interior ballistic trajectories for recoilless rifles of standard characteristics. The method is explained and the graphs and nomograms are presented in usable form in Reference 23.

2-15 SMOOTH BORE MORTARS AND WORN GUNS

Smooth bore mortars are loaded by dropping the fin-stabilized projectile into the muzzle. Therefore, there has to be an appreciable clearance between the bore and the projectile body with the result that some of the propellant gas escapes past the projectile. Thus, the space between the bore and the projectile is like a nozzle, and the theory of efflux through nozzles can be applied to smooth bore mortars. Since the flow is forward, the leakage factor k is equal to unity, (Cf. par. 2-14.2).

In rifled guns, there is no appreciable leakage when they are new; but after they are badly worn, there is considerable leakage between the rotating band and the bottom of the grooves. Therefore, the same theory can be applied to a worn rifled gun as to a smooth bore mortar.

For simplicity, the linear law of burning will be used.

$$w\frac{dz}{dt} = \beta P \tag{2-234}$$

Let

$$\Psi = \frac{\psi A_1 w}{\beta C \lambda^{1/2}} \tag{2-235}$$

where

ψ is the function of γ defined in Equation 2-180
A_1 is the leakage area
$\beta = \frac{B}{\omega}$

Corner[3] shows that a leaking gun behaves almost like an orthodox gun with the effective charge

$$C' = C(1 - \Psi) \tag{2-236}$$

Also, the muzzle velocity, V_m, and maximum pressure, P_p, vary approximately according to the relations

$$V_m \alpha\ 1 - \epsilon\Psi \tag{2-237}$$

$$P_p \alpha\ 1 - 2\Psi \tag{2-238}$$

The coefficient, ϵ, depends on the details of the gun and charge, but is usually about 0.7.

Equation 2-237 may also be expressed

$$\frac{\Delta V_m}{V_m} = -\epsilon\Psi \tag{2-239}$$

or

$$\frac{\Delta V_m}{V_m} = -\frac{\epsilon\psi w}{\beta C F^{1/2}} A_1 \tag{2-239a}$$

With some further approximations, Corner finds that the variation in muzzle velocity is

$$\Delta V_m = -V_1 A_1/A \tag{2-240}$$

where A is the cross-sectional area of the bore, and the coefficient, V_1, is about 24,000 in/sec (2,000 ft/sec). If d is the caliber of the mortar, Δd the diametral clearance between mortar and projectile

$$\Delta V_m = -2V_1 \frac{\Delta d}{d} \tag{2-241}$$

It is thus seen that the clearance should be small, not only to increase the efficiency of the mortar, but also to decrease the dispersion in muzzle velocity, and hence in range. Besides, a small clearance makes the projectile fly nearly straight after ejection, so that the air resistance is minimized.

2-16 THE USE OF HIGH SPEED COMPUTING MACHINES

Large high speed automatic computing machines are becoming increasingly available. Their use will greatly facilitate the solution of the equations of interior ballistics and the reduction of experimental data so that more sophisticated treatments of the theory and more elaborate instrumentation for experiment and testing can be used without too great an expenditure of time and labor. Once a formulation of the theory has been properly prepared for machine computation, the effect of changes in the parameters can be determined very rapidly. The parameters to which the solution is most sensitive can be readily selected and the adjustment for best fit to firing records made with relatively little expenditure of time and labor. These machines will not, however, entirely supercede the use of the simple analytical formulas or the use of charts or tables of solutions as exemplified earlier. For many problems, especially of preliminary design, the simple methods are sufficiently accurate and are rapid and easy to use and do not involve a large computing group.

For treatment of interior ballistic theory devised especially for solution by high speed digital computers the reader is referred to References 24 and 25.

REFERENCES

1. W. C. Taylor and F. Yagi, *A Method for Computing Interior Ballistic Trajectories in Guns for Charges of Arbitrarily Varying Burning Surface*, BRL Report No. 1125, 1961.
2. J. P. Vinti, *The Equations of Interior Ballistics*, BRL Report No. 307, 1942.
3. J. Corner, *Theory of the Interior Ballistics of Guns*, John Wiley & Sons, N. Y., 1950.
4. A. A. Bennett, *Tables for Interior Ballistics*, War Dept. Document No. 2039, 1921. Revision and expansion directed by H. P. Hitchcock, BRL Report No. 993, 1956 and BRL Technical Note No. 1298, 1960.
5. J. E. Mayer and B. I. Hart, "Simplified Equations of Interior Ballistics", J. Franklin Inst. 240, 401 (1945).
6. J. P. Vinti and J. Opernick, *Interior Ballistics for Powder of Constant Burning Surface*, BRL Report No. 625, 1947.
7. P. G. Baer and J. M. Frankle, *Reduction of Interior Ballistic Data from Artillery Weapons by High Speed Digital Computer*, BRL Memorandum Report No. 1148, 1958.
8. J. M. Frankle and J. R. Hudson, *Propellant Surface Area Calculations for Interior Ballistic Systems*, BRL Memorandum Report No. 1187, 1959.
9. H. P. Hitchcock, *Formulas for Differential Variations by Means of Röggla's Charts*, BRL File R-11-31, 1941.
10. H. P. Hitchcock, *Differential Coefficients for Interior Ballistics*, BRL Report No. 169, 1940.
11. R. C. Strittmater, *A Single Chart System of Interior Ballistics*, BRL Report No. 1126, 1961.
12. S. Kravitz, *Nomographs for Interior Ballistics*. Picatinny Arsenal Technical Report No. 3035, 1963.
13. AMCP 706-252, Engineering Design Handbook, *Gun Tubes*.
14. D. C. Vest, *An Experimental Traveling Charge Gun*, BRL Report No. 773, 1951.
15. *Fast Burning Propellant*, Olin Mathieson Chemical Corp., East Alton, Ill., Contract DA-23-073-ORD-369, Phases I, II, and IV, Final Report, 1955.
16. D. C. Vest et al, *A Qualitative Discussion of the Burning Mechanism of Porous Propellants*, BRL Report No. 902, 1954.
17. M. F. Ford, *Performance of a 40mm Combustion-Heated Light Gas Gun Launcher*, Arnold Engineering Development Center Technical Note No. 60-176, 1960.
18. A. C. Charters, B. P. Denardo and V. J. Rossow, *Development of a Piston-Compressor Type Light Gas Gun for Launching of Free Flight Models at High Velocity*, National Advisory Committee for Aeronautics Technical Note No. 4143, 1957.
19. P. G. Baer, "The Application of Interior Ballistic Theory in Predicting the Performance of Light Gas Hypervelocity Launchers", *Fourth Symposium on Hypervelocity Impact*, Vol. II, Air Proving Ground Center Technical Report No. 60-39 (II), 1960.
20. J. P. Vinti and S. Kravitz, *Theory of the Transient State of a Rocket Motor or of the Reservoir of a High-Low Pressure Gun*, BRL Report No. 772, 1951.
21. AMCP 706-270, Engineering Design Handbook, *Propellant Actuated Devices*.
22. D. J. Katsanis, *A New Concept of the Ballistic Efficiency of Recoilless Rifles*, Frankford Arsenal, Pitman-Dunn Lab. Report No. 1312, 1956.
23. D. J. Katsanis, *Graphical Presentation of Ballistics for Recoilless Rifles*, Frankford Arsenal Report No. 1410, 1957.
24. P. G. Baer and J. M. Frankle, *The Simulation of Interior Ballistic Performance of Guns by Digital Computer Program*, BRL Report No. 1183, 1962.
25. S. Kravitz, *A Digital Computer Program for Interior Ballistics*, Picatinny Arsenal Technical Memorandum No. 1127, 1963.
26. AMCP 706-282, Engineering Design Handbook, *Propulsion and Propellants*.
27. M. J. Zucrow, *Principles of Jet Propulsion and Gas Turbines*, John Wiley & Sons, N. Y., 1948.

CHAPTER 3

LIST OF SYMBOLS

A	Cross-sectional area of bore
B	Burning rate coefficient
B	Quantity of heat necessary to raise a unit volume of the metal to the melting point and melt it
C	Weight of propellant
C_p	Specific heat of propellant gas at constant temperature
C_s	Specific heat of steel
C_v	Specific heat of gas at constant volume
c	Weight of burnt propellant
d	Diameter of the bore: the caliber
E	Specific energy of the propellant
E	Burning parameter
EFC	Equivalent full charge factor
F	Specific force of the propellant
$F(l)$	Function of time
F_m	Maximum value of $F(l)$
$f(\tau)$	Heat transfer function
g	Gravitational acceleration
H	Dimensionless heat transfer coefficient
H	Instantaneous rate of heat input to the hot spots per unit area
H'	Time rate of heat flow
h	Heat transfer coefficient
I	Heat transfer integral, defined by Equation 3-52
j	Weight ratio: W'/C
K	Empirical constant
k	Thermal conductivity of steel
L	Heating parameter
L	Heat of fusion of the steel tube
n	Number of moles of gas formed by burning one gram of propellant
P	Pressure
P	Maximum chamber pressure
Q	Heat input
R	Molar gas constant
S	Expansion ratio
T	Temperature of the gas
T_g	Temperature of the gas
T_0	Adiabatic flame temperature
T_i	Initial temperature of the tube
T_m	Average temperature of the gas when the projectile is at the muzzle
T_m	Melting temperature of the tube
t	Time
t'	Time after ejection: $t - t_m$
U	Free volume
U_{ch}	Chamber volume
V	Velocity of projectile
V	Muzzle velocity
V_r	Speed of surface regression
v	Velocity of the gas
v'	Velocity factor
W	Wear per round
W'	Effective weight of projectile
w	Web thickness
X	Travel of projectile
x	Coordinate along the axis of the bore
x	Travel of projectile plus reduced chamber length
y	Reduced coordinate along the axis of the bore: U/A
Z	Empirical constant
z	Coordinate normal to surface
α	Time factor
β	Distance factor
γ	Ratio of specific heats
Δ	Density of loading: C/U_{ch}
δ	Density of solid propellant
ζ	Dimensionless distance from the inner surface of the barrel
η	Specific covolume of the gas
θ	Temperature rise
θ_g	Temperature of the gas
θ_s	Temperature of the metal surface
λ	Friction factor
ρ	Density of the gas
ρ_s	Density of the steel tube
τ	Dimensionless time
ϕ	Factor: $BCgF/wA$

Subscripts

0	Initial value: at time of projectile start
1	Pertaining to ammunition for which $EFC = 1$
1	Beginning of erosion interval
2	End of erosion interval
b	At time when propellant is all burnt
g	Property of the gas
m	At time when the projectile is at the muzzle
p	At time of peak pressure

CHAPTER 3

HEAT TRANSFER, TEMPERATURE DISTRIBUTION AND EROSION OF GUN TUBES

3-1 HEAT TRANSFER

3-1.1 General Discussion

The transformation of the propellant from the solid to the gaseous state produces a large amount of heat and the difference in temperature between the gas and the surface of the gun bore is always very large. This, combined with the fact that the boundary layer is very thin, leads to a large temperature gradient to the surface. This results in a high rate of heat transfer to the surface and appreciable heating of the barrel, in spite of the short time during which the hot gas is in contact with the wall. The heating effect is most marked in rapid-fire weapons, such as machine guns, where the temperature attained limits the number of rounds that may be fired continuously. In the larger caliber slower-fired weapons the heating of the bore surface is a major cause of the erosion of the bore which limits the useful life of the barrel.

The flow of the gas in a gun is highly turbulent and the heat transfer is by forced convection. In treating the problem theoretically, it has been the universal practice to assume that the equations of heat transfer for steady, fully developed flows in pipes or over flat plates can be taken over into the theory for guns, despite the existence of a highly unsteady state, and the lack of a fully developed flow. Due to these conditions the heat transfer varies rapidly with time and the boundary layer has not reached its final form, since the theory must be applied at positions too close to the entrance of the bore. The boundary layer is always very thin and has not reached its final form for steady flow anywhere in the barrel.

The theory starts by assuming the well known heat transfer equation

$$H' = h(\theta_g - \theta_s) \qquad (3\text{-}1)$$

where

H' is the time rate of heat flow
θ_g the temperature of the fluid in the flow beyond the boundary layer
θ_s the temperature of the surface and
h the heat transfer coefficient

3-1.2 Heat Transfer Coefficient

Nordheim, Soodak and Nordheim made an extensive study of thermal effects of propellant gases.[1] They assumed that Equation 3-1 is valid, in the sense that it is valid at each instant of time. Although this assumption is doubtful, the results appear to be reasonable. The following discussion is based on their work.

There exists an extensive literature on the specification of h. A very simple formula for h which is adequate for the heat transfer problem in guns was adopted by the investigators, namely:

$$h = 0.5\lambda C_p \rho v \qquad (3\text{-}2)$$

where C_p is the specific heat of the gas at constant pressure, and ρ and v its density and velocity, respectively. The dimensionless factor, λ, is called the friction factor. It is related to the frictional force on the surface due to the flow of the gas and hence on the momentum transfer to the surface. Equation 3-2 expresses the analogy between the momentum transfer and the heat transfer and is called the Reynolds analogy. λ depends on the surface condition, particularly on the roughness. It is not possible to specify the roughness, or its effect upon λ, in any simple way so that λ must be determined by comparison with experiment.

The only experimental data on guns available at the time were data derived from calorimetric measurements made, just beyond the forcing cone on a caliber .50 machine gun, by Machler.[2] Based on these measurements a value of λ for this weapon, equal approximately to 5×10^{-3}, was derived. Two assumptions were made concerning the distribution of the unburnt propellant; (a) that it was uniformly distributed in the gas, and (b) that it remained in the chamber, so that the value of λ depends on the assumption used. Assumption (a) is the better assumption and is assumed in all the systems presented in this handbook.

To evaluate λ for other calibers a formula based

on heat transfer in pipes was modified and stated in the form

$$\lambda = (Z + 4 \log_{10} d)^{-2} \qquad (3\text{-}3)$$

where d is the caliber and Z is an empirical constant. When d is expressed in centimeters, Z has the value 13.2. This formula asserts that λ depends only on d. Later experiment has shown that this is not so, as λ is also a function of position along the tube. It will also depend on the condition of the bore surface. The validity of Equation 3-3 is doubtful, but it will be used here.

3-1.3 Calculation of the Rate of Heat Input

a. Heat Transfer Coefficient. Consider the example of paragraph 2-3.9*a*, pertaining to the 105mm Howitzer firing a High Explosive Projectile M1 propelled by propellant M1. To calculate the rate of heat input, H', the heat transfer coefficient, h, must be determined by Equation 3-2.

By Equation 3-3, with

$$Z = 13.2$$

$$d = 10.5 \text{ cm}$$

the friction factor is

$$\lambda = 1\ 300$$

The effective chamber length is	$U_{ch}/A = 11.5$ in
The total travel is	$X_m = 80.4$ in
Distance from the breech to the muzzle	$= 91.9$ in
The muzzle velocity is	$V_m = 8789$ in/sec

Therefore, assuming the gas velocity to vary linearly from the breech to the projectile when the projectile is at the muzzle, the estimated gas velocity at the front end of the chamber is

$$v = \frac{11.5}{91.9} 8789 = 1100 \text{ in/sec}$$

Using a value of C_v equal to 199 cal/lb-°K and substituting these values in Equation 3-2 gives

$h = 0.187$ cal in²-sec-°K at the front end of the chamber

$h = 1.493$ cal/in²-sec-°K at the muzzle

b. Temperature Before Ejection. The temperature of the propellant gas needs also to be known. With substitution of Equation 2-14 in Equation 9 of Reference 3 and the assumption that the specific covolume of the gas is equal to the specific volume of the solid propellant, the equation of state may be written

$$\frac{cFT_v}{T_0} = PU \qquad (3\text{-}4)$$

where

F is the specific force of the propellant
T_v the absolute temperature of the gas
T_0 the adiabatic flame temperature
U the free volume
P the pressure and
c the weight of burnt propellant

It was shown in Chapter 1 that

$$T_0 = \frac{F}{(\gamma - 1)C_v} \qquad (3\text{-}5)$$

where C_v is an appropriate average value of the specific heat at constant volume. Hence,

$$T_v = \frac{PU}{(\gamma - 1)C_v c} \qquad (3\text{-}6)$$

In the example chosen,

$$P = P_m = 1040 \text{ psi}$$

$$U = U_m = 1220 \text{ in}^3$$

$$\gamma - 1 = 0.26$$

$$C_v = 5846 \text{ in-lb/lb-°K}$$

$$c = C = 0.625 \text{ lb}$$

By substitution in Equation 3-6 when the projectile is at the muzzle, the absolute temperature is

$$T_v = T_m = 1336°\text{K}$$

If the inner surface of the gun is taken as 300°K then

$\theta_v - \theta_s = T_v - 300 = 1036°$K and by Eq. 3-1 the heat input rate

$H' = 0.187\ (1036) = 194$ cal/in²-sec at the front end of the chamber and

$H' = 1.493\ (1036) = 1547$ cal/in²-sec at the muzzle

c. Density, Velocity and Temperature After Ejection. After the projectile is ejected, the hot gas remaining in the bore continues to transmit heat to the barrel. The density, velocity and temperature can be determined during this phase by the following.

Let

$$x = X + U_{ch}/A \qquad (3\text{-}7)$$

The density, ρ, pressure, P, and temperature, T_v should be nearly independent of x; but the velocity, v, may be assumed to be a linear function of x:

$$v = v'x \qquad (3\text{-}8)$$

where the factor, v', is a function of the time, t, only.

Since the motion of the gas is assumed to be one-dimensional, the equations of continuity, motion, and energy may be expressed

$$\frac{\partial \rho}{\partial t} + \rho \frac{\partial v}{\partial x} = 0 \tag{3-9}$$

$$\frac{dv}{dt} = \frac{\partial v}{\partial t} + v \frac{\partial v}{\partial x} = 0 \tag{3-10}$$

$$C_v \rho \frac{\partial T_g}{\partial t} + P \frac{\partial v}{\partial x} = 0 \tag{3-11}$$

Under the above assumptions, these equations become

$$\frac{d\rho}{dt} + \rho v' = 0 \tag{3-12}$$

$$\frac{dv'}{dt} + v'^2 = 0 \tag{3-13}$$

$$C_v \rho \frac{dT_g}{dt} + Pv' = 0 \tag{3-14}$$

Let the subscript m denote values at ejection, and let

$$t' = t - t_m \tag{3-15}$$

Then integration of Equation 3-13 leds to

$$v' = \frac{v'_m}{1 + v'_m t'} \tag{3-16}$$

Hence, by Equation 3-8, the velocity is

$$v = \frac{v'_m x}{1 + v'_m t'} \tag{3-17}$$

It is evident that

$$x_m = V_m, \qquad v'_m = V_m x_m \tag{3-18}$$

where V_m is the muzzle velocity of the projectile.

Integration of Equation 3-12 gives

$$\rho / \rho_m = v' / v'_m \tag{3-19}$$

Hence, by substituting Equation 3-16, the density is found

$$\rho = \frac{\rho_m}{1 + v'_m t'} \tag{3-20}$$

The equation of state is

$$P(1/\rho - \eta) = nRT_g \tag{3-21}$$

where

η is the specific covolume of the gas
n the number of moles of gas formed by burning one gram of propellant and
R the molar gas constant

Substituting this in Equation 3-14 gives

$$C_v \frac{dT_g}{dt} = \frac{nRT_g v'}{1 - \eta\rho} \tag{3-22}$$

Assuming

$$nR = C_v(\gamma - 1) \tag{3-23}$$

and with the help of Equations 3-16 and 3-20,

$$\frac{1}{T_g} \frac{dT_g}{dt} = \frac{(\gamma - 1)v'_m}{1 + v'_m t' - \eta\rho_m} \tag{3-24}$$

The integral of this is

$$T_g = T_m \left[\frac{1 - \eta\rho_m}{1 + v'_m t' - \eta\rho_m}\right]^{\gamma - 1} \tag{3-25a}$$

or

$$T_g = T_m \left[\frac{1/\rho_m - \eta}{1/\rho - \eta}\right]^{\gamma - 1} \tag{3-25b}$$

which is the adiabatic relation for an imperfect gas that obeys the equation of state (Eq. 3-21). Here, the ratio of specific heats, γ, should be adjusted to take account of the loss of heat; as in paragraph 2-2.1. Let us assume $\gamma = 1.30$.

By Equations 3-20, 3-21 and 3-25, the pressure is

$$P = P_m \left[\frac{1/\rho_m - \eta}{1/\rho - \eta}\right]^{\gamma} \tag{3-26a}$$

or

$$P = P_m \left[\frac{1 - \eta\rho_m}{1 + v'_m t' - \eta\rho}\right]^{\gamma} \tag{3-26b}$$

This example can be continued by calculating the rate of heat input at the muzzle 0.1 second after the projectile is ejected.

Symbol	Value	Unit	Remarks
t'	0.1	sec	Assumed
$x = x_m$	91.9	in	Given
V_m	8789	in/sec	Given
ρ_m	5.12×10^{-4}	lb/in³	Given
T_m	1336	°K	Given
P_m	1040	lb/in²	Given
C_v	199	cal/lb-°K	Given
λ	1/300		Given
η	27.7	in³/lb	Par. 2-2.1
γ	1.30		Given
v'_m	95.6	sec^{-1}	Eq. 3-18
$1 + v'_m t'$	10.56		
v	832	in/sec	Eq. 3-17
ρ	4.85×10^{-5}	lb/in³	Eq. 3-20
h	0.0134	cal/in²-sec-°K	Eq. 3-2
T_g	657	°K	Eq. 3-25a
$\theta_g - \theta_s$	357	°K	
H'	4.78	cal/in²-sec	Eq. 3-1
P	48.1	lb/in²	Eq. 3-26b

3-1.4 Nondimensional Heat Transfer Coefficient

In order to apply the calculation of heat input to all calibers, it is convenient to define a nondimensional heat transfer coefficient.

A simple interior ballistic theory similar to that of Mayer and Hart (paragraph 2-5.2) is used. The notion in the following has been changed where necessary from that used in Reference 1 to conform to the notation used in Chapter 2.

The burning rate coefficient, B, is defined by the weight burning rate law

$$\frac{dc}{dt} = \frac{BCP}{w}$$

The position of the projectile is defined by the coordinate

$$y = V/A \tag{3-27}$$

Its initial position is then $y_0 = V_{ch}/A$. The relation between the position of the projectile and its velocity is given, up to the time the charge burns out, by

$$\frac{y}{y_0} = \left[\frac{1}{1 - \dfrac{\gamma - 1}{2\phi} V}\right]^{2/(\gamma-1)} \tag{3-28}$$

where ϕ has the dimensions of velocity and is given by

$$\phi = \frac{BCF}{wA} \tag{3-29}$$

Equation 3-28 holds up to $y = y_b$, the position of the projectile at the time of charge burnout, when it becomes

$$\frac{y_b}{y_0} = \left[\frac{1}{1 - E}\right]^{2/(\gamma-1)} \tag{3-30}$$

where E is given by

$$E = \frac{\gamma - 1}{2} \frac{gF}{j\phi^2} \tag{3-31}$$

and j is equal to W/C. E is called the burning parameter. It is dimensionless and specifies the gun-ammunition system. Systems with the same E have similar ballistics. From Equation 3-28 V is given by

$$V = \frac{2\phi}{\gamma - 1}\left[\left(1 - \frac{y_0}{y}\right)^{(\gamma-1)/2}\right] \tag{3-32}$$

before the charge burns out. After burnout it is given by

$$V = \left(\frac{2E}{j(\gamma - 1)}\right)^{1/2}\left[1 - \left(\frac{y_b}{y_0}\right)^{\gamma-1}\left(\frac{y_0}{y}\right)^{\gamma-1}\right]^{1/2} \tag{3-32a}$$

The pressures before and after burnout are given respectively, by

$$P = \frac{F\Delta}{1 - \Delta/\delta}\frac{1}{E}\left(\frac{y_0}{y}\right)^{(\gamma+1)/2}\left(1 - \frac{y_0}{y}\right)^{(\gamma-1)/2} \tag{3-33}$$

and

$$P = \frac{F\Delta}{1 - \Delta/\delta}\left(\frac{y_b}{y_0}\right)^{(\gamma-1)/2}\left(\frac{y_0}{y}\right)^{\gamma} \tag{3-33a}$$

The maximum pressure comes at

$$\frac{y_{p\,max}}{y_0} = \left(\frac{2\gamma}{\gamma + 1}\right)^{2/(\gamma-1)} \tag{3-34}$$

unless $y_{p\,max}$ is not greater than y_b, when it comes at y_b. The value of the maximum pressure is given by

$$P_{max} = \frac{j\Delta}{1 - \Delta/\delta}\phi^2\frac{1}{\gamma}\left(\frac{\gamma + 1}{2\gamma}\right)^{(\gamma+1)/(\gamma-1)}$$

$$\text{for} \quad E \geqq (\gamma + 1)/2\gamma \tag{3-35}$$

$$P_{max} = \frac{j\Delta F}{1 - \Delta/\delta}(1 - E)^{(\gamma+1)/(\gamma-1)}$$

$$\text{for} \quad E < (\gamma + 1)/2\gamma \tag{3-35a}$$

The gas temperatures are given by

$$T = T_0\left(\frac{y_0}{y}\right)^{(\gamma-1)/2} \quad \text{before burnout} \tag{3-36}$$

$$T = T_0\left(\frac{y_b}{y_0}\right)^{(\gamma-1)/2}\left(\frac{y_0}{y}\right)^{\gamma-1} \quad \text{after burnout} \tag{3-36a}$$

In using the system, the values of ϕ and, hence, E are determined from Equations 3-35 and 3-35a from the observed maximum pressure. The ballistics can then be cross checked by comparing the muzzle velocity calculated from Equation 3-32a with the observed value. The calculation of ϕ from Equation 3-29 leads to poor results because the value of B is not well known.

It is to be noted that in Equations 3-32 to 3-36 the dimensions of the gun do not appear. Also since $V/y_0 = d/dt(y/y_0)$, an examination of Equations 3-32 and 3-32a shows that if a reduced time defined by

$$\tau = \frac{2\phi}{y_0(\gamma - 1)}t = \alpha t \tag{3-37}$$

is introduced, the velocity-time curves for all guns are the same on the reduced scale. The result is that for a given gun class defined by E, a change in the size of the gun means simply a change in the time scale. All ballistic curves are the same except for multiplicative factors when expressed as functions

of the reduced time. This result is true, of course, only to the approximation of the simple theory.

It follows from the above discussion that, to this approximation, the heat transfer coefficient, h, is a universal function of the reduced time variable, τ, except for the multiplicative factor, λ, so that

$$h = \lambda h_u \tag{3-38}$$

where h_u applies to all cases if expressed in the τ scale.

3-2 TEMPERATURE DISTRIBUTION

3-2.1 The Equations of Temperature Distribution in Reduced Variables

To calculate the temperature distribution in the gun one must solve the Fourier equation of heat conduction subject to the proper boundary condition. The curvature of the bore surface is neglected and the equation is restricted to one dimension. This approximation is also used by Corner (Reference 1 of Chapter 1) and is probably sufficient in view of the other approximations in the theory. Variations in the thermal properties of the barrel material are also neglected and constant average values are assumed.

The Fourier equation in one dimension is

$$\frac{\partial \theta}{\partial t} = \frac{k}{C_s \rho_s} \frac{\partial^2 \theta}{\partial z^2} \tag{3-39}$$

where k, C_s and ρ_s are the thermal conductivity, the specific heat and the density, respectively, of the material in which the heat is being conducted; in the case of the gun, the steel of the barrel wall. The boundary condition at the wall expressing the conservation of heat flux is

$$h(\theta_g - \theta_s) + k \frac{\partial \theta}{\partial z} = 0 \tag{3-40}$$

where z is a coordinate normal to the surface in the direction of heat flow. The initial condition is

$$\theta(0, z) = 0 \tag{3-41}$$

so that θ represents temperature above the initial temperature of the barrel.

Substituting the reduced variables $\tau = \alpha t$ and $\zeta = \beta z$ where $\beta^2 = C_s \rho_s \alpha / 2k$ Equations 3-39, 3-40 and 3-41 become, respectively,

$$\frac{\partial \theta}{\partial \tau} = \frac{1}{2} \frac{\partial^2 \theta}{\partial \zeta^2} \tag{3-39a}$$

$$H(\theta_g - \theta_s) + \frac{\partial \theta}{\partial \zeta} = 0 \tag{3-40a}$$

$$\theta(0, \zeta) = 0 \tag{3-41a}$$

where

$$H = \frac{\sqrt{2}h}{\sqrt{\alpha k C_s \rho_s}} = \frac{\sqrt{2}\lambda h_u}{\sqrt{\alpha k C_s \rho_s}} \tag{3-42}$$

is the reduced heat transfer coefficient.

If it is assumed that the unburnt propellant is uniformly distributed in the gas the mass flow of the gas is given by

$$\rho r = \frac{A_s \rho_p \dfrac{dx}{dt}}{A_s \left[A x - \dfrac{(C - c)}{\rho_p} \right]} \tag{3-43}$$

where x is the axial coordinate of position along the barrel defined by

$$x = V_x / A \tag{3-44}$$

where V_x is the volume between the position, x, and the breech. x_s is the position at which ρr is determined, x is the position of the projectile and dx/dt its velocity. ρ_p is the density of the propellant.

The coefficient H can be expressed as a function of the reduced distance down the bore x_s / x_0 (where $x_0 = V_{x_0} / A$), and the reduced time, τ, in the form

$$H = (x_s / x_0) L f(\tau). \tag{3-45}$$

L, which is called the heating parameter, is given by

$$L = \frac{\lambda C_p}{\sqrt{2k C_s \rho_s}} \left[\frac{C}{A} \right]^{1/2} \frac{1}{E} \left[\frac{\Delta}{1 - \Delta / \rho_p} \frac{2\phi}{\gamma - 1} \right]^{1/2} \tag{3-46}$$

where Δ is here defined as C / C_{x_0}. L is a function only of specific quantities related to the gun system. The time dependence is given by $f(\tau)$ which is expressed as

$$f(\tau) = \frac{\left[1 - (y_0 / y)^{(\gamma - 1)/2} \right]^2}{\left[1 - \dfrac{\Delta}{\rho_p} \right] \dfrac{y}{y_0} + \dfrac{\Delta}{E \left[1 - \dfrac{\Delta}{\rho_p} \right]} \left\{ 1 - \left(\dfrac{y_0}{y} \right)^{(\gamma - 1)/2} \right\} \left| \dfrac{y}{y_0} + \dfrac{\Delta / \rho_p}{1 - \dfrac{\Delta}{\rho_p}} \right|} \tag{3-47}$$

before burnout, and

$$f(\tau) = \frac{E^{3/2}\left[1 - \frac{1}{1-E}(y_0/y)^{\gamma-1}\right]^{1/2}}{\left[1 - \frac{\Delta}{\rho_p}\right]\left[\frac{y}{y_0} + \frac{\Delta/\rho}{1-\frac{\Delta}{\rho_p}}\right]^2} \qquad (3\text{-}47a)$$

after burnout.

$f(\tau)$ is tabulated in Tables 3-1 and 3-2.

The theory so far developed holds up to the time of exit of the projectile. After exit the hot gases continue to flow from the tube and so continue to transfer heat by turbulent forced convection. For location near the muzzle most of the heat is so transferred. If the gases in the barrel undergo a uniform adiabatic expansion, from Equations 3-16, 3-17 and 3-26a,

$$H = H_m \frac{1}{[1 + b(\tau - \tau_m)]^2} \qquad (3\text{-}48)$$

$$T = T_m\left[\frac{1 - \eta C' A x_m}{1 - \eta C' A x_m + b(\tau - \tau_m)}\right]^{\gamma-1} \qquad (3\text{-}49)$$

where the subscript m indicates values when the projectile is at the muzzle and $b = V_m/\alpha x_m$. The problem is now completely specified.

Equations 3-39a, 3-40a and 3-41a cannot be solved analytically. They have been solved numerically for a limited range of the parameters and tables of the solutions are published in Reference 1. The theory has been coded for machine computation at the Ballistic Research Laboratories.

3-2.2 Heat Input

After the temperature distribution for any specified time has been computed, the heat input, Q, up to the specified time can be found by means of the integral

$$Q = \int_0^\infty C_s \rho_s \theta(z, \tau)\, dz \qquad (3\text{-}50)$$

In terms of the nondimensional distance, ζ

$$Q = (2kC_s\rho_s/\alpha)^{1/2} I(\tau, y/y_0), \qquad (3\text{-}51)$$

where

$$I(\tau, y/y_0) = \int_0^\infty \theta(\zeta, \tau)\, d\zeta. \qquad (3\text{-}52)$$

Two values of Q are of special interest: at the time when the projectile leaves the muzzle, and at an infinite time. Therefore, the heat transfer integral, I, is tabulated in Table 3-3 as a function of y/y_0 and the heating parameter, L, for two values of the burning time, τ_b, at muzzle time corresponding to two values of y_m/y_0, and also at $\tau = \infty$.

3-2.3 The "Thermal Analyzer"

The solution of the Fourier equation is quite complicated, even for a single round, and even more

TABLE 3-1. HEAT TRANSFER FUNCTION, $f(\tau)$, FOR GUNS DURING BURNING

τ	$1000\,f(\tau)$	τ	$1000\,f(\tau)$	τ	$1000\,f(\tau)$
0	0.068	12	1.51	24	3.90
1	0.100	13	1.78	25	3.88
2	0.132	14	2.06	26	3.88
3	0.177	15	2.34	27	3.88
4	0.230	16	2.62	28	3.84
5	0.310	17	2.89	29	3.78
6	0.404	18	3.15	30	3.72
7	0.524	19	3.35	31	3.64
8	0.661	20	3.54	32	3.54
9	0.840	21	3.68	33	3.43
10	0.999	22	3.79	34	3.31
11	1.24	23	3.86	35	3.20

TABLE 3-2. HEAT TRANSFER FUNCTION, $f(\tau)$, FOR GUNS AFTER ALL BURNT FOR τ_b = 24 AND 28

	$\tau_b = 24$				$\tau_b = 28$		
τ	$1000\,f(\tau)$	τ	$1000\,f(\tau)$	τ	$1000\,f(\tau)$	τ	$1000\,f(\tau)$
25	3.80	53	.675	29	3.80	62	.552
26	3.60	57	.550	30	3.60	66	.446
27	3.40	61	.456	31	3.39	70	.367
28	3.20	65	.386	32	3.18	74	.308
29	3.00	69	.322	33	2.99	78	.262
30	2.81	73	.285	34	2.80	82	.226
31	2.63	77	.248	35	2.62	86	.197
32	2.46	81	.219	36	2.46	102	.122
33	2.30	85	.194	37	2.30	118	.0835
34	2.14	89	.175	38	2.16	134	.0605
35	2.01	105	.117	39	2.00	150	.0458
36	1.88	121	.0844	40	1.88	166	.0358
37	1.76	137	.0632	41	1.76	182	.0289
38	1.65	153	.0494	42	1.64	198	.0237
39	1.54	169	.0396	46	1.31	214	.0199
40	1.45	185	.0325	50	1.04	230	.0168
41	1.36	201	.0270	54	0.850	246	.0145
42	1.28	217	.0230	58	0.699		
43	1.21	233	.0197	Projectile			
44	1.14	249	.0171	leaves muzzle			
45	1.07						
46	1.01						
47	0.961						
48	0.910						
49	0.860						
Projectile							
leaves muzzle							

so for a series in rapid succession since the solution must be repeated for each round using as initial conditions the temperature distribution resulting from the previous rounds. For points a short distance below the surface, however, the temperature history is insensitive to the details of the heat transfer and the problem can be simplified by assuming that the heat is transferred in a series of instantaneous pulses. This assumption is usually made in treating the problem of heating in machine guns.

Purdue University has built an electrical analog computer or "thermal analyzer" to determine the temperature distribution in machine guns.[4]

TABLE 3-3. HEAT TRANSFER INTEGRAL, *I*.

			I			
τ_0	η_0	η/η_0	28.4	49.4	86.5	148
21	8.3	1.0	1830	2730	3880	4910
		1.2	1970	2880	3910	4910
		1.6	2000	2810	3770	4590
		2.1	1840	2600	3510	4140
		2.7	1620	2320	3050	3710
		4.7	900	1330	1840	2350
		8.3	0	0	0	0
	10.3	1.0	1830	2820	3980	5030
		1.2	2030	2960	4020	5030
		1.6	2070	2920	3850	4740
		2.1	1940	2730	3570	4330
		2.7	1750	2470	3240	3940
		4.7	1080	1590	2200	2760
		8.3	440	650	920	1230
	$\tau = \infty$	1.0	2100	3000	4260	5330
		1.2	2220	3200	4310	5350
		1.6	2310	3190	4210	5120
		2.1	2210	3080	4010	4840
		2.7	2060	2910	3810	4630
		4.7	1590	2300	3090	3870
		8.3	1390	1980	2750	3450
28	8.9	1.0	2030	2980	4350	5270
		1.6	2220	3120	4090	4920
		2.5	2000	2780	3580	4240
		3.1	1700	2340	3020	3650
		5.5	1030	1480	1990	2420
		8.3	0	0	0	0
	11.3	1.0	2100	3070	4280	5330
		1.6	2320	3230	4240	5070
		2.5	2120	2940	3780	4450
		3.1	1870	2560	3330	3960
		5.5	1310	1850	2440	2950
		8.3	580	860	1210	1550
	$\tau = \infty$	1.0	2320	3320	4530	5580
		1.6	2570	3510	4550	5400
		2.5	2420	3310	4200	4950
		3.1	2230	3040	3870	4650
		5.5	1870	2610	3380	4050
		8.3	1450	2070	2800	3460

3-2.4 Comparison With Experiment

A detailed and extensive comparison of the results of the theory of Reference 1 with the experimental measurements available at the time is given in Reference 5. A more recent comparison with measurements made in a 37mm gun can be found in Reference 6. The general conclusion from these studies is that the theory yields results which are fairly reliable, perhaps better than one might expect in view of the drastic assumptions underlying it. In most cases the agreement is within 20 percent using values of λ for different calibers derived from Equation 3-3. If λ is fitted to the experimental data, it turns out that λ is a function not only of caliber but of position in the bore as well as propellant type and probably other factors. It would be expected to depend on position in the bore because when a gun is used the bore always becomes roughened preferentially near the breech and near the muzzle. In general the fitted values of λ seem to follow a corresponding pattern.

Except on the outer surface accurate measurements of barrel temperature are difficult to make. This is especially true of the bore surface temperature (see paragraph 4-9.1). In fact it is doubtful that a uniform bore surface temperature actually exists. The measurements usually show large round to round variations so that the fitted value of λ depends on the particular firing. The total heat input, Q, is much less variable and it is better to fit λ to Q. When this is done and the resulting values of λ used to calculate the temperatures, the agreement with the measured values is usually within the uncertainty in the measured values. For further details the reader should consult the original papers.

3-3 EROSION

3-3.1 General Discussion

The phenomenon described as erosion is the progressive wearing away of the bore surface as the gun is used. It is greatest on the surface of the lands and near the origin of the rifling so that the bore tends to become enlarged preferentially in this region. The effect is to lower the engraving forces and to shift the forcing cone somewhat toward the

muzzle. This is equivalent to increasing the effective chamber volume and to lowering the engraving resistance and the starting pressure. The result on the interior ballistics is to lower the maximum pressure and the muzzle velocity, an effect called pressure and velocity drop. These effects were studied by Nobel[7].

The details of the erosion process are not understood. The process is extremely complex and involves mechanical, chemical and thermal effects which are interrelated in unknown ways and no doubt interrelated differently depending on the particular circumstances. It is a fact of observation, however, that erosion is very sensitive to the heating of the barrel. Low energy weapons using cool propellants erode very slowly. As the muzzle velocity is increased the erosion per round increases rapidly so that a high velocity tank gun erodes at a rate many times that of a howitzer of similar caliber. The erosion is particularly severe if hot propellants are used. As the flame temperature is increased, for constant ballistics, the erosion rate increases much more rapidly than the rate of increase of the flame temperature, so much so that the thermal effects become dominant. That the erosion is intimately related to the heating is indicated by Figure 3-1 which is a plot of the observed erosion per round versus the heat input Q calculated by the method of Reference 1.

There are other forms of damage to the tube due to firing, some of them due to thermal effects. When a gun is fired, the firing cycle is very short, of the order of milliseconds. During this interval, the tube is subjected to very large thermal and mechanical stresses. The most characteristic result of this is heat checking. The bore surface develops a characteristic pattern of cracks which lead to a developing roughness which increases the heat transfer. These cracks erode locally so that the surface eventually becomes quite rough and gas tends to leak past the rotating band which causes large local erosion. For more details on erosion and other types of damage of gun tubes and methods of dealing with them, reference should be made to another handbook in this series, Reference 8.

3-3.2 Estimation of the Erosion of Gun Tubes

A general theory of erosion of guns has not been formulated. The erosion rate decreases as the gun is used due to changes in the interior ballistics resulting from the erosion. It does not seem possible to formulate a complete theory from first principles in any general way. Jones and Breitbart[9] developed a semi-empirical thermal theory applicable to the erosion near the commencement of firing in a new gun for slow rates of fire. In discussing erosion by propellant gases, it is usually assumed that the surface is first brought to the melting point and then removed in the molten form by the frictional forces of the gas flowing over the surface. A mathematical treatment of this problem has been given by Landau.[10] Jones and Breitbart could not fit this picture to the observed data for guns and were led to assume that, due to the roughness, the surface reaches the melting point only locally so that erosion occurs at "hot spots". The heat involved in the erosion is only a small fraction of the total input. The hot spots occur for short times and shift about on the surface. The instantaneous rate at which material is being removed can be averaged over the surface and will define an instantaneous average rate of surface regression, V_r. The surface will move back on the average in one round an amount

$$W = \int_{t_1}^{t_2} V_r \, dt \tag{3-53}$$

where t_1 and t_2 specify the beginning and end of the erosion interval, respectively. If

H is the instantaneous rate of heat input to the hot spots per unit area and

B is the quantity of heat necessary to raise a unit volume of the metal to the melting point and melt it,

$$V_r = H/B \tag{3-54}$$

Evidently,

$$B = \rho_s[C_s(T_m - T_i) + L] \tag{3-55}$$

where

ρ_s is the density of the tube material
C_s the specific heat of the tube material
T_m the melting temperature of the tube material
T_i the initial temperature of the tube material and
L the heat of fusion of the tube material

Taking

$$\rho_s = 7.8 \text{ gm/cm}^3$$
$$C_s = 0.13 \text{ cal/gm-°K}$$
$$T_m - T_i = 1400°\text{C}$$
$$L = 60 \text{ cal/gm}$$

one finds that $B = 1.9 \times 10^3$ cal/cm^3. Using Equations 3-1 and 3-2 it is assumed that an erosion function, A, can be defined by the equation

$$H = AC_p\rho(T_g - T_m) \tag{3-56}$$

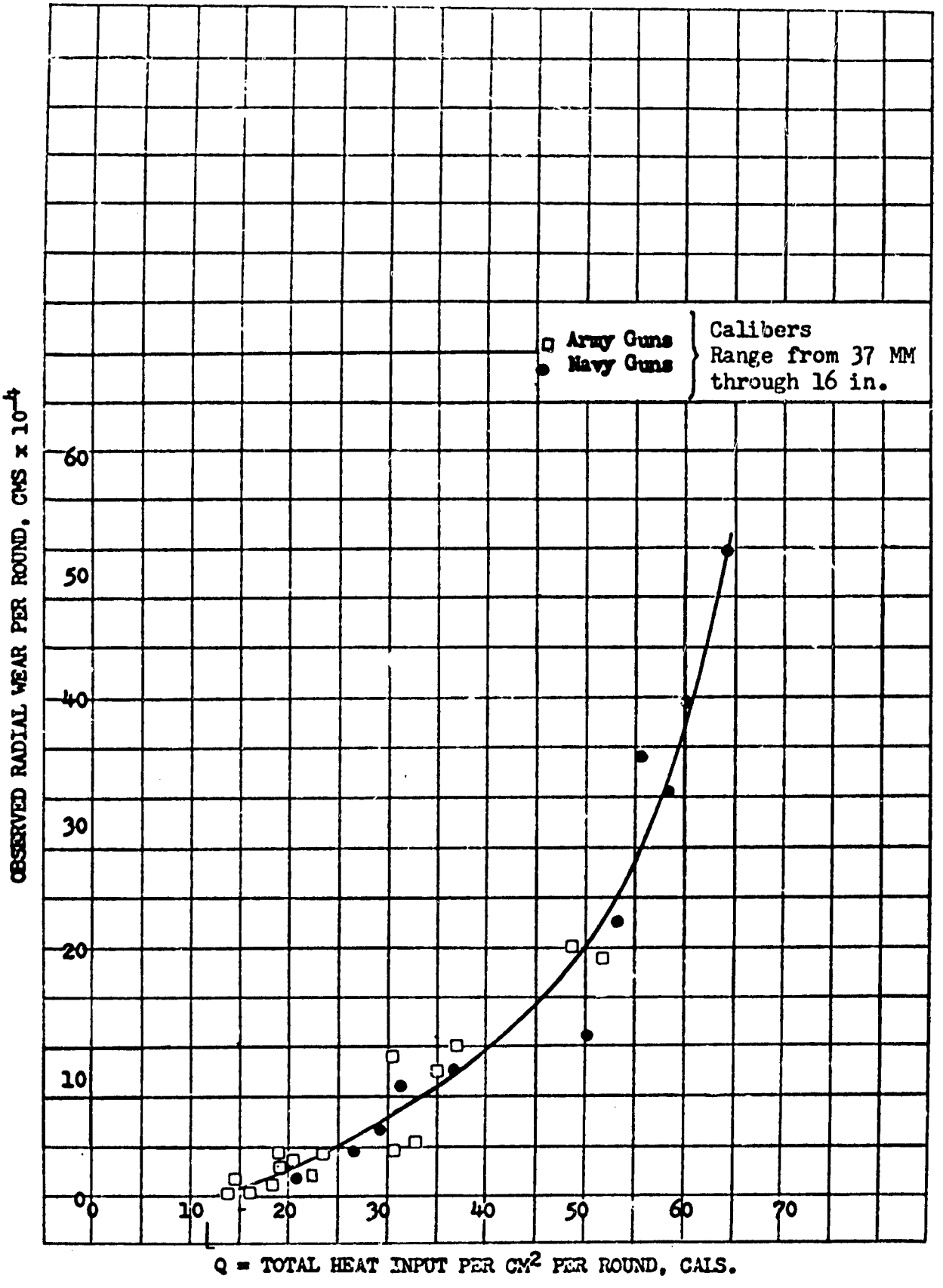


FIGURE 3-1. *Observed Radial Wear per Round at the Commencement of Rifling versus Calculated Heat Input per cm² per Round.*

where T_g = temperature of the propellant gas. This effectively determines the fraction of the heat input responsible for the erosion. Based on general arguments regarding the behavior of hot spots it is further assumed that

$$A = Kt_1F_m \qquad (3\text{-}57)$$

where F_m is the maximum value of the function

$$F(t) = \rho r(T_g - T_m)$$

and K is an empirical constant.
Equation 3-53 then becomes

$$W = \frac{KC_p t_1 F_m}{B} \int_{t_1}^{t_2} F(t)\, dt \qquad (3\text{-}58)$$

The values of t_1 and t_2, the times at which erosion starts and ends, are taken as the times at which $F(t)$ for the weapon in question, rises above and falls below the value of the maximum value of $F(t)$ for a low velocity gun like a howitzer for which the erosion is negligible. A standard value, based on a study of such low velocity weapons, of 200×10^4 cgs units was chosen. The interval during which the value of $F(t)$ for the weapons under consideration was above the standard value was taken as the interval over which the integral in Equation 3-58 was to be evaluated.

The function $F(t)$ was evaluated using the formulas of Reference 1 and then plotted and the integral determined from the graph. K was then evaluated by fitting to the observed rate of wear at the origin of rifling for 29 guns of various types, and an average value of K determined. The value of K so determined was equal to 3.28×10^{-8} cm^2/gm°K/rd. The wear

TABLE 3-4. WEAR OF GUNS

Gun	Propellant	Projectile Type	Nominal M.V., fps	W(obs), cm × 10^{-3}	$K \times 10^8$	W(calc), cm × 10^{-3}	W(calc) − W(obs)	$\frac{W(calc) - W(obs)}{W(obs)}$, %
Army								
37mm M3	M2	AP	2900	.11	3.74	.097	−.013	−12
40mm M1	M1	HE	2870	.043	2.79	.050	.007	18
57mm M1	M6	APC	2700	.28	3.85	.239	−.041	−15
57mm M1	M6	HE	2700	.13	1.71	.250	.120	92
75mm T22	M1	HE	2300	.049	3.33	.048	−.001	− 1
76mm T91	M6	AP	4000	.38	3.96	.315	−.065	−17
3-inch M7	M6	APC	2600	.19	3.24	.192	.002	1
90mm M3	M6	HE	2700	.30	4.04	.244	−.056	−19
90mm T19	M2	APC	2650	1.10	3.18	1.137	.037	3
90mm T5	M6	APC	3300	1.90	4.27	1.462	−.438	−23
90mm T54	T12	APC	3300	2.00	3.41	1.920	.080	4
90mm T54E2	M6	APC	3200	1.20	8.40	.469	−.731	−61
120mm M1	M6	HE	3100	1.00	2.99	1.100	.100	10
6-inch	M6	TP	2800	1.20	3.28	1.202	.002	.1
155mm M2	M6	HE	2800	.36	1.57	.528	.168	47
155mm M1 How.	M1	HE	1850	.058	3.07	.062	.004	7
8-inch M1	M6	HE	2800	2.00	3.44	1.911	−.089	− 4
240mm M1 How.	M1	HE	2300	.44	3.50	.382	−.058	−13
Navy								
3-inch/50 Mk2	NH		2700	.15	1.77	.279	.129	86
5-inch/38 Mk12-1	NC		2600	.34	1.61	.498	−.158	−46
5-inch 51 Mk7&8	NC		3150	.86	3.84	.735	−.125	−14
5-inch/54 Mk16	NC		2650	.51	2.87	.583	.073	14
6-inch/47 Mk16	NC		2500	.83	2.25	1.212	.382	46
8-inch/55 Mk15	NC		2500	1.27	2.60	1.605	.335	26
12-inch/50 Mk8	NC		2500	2.21	2.58	2.815	.605	27
14-inch/45 Mk12	NC		2600	3.95	3.37	3.852	−.098	2
14-inch/50 Mk11	NC		2700	3.55	3.55	3.287	−.263	− 7
16-inch/45 Mk6	NC		2300	3.25	3.12	3.424	.174	5
16-inch/50 Mk7	NC		2500	5.13	3.84	4.390	−.740	−14

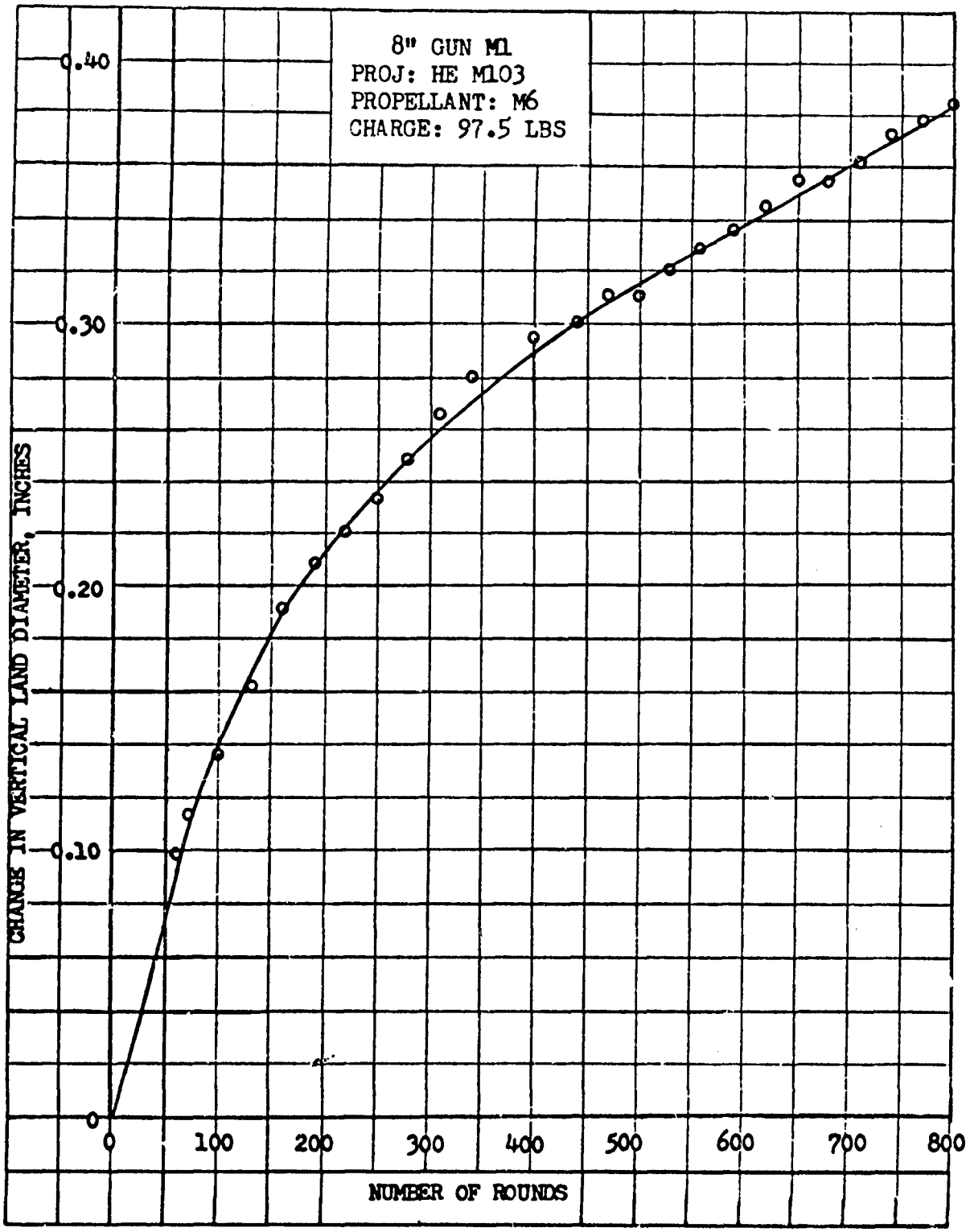


FIGURE 3-2. *Change in Vertical Land Diameter at 0.1 inch from Commencement of Rifling versus Number of Rounds in the 8-inch Gun, M1.*

per round as calculated using this average value is presented in Table 3-4 along with other pertinent data and compared with the measured values. It is shown that the theory correlates the data with the interior ballistics fairly well over a wide range of different guns and ammunition. The measured values themselves are subject to considerable uncertainty, because they vary for different tubes of the same model and with the amount of use the particular tube has undergone (Cf. Figures 3-2 and 3-3). The agreement is also, at least in part, a reflection of the fact that the guns studied are approximately scale models of each other. The erosion rate depends on minor differences in the guns such as the design of the forcing cone and the rifling which are not taken account of in the theory. Some of the scatter may, therefore, be due to such factors.

The theory applies only to erosion at the origin of rifling since the specification of A by Equation 3-57 is not possible at other locations.

The evaluation of W' from Equation 3-58 is time consuming. By making a number of quite drastic approximations, Breitbart[11] recast the procedure in analytical form and derived a simple algebraic expression for W' which yields results in almost as good agreement with observed values as Equation 3-58, namely:

$$W' = \frac{K\Delta^2 X_m^2}{S^2}\left[\frac{P_m^2 - 16000^2}{P_m^3}\right] \qquad (3\text{-}59)$$

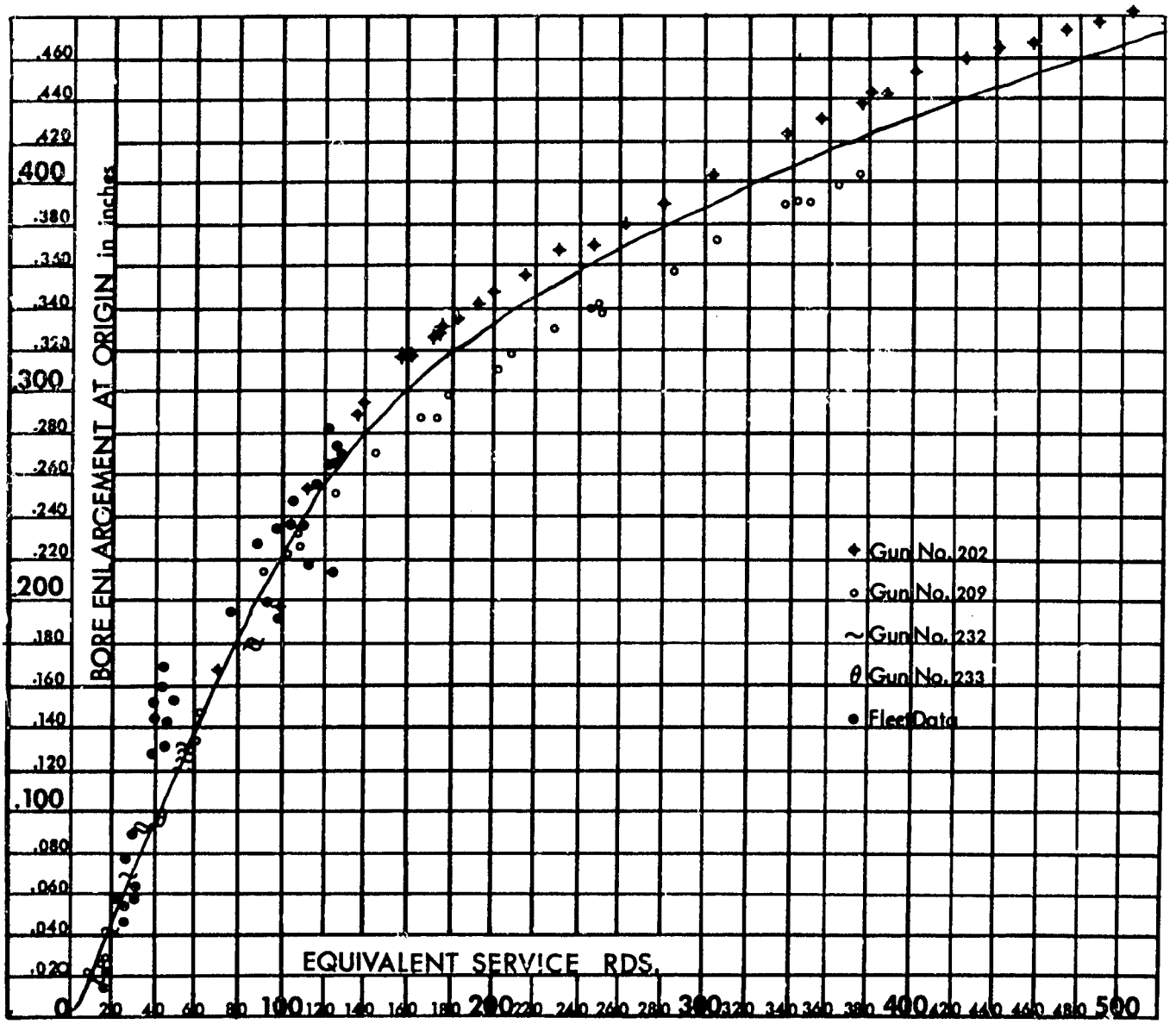


FIGURE 3-3. *Bore Enlargement at Origin versus Equivalent Service Rounds. 16-inch/45 Caliber Guns Marks 6 and 8. (Data from U. S. Naval Weapons Laboratory, Dahlgren, Virginia)*

where Δ is dimensionless and is equal to $27.68\ C/U_{ch}$. Numerically it corresponds to the density of loading in gm/cc. X_m is the travel to the muzzle (in), S the expansion ratio and P_m the maximum pressure (psi).

Breitbart evaluated the empirical constant, K, by fitting the formula to the measured wear per round at the commencement of rifling in the 8-inch gun M1. If W represents the increase in the diameter per round in inches and the units of the other quantities are as indicated above, K has the value 4.29×10^{-2}.

The formula as written applies to standard guns. Breitbart showed that it can be applied to howitzers by introducing an empirical correction factor equal to $CX_m\ 4.87d^{1.1}$ so that Eq. 3-59 becomes for howitzers

$$W = \frac{K'C\Delta^2 X_m^3}{S^2 d^{1.1}} \left[\frac{P_m^2 - 16000^2}{P_m^3}\right] \qquad (3\text{-}59a)$$

where C is the charge, d the caliber and $K' = K\ 4.87 = 8.81 \times 10^{-3}$.

3-3.3 Life of Gun Tubes

a. Estimation of Gun Life. Paragraph 3-3.2 gives formulas for the rate of wear of gun tubes, derived by Jones and Breitbart. Eventually, a tube wears so much that it cannot be used, either because the muzzle velocity is so low that it cannot be properly allowed for in firing, or because the spin of the projectile is too low to stabilize it properly. The instability of the projectile can usually be traced to shearing of the engraved part of the rotating band while it is still in the tube. Examination of the bands of recovered projectiles will usually indicate the expected remaining accuracy life.

After studying data pertaining to cannon from 37mm to 203mm (8-inch) caliber, Jones and Breitbart found that the useful life can be correlated rather well with the wear at the commencement of rifling.[12] The *commencement of rifling* is defined as the point at which the full height of the land is first encountered, in contrast to the *origin of rifling*, which is the point at which the land starts to rise. At the end of the useful life of these guns, the wear at the commencement of rifling was between 3.5 and 5 percent of the original diameter between the lands. Therefore, a wear of 5 percent of the original bore diameter may be taken as the tolerable limit and having calculated the rate of wear, the life of the gun can be estimated.

b. Equivalent Full Charge Factors. In order to estimate the useful life of guns that fire different kinds of projectiles with different charges, it is necessary to determine a factor that represents the relative erosiveness of the ammunition. Such a factor is called the equivalent full charge (*EFC*) factor.

After studying all available data, Riel found an empirical formula that satisfies the experimental results quite well.[13] This formula is

$$EFC = (P/P_1)^{n-1}(C/C_1)^2(V/V_1)(E/E_1) \qquad (3\text{-}60)$$

where

EFC is the equivalent full charge factor
P the maximum chamber pressure
C the weight of propellant
V the muzzle velocity
E the specific energy of the propellant

and the subscript 1 denotes the value pertaining to the ammunition for which the *EFC* is chosen to be unity. Of course, the data for both types of ammunition must be expressed in the same units; if two types of propellant are used in a mixed charge, their average specific energies may be substituted for E.

Riel has tabulated the estimated life and *EFC* for most of the present artillery ammunition.[14]

3-3.4 Erosion in Vents

Many experiments, going back over many years have been conducted to study the erosion of materials by propellant gases. These experiments have been conducted to study the basic processes involved as well as to develop materials more resistant to gas erosion. The technique most often used is to burn the propellant in a combustion chamber and allow the gases to flow out through a nozzle or vent and to study the effect upon the nozzle surface. There is an extensive literature on the subject some of which will be reviewed here.

a. Greaves, Abram and Rees used three chambers of different volumes and tested several different propellants with different adiabatic flame temperatures.[15] They measured only peak pressures, using copper crusher gages. They rated their materials on a relative scale of "erodability": the slope of the linear part of the graph of weight loss versus peak pressure.

They established a strong dependence of weight loss on the "calorific value" of the propellant. In their experiments, for a given maximum pressure, the weight loss per unit charge is independent of the chamber volume. Their data confirm the expected result that the weight loss tends to go up as the melting point of the vent material goes down. In the case of steels, the milder the steel, the less

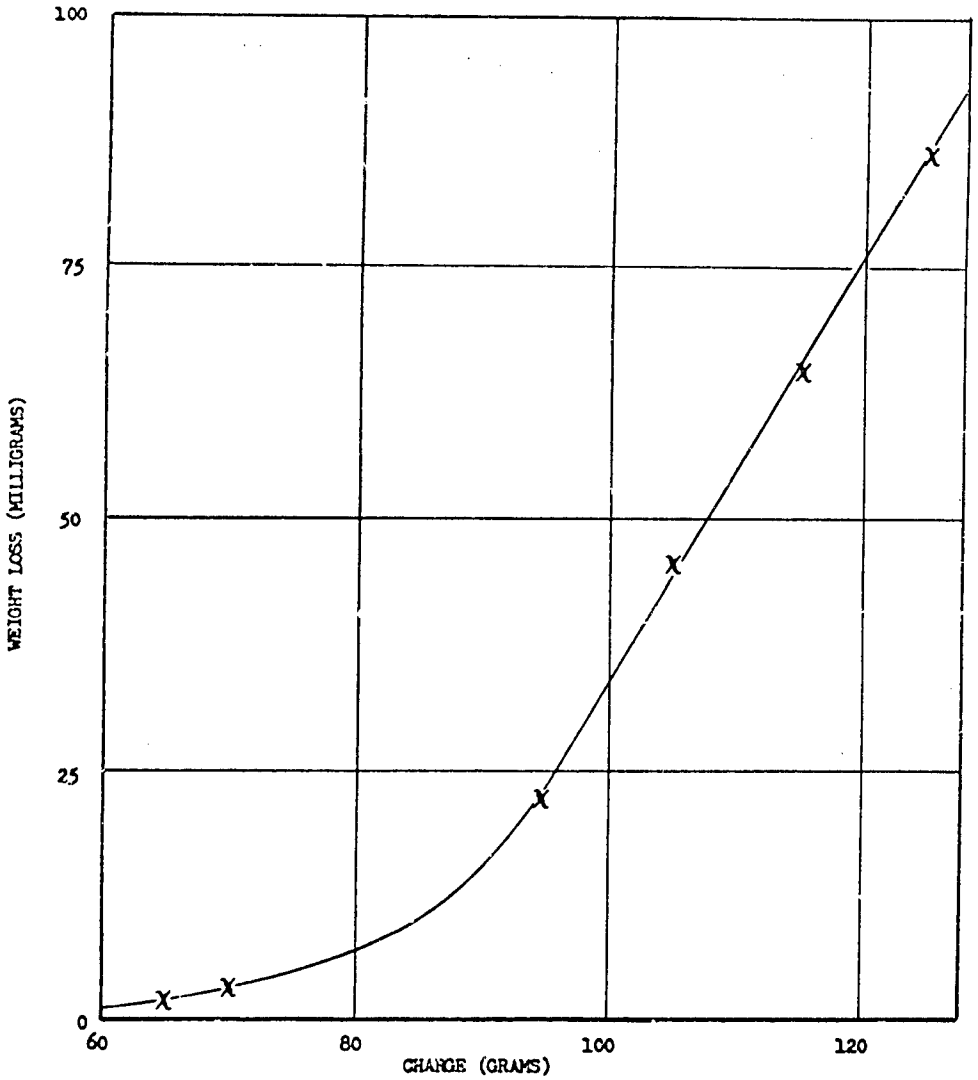
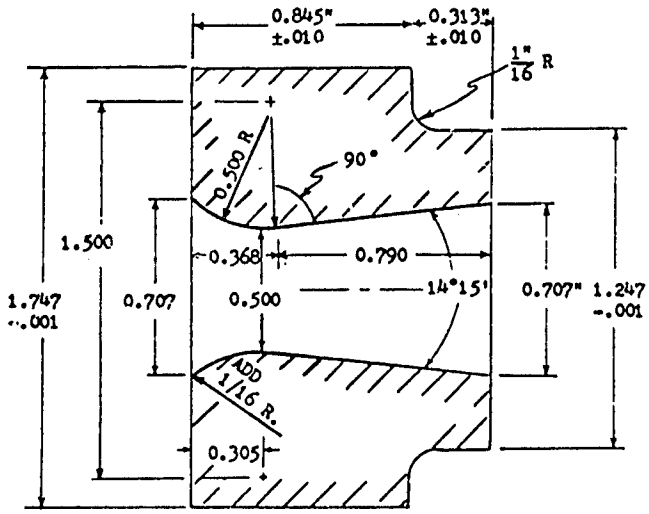


FIGURE 3-4. *The General Shape of Vent Erosion versus Charge*

the erosion. They conclude that the principal factor of erosion in both guns and vents is generally the heating of the surface with its consequent melting. They are convinced that direct chemical reaction of the gases with the surface material plays a minor role, if any, under the conditions of their experiments.

b. Evans, Horn, Shapiro and Wagner studied the erosion by the gases produced by the explosion of carbon monoxide and oxygen.[16] Their apparatus was fitted with a blowout seal. Several blowout pressures and chamber volumes were used. The weight loss of the vents was measured and correlated with the number of moles of the product gases, the explosion temperature, and the ratio of CO to CO_2 in the product.

For an equal number of moles, the weight loss increased with the gas temperature, but in a non-linear manner: the plots were concave upwards with a curvature that was quite sharp initially, but



1. Entrance Radius Tangent to Exit Cone.
2. Inner Surface Must be Smooth and Free of Tool Marks.
3. All Tolerances ±.001 Except as Noted, Scale 2/1.

FIGURE 3-5. *Early Design of Erosion Test Vent*

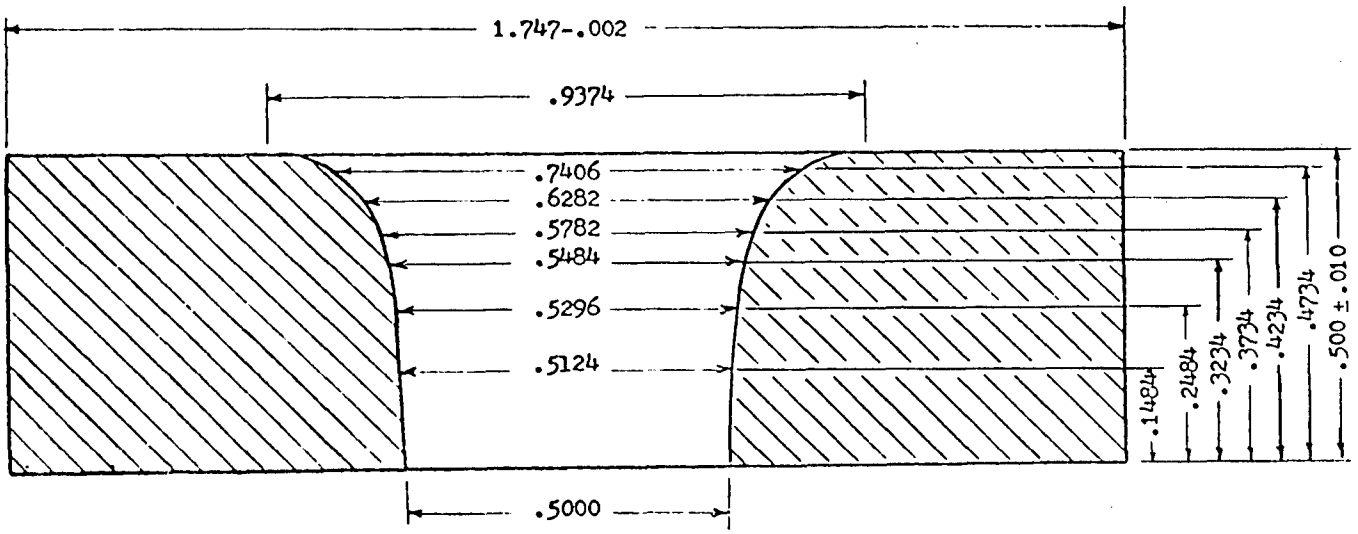


FIGURE 3-6. *Final Design of 0.50-inch Erosion Test Vent.*
(Vents with different diameters are obtained by adding a constant increment to the numbers shown.)

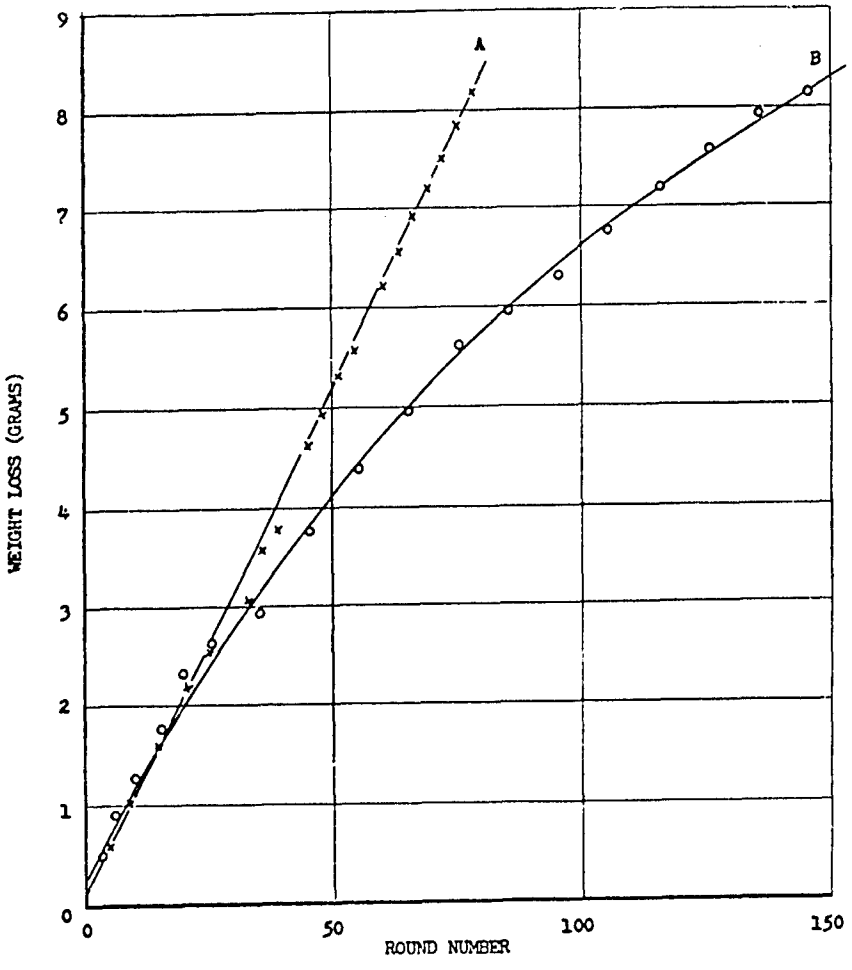


FIGURE 3-7. *Weight Loss versus Round Number*
A- C/D Constant
B- C Constant

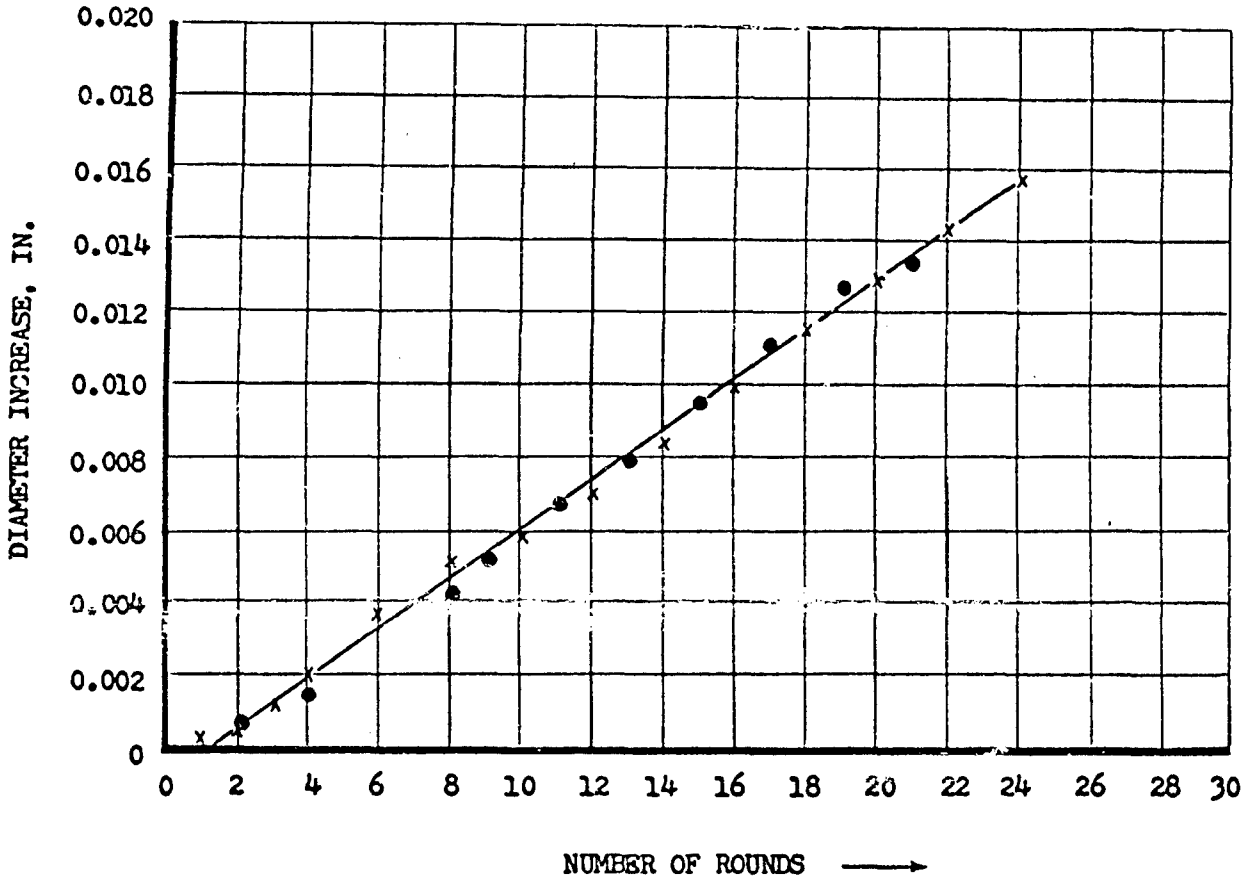


FIGURE 3-8. *Diameter Increase versus Number of Rounds*
Nozzle Type: E1
Material: ARMCO Iron
Charge: 70 GMS. of M2 Propellant
⊙●*Nozzle Diameter 0.358"—Total Throat Area = .2012" in²*
×*Nozzle Diameter 0.500"—Total Throat Area = .1963" in²*
(*Nozzles represented by* ⊙, ● *were fired together and were subjected to the same pressure-time gas flow as the single nozzle represented by* ×.)

decreased almost to linearity. At a given calculated temperature, the weight loss increased rapidly as the ratio of CO to CO_2 decreased. The addition of small amounts of sulfur, nitrogen, and hydrogen-bearing compounds to the gas mixtures as well as hydrogen itself usually caused a large increase in erosion. This was interpreted as a catalytic effect upon the reaction of CO with the iron of the steel vent to form iron pentacarbonyl. Evans et al suggested that two fundamental phenomena underlie the erosion of the vents: at low temperatures and large CO/CO_2 ratios, material is removed by converting iron to volatile iron carbonyl; as the temperature increases, direct melting of the surface sets in and increases until it becomes predominant.

c. The Ballistic Research Laboratories have conducted several experiments on vent erosion. Wiegand[17] found that their early data and also those of Greaves, Abram and Rees produced better correlation when the weight loss was plotted against charge weight rather than against peak pressure. A representative curve is shown in Figure 3-4. This indicates a region of low severity, where the removal of material is related to some chemical reaction of one or more constituents of the gas with the material of the channel wall, followed by a region of high severity, wherein the material is removed predominantly by melting of the surface. In the latter region, the points can be fitted closely with a straight line, whose intercept with the axis of abscissas roughly divides the two regions. The slope of the curve at any point depends upon the experimental arrangement; that is, upon chamber volume, vent diameter, material and shape of the

vent, type and granulation of the propellant, method of ignition, and any other factor that affects the rate of heat transfer.

The apparatus consists of the breech and chamber of a 37mm gun with the barrel cut off just before the forcing cone, and an adapter to hold the vent in place. In the early experiments[13] vents like that of Figure 3-5, with various throat diameters and an expanding cone beyond the throat, were used. It was found that the erosion varied along the vent so as to change its shape. The result was that the erosion per round was not constant but depended on the round number. That is, the plot of the integrated erosion, as measured by total weight loss, against round number was not a straight line and no valid erosion rate per round could be determined. To circumvent this difficulty the shape of the vent was changed to conform to Figure 3-6 and also steps were taken to adjust the charge to maintain constant maximum chamber pressure. It was found that this could be done over a considerable change in vent diameter by simply keeping the ratio of charge to vent diameter constant. This would ensure that the characteristics of the gas flow were nearly constant from round to round. The type of data obtained is illustrated in Figure 3-7. The results

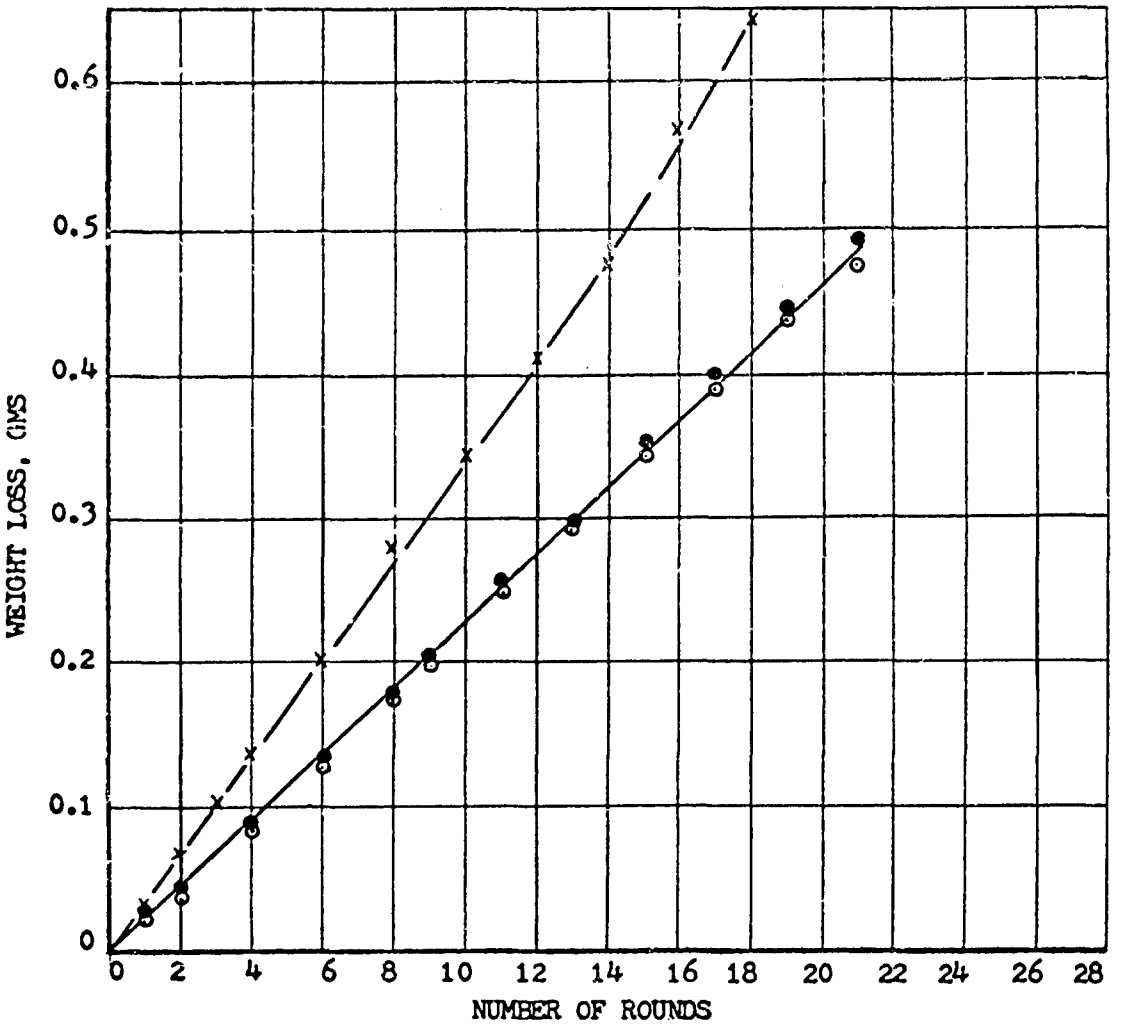


FIGURE 3-9. *Weight Loss versus Number of Rounds*
Nozzle Type: E1
Material—ARMCO Iron
Charge: 70 GMS. of M2 Propellant

⊙ ● *Nozzle Diameter 0.358"—Total Throat Area = .2012" in²*

× *Nozzle Diameter 0.500"—Total Throat Area = .1983" in²*

(Nozzles represented by ⊙, ● were fired together and were subjected to the same pressure-time gas flow as the single nozzle represented by ×.)

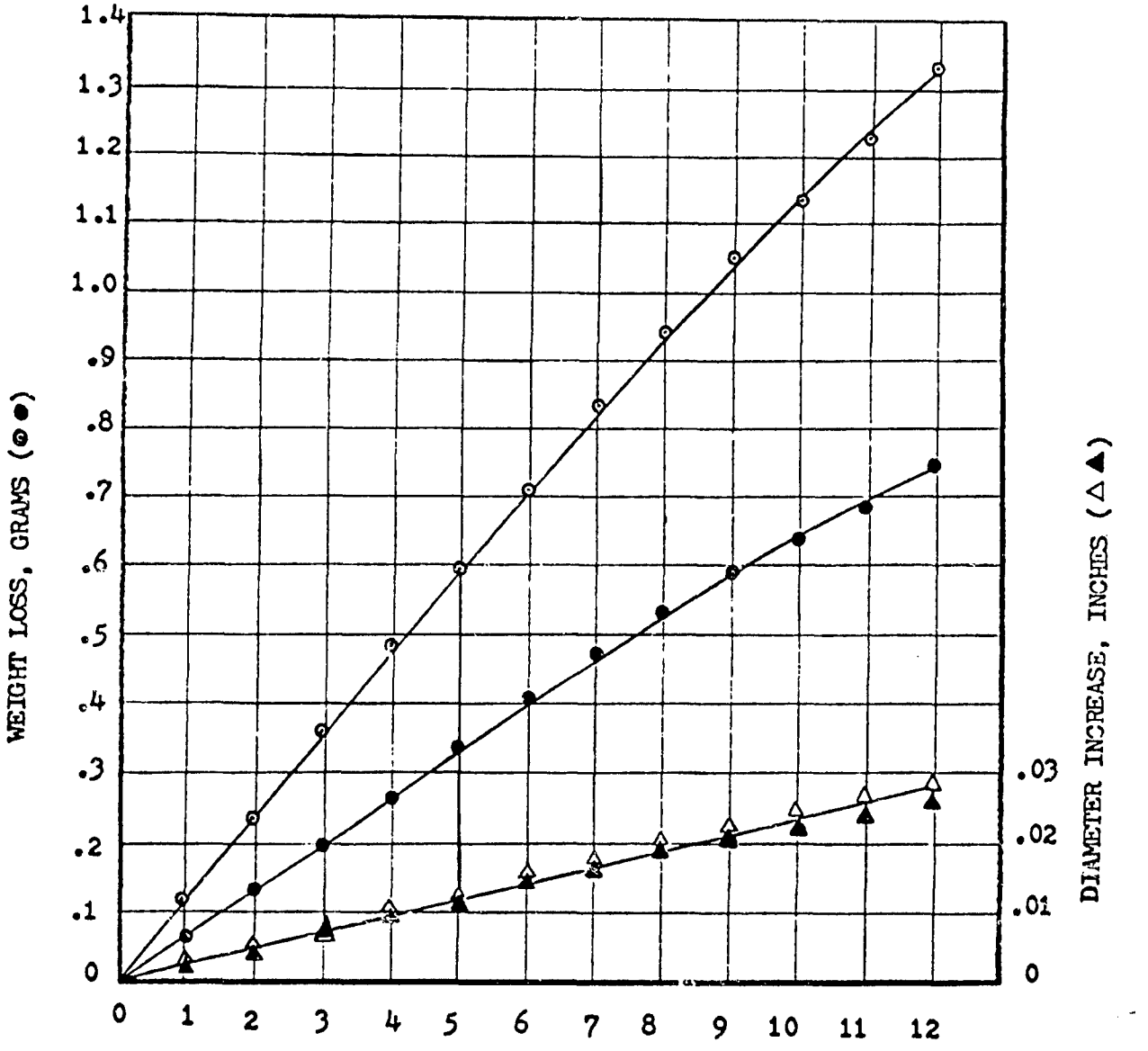


FIGURE 3-10. *Weight Loss and Diameter Increase versus Number of Rounds.*
Nozzle Type—E1
Material—Gun Steel (4140)
Charge—88 GMS. of M2 Propellant
Maximum Chamber Pressure—22,600 psi.
⊙ △ *Nozzle No. J41-3. Diam. = 0.4171" Throat Area = 0.1367 in²*
● ▲ *Nozzle No. J29-3. Diam. = 0.2866" Throat Area = 0.0645 in²*

also show that when these procedures are used, the weight loss per round is proportional to the diameter increase per round so that either may be used as a measure of erosion.

Figure 3-8 shows the increase in throat diameter versus round number for three different vents of the later type. The two small ones were fired simultaneously, using a manifold attached to the chamber. Their combined throat area was approximately the same as that of the larger one, which was fired alone from the same chamber with the same charge so as to produce the same flow conditions. With all vents tested, the rate of diametral increase was independent of the diameter.

Figure 3-9 shows the weight loss versus round number for the same series of firings. The fact that the weight losses of the two small vents are nearly the same proves the reproducibility of the data. With vents of different sizes, the ratio of the weight losses is larger than the ratio of diameters Figure 3-10. Since the weight loss is a measure of the integrated erosion over the entire inner surface of

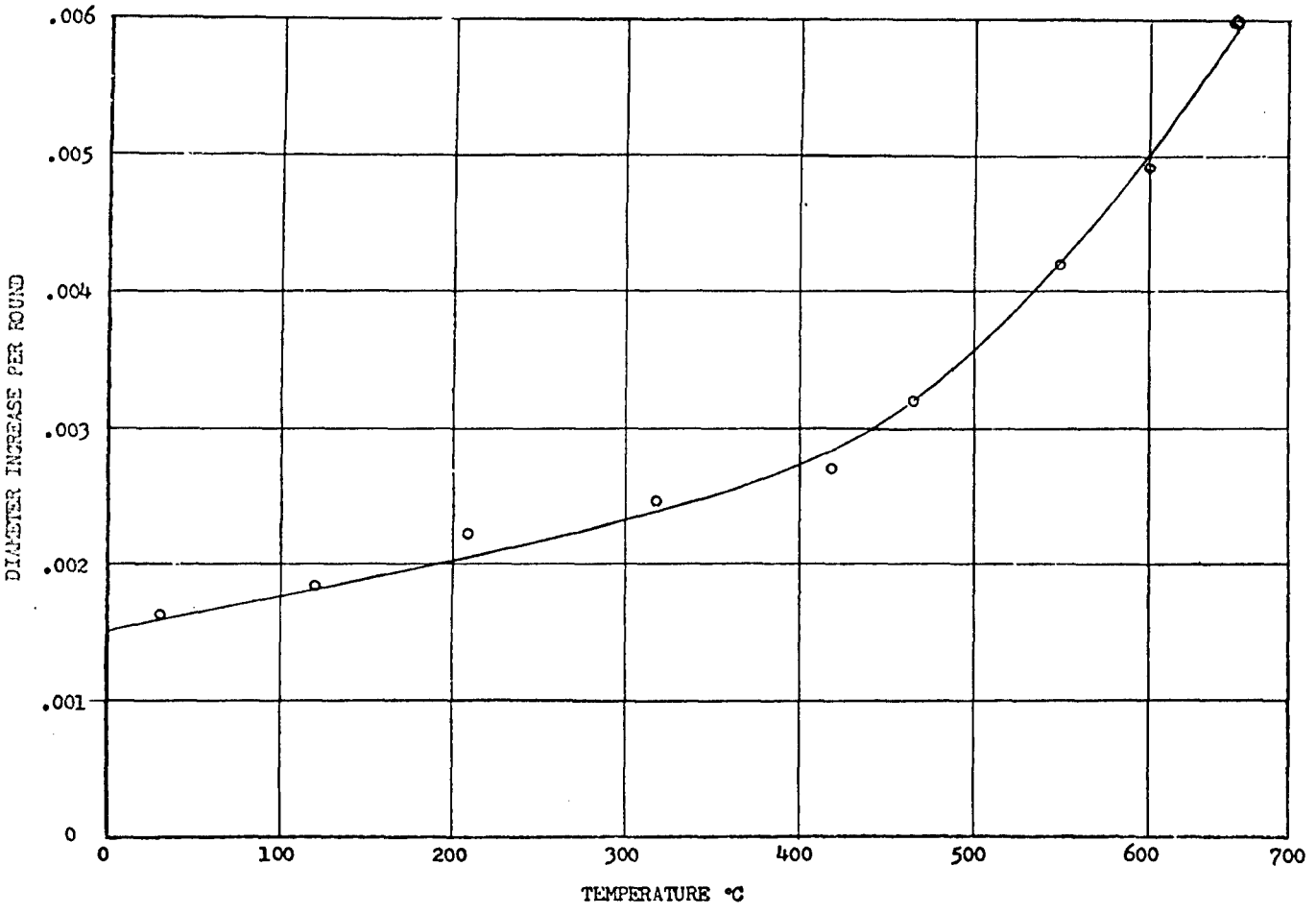


FIGURE 3-11. *Dependence of Erosion on Initial Wall Temperature*

the vent, its relatively greater variation indicates that, at upsteam locations, the thickness eroded in the larger vent increases relative to that in the smaller one. This may be partly caused by the fact that, as one proceeds upstream, the relative increase in cross section is smaller for the larger vent, so that the gas velocity will not decrease as rapidly from its sonic velocity at the exit and consequently will be higher in the larger vent than at the corresponding location in the smaller vent. Experiments indicate that the erosion rate is very sensitive to the gas velocity and increases rapidly with it.[18]

The temperature of the vent before firing also affects the rate of erosion. To determine the temperature, the thermocouple was imbedded in the vent so that the junction was about $\frac{1}{16}$th inch from the surface. The vent was well insulated from the mount and heated by means of an electrical resistance heater inserted into the opening. The heater was withdrawn immediately before firing. The results for a 70-gram charge of M2 propellant are shown in Figure 3-11.

It should be noted that, in both vents and guns, the rate of erosion is affected by the roughness of the surface.[19] With a given propellant, a particular combination of the gas velocity and heat transfer rate can be duplicated only under conditions where the nature of the surface roughness is similar.

REFERENCES

1. L. W. Nordheim, H. Soodak and G. Nordheim, *Thermal Effects of Propellant Gases in Erosion Vents and in Guns*, National Defense Research Committee Report A-262, 1944.
2. R. C. Machler, *The Temperature of the Bore Surface of Guns*, National Defense Research Committee Report A-201, 1943.
3. J. O. Hirschfelder, R. B. Kershner and C. F. Curtiss, *Interior Ballistics I*, National Defense Research Committee Report A-142, 1943.
4. E. A. Trabant and W. E. Thompson, *Description and Schematic Diagrams of the Purdue Thermal Analyzer*, Lafayette, Indiana, Purdue University Engineering Experiment Station Report S-1-10-53, 1953.
5. M. Boyd, J. A. Dooling, V. Griffing and R. Moller, *Heating and Erosion Studies in Guns*, Catholic University Final Report, Task 3, Contract NOrd 10,260, 1956.
6. E. Bannister, R. N. Jones and D. R. Bagwell, *Heat Transfer, Barrel Temperature and Thermal Strains in Guns*, BRL Report No. 1192, 1963.
7. H. A. Noble, Jr., *Interior Ballistic Effects of Gun Erosion*, Aberdeen Proving Ground Miscellaneous Report No. 156, 1948.
8. AMCP 706-252, Engineering Design Handbook, *Gun Tubes*.
9. R. N. Jones and S. Breitbart, *A Thermal Theory for Erosion of Guns by Powder Gases*, BRL Report No. 747, 1951.
10. H. G. Landau, Quart. Appl. Math. **1**, 81 (1950).
11. S. Breitbart, *A Simplified Method for Calculating Erosion in Guns*, BRL Memorandum Report No. 549, 1951.
12. R. N. Jones and S. Breitbart, *On the Estimation of Gun Life*, BRL Memorandum Report No. 497, 1949.
13. R. H. Riel, *An Empirical Method for Predicting Equivalent Full Charge Factors for Artillery Ammunition*, Aberdeen Proving Ground D&PS Report No. 271, 1961.
14. R. H. Riel, *EFC Factors and Percent Remaining Life for Gun, Howitzer, and Recoilless Rifle Tubes*, Aberdeen Proving Ground D&PS Report TW-417/1, Revised 1960.
15. R. H. Greaves, H. H. Abram and S. H. Rees, "The Erosion of Guns", J. Iron & Steel Inst. **117**, 113 (1929).
16. R. C. Evans, F. H. Horn, Z. M. Shapiro and R. L. Wagner, "The Chemical Erosion of Steel by Hot Gases Under Pressure", J. Phys. and Coll. Chem. **51**, No. 6 (1947).
17. J. H. Wiegand, *Erosion of Vent Plugs*, BRL Report No. 520, 1945.
18. R. N. Jones and E. R. Weiner, *Experiments on the Erosion of Steel by Propellant Gases Using the Vent Technique*, BRL Report No. 1012, 1957.
19. E. R. Weiner, *The Development of Surface Roughness in Gun and Vent Bores*, BRL Report No. 904, 1954.

CHAPTER 4

LIST OF SYMBOLS

A	Area of the bore
A_p	Area of the piezoelectric gage piston
a	Acceleration of projectile or piston
C	Ballistic coefficient
D	Distance between sky screens
f	Bore friction
M	Mass of projectile
m	Mass of piston
P	Breech pressure
P_b	Base pressure
P_g	Gage pressure
t	Time of passage of projectile over measured distance, D
X	Distance from the muzzle to the midpoint of sky screens
Z	Reduced distance: X/C
δ	Phase difference
ℓ	Difference in distance traveled by two beams
λ	Wave length of radiation

CHAPTER 4

EXPERIMENTAL METHODS

4-1 INTRODUCTION

The preceding chapters have been, in the main, concerned with the theoretical aspects of interior ballistics. From the earliest days of the use of firearms, attempts have been made to measure ballistic quantities. Because the quantities to be measured have values outside the range normally experienced in other fields, the apparatus necessary to measure them is rather specialized. Because the values are extreme, exist for very short times and vary with great rapidity, they are difficult to measure by mechanical means. The tendency in recent times is to depend more and more on sophisticated electrical and optical devices. Firing ranges are often elaborately instrumented, and for work in the field much of the apparatus is installed permanently in vehicles which can be transported to the site.

A great deal of interior ballistic measurement, that related to routine testing of guns and ammunition and also a considerable amount of development work, does not require more than the measurement of the maximum pressure and the muzzle velocity, but these must often be made repeatedly to derive a statistical result. Simple devices which will make these measurements quickly, without requiring instrumentation attached to the gun, are essentials. Experimental work of this kind has been called by Corner "practical ballistics."

Research in the subject and more sophisticated development procedures, however, require a more elaborate instrumentation. The maximum pressure and muzzle velocity are the results of complex phenomena going on inside the tube which the ballistician would like to relate to the theoretical approach. To make measurements within the thick-walled tube often requres that openings be made in the tube wall to accommodate the measuring devices. This makes the tube useless for any other service and such instrumentation cannot be used for routine testing. Some measurements can be made by apparatus designed to look down the tube from the muzzle and others by placing instruments in the projectile and bringing the signal out on wires or by telemetering; that is, by modulating an electromagnetic wave with the signal from the device in the projectile and transmitting the modulated wave to an external detecting apparatus.

In recent years there has been a rapid development of apparatus suitable for interior ballistic measurement and much of it is available commercially. The ballistician needs only to fit it to his special problems. Examples of such apparatus are high speed motion picture cameras, rotating drum and mirror cameras, cathode ray oscilloscopes, electronic chronographs, etc. It will be assumed that the reader is familiar in general with most standard devices which are in wide use and generally available.

Details of experimental studies of the interior ballistics of certain guns covering a great many of the measurable parameters have been published.[1,2] Since these general experiments were done, development has continued to improve apparatus and methods and to develop devices to measure directly quantities previously not possible to measure; such as for example, the motion of the propellant grains. In what follows, measuring devices and associated apparatus will be described mainly in principle. There are usually several models extant of the different measuring devices and the associated equipment and procedures vary at different places and at different times. The references should be consulted for details and for further references to pertinent literature. It should be pointed out also that rapid development of instrumentation of all sorts is taking place and the tendency is toward more and more automation of methods and procedures.

4-2 PRESSURE MEASUREMENTS

4-2.1 General Principles

Pressure gages are of two classes, (a) those which measure maximum pressure only, called crusher gages, and (b) those which measure the pressure as a function of time. Gages of class (b) are of two types, those which make use of the mechanical strain produced by the pressure, and those which depend on the piezoelectric effect. The earliest gages of class (b) were of the mechanical type. The strain element was usually a diaphragm subject to the gas pressure on the inside, and having the outside

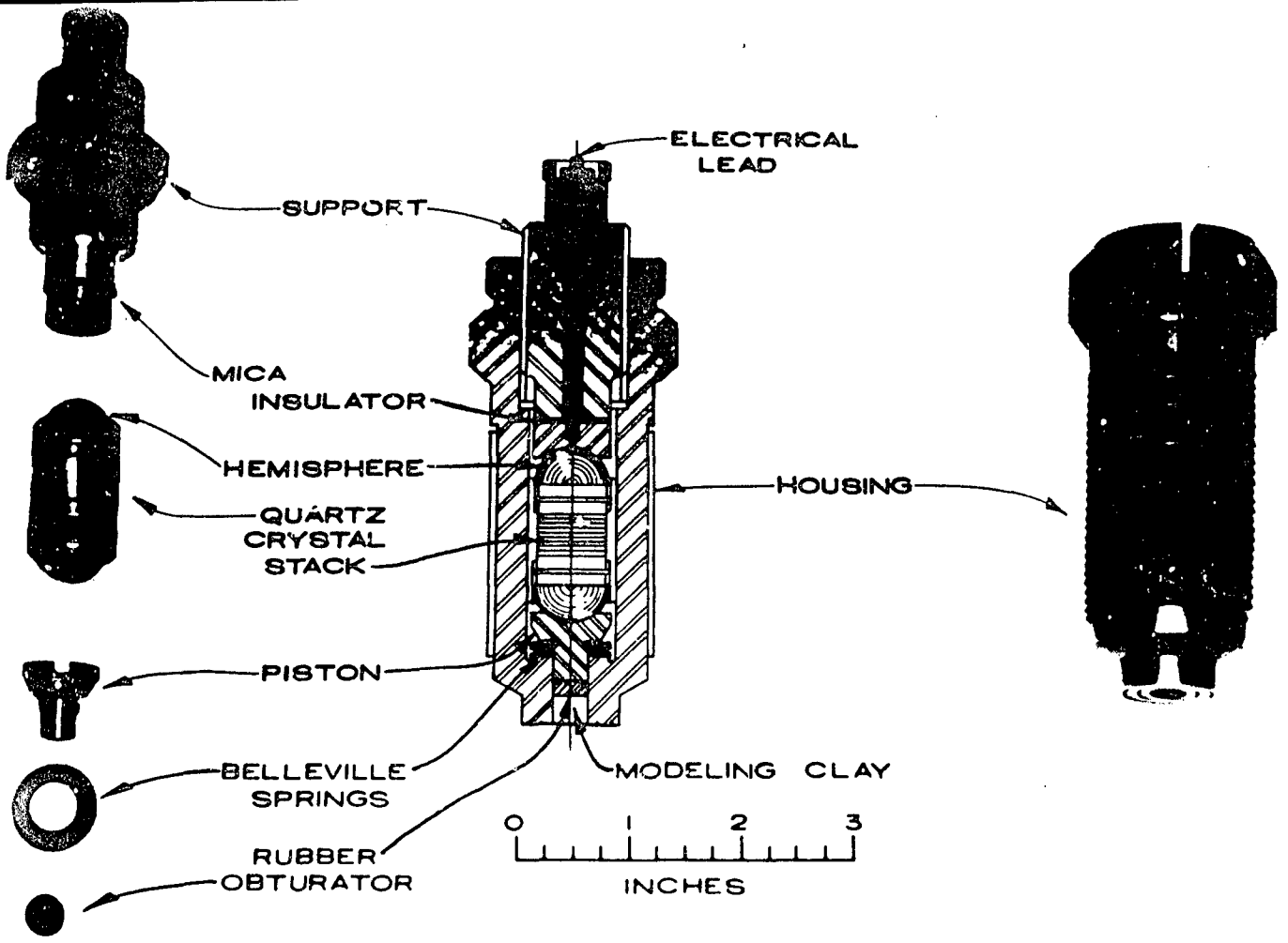


FIGURE 4-1. *Quartz Piezoelectric Pressure Gage.*

coupled mechanically to a small mirror to form an optical lever to deflect a spot of light onto a moving film. These gages are quite accurate and reliable but cannot be used on guns because of the recoil. They have been much used on closed chambers. For use on guns, strain type gages have a resistance strain wire coupled to the strain element so that the strain appears as an electrical signal which can be displayed on a cathode ray oscilloscope.

The piezoelectric gages depend on the fact that certain crystals develop a surface charge when subjected to an external pressure. Quartz crystals have been used most frequently. Gages have also been made using tourmaline. Tourmaline has the advantage that it responds to hydrostatic pressures so that the crystal need only be immersed in a medium such as a grease to protect it from the hot gases, and the pressure applied directly to the surface of the grease. The response of quartz, on the other hand, depends on the direction of the stress with respect to the crystal structure. For optimum effect, the crystal plates must be cut with their faces properly oriented with respect to the crystal axes and the forces must be applied to the crystal by means of a piston or anvil. Tourmaline crystals of sufficiently high quality are not readily available, however, and, as they are considerably more fragile than quartz, they have been infrequently used in the United States. Quartz is readily available and has the highest breaking stress of all the more commonly used piezoelectric crystals. The use of the piston complicates the gage but it has the advantage that the range of the gage can be adjusted by varying the ratio of the piston area to the area of the crystal plates.

4-2.2 The Quartz Piezoelectric Gage

The piezoelectric element of one model of this gage is a stack of X cut* crystal plates in the form of discs. The plates are stacked so that contiguous faces will generate charges of the same sign when pressure is applied. Metal foil charge-collectors are

* An X cut crystal plate has the normal to its face parallel to the electric axis of the crystal and the optic axis parallel to its face. For a given pressure on its face, such a plate produces a maximum charge.

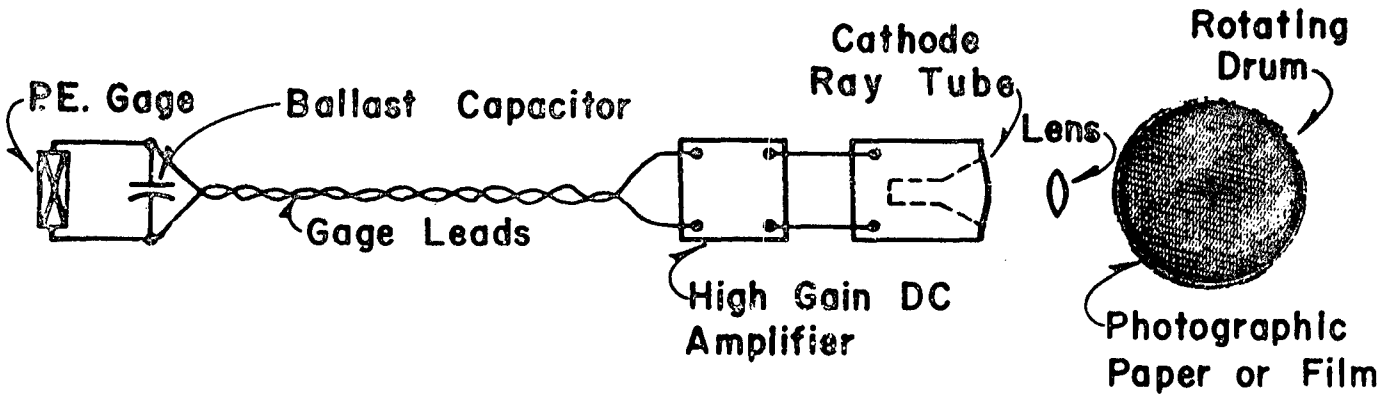


FIGURE 4-2. *Diagram of Recording System for Piezoelectric Pressure Gage.*

placed between the plates and so connected that the total charge of each sign appears at the electrodes at opposite ends of the stack. The end surfaces are in contact with electrodes of hemispherical shape. This shape, which fits into corresponding sockets on the element through which the pressure is applied, tends to assure that the pressure will be uniformly distributed over the surface of the crystals to minimize the possibility of cracking. To further assure that the pressure will be uniformly distributed the surfaces of the crystal plates and metal parts in contact with them must be optically ground and lapped. The details of the construction and mounting of the gage element are shown in Figure 4-1 for a model much used at Ballistic Research Laboratories.

The recording circuit and apparatus are illustrated in Figure 4-2. The charge developed by the gage is shared with a ballast capacitor in parallel with the gage and the voltage developed across the gage and capacitor fed through a high gain direct current amplifier to a cathode ray oscilloscope. The cathode spot is then photographed by a running film or rotating drum camera. A time scale is simultaneously placed on the record by photographing an intermittent light source. This can also be done by blocking the cathode spot intermittently to make breaks in the record. A typical record is shown in Figure 4-3.

To determine the pressure from the record requires that the gage and recording apparatus be calibrated. The gage is calibrated separately in the laboratory because it is not practicable to calibrate the gage when mounted in the gun. This is done using a dead weight hydraulic pressure apparatus, Figure 4-4. The gage is mounted in a hydraulic chamber provided with a piston which is attached through a mechanical linkage to a scale platform carrying a series of weights. Oil is then pumped into the hydraulic chamber until the weights are lifted and the pressure in the chamber determined from the piston area and the weight lifted. The hydraulic chamber is provided with a quick release valve which releases the pressure very rapidly. To make a calibration, the charge developed by the gage under pressure is first removed by shorting the gage and then the pressure is suddenly released. An equal charge of opposite sign is generated by the gage. This charge is immediately sent through a ballistic galvanometer and its magnitude determined from the deflection of the galvanometer. The recording apparatus is calibrated by applying a known charge across the ballast capacitor and observing the deflection of the cathode ray spot.

Quartz piezo gages are rugged and tend to hold their calibration well. By varying the number of plates in the stack the sensitivity can be adjusted. The crystals will not withstand stresses much above 15000 psi but the working stress on the crystals can be varied by adjusting the piston area. The piston size has a practical lower limit, below which it will deform and bind. This imposes an upper limit on the pressures that can be measured. Practical gages can be made to measure pressures between 15,000 and 70,000 psi. The gage has a high impedance and problems of grounding and shielding have to be dealt with, especially in field use where the leads from the gage to the recording equipment may be

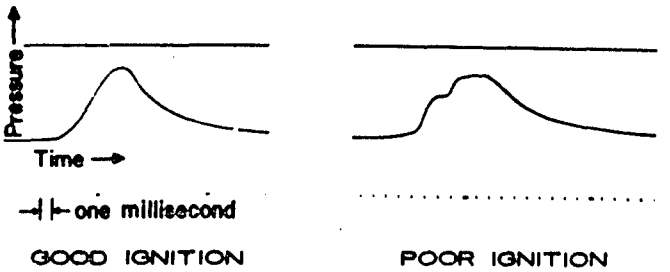


FIGURE 4-3. *Typical Pressure-Time Records from Quartz Piezoelectric Gage (155mm Gun).*

long, even with mobile equipment. Piezoelectric gages are not suitable for measuring low pressures of long duration such as exist in rocket motors because the gage discharges too rapidly, mainly through the input impedance of the amplifier. Also, for use at low pressures, the gage would have to be large to generate sufficient charge for ease of measurement.

4-2.3 Strain Type Pressure Gages

The sensitive element in these gages is a short tube or ferrule closed at one end and so mounted as

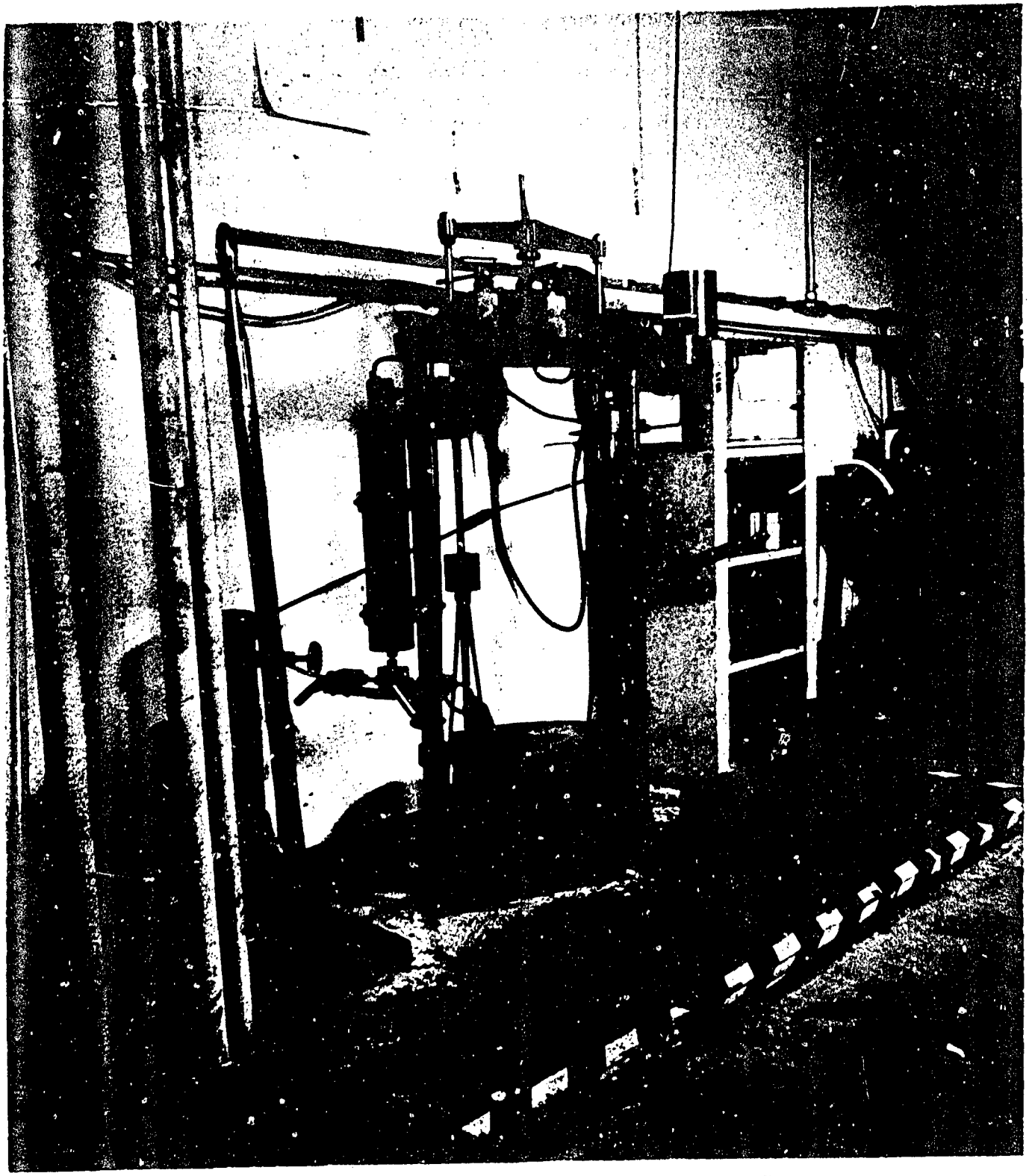


FIGURE 4-4. *Dead Weight Apparatus for Calibration of Pressure Gages.*

to be subjected to the gas pressure either on the inside or outside surface. In the earlier models the pressure is exerted on the inner surface, the ferrule being filled with a hydraulic medium such as grease or oil. A strain wire is wound on the outside of the ferrule and cemented to the surface or applied in the form of a commercial strain patch cemented to the surface in the usual way. The strain wire or patch forms one arm of a Wheatstone bridge circuit. When the pressure is applied, the bridge is unbalanced; the degree of unbalance being a measure of the pressure. The emf developed across the bridge by the unbalance is fed to a suitable amplifier and then to a cathode ray oscilloscope. The deflection of the cathode spot is then photographed with a running film or drum camera.

One model in which the pressure is applied to the outside of the ferrule has been referred to as a "hat" gage because of the shape of the ferrule. In this model the strain wire or patch is on the inner surface. The operation of the gage is the same as for the other models. Some typical models are shown in Figures 4-5, 4-6, 4-7, and 4-8, which are self-explanatory.

A typical recording circuit is shown in Figure 4-9. The circuit is calibrated by a suitable variable resistor in the gage arm of the bridge which establishes the relation between bridge output and resistance change in the gage. The gage itself is calibrated in the laboratory on the dead weight calibrator to establish the relation between the resistance change in the gage and the applied pressure.

Strain type gages can be used to measure lower pressures of long duration. The pressure range of the

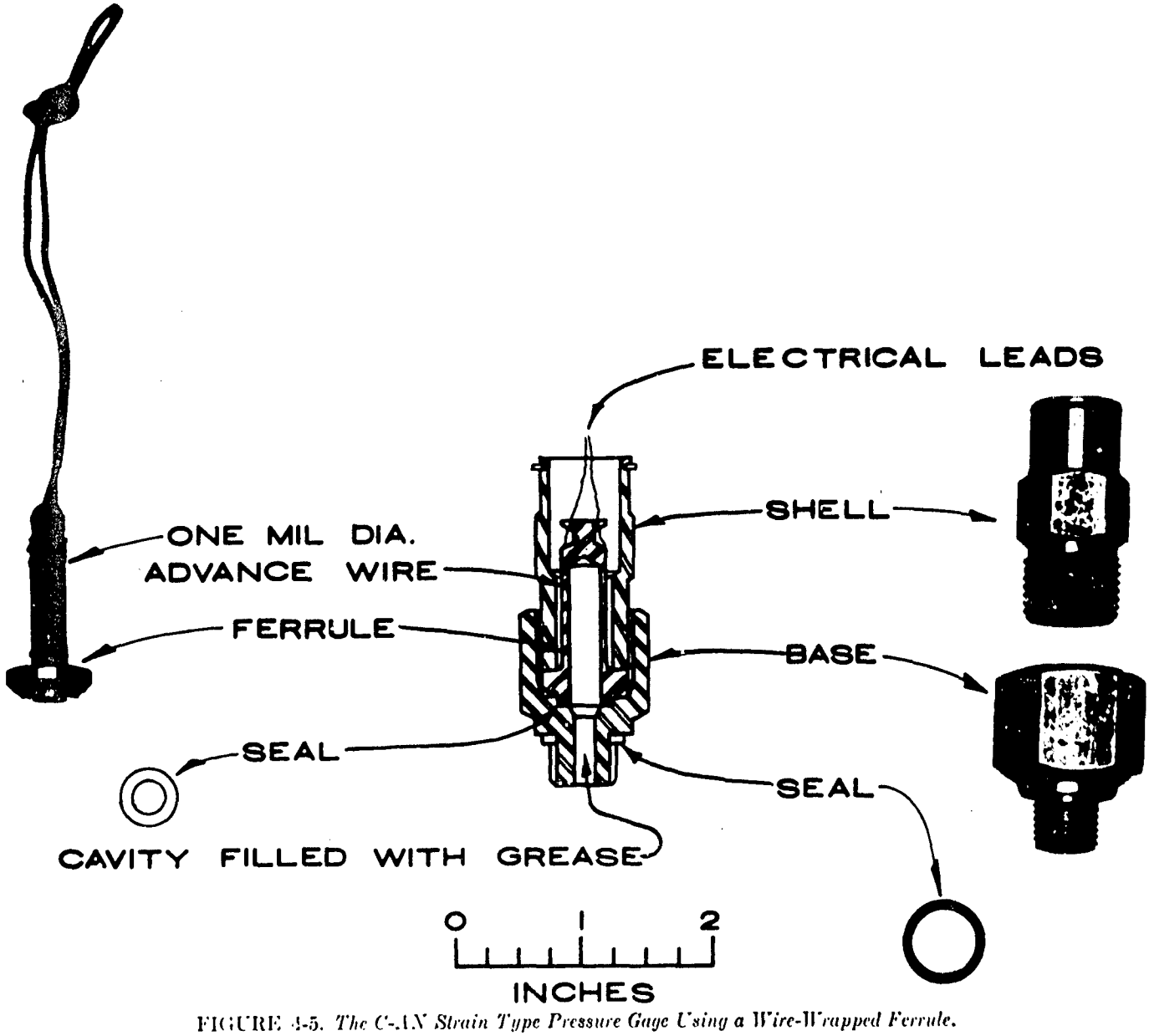


FIGURE 4-5. *The C-AX Strain Type Pressure Gage Using a Wire-Wrapped Ferrule.*

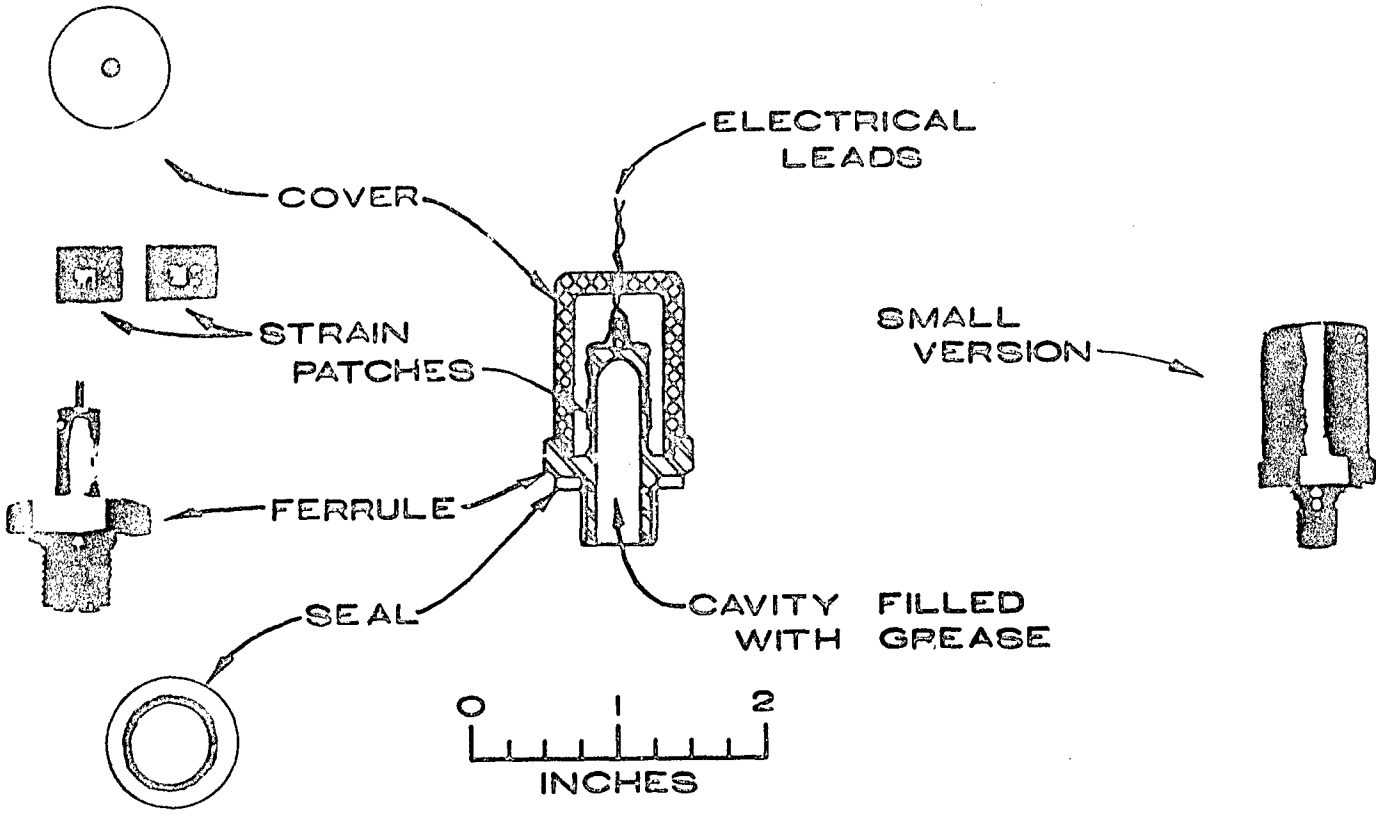


FIGURE 4-6. *An Improved Strain Type Pressure Gage Using Cemented Foil Strain Patches to Permit the Use of a Smaller Ferrule to Reduce Dimensions of the Gage.*

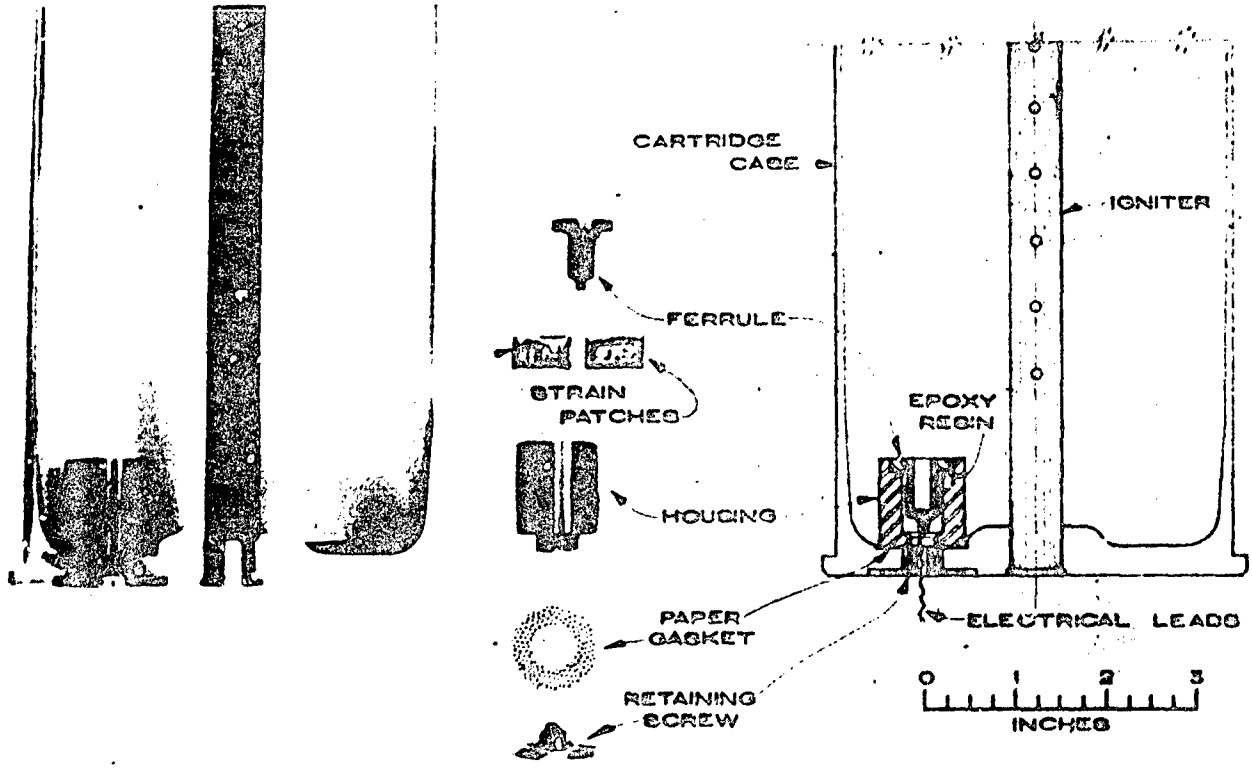


FIGURE 4-7. *Internal Strain Type Pressure Gage Mounted in Cartridge Case to Measure Breech Pressure.*

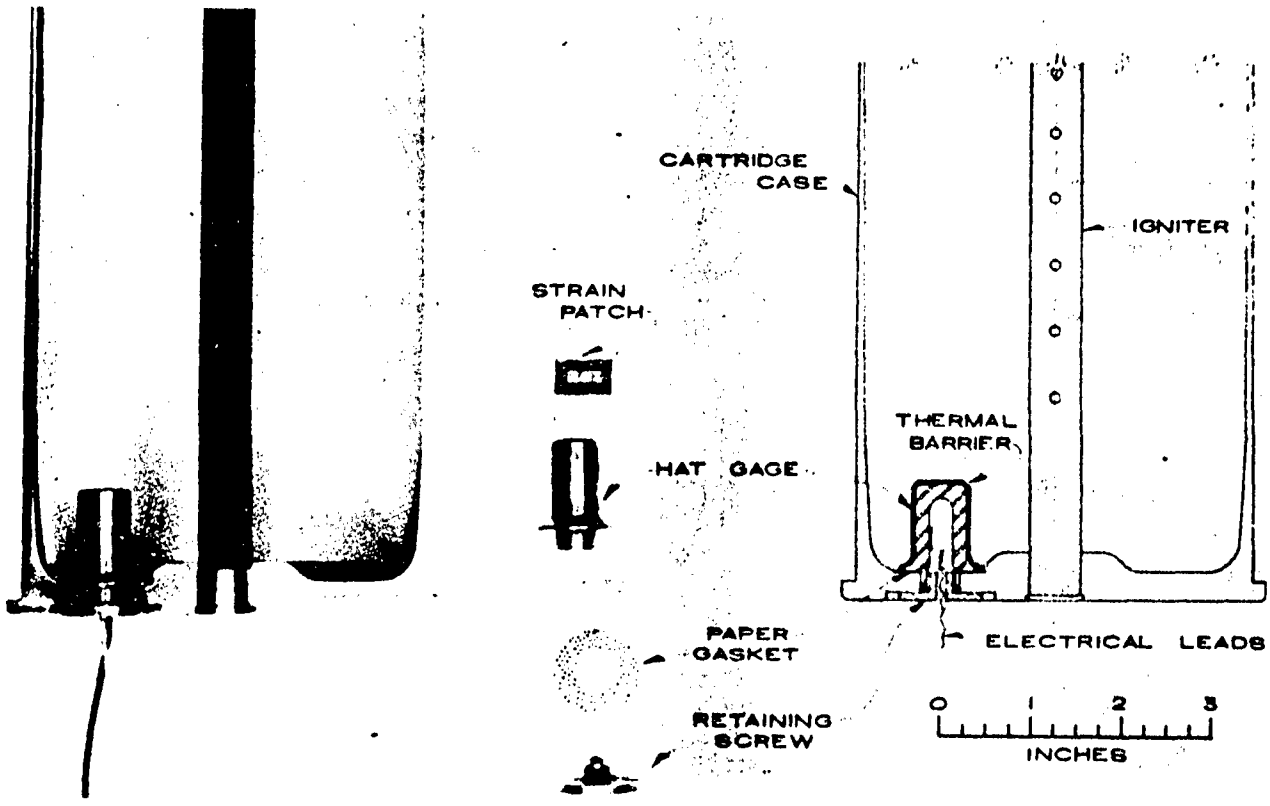


FIGURE 4-8. *The Hat Gage Mounted in Cartridge Case to Measure Breech Pressure.*

gage can be adjusted by design of the ferrule. They can also be made smaller than piezoelectric gages of the same pressure range and can be used in locations where space is restricted.

All pressure gages possess natural frequencies of oscillation. They will, therefore, overshoot and oscillate when subjected to rapid pressure changes. These oscillations will damp out more or less rapidly depending on the design of the gage and its mount. If too much damping is designed into the gage, however, it will be sluggish in response and will not accurately follow rapid pressure changes. Compromises must therefore be introduced. A high natural frequency is desirable for rapid response. The gage should be small and rigid. The hat gage shows up well in this respect. Figure 4-10 shows the response of the different types of gages when subjected to an almost instantaneous rise in pressure due to the impact on the gages of a shock wave generated in a high pressure shock tube.

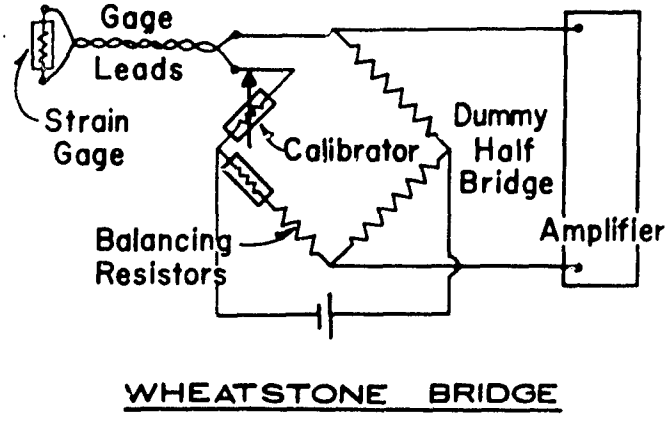


FIGURE 4-9. *Typical Input Circuit of Strain Type Pressure Gages.*

For further information on pressure-time recording gages and their use the reader is referred to References 3, 4, 5 and 6. Reference 4 gives a brief review of pressure gage development at Ballistic Research Laboratories and is the source of the figures used in paragraphs 4-2.2 and 4-2.3.

4-2.4 Crusher Gage[7]

For routine proof firing and most developmental firing, the pressure-time relation is not needed, but the maximum pressure is desired. For this purpose, crusher gages are used. A crusher gage consists of a steel cap, a copper gas-check cap, and a steel housing that contains a steel piston and a copper or lead cylinder. For recording very low pressures, the lead cylinder is required. An illustration of the crusher gage is given by Figure 4-11.

The copper gages are made in three sizes; their uses and the mean dimensions of their cylinders

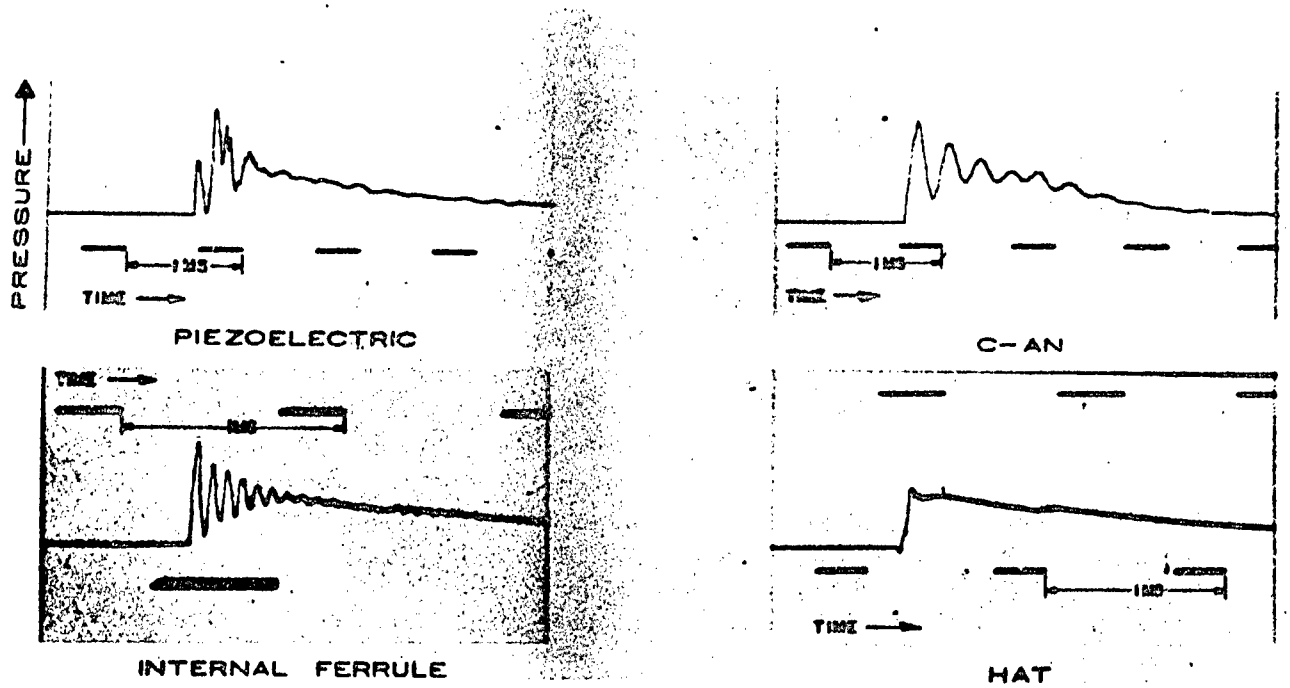


FIGURE 4-10. *Frequency Response Curves for Different Types of Pressure Gages when Subjected to a Stepwise Pressure Signal in a High Pressure Shock Tube.*

are tabulated below. The medium and major caliber gages use the same copper cylinders but have different size housings.

Size	Guns	Diameter	Length
Minor caliber	Small arms	.226	.400
Medium caliber	Small and medium cannon	.2525	.500
Major caliber	Major cannon	.2525	.500

For work on small arms, one minor caliber gage is inserted in the wall of a gun that is set aside for this purpose. For medium calibers, two medium caliber gages are placed in the chamber. Two major caliber gages are placed in depressions on the inner side of the breechblock for recording pressures in separate loading, major caliber, weapons.

The propellant gas pressure is exerted against the gas-check cap and transmitted to the piston, which compresses the cylinder against the cap. The length of the cylinder is measured in ten thousandths of an inch with micrometer calipers, both before and after firing. A table, which relates the compression to the static pressure that produces it, is based on values obtained by subjecting representative samples of cylinders from a lot to various pressures in a hydraulic press for 15 seconds. The pressures taken from the table are recorded and corrected, since they are less than the dynamic pressures corresponding to the same compression. Comparisons with piezoelectric gage pressures show that copper crusher gage pressures, when determined from copper crushers calibrated statically, should be multiplied by 1.20 to obtain the true chamber pressure, which is used in interior ballistic calculations. For the lead crusher gages, used for low pressures, the static pressure obtained is less than half the dynamic pressure.

Recent developments in dynamic calibration techniques have made it possible to reduce the difference between the maximum pressure as determined by a crusher gage and by a piezoelectric or strain type gage. The crusher elements are calibrated under pressures applied at rates approximating those occurring in guns. These techniques have been developed to the point where, for the larger caliber guns, crusher gages can be made to yield maximum pressures equivalent to those given by the pressure time measuring gages.

4-3 MEASUREMENT OF MUZZLE VELOCITY

4-3.1 General Principles

Before the invention of chronographs capable of recording very short intervals of time and of cameras capable of photographing projectiles in flight, there

was no way of making direct measurements of muzzle velocity by the simple method of measuring the time it took a projectile to traverse a previously measured distance or the distance traversed in a previously determined time.

After the invention of modern chronographs, muzzle velocity determination no longer posed a difficulty. In the method now commonly used, the projectile is timed over a measured distance by recording its passage as it enters and leaves the measured course. A device which determines the time between these two events is called a chronograph.

In the other method, the projectile is photographed against a distance scale by means of a high speed motion picture camera whose frame rate is known or by taking two or more photographs of the projectile against a distance scale using a series of fixed film cameras and a set of flash lamps with fixed time delays between them. Photographic methods are usually used when observations on the behavior of the projectile are desired, as well as determining its velocity. They cannot be classed as standard methods of muzzle velocity measurement. A discussion of these methods and the details of some applications are given in Reference 8.

4-3.2 Chronographs

There are two types of chronographs in general use; those which display the time interval directly, known as counter chronographs, and those which record the passage of the projectile as it enters and leaves the measured distance, known as camera chronographs. The former type makes use of electronic cycle counters which are started and stopped by the passage of the projectile and arranged to display the elapsed time on an indicating panel which is read directly. In the camera type of chronographs the output of the detecting device is fed to an oscilloscope and the face of the scope photographed with a drum or running film camera. The elapsed time, therefore, is determined from the distance on the film between the indications of the passage of the projectile by the detecting devices. This requires that a time scale be simultaneously recorded on the film. Figure 4-12 is a photograph of a standard model of camera chronograph using a drum camera.

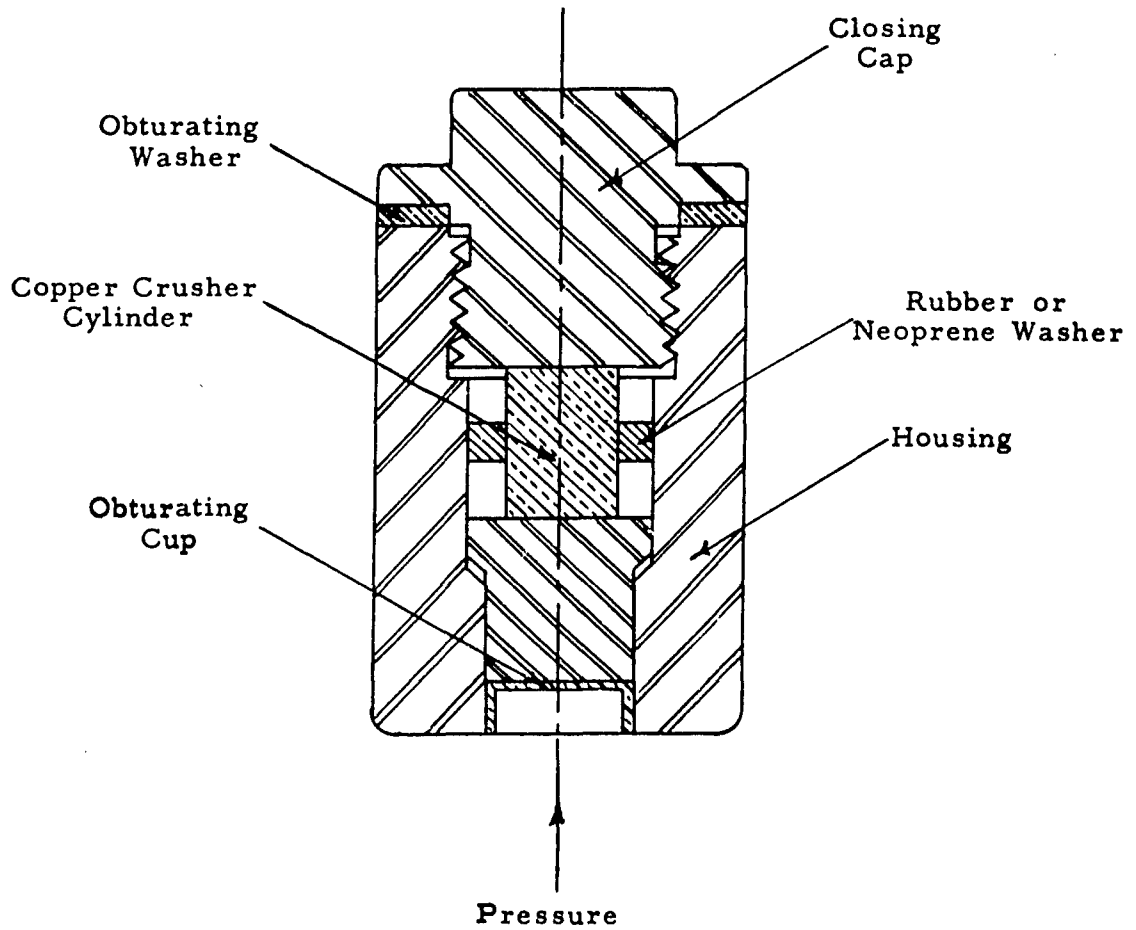


FIGURE 4-11. *Cross Section of Internal Copper Crusher Pressure Gage Using Cylindrical Copper Crusher.*

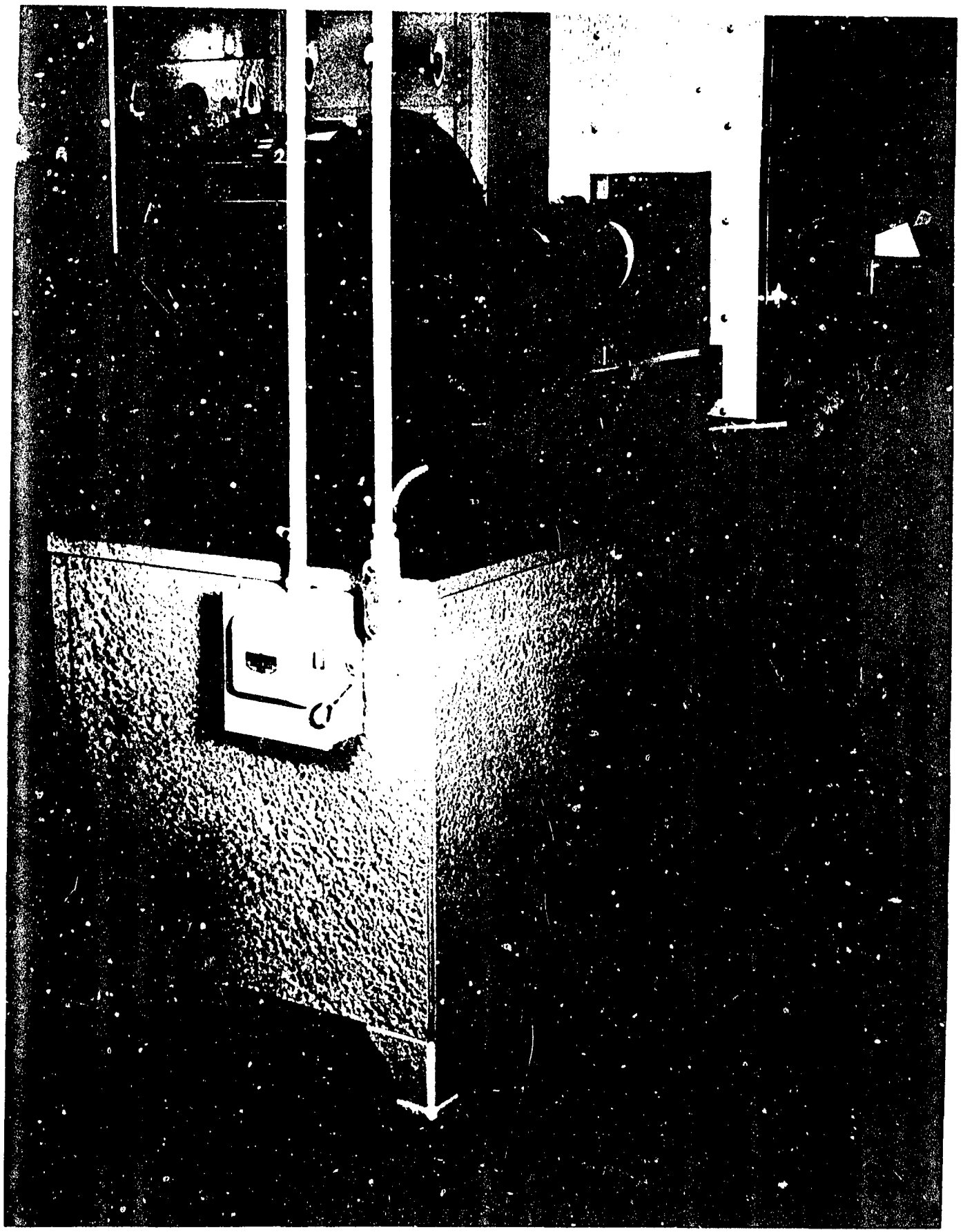


FIGURE 4-12. *Photograph of a Drum Camera Chronograph Mounted in Range Recording Room.*

The camera chronograph provides a permanent photographic record, which can be checked at any time; but about 20 minutes is required to develop, fix, and dry the film before it can be read. With the counter chronograph, about one minute is required to compute the velocity and report it; but the reading is erased after the time interval is noted. A permanent record can be provided by photographing the display panel or the process can be simplified by having the elapsed time printed out automatically.

Some of the earlier models of counter chronographs were rather critical in operation and difficulty arose because they could be activated by noise on the lines. In newer models, the operating conditions are less critical and these difficulties have been largely eliminated. The present tendency is to increasing use of the counter chronograph because of its speed and portability. For field use it has the great advantage that it does not require photographic processing facilities.

4-3.3 Detecting Devices

Commonly used devices to detect the passage of the projectile are of two types. One depends on the inductive effect as the projectile, which has been previously magnetized, passes through a coil of wire, and the other by the variation in the intensity of the light falling on a photoelectric cell caused by the passage of the projectile. The coil is the simpler device." It requires little care and can be used in the open without special protection or attention. Two coils can be easily mounted at opposite ends of a frame and the assembly elevated on a tower at an angle so that the gun can be fired at its normal operating elevation. This is more difficult to do with the more elaborate and fragile photoelectric devices. The coils, however, cannot be used with nonmagnetizable projectiles, such as small arms bullets and the other devices must be used. Nonmagnetizable, developmental projectiles used in interior ballistic research have been provided with small imbedded permanent magnets to permit the use of coil detectors.

The design of the coil detector is important." As the projectile approaches the coil the increasing magnetic flux through the coil induces an emf in it which increases and reaches a maximum value when the projectile is in such a position that the rate of change of flux is a maximum. The emf then begins to decline as the rate of change of flux declines and becomes equal to zero, at which time the emf is zero. The flux then tends to decrease as the projectile starts to leave the coil and the emf reverses

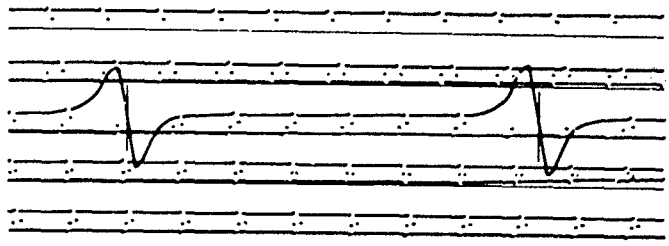


FIGURE 4-13. *Drum Camera Chronograph Record of Signal from Velocity Coils.*

sign and follows a course similar to the approach but reversed in direction. The coil should be so designed that the signal reversal is sharp so that the record crosses the axis steeply. The film distance between the crossing points is then accurately determined and serves to determine the time accurately. Figure 4-13 shows a drum camera chronograph record from coil detectors.

There are two types of photoelectric detectors, lumiline screens and sky screens. Lumiline screens use a light source incorporated in the apparatus and sky screens use the light from the sky. In the latter the photocell is screened so that it is illuminated by the light from a narrow region of the sky transverse to the trajectory. When the projectile crosses this region of the sky, the illumination of the cell is reduced sufficiently to induce a voltage change in the cell circuit which deflects a cathode ray oscilloscope and the deflection is photographed on a moving film camera or the signal can start or stop a counter chronograph. Sky screens have been developed for field use and are fully described together with the associated counter chronograph in Reference 10.

The light source in the lumiline screen is a long filament electric lamp mounted in a metal frame behind a narrow slit transverse to the trajectory. A photocell is mounted behind another slit on the opposite side of the frame. A projectile passing through the frame reduces the illumination on the cell in a manner similar to that of the sky screen. Lumiline screens are used mainly in indoor ranges for measuring the velocity of small caliber projectiles such as bullets from small arms. Screens in use are shown in Figure 4-14.

4-3.4 The Calculation of the Muzzle Velocity

Once the time of passage, t, of the projectile over the measured distance, D, is known, the ratio, D/t, gives the average velocity over the distance, D. This average velocity will occur at the midpoint of D provided the acceleration of the projectile is constant. The latter condition will hold if the air

resistance to the motion of the projectile does not change appreciably over the distance D. This is closely the case so that the velocity furnished by the instrumentation can be assumed to occur at the midpoint of D.

On account of the air resistance, the velocity decreases between the muzzle and the midpoint of the detecting devices. The small correction required to give the velocity at the muzzle is proportional to the ratio

$$Z = X/C \tag{4-1}$$

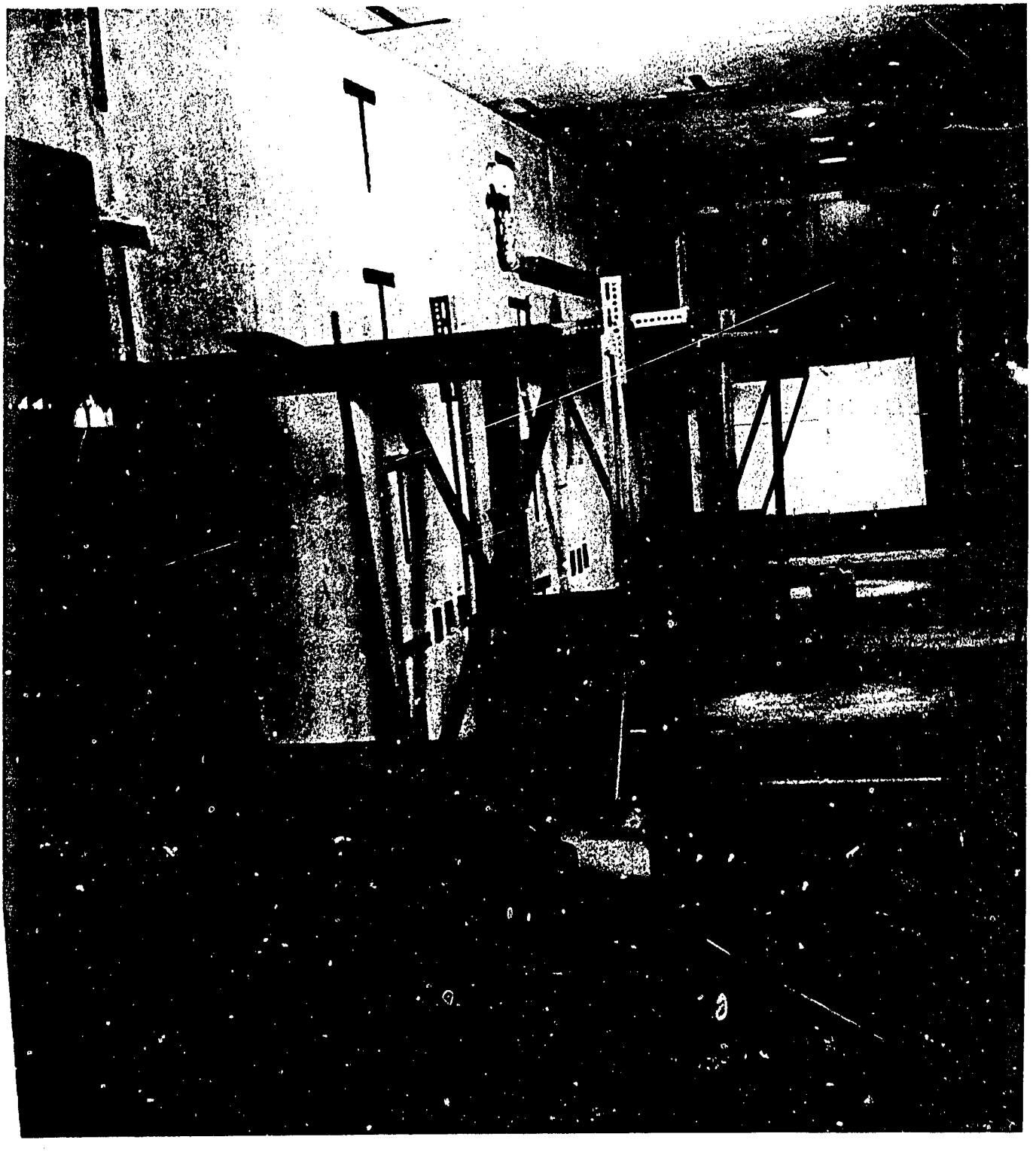


FIGURE 4-14. *Lumiline Screens in Use in an Indoor Range.*

where

X is the distance from the muzzle to the midpoint and

C is the ballistic coefficient

C is a function of the weight, caliber and shape of the projectile, the density of the atmosphere, and the range wind. The correction factor, which depends on the velocity and the drag function, has been tabulated by the Instrument Laboratory of the Development and Proof Services at Aberdeen Proving Ground.[10,11]

For a short distance in front of the muzzle, the projectile is surrounded by propellant gas. Since the muzzle blast increases the projectile velocity, another correction must be subtracted from the apparent muzzle velocity to obtain the true one. From the measurements of the spin of several projectiles by a radiosonde, extrapolated to the muzzle, Hitchcock found that the increase in velocity due to the muzzle blast is about 1.2 percent of the apparent muzzle velocity for guns having a normal expansion ratio.[12]

4-4 TRAVEL-TIME MEASUREMENTS

4-4.1 Barrel Contacts

The position of the projectile in the barrel as a function of time can be determined by inserting insulated probes through holes bored in the barrel wall which make contact with the projectile as it passes. Each probe is part of an electrical circuit which is completed through the projectile and the barrel. The projectile acts as a switch which closes the circuits momentarily. The current in the circuits can be detected and displayed on a cathode ray oscilloscope and the face of the oscilloscope photographed on a moving film or drum camera in the usual way and related to a time scale on the film. The zero of time is usually indicated on the film by detecting the initiation of the primer or by a contact at the muzzle.

Barrel contacts have to be designed and used with care if the signal is to occur when the projectile has the same position with respect to the contact at each location. This can be assured in part by machining a notch in the forward part of the projectile. The shape of the notch is such that a vertical surface is presented to the contact. If care is taken to insert the contacts only in the rifling grooves of the gun, they will then establish contact with the rotating band only.[1] For smooth bore weapons and when firing jacketed bullets, the notch in the projectile becomes necessary.[2] If the electrical potential of the contacts is too high the current may start before mechanical contact is made. This is especially likely if the gas ahead of the projectile becomes ionized. This can happen if hot gas leaks past the projectile or if the air in the tube is compressed by the motion of the projectile itself.

Barrel contacts are extensively used in interior ballistic research, the exact form varying with the user, often as check points against other methods of measuring projectile displacement.[13]

When it is desired to derive from the measurements an accurate travel-time relation, a rather large number of contacts must be used. This involves considerable damage to the barrel thus making it useless for other purposes. Considerable time and expense is involved in doing the necessary machine work.

4-4.2 Microwave Interferometer

The microwave interferometer is the microwave analog of the well known Michelson moving mirror interferometer which is used to measure small distances using light of optical wave lengths. In both instruments a beam of radiation is divided into two beams. One beam is sent to a reflector at a fixed distance and the other beam to a reflector which can be moved. The reflectors return the radiation to the point of separation where the beams are superimposed and combine to form a beam of radiation whose intensity depends on the amplitudes of the reflected beams and their phase difference. The phase difference depends on the difference in the distance traveled by the two beams from the point of separation and back again according to the relation

$$\delta = \frac{2\pi\ell}{\lambda} \qquad (4\text{-}2)$$

where δ is the phase difference, ℓ the difference in distance and λ the wave length of the radiation. Now, if the movable reflector is displaced parallel to the direction of the reflected beam, ℓ will be changed and δ will be different. This will change the intensity of the combined beam. If ℓ is changed continuously δ changes continuously and by one cycle (2π radians) every time ℓ changes by one wave length. The intensity of the combined beam changes cyclically, going through one cycle every time δ does. Since ℓ changes by one wave length when the movable reflector moves one-half wave length, one cycle of intensity change indicates a displacement of the reflector of one-half the wave length of the radiation.

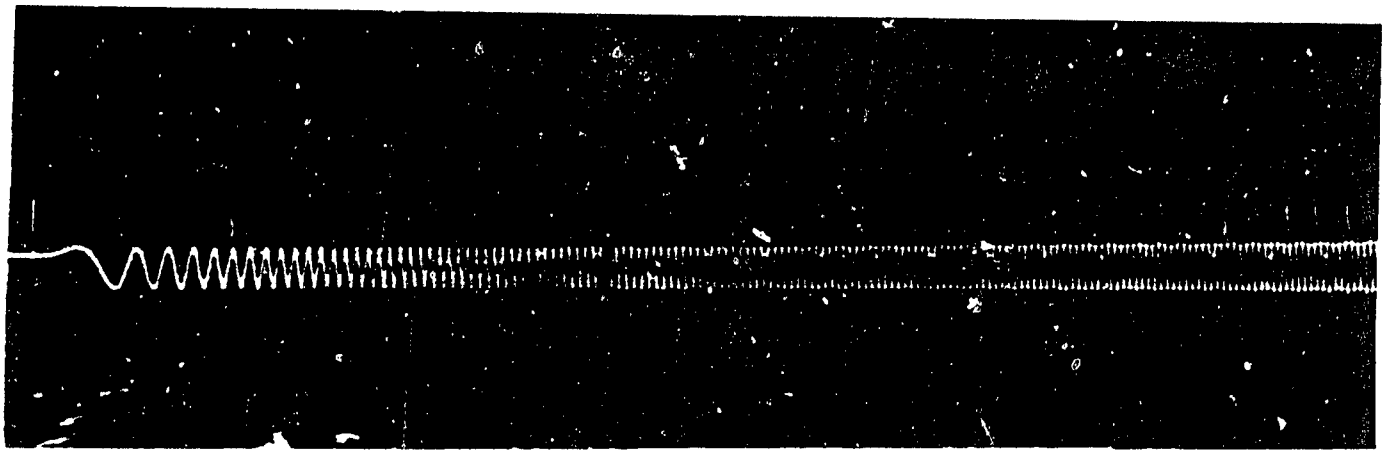


FIGURE 4-15. *Typical Microwave Interferometer Record of Projectile Travel versus Time (Caliber .50)*

For the wave length range used in the microwave interferometer, the radiation is propagated in a wave guide. The source of the radiation is a Klystron oscillator. The radiation is divided at a "magic tee". One part is led by wave guide and directed down the barrel of the gun to the projectile which constitutes the moving reflector. The other part is led to the fixed reflector and in this arm of the circuit there is provided an attenuator and a phase shifter so that the intensity of the output signal can be adjusted to a convenient value initially and the phase difference adjusted to zero.

The combined output is detected by a crystal detector and fed to a cathode ray oscilloscope through suitable amplifiers. The face of the oscilloscope is then photographed on moving film along with a time scale. A typical record is shown in Figure 4-15 and a block diagram of the apparatus in Figure 4-16. For further details of the construction and use of the interferometer the reader is referred to References 14 and 15.

The microwave interferometer has obvious advantages over the barrel contacts. It requires no modification of the tube and yields a continuous record of the travel of the projectile so that a more accurate travel-time curve can be derived. The relative accuracy for the two methods is discussed in Reference 13 where it is shown that even with

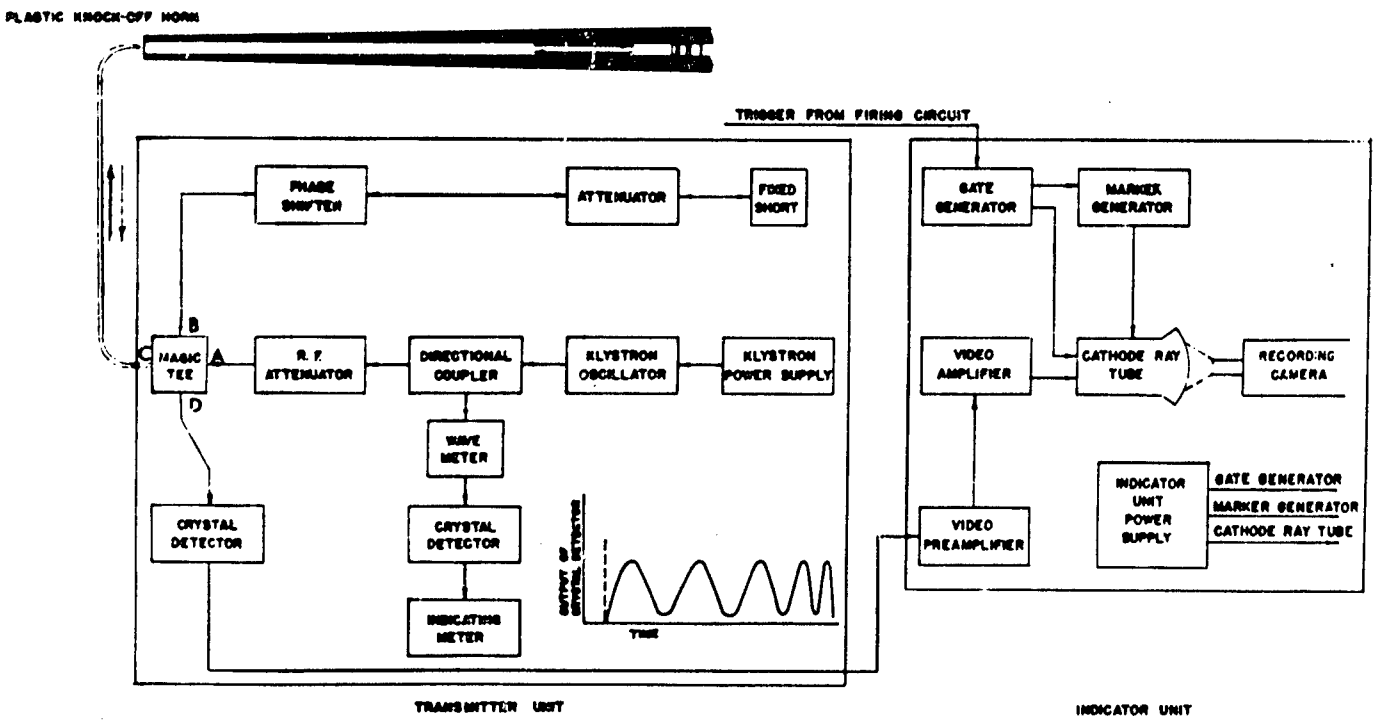


FIGURE 4-16. *Block Diagram of the Microwave Interferometer for Measuring Projectile Travel versus Time.*

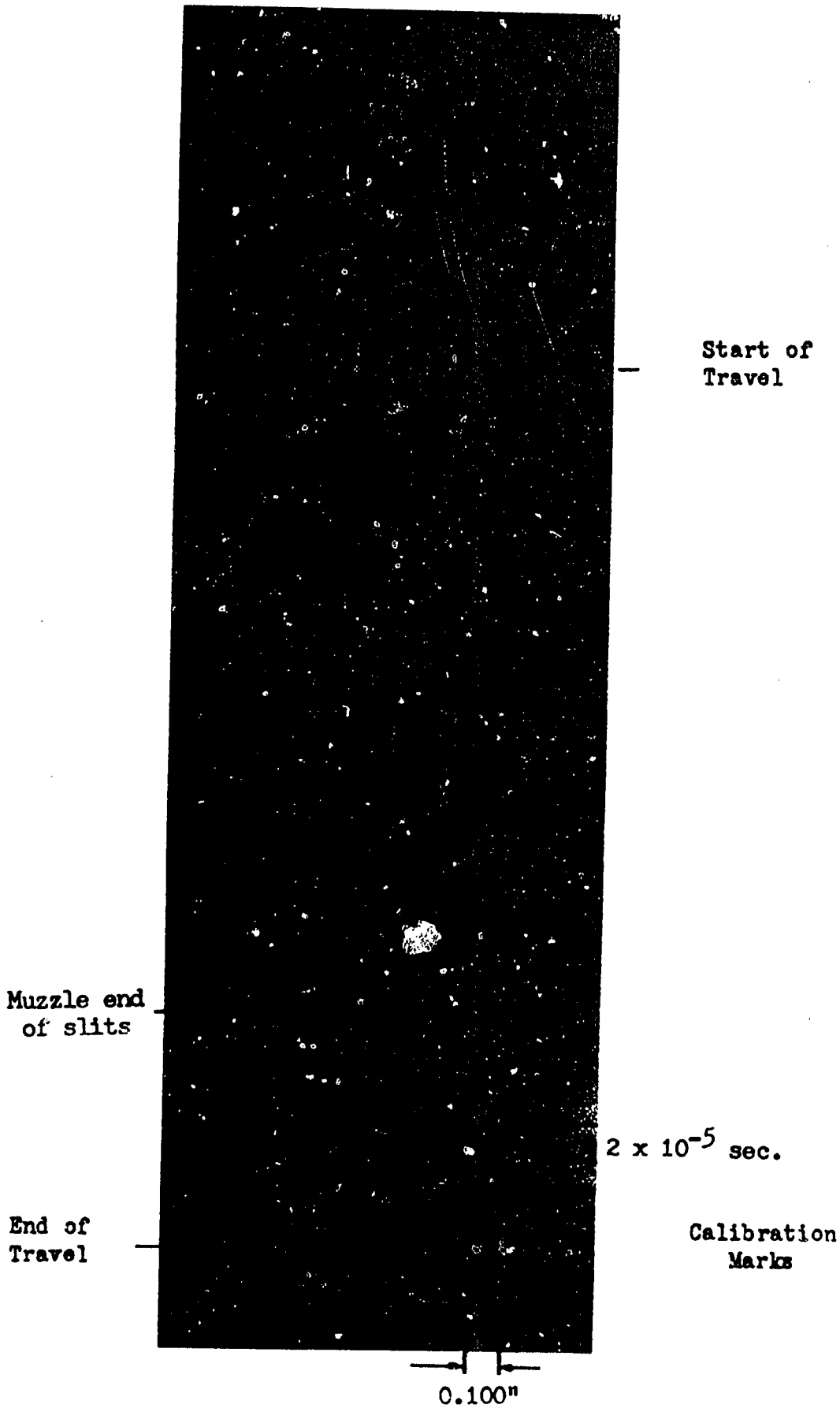


FIGURE 4-17 *Typical Travel-Time Record at Start of Travel Using Back-Lighted Slits in Cutoff Tube (Caliber .50), Back-Lighting Intermittent, 10^5 Exposures per Second.*

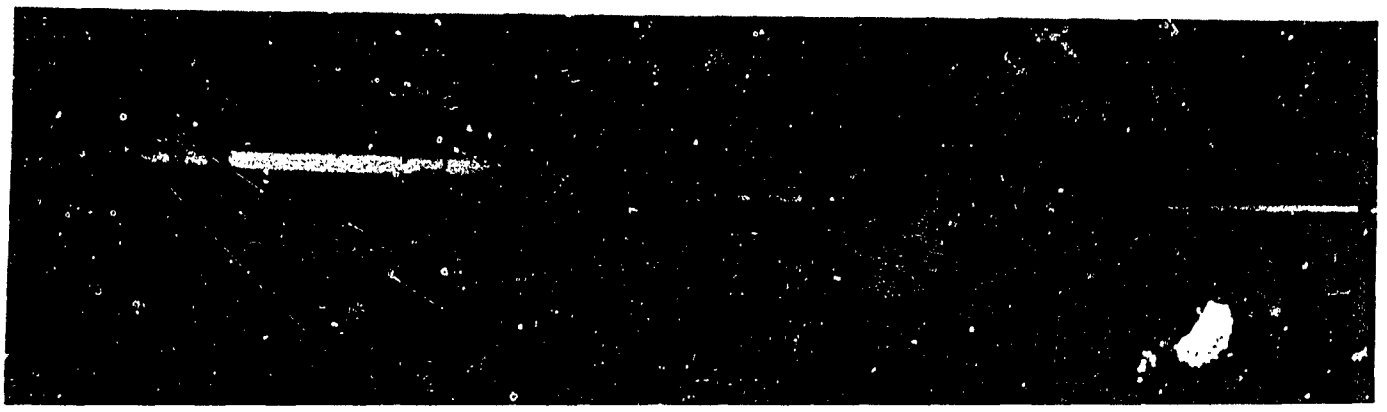


FIGURE 4-18. *Foil Contactor Assembly for Measuring Travel During the Engraving Process, 105mm Howitzer.*

great care in the design and placement of the contacts they exhibited some erratic behavior although there was no systematic error in the results derived from their use. There were no systematic errors in the results for either system, however.

4-4.3 Measurement of Projectile Travel Near the Start of Motion

Neither the barrel contacts nor the interferometer gives a sufficiently detailed and accurate account of the motion of the projectile at the start of motion and during engraving to permit entirely satisfactory conclusions to be drawn about engraving forces and starting pressures.

If extra tubes are available, for research purposes it is often permissible to cut the tube off so that the nose of the projectile is visible and then take a high speed motion picture of the projectile as it moves. Another method[2] is to machine two slits on opposite sides of the tube so located that the nose of the projectile projects slightly beyond the breech end of the slits. The slits are then backlighted and an image of the illuminated slits formed on the film of a moving film camera so that the film runs perpendicular to the image. As the projectile moves the slits are progressively covered and the boundary between the illuminated and unilluminated part of the film is the locus of the travel-time curve, Figure 4-17. The tube must be cut off just beyond the end of the slits since the slits relieve the pressure when the projectile base passes and the projectile may stop in the tube.

If damage to the tube is not permissible other methods must be used. One of these which has been used for measurements on a 105mm Howitzer is described in Reference 16. In this method, a rod is inserted down the barrel and fixed at the muzzle. At the other end, the rod holds a set of foil contactors inside the hollowed out projectile. An internal contact is provided in the projectile, arranged so that the projectile movement causes the internal contact to touch the foil contactors in succession. The arrangement is shown in Figure 4-18. The rod and contactor assembly are insulated from the barrel electrically and an electrical circuit is completed through the projectile and the barrel when contact is made with the foils. After a travel of about four inches the base of the projectile comes in contact with the end of the rod and forces it out of the barrel. In the 105mm Howitzer the rod comes out smoothly. It may not do this if used in higher velocity weapons where the accelerations are larger and the force on the rod greater.

The results of the measurements were differentiated twice to yield the acceleration, and from a simultaneous measure of the pressure the resistance to the motion is determined from the relation

$$PA - f = Ma \qquad (4\text{-}3)$$

where f is the resistance to the motion. A typical result is shown in the consolidated plot, Figure 4-19.

4-5 IN-BORE VELOCITY AND ACCELERATION MEASUREMENT

4-5.1 Differentiation of the Travel-Time Data

The velocity and acceleration in the bore can be determined by differentiating the travel-time data provided by the interferometer or barrel contacts. To do this requires a complicated data reduction process and if the differentiations are to yield accurate results, not only must the records be read with great accuracy but the records must be very precise to begin with. In no case is the original data obtained from the records sufficiently accurate to be used directly. It must be first smoothed and the smoothed data differentiated. The result of the

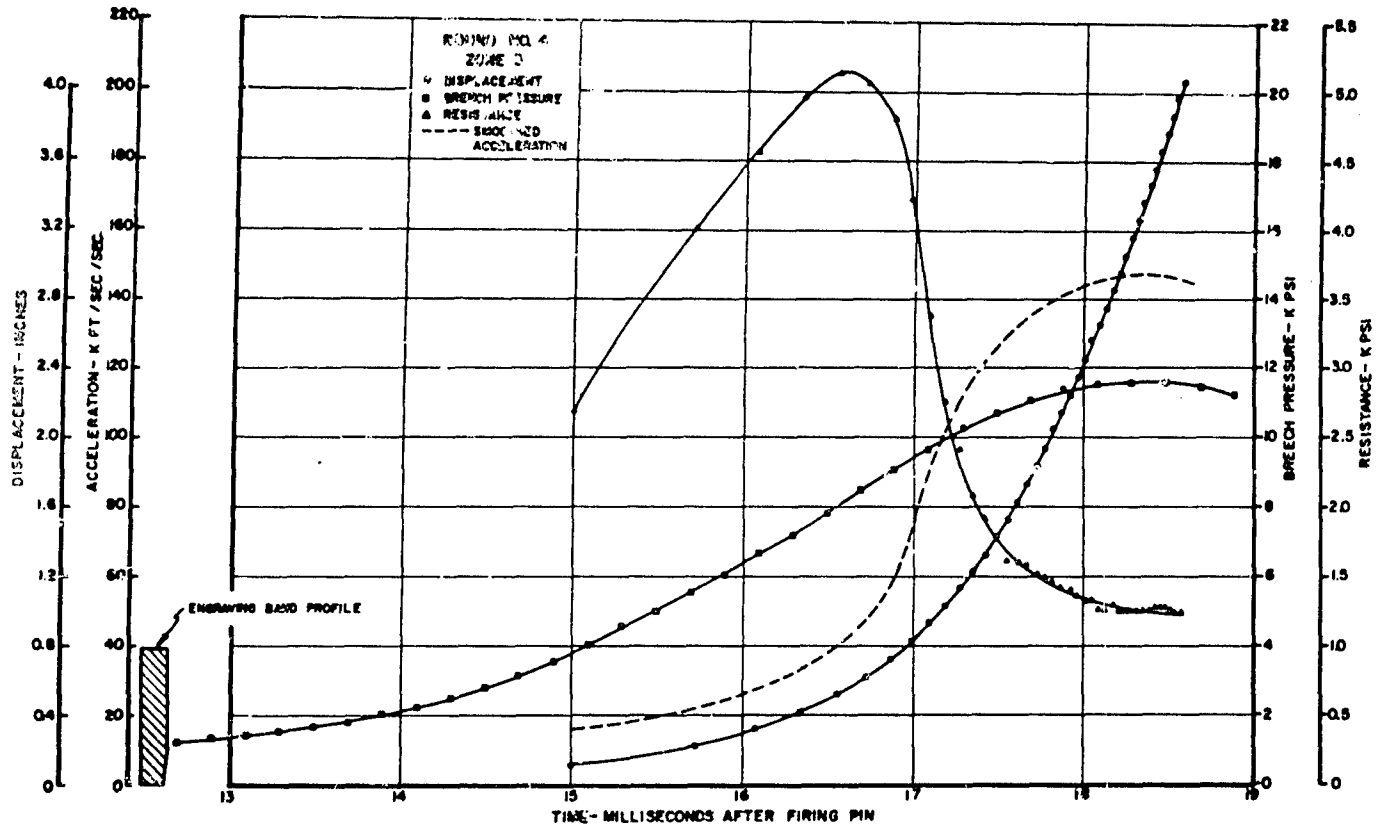


FIGURE 4-19. *Consolidated Plot of the Data and Results for the First Four Inches of Travel in the 105mm Howitzer.*

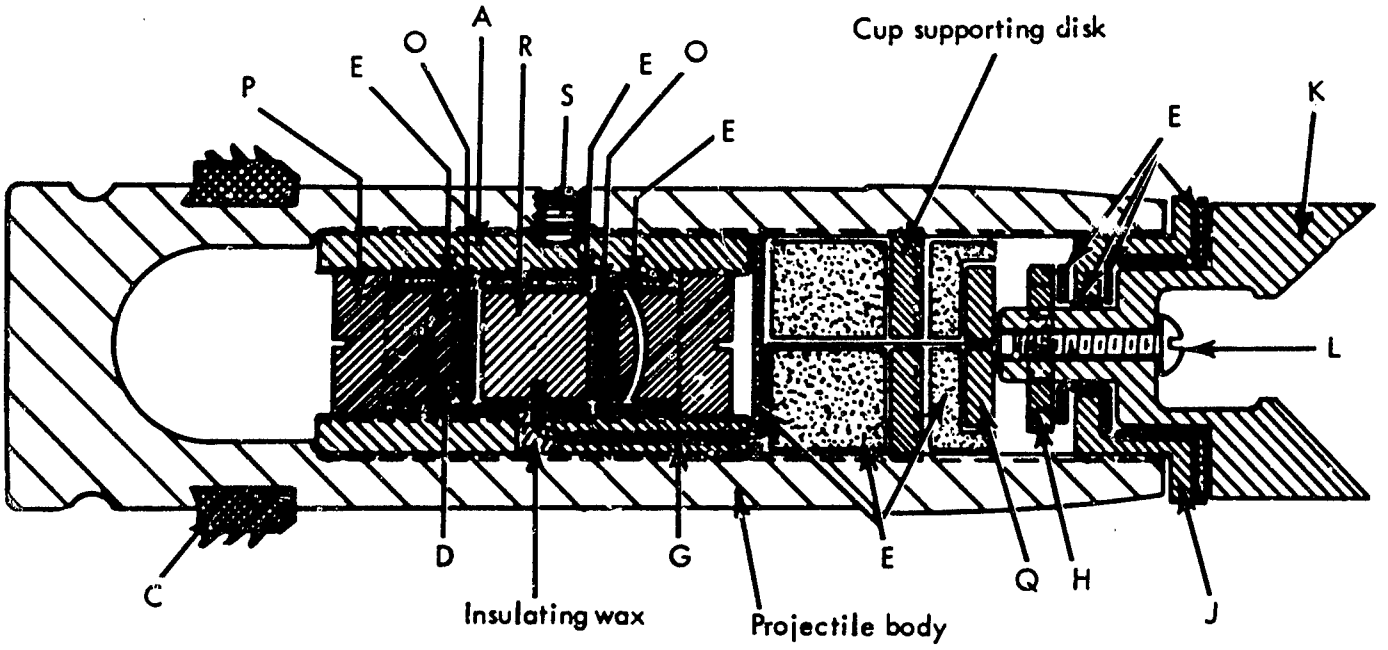
first differentiation must also be smoothed before the second differentiation, and the final result will usually require some final smoothing. The amount of work required to reduce the data and make the calculations for a single round is considerable[2,17] and the results may be subject to unknown errors. It is desirable to measure the velocity and acceleration directly.

4-5.2 The Measurement of Velocity

A standard method of measuring the velocity of projectiles makes use of the Doppler effect; that is, the change in frequency which occurs when a radar beam is reflected from the projectile. There are a number of ways, differing in detail, which theoretically can be used to measure the Doppler shift.

One method is to use two stabilized Klystrons differing in frequency by a few megacycles. The radiation from one is led down the barrel of the gun and reflected from the projectile. The second Klystron is provided with a control system which locks its frequency to the signal from the first after reflection, which serves as a reference signal. When the projectile is not moving, the control voltage required to lock the second Klystron to the radiation of the first is constant. Another method of providing the reference signal, using only one Klystron, is to lead part of the signal from the Klystron out and shift its frequency, thus taking the place of the signal from the second Klystron. If now the projectile starts to move, the reference signal will be increased in frequency and the control voltage will increase or decrease depending upon whether the difference in frequency between the two Klystrons is increased or decreased. The change in the control voltage is proportional to the frequency change and hence to the change in velocity. The control voltage is recorded as a measure of the velocity. It has been found that the controlled Klystron has a locking range of about 200 kc which corresponds to projectile velocities of about 5000 feet per second.

These methods for measuring the velocity directly simplify the determination of displacement and acceleration. Not only will the tedious smoothing and differentiating processes be reduced but the accuracy of the final results should be improved. The direct measurement of the velocity by the Doppler effect is simple in principle and from an accurate measurement, the displacement can be determined by integration, which is a more accurate process than differentiation, and the acceleration determined by a single differentiation which will eliminate the errors due to the second differentiation.



A Gage body
C Copper rotating band with obturation skirts
D Ball contactor
E Lucite bushing
G Signal conductor
H Lock nut
J Cup retainer
K Wire-collector cup
L Bore wire terminal screw
O Quartz crystal
P Retaining screw
Q Brass contact button
R Weight
S Set screw

FIGURE 4-20. *Diagram of Quartz Piezoelectric Acceleration Gage Assembled in the Projectile.*

4-5.3 The Measurement of Acceleration

To measure the acceleration directly requires instrumentation in the projectile. The earliest acceleration gages for mounting in projectiles depended upon the pressure developed on a quartz crystal plate by the inertial reaction to the acceleration of a weight bearing against the crystal plate. One model is shown in Figure 4-20.[18]

To record the signal from the gage one must transmit the signal out of the barrel. This is done by leading a wire down the barrel and connecting it to one terminal of the gage, the circuit being completed by grounding the other terminal to the projectile wall which makes contact with the barrel through the rotating band. As the projectile moves the wire is gathered up in a cup-shaped receptacle at the forward end of the projectile.

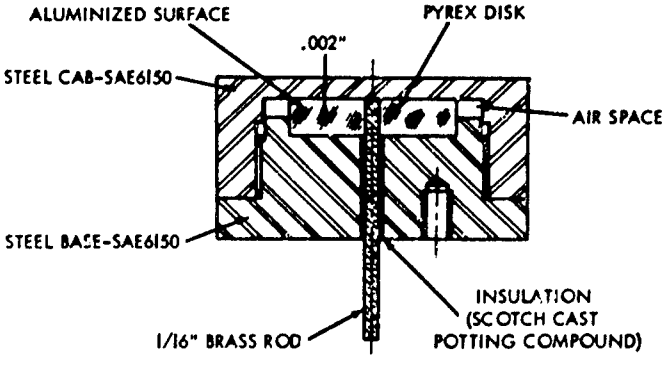
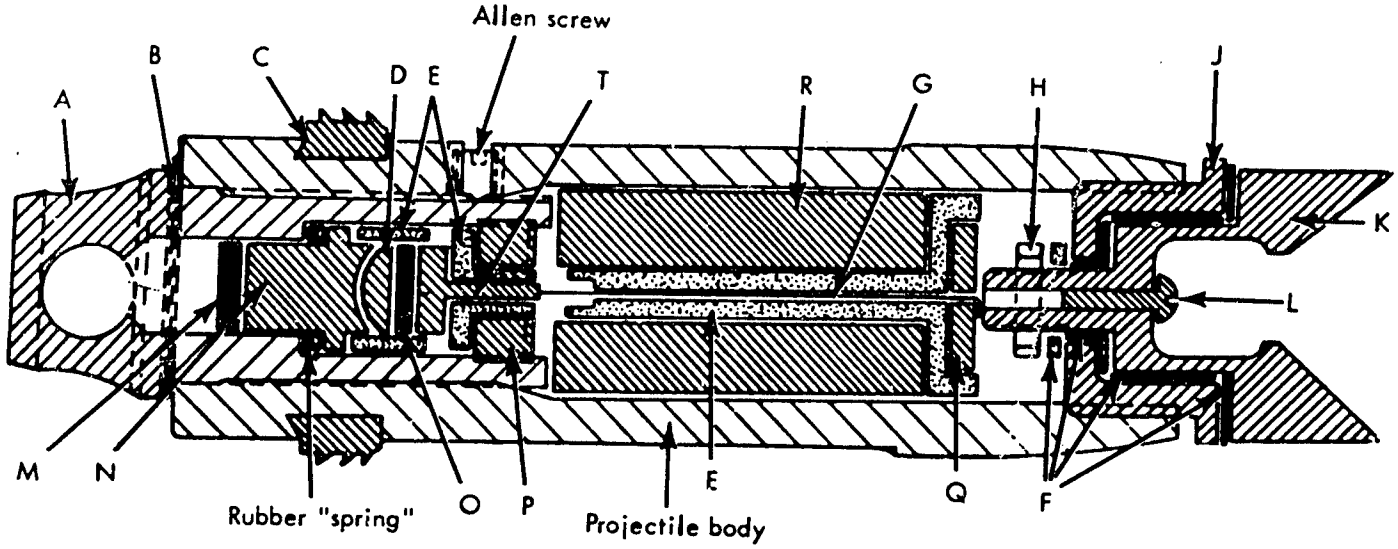


FIGURE 4-21. *Diagram of the Variable Capacitance Acceleration Gage.*

Considerable difficulty is usually encountered with this system of measurement. It requires direct current operation and it is difficult to eliminate the noise generated by the sliding contact at the rotating band. In the process of gathering up the wire, it may shatter at the higher velocities which will generate noise as will leakage of ionized gases past the projectile.

In an attempt to circumvent these difficulties, apparatus has been developed[19] using an acceleration gage depending on the change in capacitance when subjected to acceleration. The design of one model of the gage is shown in Figure 4-21. When the projectile is accelerated, the body of the gage is slightly flattened which decreases the separation between the metal plated surfaces and hence increases the capacitance. In use the gage is part of an oscillator circuit. If the capacitance of the gage is changed the frequency of the oscillator is shifted; the frequency shift being a measure of the acceleration.

This scheme permits the use of alternating current



A Gage body
B Copper gasket
C Copper rotating band with obturation skirts
D Ball contactor
E Lucite bushing
F Lucite insulators
G Signal conductor
H Lock nut
J Cup retainer
K Wire-collector cup
L Bore wire terminal screw
M Neoprene disk
N Piston
O Quartz crystal
P Retaining screw
Q Brass contact button
R Weight
T Top contactor

FIGURE 4-22. *Diagram of Quartz Piezoelectric Base-Pressure Gage Mounted in the Projectile.*

operation so that much of the unwanted noise can be blocked out of the recording circuits by proper filtering. It introduces other difficulties, however, in that the instrumentation in the projectile is much more complicated, and as it must function while under large acceleration, the design requirements are very stringent. One is also never quite certain that the frequency of the oscillator will be stable under the conditions of firing. Models have been used successfully in the 105mm Howitzer where the conditions are not too drastic. There seems to be no difficulty in designing apparatus rugged enough to withstand high velocity gun accelerations. The question of stability will remain.

Trouble also arises with the uncertainty of the calibration of the capacitance gage. It is obviously not possible to subject the gage to a known acceleration of the required magnitude. Recourse has, therefore, been made to subjecting the gage to a mechanical force applied externally with a press. Under acceleration, however, the force system acting on the gage is not the same as that used in the calibration. The gage has a complex shape and any distortion due to acceleration cannot be predicted accurately by theory so that it could be allowed for. The piezoelectric crystal gages, discussed in paragraph 4-2.2, could be calibrated much more confidently as the effect of the acceleration in the crystal itself was considered negligible, the charge developed therefore being entirely due to the inertial pressure of the weight.

4-6 THE MEASUREMENT OF BASE PRESSURE

The methods described to measure acceleration can be used to measure base pressure.[18] All that is needed is to modify the gages and their installation in the projectile to withstand and be subjected to the pressure of the gases and to make the effects of the acceleration negligible with respect to those due to the gas pressure. The design of a piezoelectric base pressure gage is shown in Figure 4-22. It is similar to the acceleration gage except that the crystal is now compressed by a piston subject to the gas pressure through an opening in the base of the projectile. Because the piston also has inertia, the pressure on the gage, P_g, is not equal to the base pressure, P_b, but is given by

$$P_b - \frac{ma}{A_p} = P_g \qquad (4\text{-}4)$$

where m is the mass of the piston and A_p its area.

A variable capacitance base pressure gage designed for alternating current operation in a manner

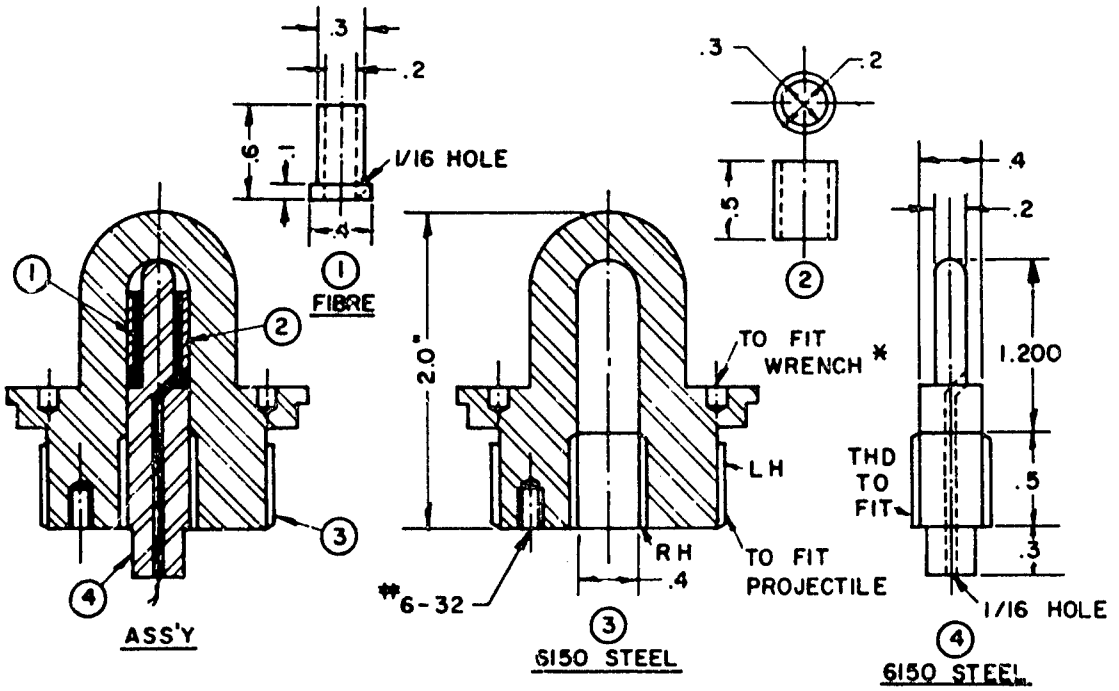


FIGURE 4-23. *Variable Capacitance Base-Pressure Gage Diagram of Parts and Assembly.*

similar to the variable capacitance acceleration gage is illustrated in Figure 4-23. It does not make use of a piston; the gas pressure being applied directly to the outside of the pressure element which serves also as the outer electrode. The pressure reduces the inner diameter of the pressure element and hence reduces the clearance from the inner electrode. This increases the capacitance of the gage.

4-7 THE MEASUREMENT OF BORE FRICTION

If the acceleration and the base pressure are known one can derive the bore friction, f, from the relation,

$$f = P_b A - Ma \qquad (4\text{-}5)$$

where P_b is the base pressure, a the acceleration, M the mass of the projectile, and A the bore area.

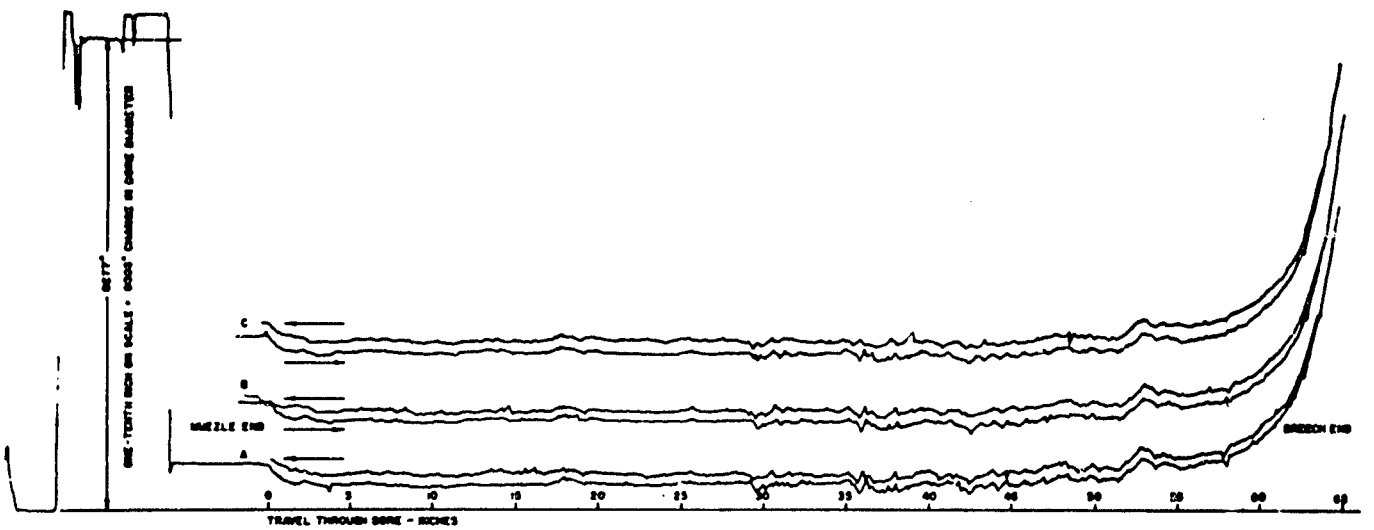


FIGURE 4-24. *Record Produced by the Automatic-Recording Bore Gage. Three Complete Scans in Both Directions to Test Repeatability.*

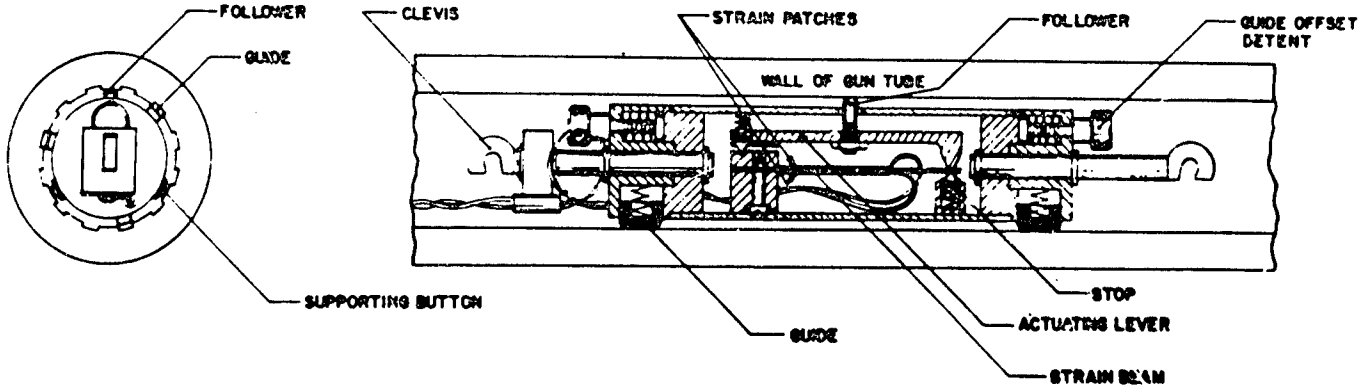


FIGURE 4-25. *Diagram of One Model of the Automatic-Recording Bore Gage*

An examination of Equations 4-4 and 4-5 shows that if the mass of the piston, m, is so chosen that $m A_p = M_c A$, then $f = P_g A$ so that under these circumstances the output of the gage is proportional to the bore friction. By use of this property, a base pressure gage can be designed to yield a simultaneous measure of the bore friction.

4-8 THE MEASUREMENT OF BARREL EROSION

4-8.1 General

The standard devices used to measure changes in bore diameter are the star gage and the pullover gage. They are both mechanical micrometers designed especially to measure both the diameter of the tube at a certain location and the distance to the point of measurement. The measuring head is attached to a long staff. The staff serves to manipulate the head to make the diameter measurement and is also provided with a scale to measure the distance to the point of measurement. Both gages are made in a number of sizes for use with the various calibers. The details of their construction and use are given in Reference 20.

4-8.2 The Star Gage

There are several types of star gages but the principal ones are the lever and small bore gages used for large and small calibers. They do not differ in principle, the difference being only in the mechanism used to manipulate the measuring head. In both types, the head is provided with contactors which are forced out radially to make contact with the surface of the bore by advancing a cone shaped piece upon which the inner ends of the contactors ride. When the cone is retracted the contactors disengage from the surface. The position of the cone when contact is made with the bore surface is an indication of the diameter, and is read on a scale at the operating end of the staff.

4-8.3 The Pullover Gage

This gage functions in a manner similar to a telescoping inside micrometer. The head which is constructed so that it will telescope and retain its minimum size is initially set larger than the bore diameter and inserted with its staff into the barrel to the distance at which the measurement is to be made. This requires that it be set at an angle with respect to the staff. It is then "pulled over" which forces it to telescope until its length is equal to the inner diameter of the tube. A vernier scale is provided on the head so that the diameter can be read off when the gage is withdrawn.

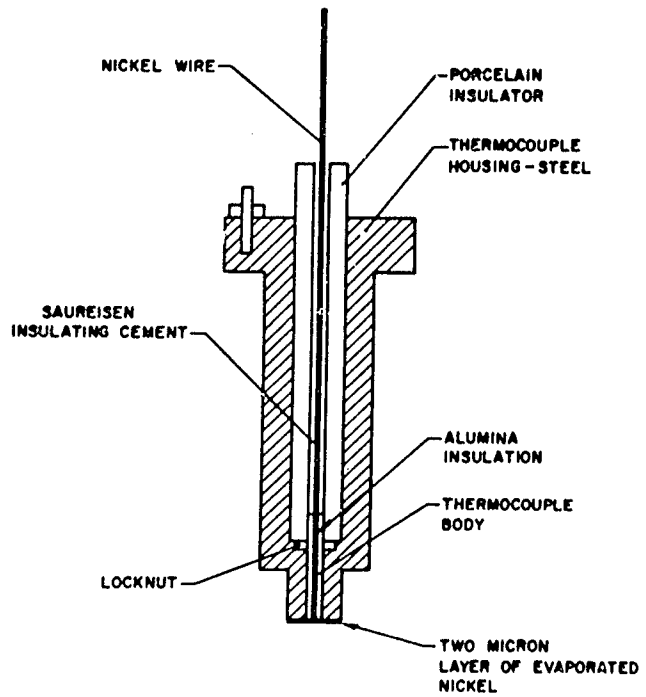


FIGURE 4-26. *Diagram of Bore Surface Thermocouple and Housing, BRL Model.*

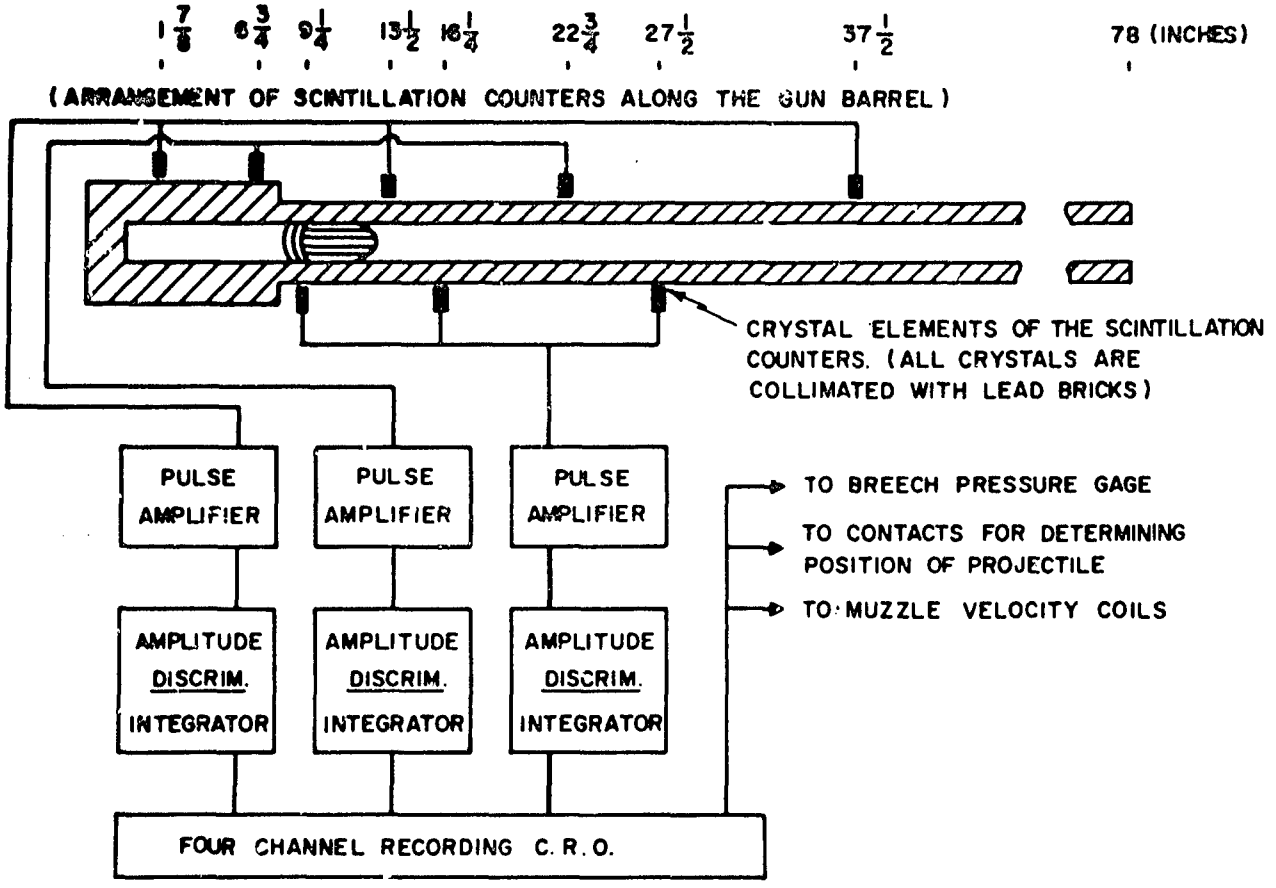


FIGURE 4-27. *Block Diagram of Apparatus for Observing Motion During Firing of a Radioactive Source Imbedded Initially in a Propellant Grain.*

4-8.4 The Automatic Recording Bore Gage

Bore gages have been constructed which depend on the strain produced at the surface of a cantilever beam. The beam is mounted in a frame which fits into the barrel and carries one or more contactors which bear on the bore surface. When the frame is forced into the bore, the beam is bent from its initial position by the force on the contactors. The strain produced in the beam is recorded by a system of two strain gages cemented to opposite surfaces of the beam and forming two arms of a Wheatstone bridge so arranged as to maximize the bridge output. When calibrated by applying known deflections to the beam the imbalance of the bridge is a measure of the bore diameter.

A gage of this type was developed[21] to record automatically a continuous measurement of the bore diameter (or radius, depending on the model) when it was pulled through the barrel by a motor driven mechanism. The gage is provided with supports which engage the rifling so that the contact stays on the same land throughout the travel. The output of the gage is fed to an automatic recorder which traces on a moving paper a record of the bore diameter as a function of distance. A calibration is placed on the record by pulling the gage through a calibration tube provided with stepwise diameter changes or by a micrometer calibrator which can be varied continuously by a micrometer screw.

These gages have been found to be consistent in operation and to give reproducible results. The records can be read to .0005 inch and the precision is about of this order. By reducing the radius of curvature of the tip of the contactor they can be made to record the major roughnesses of the surface and yield knowledge of the condition of the surface. The type of record produced is shown in Figure 4-24 and a diagram of one model of the gage in Figure 4-25.

4-9 BARREL TEMPERATURE MEASUREMENTS

4-9.1 Thermocouples

A variety of thermocouples have been used for barrel temperature measurement. On the outside surface where the temperature variations are low, no special difficulty is encountered; all that is necessary is a good bond to the surface which can be obtained by soldering or welding.

To make measurements within the wall, holes must

be bored to the desired depth and an insulated thermocouple wire inserted to make good thermal and electrical contact with the bottom of the hole. This usually requires welding although mechanical pressure can be made to work. Such contact may be unreliable, however, in a gun during firing. Electric welding of the contact requires care. If too much metal is melted, the exact location of the contact is uncertain. Just enough and no more should be melted. This usually requires an automatically controlled switching mechanism and the time to just make the weld is determined by trial in a separate test sample.

The hole and wire should be small and the thermal diffusivity of the wire and weld should be as close to that of the barrel material as possible. This is to minimize the disturbance to the heat distribution brought about by the presence of the hole and

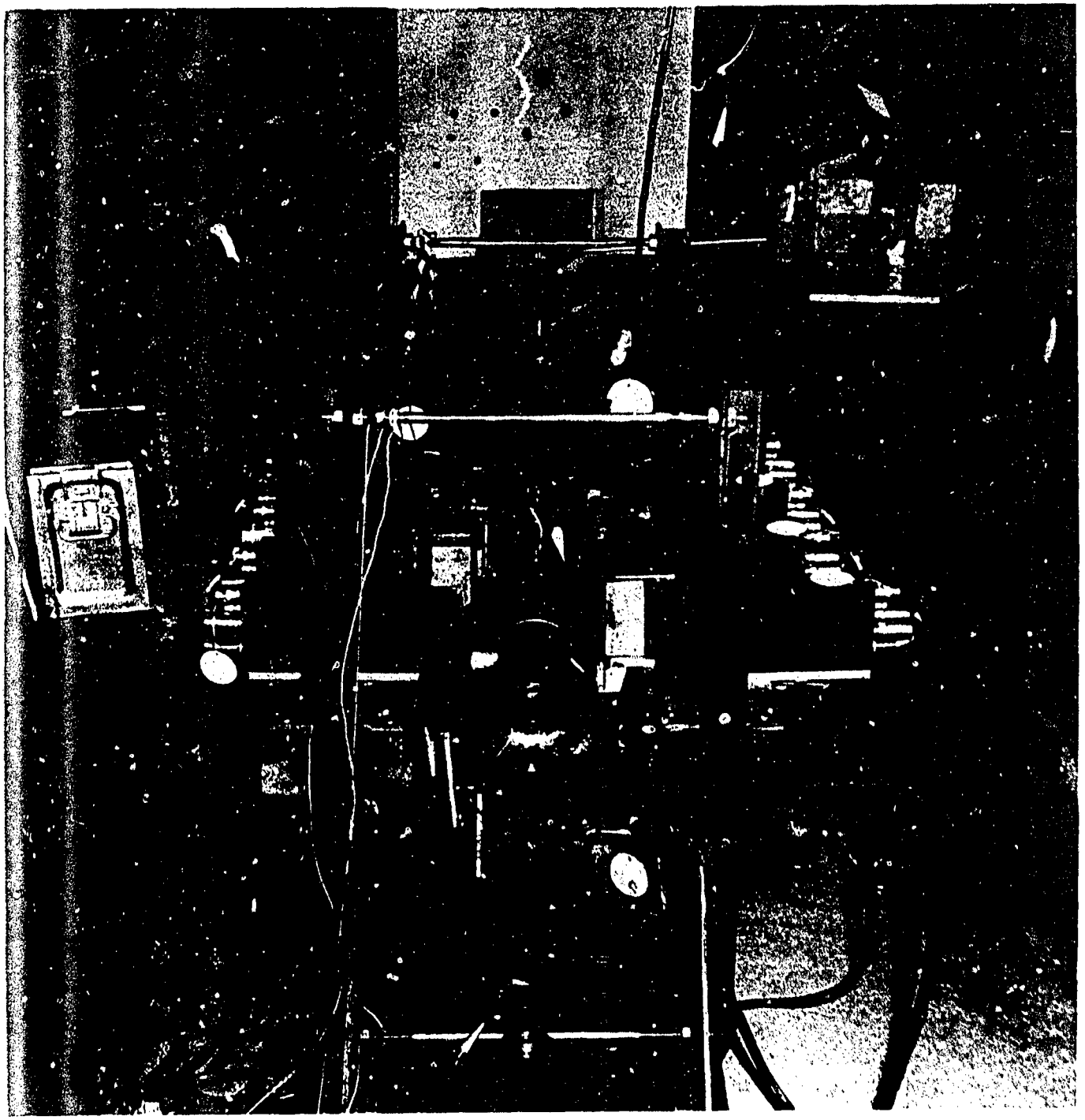


FIGURE 4-28. *Photograph of Apparatus for the Study of Propellant Motion During Firing Using Radioactive Tracer Technique. 37mm Gun with Four Scintillation Counters on Each Side of the Barrel.*

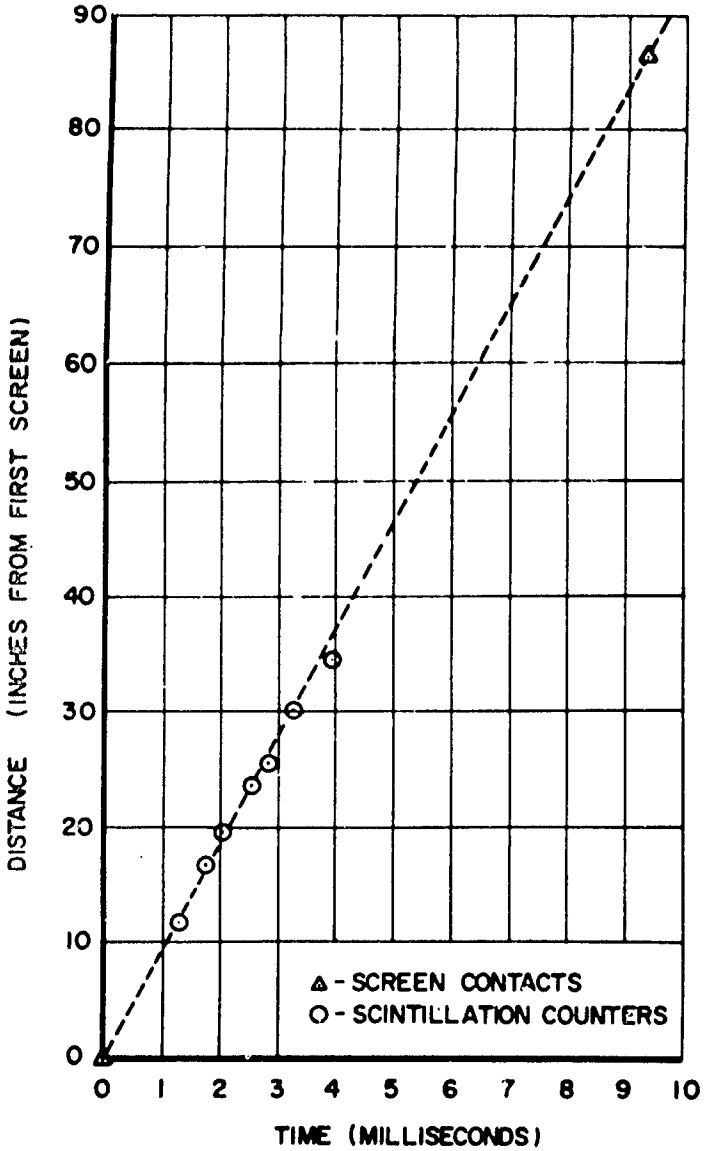


FIGURE 4-29. *Calibration Curve Showing Radioactive Source Position versus Time.*

thermocouple wire. The thermojunction formed by a single wire inserted in this manner in a steel barrel is that between iron and the material of the wire. Nickel is a good material for the wire since its thermal properties are similar to those of iron.

Two wire thermocouples can be used for in-wall temperatures but these require a larger hole and would be expected, in general, to disturb the temperature distribution more than the single wire. For very rapidly varying temperatures they would also be expected to follow the temperature changes less accurately then the welded single wire.

Thermocouples have been developed especially for bore surface temperature measurements. The original model was developed in Germany[22]. Various other models have been developed in different laboratories but they do not differ in principle from the original. Figure 4-26 is a diagram of one model.[23] The thermocouple consists essentially of an insulated nickel wire inserted through a hole in the gun steel mounting plug. The wire and plug are then faced off and ground and polished. A thin layer of known thickness (2-5μ) of nickel is then deposited on the polished surface. The deposited nickel bridges the thin layer of insulation on the wire and a thermojunction is formed between the nickel and the steel. The emf generated is that for nickel and iron. In the original model the nickel wire was insulated by heating in air to form a layer of nickel oxide. Later models use aluminum oxide (Al_2O_3) as an insulating material because it stands up better at higher temperatures. These thermocouples require care in fabrication. They are fragile and last only a few rounds in high performance guns.

In use the thermocouple is so mounted that the surface of the nickel plate forms part of the bore surface. It has been found not to be necessary to match the surface of the nickel layer exactly to the surface. It is an advantage to withdraw the thermocouple surface somewhat to protect it and this can be done up to a millimeter or so without apparently reducing the indicated temperature. The temperatures indicated by these thermocouples show large round to round variations[23]. This may be partly due to the deposition of variable layers of contamination from the propellant which is observed to occur. Much of the variation is, however, real. The temperature of the propellant gases is not uniform. Gas produced early in the cycle has expanded more than gas produced later and is cooler. The reading of the thermocouple will record this fact by random round-to-round variations in response. It has been shown experimentally[23] that if rounds are fired with charges of mixed hot and cool propellants the responses of the thermocouples are much more variable. In a gun, the firing cycle is so brief that there is not time for parts of the gas at different temperatures to mix and come to a uniform average temperature.

4-9.2 Resistance Type Temperature Measuring Gages

These gages measure surface temperature changes by noting the change in electrical resistance of a fine wire in contact with the surface. One model, which is available commercially, resembles in appearance an ordinary cemented-on strain gage. They are very convenient for measuring external barrel temperatures. They are mounted in a manner similar to a strain gage and form an arm of a Wheatstone bridge circuit. When the gage is heated the

emf appearing across the bridge is an indication of the temperature rise if multiplied by the proper calibration factor.

4-10 MOTION OF THE PROPELLANT DURING BURNING

In any theory of interior ballistics some assumption must be made about the distribution of the unburnt propellant. It is usual to assume either one of two limiting situations, namely; that the propellant remains in the chamber during burning and burns at the chamber pressure; or is uniformly distributed in the gas column behind the projectile and burns, on the average, at the average pressure in the gas. The actual situation is neither of these extremes but until recently there was no way of measuring even approximately the actual motion of the grains of propellant. This difficulty has been overcome, at least to a large extent, by the availability of radioactive tracer techniques.[21]

The method is to incorporate in one of the grains of the charge a gamma radioactive source of sufficient strength that a measurable amount of the gamma radiation from the source will penetrate the barrel wall and activate gamma ray detectors placed along the outside of the barrel. The detectors are shielded with lead shielding except for a narrow opening on the side toward the barrel. When the source passes in front of the opening the detector is activated and the fact recorded as a displacement of the spot on the screen of a cathode ray oscilloscope. The motion of the spot is recorded with a moving film camera and related to a time scale so that one derives from the observations a displacement-time curve for the activated grain. By repeated firings, with the activated grain initially at different distances from the breech end of the chamber, a composite picture of the motion of the charge can be derived.

The sources used were either Ta^{182} or Co^{60}, 50-100 millicuries in strength. They were sheathed in stain-

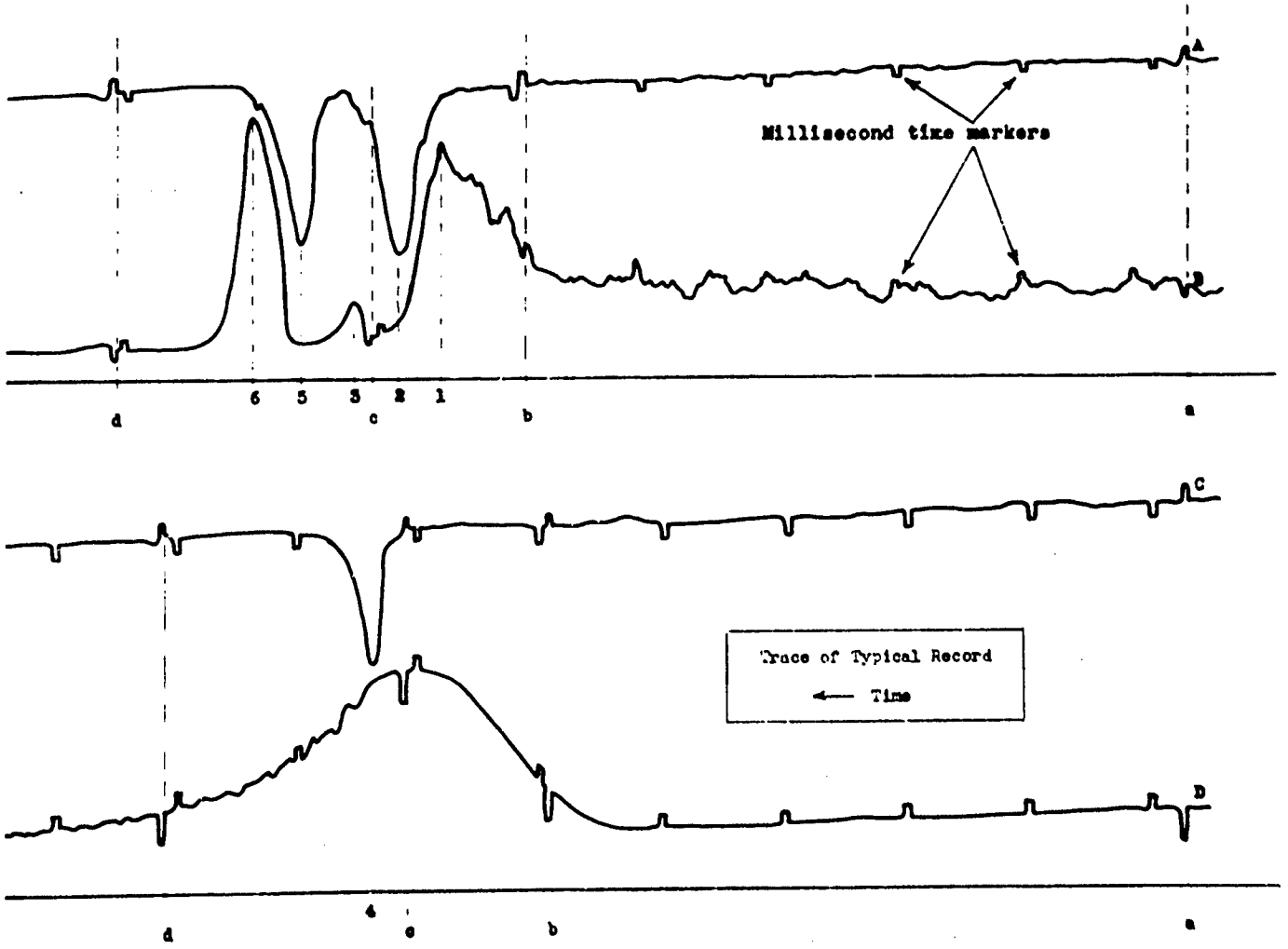


FIGURE 4-30. *Typical Record of Source Position and Pressure versus Time.*

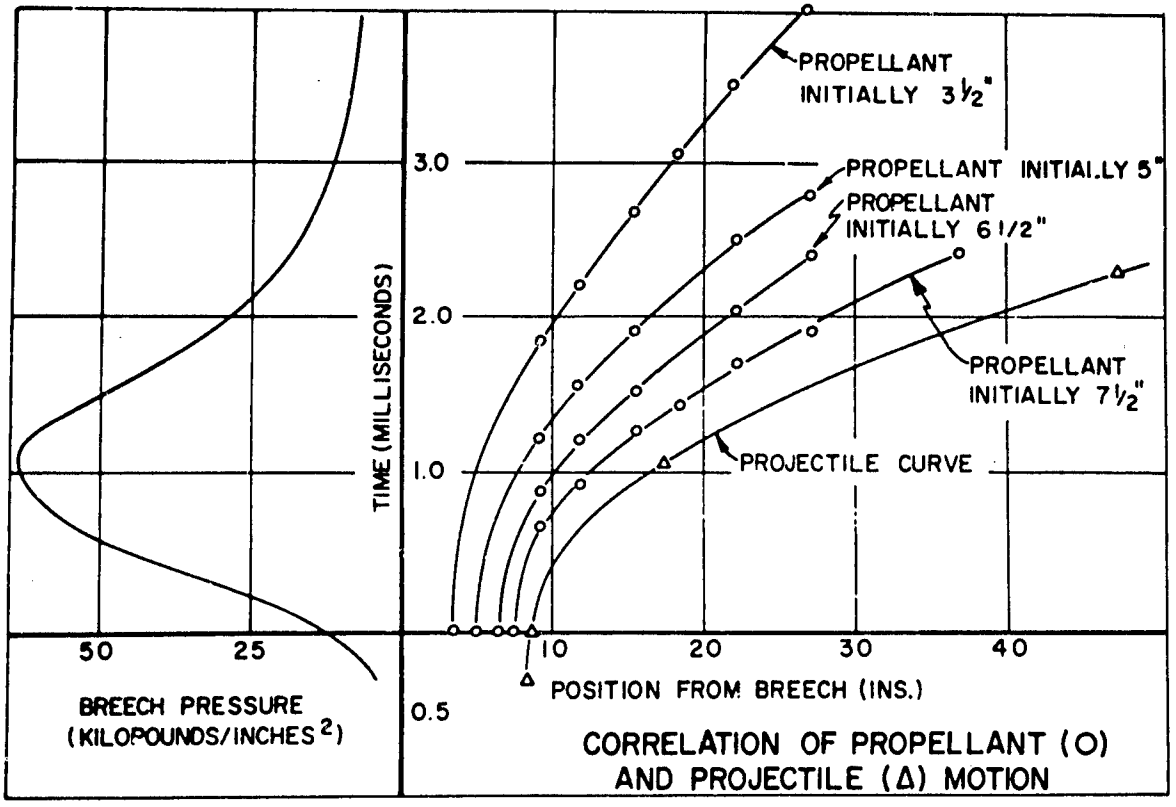


FIGURE 4-31. *Consolidated Plot of Observations Showing Correlation of Radioactive Source and Projectile Positions versus Time.*

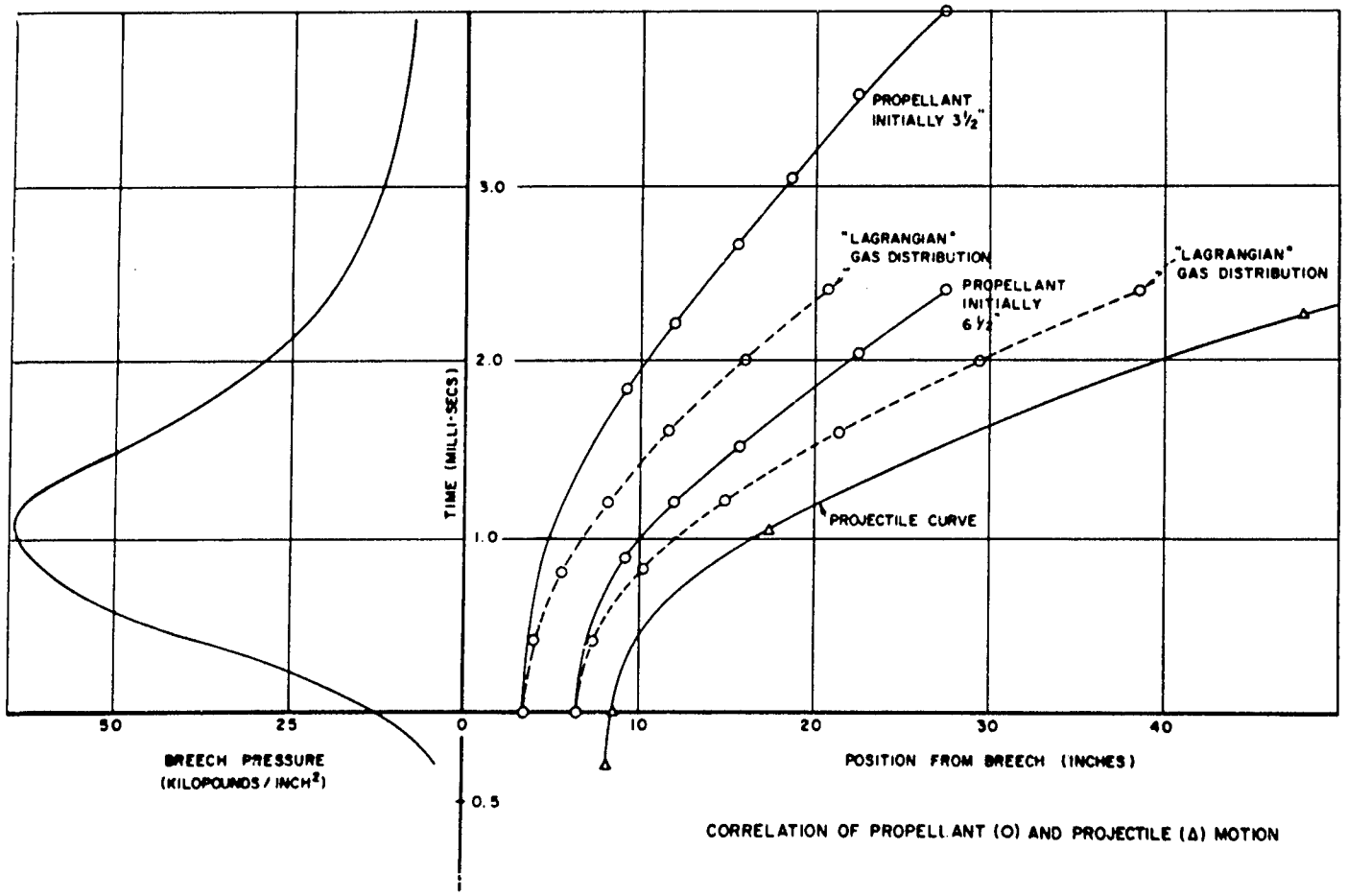


FIGURE 4-32. *Consolidated Plot of Radioactive Source and Projectile Motion Compared with Gas Motion as Predicted by the Lagrange Approximation.*

less steel and imbedded in a small hole drilled in the center of the grain. The activated grain was about 30 percent heavier than the normal grain because of the higher density of the source.

The motion of the grain was followed by eight collimated scintillation counters placed along the barrel. The individual scintillation pulses from the scintillation counters have a time duration of approximately 0.1 microsecond. The possible counting rate is, therefore, several million per second. The counting rate must be high to obtain the necessary statistical accuracy because the time interval over which the measurements are made is of the order of a few milliseconds. The individual pulses are amplified and fed to pulse height discriminator circuits. The uniform output pulses of these circuits are then fed to integrator circuits with time constants small compared to the time intervals to be measured and large compared to the individual pulse widths. A block diagram of the apparatus is shown in Figure 4-27 and a photograph of the apparatus and the gun in Figure 4-28.

The apparatus was checked by firing a metal pellet containing the source through the barrel with an air gun. Screen contacts were placed at the breech and muzzle to detect the passage of the pellet. Data from the screens and the counters are shown in Figure 4-29 which shows that the counters record faithfully the position of the source.

Figure 4-30 is a typical record. The upper and lower parts were recorded on different oscilloscopes on a common time scale. The numbers 1-6 indicate the times of the maxima of the detector pulses, starting at the breech. The letter *a* indicates firing pin contact, *b* the time when the projectile had moved one-half an inch, *c* the time when the projectile had moved 9½ inches and *d* the time when the projectile was at the muzzle. The trace *D* indicates the pressure.

Figure 4-31 is a consolidated plot of the data for four different initial positions of the activated grain. The early motion of the source could not be followed because of the excessive thickness of the walls of the chamber.

Figures 4-32, 4-33 and 4-34 derived from Figure 4-31 exhibit the relation between the motion of the activated grain as compared with the motion of the gas as predicted by the Lagrange approximation. The grains will always lag behind the gas because of the higher density of the grain. The activated grain will lag even more because of its still higher density and this effect will be enhanced as the grain burns away leaving the source itself. A great deal

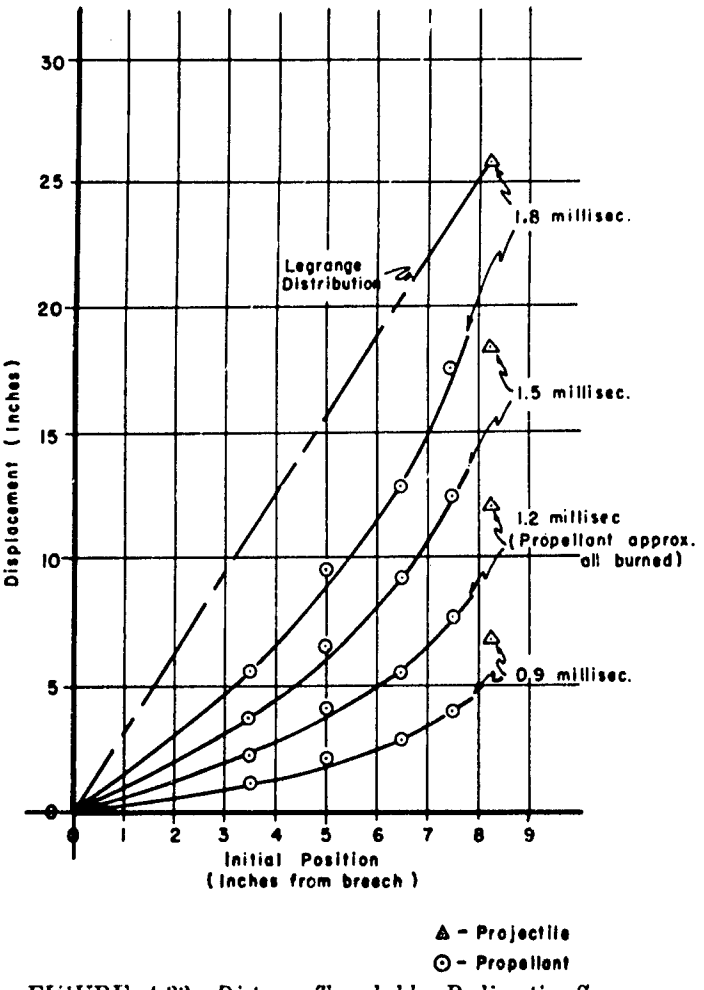


FIGURE 4-33. *Distance Traveled by Radioactive Source as a Function of Initial Position Compared with the Displacement of the Gas Given by the Lagrange Approximation.*

of the lag probably occurs early when the velocity of the gas is low and the gas density also low. The Lagrange approximation does not hold in the early stages when the charge is still burning. The results show in general that the propellant grains follow the gas motion as predicted by the Lagrange approximation more closely the farther forward they are initially and tend to approach it more closely in the later stages of the burning.

4-11 ROTATING MIRROR CAMERA

When using the microwave interferometer to measure projectile displacement, a long continuous record is usually desired, and for higher projectile velocities the film speed must be large to resolve the oscillations sufficiently. This can be done with the commercially available running film cameras up to about 2000 fps at which velocity the oscillation frequency is 100 kc per second.

For use at higher velocities a specially designed

rotating mirror camera was built.[25] Rotating mirror cameras sweep the image over a stationary film by means of a rotating mirror. They are available commercially but the design is not advantageous for use with the interferometer. In most models the image is on the film for only a fraction of the time of one revolution of the mirror and the length of the film is too short for a long record.

In the Ballistic Research Laboratories model use is made of a four-sided mirror which, as it rotates, divides the incident beam of light from the lens of the camera so as to form two images, at least one of which is always on the film. The record, therefore, is continuous.

Figure 4-35 shows the design of the basic optical system. The two images are always 180° apart, and as the film is carried around the focal surface more than 180°, one image always comes on the film before the other leaves it. When photographing the spot of a cathode ray oscilloscope the spot can be stepped across the screen and a record several times the length of the film can be recorded. Since the axis of rotation of the mirror is not at the reflecting surfaces, the focal curve is not a circle. Also the image of an extended object is not everywhere in exact focus on the film so that as the spot changes position on the screen the sharpness of focus of the spot image on the film will change. These effects are not large in the present model where the distance from the lens to the film is about 40 inches. The instrument works at approximately one to one magnification so that the image of the spot is the same size as the spot itself and any fuzziness is reproduced in the image. The instrument uses an ordinary balloptican projection lens. The mirror is made of stainless steel and is driven by a one-half horse power motor. The faces of the mirror are 3 by 4 inches. The film is held on the focal curve by being wrapped on a plexiglass surface, emulsion side toward the mirror, the plexiglass surface being formed to the focal curve. The film is loaded in daylight from a built-in film supply and loading arrangement. A photograph of the camera with the cover removed is shown in Figure 4-36. This is a prototype model in which no attempt was made to optimize the design either mechanically or optically.

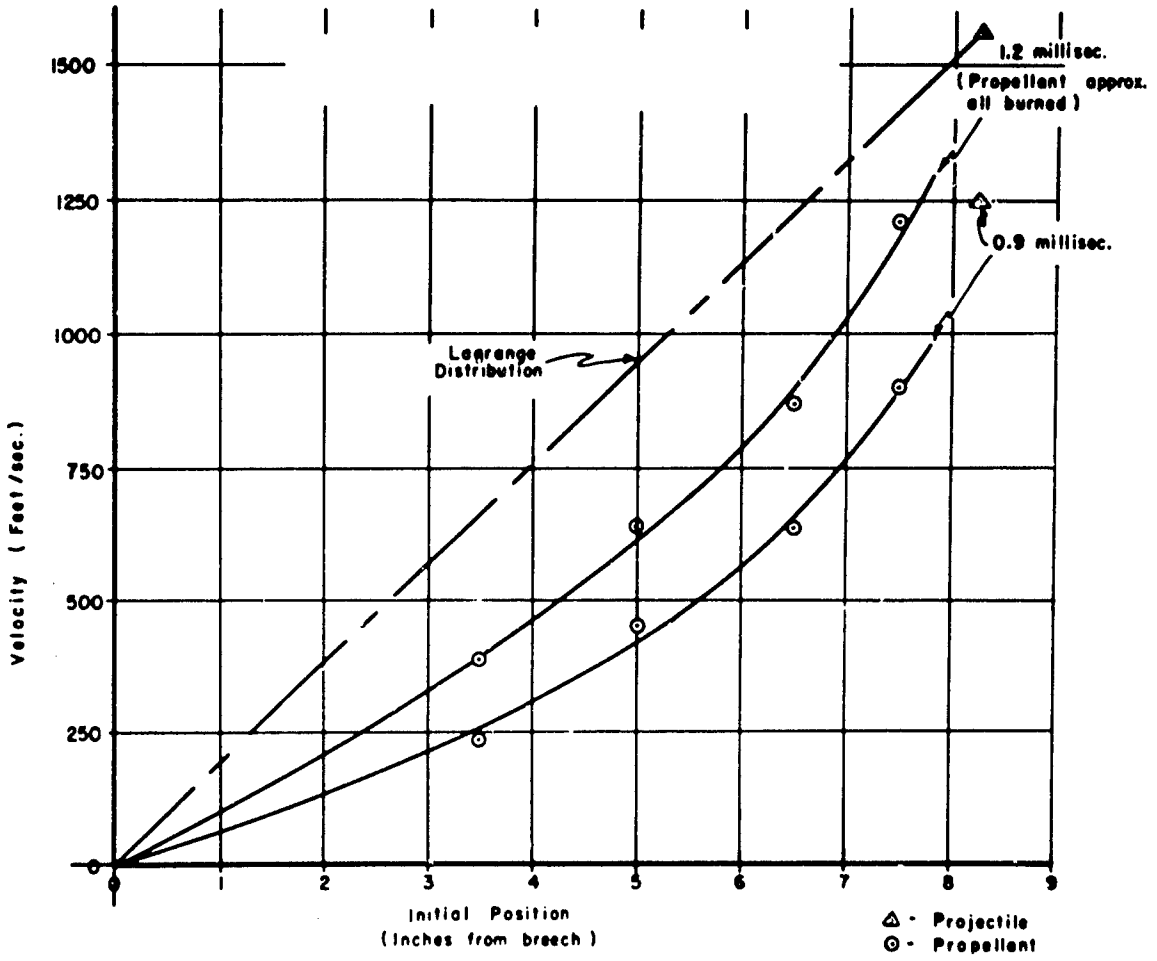


FIGURE 4-34. *Velocity Attained by Radioactive Source as a Function of Initial Position Compared with the Velocity of the Gas Given by the Lagrange Approximation.*

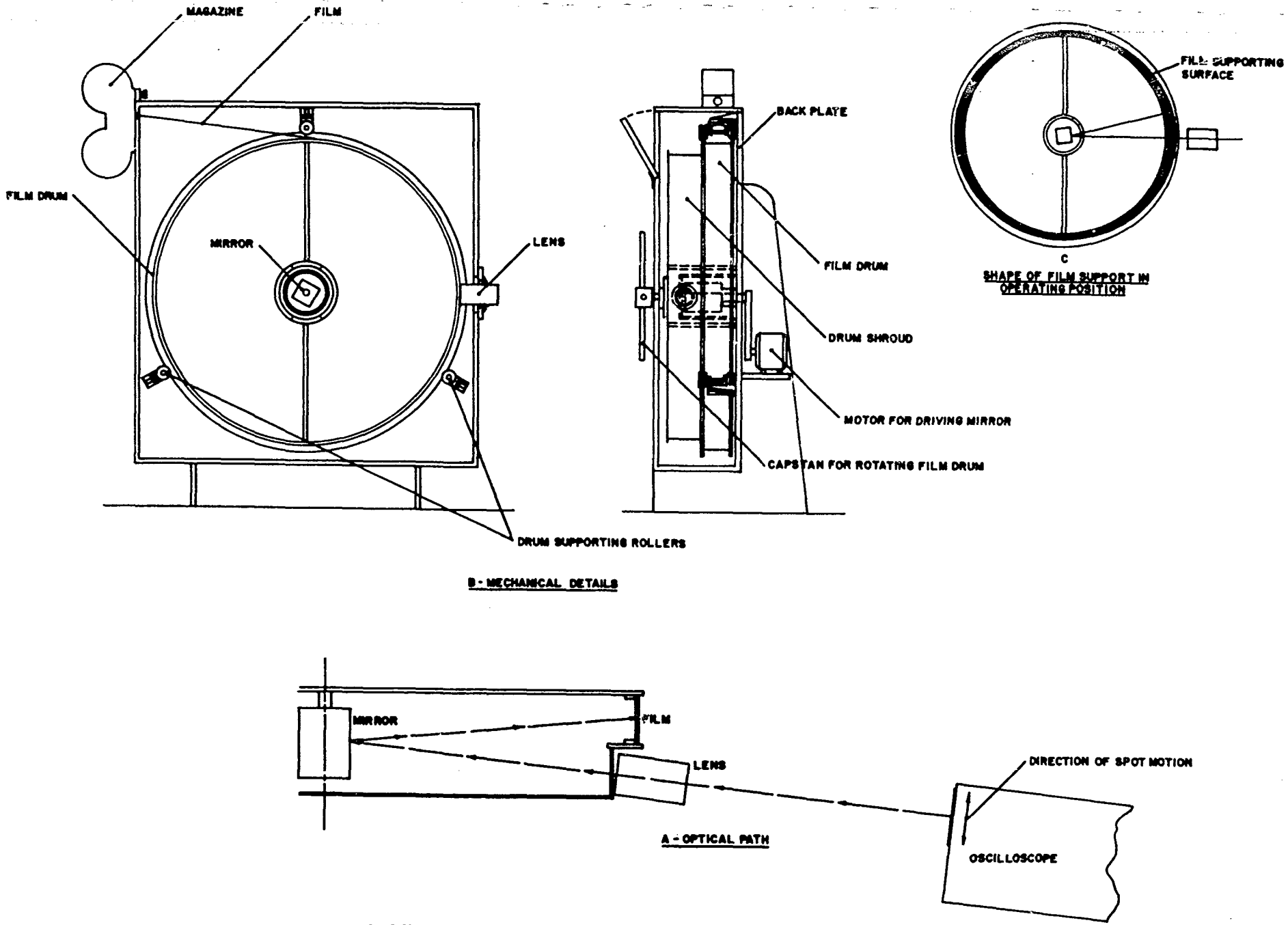


FIGURE 4-35. *Schematic Diagrams of the BRL Rotating Mirror Camera.*

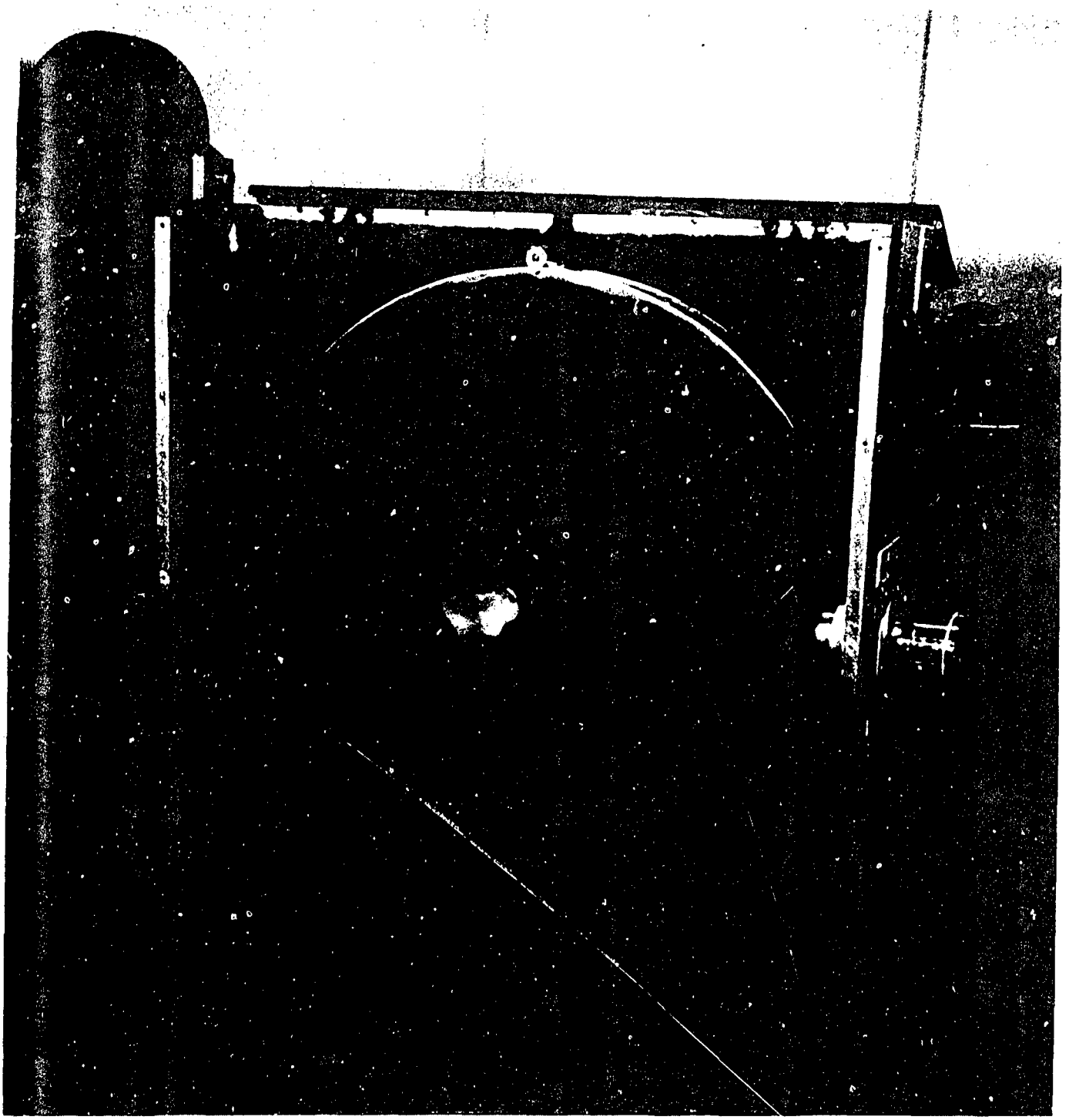


FIGURE 4-36. *Photograph of BRL Four-Surface Rotating Mirror Camera for Recording Interior Ballistic Trajectories (Cover Removed).*

The intensity of the image changes with position on the film because of the way the mirror divides the light between the two images but this has been found not to be serious. Under the best of conditions of spot intensity, color and focus, and using the most sensitive film, interferometer frequencies up to 1200 kc per second have been resolved and recorded. Projectile velocity for this frequency would be about 20,000 fps for the wave length used in the present interferometer.

REFERENCES

1. (a) C. F. Curtiss et al, *Second Report on Firings in 3-Inch Gun at David W. Taylor Model Basin*, National Defense Research Committee Report No. A-323, 1945.
   (b) *Report of National Bureau of Standards to Bureau of Ordnance, Navy Department on Firings in 90mm Gun at David W. Taylor Model Basin*, NAVORD Report No. 430, 1947.
2. *Results of Firings in the Caliber .50 Velocity or Pressure Test Barrel at New York University*, NYU Research Division, College of Engineering, Final Report No. 78.05, 1950.
3. F. W. Whitlock, *Piezoelectric Pressure-Time Recording Equipment: Its Construction and Use as a Ballistic Measuring Tool*, Independence, Mo., Lake City Arsenal Industrial Engineering Division Report 59-1, 1959.
4. H. P. Gay, *The Evolution of Gages for Measuring Pressure in Guns and Rockets at the Ballistic Research Laboratories*, BRL Memorandum Report No. 1402, 1962.
5. A. J. Hodges, *Equipment for Dynamic Pressure Measurements at the New Mexico Experimental Range*, New Mexico School of Mines, Research and Development Division, Task D, Contract NOrd-9817, Interim Report, 1950.
6. V. H. McNeilly and J. W. Hanna, *Strain-Resistance Pressure Gage, Model C-AN*, BRL Memorandum Report No. 422, 1947.
7. OPM 80-10, *Weapon Pressure Instrumentation*, Volume IV, Aberdeen Proving Ground, 1963.
8. E. L. Bonhage and H. G. McGuire, *Microflash Photographic Instrumentation of the Interior Ballistic Laboratory*, BRL Memorandum Report No. 1216, 1959.
9. R. H. Kent, *Description and Instruction for the Use of the Solenoid Chronograph*, Ordnance Technical Note 8, 1927.
10. TM 9-1860-7, *Field Sky Screen and Counter Chronograph*, Dept. of Army, 1956.
11. *Tables of Drag Coefficient*, Aberdeen Proving Ground Instrumentation Lab. Report No. 4, 1955.
12. H. P. Hitchcock, *Effect of Muzzle Blast on Maximum Yaw*, BRL Memorandum Report No. 649, 1953.
13. I. Slawsky, A. E. Seigel, L. T. Ho and J. T. Vanderslice, *A Comparison Study Between a Microwave Interferometer and an Electrical Contact System for Following the Motion of a High Speed Projectile*, University of Maryland, Institute of Molecular Physics, 1958.
14. D. C. Vest et al, *Ballistic Studies With a Microwave Interferometer: Part I*, BRL Report No. 968, 1955.
15. D. C. Vest et al, *Ballistic Studies With a Microwave Interferometer: Part II*, BRL Report No. 1006, 1957.
16. J. A. Petersam, H. G. McGuire and T. E. Turner, *Measurement of Projectile Motion During Engraving Process*, BRL Memorandum Report No. 1070, 1957.
17. P. G. Baer and J. M. Frankle, *Reduction of Interior Ballistic Data from Artillery Weapons by High Speed Digital Computer*, BRL Memorandum Report No. 1148, 1958.
18. N. M. Smith, Jr. and J. A. Crocker, *Measurement of Various Ballistic Quantities on a Projectile Moving in the Bore of a Gun*, National Defense Research Committee Report A-259, 1944.
19. W. M. Kendrick and L. A. Peters, *Interior Ballistic Telemetering*, BRL Memorandum Report No. 1183, 1958.
20. OPM 80-41, *Measurement of Internal Diameters of Cannon*, Aberdeen Proving Ground, 1957.
21. B. L. DeMare, *The Mouse Automatic Boregage*, BRL Report No. 1054, 1958.
22. P. Hackemann, *A Method for Measuring Rapidly Changing Surface Temperatures and Its Application to Gun Barrels*, Armament Research Establishment Translation 1/46 by C. K. Thornhill.
23. E. Bannister, R. N. Jones and D. R. Bagwell, *Heat Transfer, Barrel Temperature and Thermal Strains in Guns*, BRL Report No. 1192, 1963.
24. K. A. Yamakawa, R. H. Comer and R. J. Epstein, *Propellant Motion in a 37mm Gun Using Gamma Ray Tracer Techniques*, BRL Report No. 940, 1955.
25. B. L. DeMare, H. G. McGuire and E. L. Bonhage, *A High Speed Rotating Mirror Camera*, BRL Report No. 1069, 1959.

CHAPTER 5

LIST OF SYMBOLS

a_n	Parameter characteristic of the Pidduck-Kent solution
C	Mass of charge
c_1	A function of ϵ and n
c'	Heat capacity of the propellant per unit volume
E	Activation energy for the reaction
e	Base of natural logarithm
f	Frequency factor
h	Heat transfer coefficient
K	Thermal conductivity of the propellant
K_g	Kinetic energy of the gas and unburnt propellant
K_p	Kinetic energy of the projectile
M	Effective mass of the projectile
n	Polytropic index: $1/(\gamma - 1)$
P	Average pressure
P_c	Breech pressure
P_s	Base pressure
Q	Heat evolution per unit volume
q	Heat of reaction per unit volume
R	Universal gas constant
T	Temperature at any point in the propellant
T_g	Gas temperature
t	Time
t_0	Heating time
U	Reduced temperature variable
V	Velocity of the projectile
x	Distance from gas-solid interface
α	Initial slope of $(2n + 3)/\delta$ versus n
β	Ratio (final slope/initial slope) of $(2n + 3)/\delta$ versus n
γ	Effective ratio of specific heats
δ	Pidduck-Kent constant
ϵ	Ratio: C/M
μ	Dummy variable
ξ	Reduced distance variable
τ	Reduced time variable

Subscripts

g	Gas phase
i	Ignition
ia	Adiabatic ignition
im	Minimum ignition
0	Shut-off or end of heating
0c	Critical heating

Superscripts

(0)	Initial value
(1)	A subsequent value

CHAPTER 5

SPECIAL TOPICS

5-1 THE HYDRODYNAMIC PROBLEMS OF INTERIOR BALLISTICS

5-1.1 Pressure Distribution and Kinetic Energy of the Propellant Gases

In most formulations of the theory of interior ballistics, it is customary to account for the effects of the motion of the gas and the unburnt propellant by means of certain simple formulas. These purport to define (a) the relations between the different pressures occurring in the basic equations of the theory; namely, the breech pressure, P_c, the pressure on the base of the projectile, P_p, and the average space pressure, P, consistent with the equation of state of the gas, and (b) the amount of kinetic energy to be attributed to the gas and unburnt propellant, (Cf. paragraphs 2-2.2 and 2-2.3). If ϵ denotes the ratio of the mass of the charge, C, to that of the projectile, M, where M may be an effective mass as in Chapter 2, these relations can be stated as:

$$P_c = P_p\left(1 + \frac{\epsilon}{2}\right) \tag{5-1}$$

$$P = P_p\left(1 + \frac{\epsilon}{3}\right) \tag{5-2}$$

$$K_g = \frac{\epsilon}{3}\left(\tfrac{1}{2}MV^2\right) = \frac{\epsilon}{3}K_p \tag{5-3}$$

where K_g is the kinetic energy of the gas and unburnt propellant and K_p the kinetic energy of the projectile.

These relations are very approximate and relate rather remotely to the actual situation in a gun. They can be justified under certain conditions by appeal to solutions of what is called the Lagrange Ballistic Problem.

This problem was first formulated by Lagrange in 1793 and is based on the following simple model. The propellant is all burnt instantaneously so that one deals only with the gas. For the black powder used as a propellant in Lagrange's day this is not too bad an assumption. The gas is then initially at uniform pressure, density, and temperature, and at rest. It is assumed also that the bore and chamber are of uniform cross section so that they are parts of a uniform tube closed at one end. At the origin of time the projectile is released. The problem then is to find the distribution of pressure, density and velocity of the gas between the breech and the projectile at all subsequent times during the travel of the projectile to the muzzle.

The problem was first solved completely using analytical methods by Love and Pidduck.[1] The treatment assumes that the flow is one-dimensional and adiabatic, that is there is no heat loss to the wall, and that gas friction at the wall is negligible.

A general discussion of the Love and Pidduck solution as applied to guns is given in Corner.[2] The rigorous solution is characterized by rarefaction waves traveling back and forth between the breech and projectile base and the ratios P_c/P_p and K_g/K_p oscillate and approach certain limiting values corresponding to a certain special solution of the equation of motion of the gas. This special solution was worked out by Pidduck[3] and by Kent[4] and is called the Pidduck-Kent special solution of the Lagrange problem. It has not been proved that the rigorous solution approaches the special solution in the limit of large travel, but it is usually assumed that it does. The Pidduck-Kent solution does not satisfy the initial conditions of the Lagrange problem but corresponds to an initially nonuniform distribution of pressure and density.

The Pidduck-Kent solutions for the pressure and kinetic energy ratios can be expanded in powers of ϵ and are given in Corner.[2] When all the terms in the expansions beyond those in the first power of ϵ are dropped, Equations 5-1, 5-2 and 5-3 result. These equations are, therefore, only valid, even as approximations, for small values of ϵ; that is, for relatively low velocity guns.

The complete Pidduck-Kent solutions for the pressure and kinetic energy ratios can be stated in the form

$$P_c = P_p(1 - a_0)^{-n-1} \tag{5-4}$$

$$P = P_p\left(1 + \frac{\epsilon}{\delta}\right) \tag{5-5}$$

$$K_g = K_p\frac{\epsilon}{\delta} \tag{5-6}$$

where δ, the Pidduck-Kent constant, is given by

$$\frac{1}{\delta} = \frac{1}{2n+3}\left[\frac{1}{a_0} - \frac{2(n+1)}{\epsilon}\right] \qquad (5\text{-}7)$$

where a_0 is a parameter characteristic of the Pidduck-Kent solution, $n = 1/(\gamma - 1)$ and γ can be an effective value of γ adjusted as in paragraph 2-2.1 of Chapter 2.

Vinti and Kravitz[5] prepared tables and graphs for calculating numerical values of $1/\delta$ for different values of ϵ and n and these are reproduced in Tables 5-1, 5-2, 5-3 and 5-4 and Figures 5-1 and 5-2. In these tables $1/\delta$ is expressed in terms of new variables α, β and c_1 in the form

$$1/\delta = \frac{1}{2n+3}\left[1 + \alpha n \frac{1 + c_1\beta n}{1 + c_1 n}\right] \qquad (5\text{-}7a)$$

and the tables and graphs are for α, β, and c_1 in terms of ϵ and n. These tables and graphs permit theoretical values of the ratios to be calculated over the range of practical values of C and γ.

Equations 5-4, 5-5 and 5-6 assert that the pressure

TABLE 5-1.

TABLE FOR THE PIDDUCK-KENT SOLUTION

In the following table α is given as a function of ϵ for the following values: ϵ = 0(.05) 1 (.1) 4 (.2) 10. It is found from the following formula:

$$\alpha = 2/\epsilon\{\sqrt{1 + 2/\epsilon}\{\ln(1 + \epsilon + \epsilon\sqrt{1 + 2/\epsilon})\} - 2]$$

The first forward differences of the function are given in the third column marked Δ_1. Linear interpolation is permissible.

ϵ	α	Δ_1	ϵ	α	Δ_1	ϵ	α	Δ_1
.00	.6667	−66	1.0	.5621	−81	4.0	.4038	−67
.05	.6601	−64	1.1	.5540	−78	4.2	.3971	−65
.10	.6537	−62	1.2	.5462	−75	4.4	.3906	−62
.15	.6475−	−61	1.3	.5387	−73	4.6	.3844	−59
.20	.6414	−59	1.4	.5314	−70	4.8	.3785−	−57
.25	.6355+	−57	1.5	.5244	−67	5.0	.3728	−56
.30	.6298	−56	1.6	.5177	−65	5.2	.3672	−53
.35	.6242	−55	1.7	.5112	−63	5.4	.3619	−51
.40	.6187	−53	1.8	.5049	−61	5.6	.3568	−49
.45	.6134	−52	1.9	.4988	−59	5.8	.3519	−48
.50	.6082	−51	2.0	.4929	−57	6.0	.3471	−46
.55	.6031	−50	2.1	.4872	−56	6.2	.3425+	−44
.60	.5981	−48	2.2	.4816	−53	6.4	.3381	−43
.65	.5933	−48	2.3	.4763	−53	6.6	.3338	−42
.70	.5885+	−46	2.4	.4710	−50	6.8	.3296	−41
.75	.5839	−46	2.5	.4660	−50	7.0	.3255+	−39
.80	.5793	−44	2.6	.4610	−48	7.2	.3216	−38
.85	.5749	−44	2.7	.4562	−46	7.4	.3178	−37
.90	.5705+	−42	2.8	.4516	−46	7.6	.3141	−36
.95	.5663	−42	2.9	.4470	−44	7.8	.3105+	−35
			3.0	.4426	−43	8.0	.3070	−34
			3.1	.4383	−42	8.2	.3036	−33
			3.2	.4341	−41	8.4	.3003	−32
			3.3	.4300	−40	8.6	.2971	−31
			3.4	.4260	−39	8.8	.2940	−31
			3.5	.4221	−39	9.0	.2909	−30
			3.6	.4182	−37	9.2	.2879	−29
			3.7	.4145+	−36	9.4	.2850+	−28
			3.8	.4109	−36	9.6	.2822	−27
			3.9	.4073	−35	9.8	.2795−	−27
						10.0	.2768	

TABLE 5-2.

TABLE FOR THE PIDDUCK-KENT SOLUTION

In the following table β is given as a function of ϵ for the following values: ϵ = 0(.1)2.6(.2)5(.25)10.

$$\beta = 1/\alpha[1/k - 2/\epsilon]$$

where k is the solution of

$$\epsilon = 2ke^k \int_0^1 e^{-k\mu^2}\, d\mu$$

The first forward differences of the function are given in the column marked Δ_1. Linear interpolation is permissible.

ϵ	β	Δ_1	ϵ	β	Δ_1	ϵ	β	Δ_1
0.0	1.0000	67	2.5	1.1686	63	5.00	1.3160	136
0.1	1.0067	69	2.6	1.1749	125	5.25	1.3296	135
0.2	1.0136	69				5.50	1.3431	134
0.3	1.0205−	69	2.8	1.1874	124	5.75	1.3565+	132
0.4	1.0274	70						
0.5	1.0344	69	3.0	1.1998	122	6.00	1.3697	131
0.6	1.0413	70	3.2	1.2120	121	6.25	1.3828	129
0.7	1.0483	70	3.4	1.2241	119	6.50	1.3957	128
0.8	1.0553	69	3.6	1.2360	118	6.75	1.4085−	126
0.9	1.0622	69	3.8	1.2478	117			
1.0	1.0691	69	4.0	1.2595−	115	7.00	1.4211	126
1.1	1.0760	69	4.2	1.2710	114	7.25	1.4337	124
1.2	1.0829	68	4.4	1.2824	113	7.50	1.4461	123
1.3	1.0897	68	4.6	1.2937	112	7.75	1.4584	121
1.4	1.0965+	68	4.8	1.3049	111			
1.5	1.1033	67				8.00	1.4705+	121
1.6	1.1100	67				8.25	1.4826	120
1.7	1.1167	66				8.50	1.4946	118
1.8	1.1233	66				8.75	1.5064	118
1.9	1.1299	65						
2.0	1.1364	66				9.00	1.5182	116
2.1	1.1430	64				9.25	1.5298	116
2.2	1.1494	65				9.50	1.5414	115
2.3	1.1559	64				9.75	1.5529	113
2.4	1.1623	63						
						10.00	1.5642	

TABLE 5-3.

TABLE FOR THE PIDDUCK-KENT SOLUTION

In the following table c_1 is given as a function of ϵ and n for all combinations of the following values: $\epsilon = 0(.2)1(1)10$; $n = \frac{1}{2}, 1(1)5$.

	n					
ϵ	½	1	2	3	4	5
0.0	1.000	1.000	1.000	1.000	1.000	1.000
.2	1.016	1.016	1.016	1.016	1.016	1.016
.4	1.029	1.029	1.029	1.029	1.029	1.030
.6	1.038	1.039	1.039	1.039	1.039	1.039
.8	1.045	1.046	1.046	1.047	1.047	1.047
1	1.051	1.051	1.052	1.052	1.053	1.053
2	1.059	1.061	1.063	1.064	1.065	1.065
3	1.053	1.057	1.061	1.063	1.064	1.065
4	1.042	1.047	1.053	1.055	1.057	1.058
5	1.029	1.036	1.042	1.046	1.048	1.049
6	1.015	1.023	1.031	1.035	1.037	1.039
7	1.000	1.010	1.019	1.024	1.027	1.029
8	.986	.997	1.008	1.013	1.016	1.018
9	.973	.985	.997	1.002	1.006	1.008
10	.960	.973	.986	.992	.996	.998

and kinetic energy ratios are constant for fixed values of γ and ϵ and are independent of the velocity of the projectile. As was mentioned earlier, the general solution predicts that the ratios are initially oscillatory but the oscillations tend to die out. Love and Pidduck appled their formulas to the case of a gun for which $\epsilon = 0.24$ having a muzzle velocity of about 2500 feet per second. These results are reproduced in Corner[2] and show that, for this case, the theory predicts that the pressure and energy ratios, apart from the oscillations, are nearly constant up to exit of the projectile.

Recent interest in the development of high velocity guns, especially the so-called light gas guns, has stimulated a revived interest in the hydrodynamic problems of interior ballistics. The recent practice is to solve the problems numerically by the method of characteristics rather than analytically as was done by Love and Pidduck. With modern computers, it is probably less work to solve the individual problem numerically from the beginning than to use the analytical formulas which are complicated. Recent treatments of the problem by the method of characteristics for different assumed forms of the equation of state of the gas are given in References 6, 7 and 8. An experimental investigation of the problem is described in Reference 9.

A treatment of the problem taking account of chambrage and chamber geometry is given in Reference 10 in connection with a study of light gas gun performance.

5-1.2 The Emptying of the Gun

The emptying of the gun after the projectile leaves is a problem of some interest in interior ballistics. The gas flowing from the tube continues to impart recoil momentum to the barrel which can be estimated by integrating the breech pressure over the time of emptying. This contribution to the recoil momentum can be appreciable especially for the higher velocity guns.

Theoretical treatments of the flow of the gas from the gun have been given by several authors. In general, they assume that the initial conditions for the problem are those given by the solution of the Lagrange problem when the projectile is at the muzzle. Such a treatment is given by Corner,[2] who also gives references to other work on the subject as well as a general discussion of the problem.

The gas flowing from the muzzle can be made to reduce the recoil forces by attaching a system of baffles just beyond the muzzle. These baffles are designed so as to deflect the muzzle gases sideways and to the rear. The gases, therefore, tend to force the barrel forward and so reduce the recoil forces.

TABLE 5-4.

TABLE FOR THE PIDDUCK-KENT SOLUTION

Values of ϵ as a function of c_1 and n.

	n					
c_1	½	1	2	3	4	5
1.000	0.00	0.00	0.00	0.00	0.00	0.00
1.010	0.11	0.11	0.11	0.11	0.11	0.11
1.020	0.25	0.25	0.25	0.25	0.25	0.25
1.030	0.43	0.42	0.42	0.41	0.40	0.40
1.040	0.65	0.65	0.64	0.64	0.63	0.60
1.050	0.97	0.97	0.94	0.92	0.91	0.90
1.060	———	1.69	1.50	1.44	1.40	1.35
1.063	———	———	1.98	1.75	1.63	1.60
1.065	———	———	———	———	2.00	1.92
1.065	———	———	———	———	2.73	.208
1.063	———	———	2.45	2.95	3.18	3.35
1.060	———	2.50	3.12	3.43	3.62	3.75
1.050	3.29	3.73	4.28	4.55	4.75	4.87
1.040	4.15	4.60	5.20	5.52	5.73	5.89
1.030	4.92	5.44	6.06	6.45	6.70	6.85
1.020	5.65	6.23	6.90	7.37	7.65	7.85
1.010	6.34	6.98	7.80	8.30	8.60	8.83
1.000	7.00	7.75	8.70	9.22	9.58	9.80
.990	7.72	8.57	9.65	———	———	———
.980	8.45	9.40	———	———	———	———
.970	9.20	———	———	———	———	———

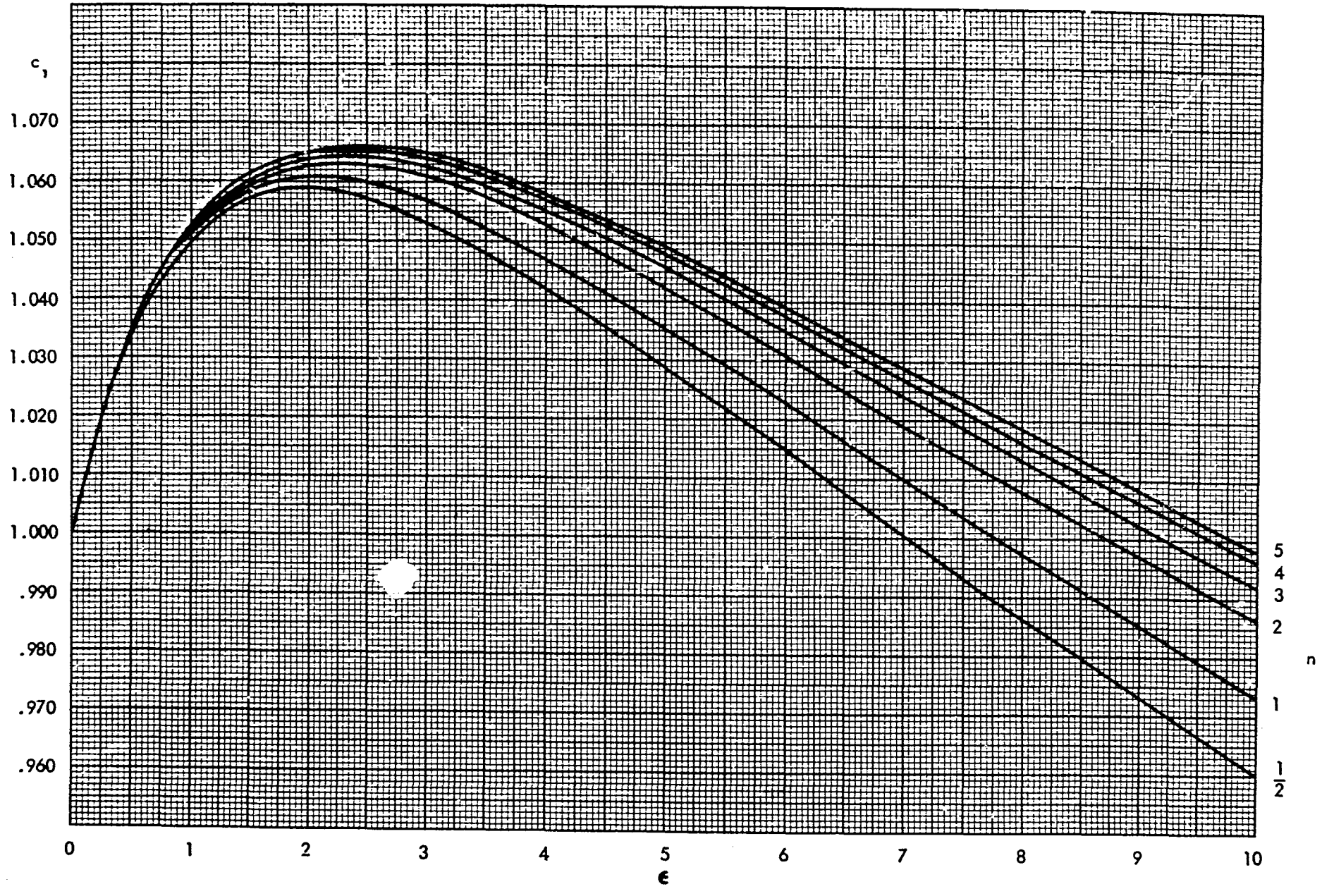


FIGURE 5-1. *Graph of c_1 as a Function of ϵ and n (Data from Table 5-3)*

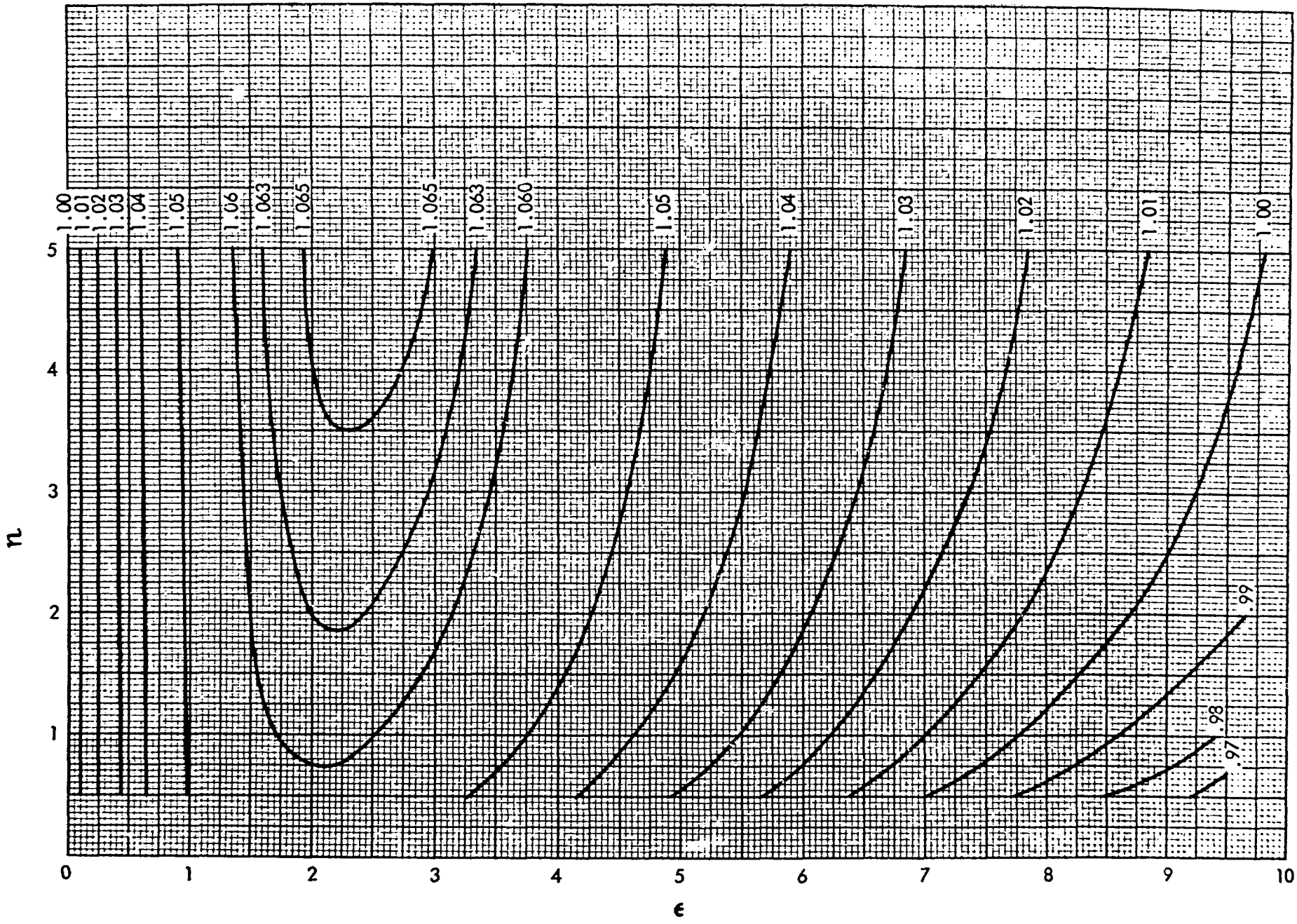


FIGURE 5-2. *Contour Map of Lines of Constant* c_1 *(Data from Table 5-4)*

A device of this type is called a muzzle brake. For a general discussion of the design features and use of muzzle brakes, the reader is again referred to Corner.[2]

The emptying of the gun is also of importance in tank applications and automatic weapons. If the breech is opened before the breech pressure has become negligible, gases will flow from the breech. This can be serious especially when the gun is operated in an enclosed turret, where the gases can accumulate. The gases can form a combustible mixture with air and are also initiating as well as toxic to personnel since they contain ammonia fumes and carbon monoxide.

Even when the breech pressure has fallen to atmospheric pressure, some propellant gas will remain in the barrel. This gas can emerge from the open breech. To permit early opening and to prevent gas flow from the breech, a device known as a bore evacuator has been invented. It consists essentially of a chamber located near the muzzle, surrounding the tube and opening into it, so that when the projectile passes the openings, gas flows into the chamber and fills it to a pressure near that in the tube. When the projectile leaves the muzzle and the pressure in the tube falls below that in the evacuator chamber, the gas in the chamber flows back into the tube. The openings are so designed that the reverse flow has a component toward the muzzle. The effect is to drive the gases in the tube toward the muzzle and so prevent their emergence from the breech.

5-2 IGNITION OF PROPELLANTS

5-2.1 General Discussion

When a solid propellant is burned, the preponderance of experimental evidence supports the conclusion that the burning proceeds in two stages.[11] The first stage takes place in a thin layer of the solid at the surface, and is characterized by a chemical reaction in the solid material. The reaction converts the solid propellant into gaseous products which stream away from the surface in a perpendicular direction. These products continue to react in the gas phase which constitutes the second stage of the process. If the ambient pressure is sufficiently high, the gas phase reactions continue until the final products are produced and, under these circumstances, the temperature of the product gases becomes high enough somewhere along the stream that the gases become luminous and a flame appears. The base of the flame is quite sharply defined and its position with respect to the surface is dependent on the ambient pressure; the base of the flame moving closer to the surface as the ambient pressure increases. At pressures of about 1000 psi, the separation of the flame from the surface becomes too small to be easily observable.

At pressure around an atmosphere or less, it is possible for the propellant to burn without the occurrence of the flame. This would indicate that the gas phase reaction does not go to completion, leaving combustible products. This condition can be brought about by gentle ignition so that the igniter itself does not start the flame reaction which then would be self-sustaining. For pressures below about 100 atmospheres, the presence of the flame does not appreciably alter the rate of regression of the surface. The solid phase reaction can, therefore, proceed without the reception of heat from any outside source. It will be accelerated, however, by heating from the environment, and this accounts for the effect of pressure on the burning rate, which forces the hot flame zone closer to the surface and hence increases the rate of heat transfer back to the surface.

When a propellant burns without the presence of flame it is said to fizz burn. The surface appears to boil and bubble and a fizzing sound is audible. The nature of the products produced when a propellant fizz burns is not completely known. The absorption spectrum of the dark zone exhibits the absorption bands of nitrous oxide. The products of the thermal decomposition of nitrocellulose have been studied by Wolfram.[12] The products of the fizz burning of propellants probably contain similar fractions but in greater variety and in different proportions.

5-2.2 Laboratory Investigations of Ignition

Ignition is brought about by the application of heat to the surface of the propellant. A great deal of research on a laboratory scale has been done in attempts to study the process in detail. In most cases, the procedure has been to apply heat suddenly to a selected sample of propellant and then to observe by photographic and photo-electric means the behavior of the surface and the initiation of the flame as a function of the time. Apart from qualitative description, the experiments yield quantitative measurements of the times necessary to initiate the solid phase and gas phase reactions. The former is assumed to begin when evidence of surface disintegration appears and the latter when the gases become sufficiently luminous for the luminosity to be detected by the measuring apparatus. These limits are obviously somewhat arbitrary as is the

sharp division of the total combustion reaction into two phases sharply separated in time and space. The flame zone will appear where and when the total reaction has proceeded to the point at which the temperature of the products is high enough to stimulate the emission of observable radiation. In studies of ignition, it is usually assumed that when observable radiation appears effective ignition has taken place. In some experiments, thermocouples have been imbedded in the propellant sample close to the surface and measurements made of the way the temperature in the surface layer changes during ignition and early burning of the propellant.

To apply the heat several methods have been used. They differ in detail but can be classified as (a) contact with a hot solid such as a heated wire,[13] (b) contact with or immersion in a quiescent hot gas,[14] (c) immersion in a stream of hot gas[15] and (d) irradiation of the surface by a source of heat radiation.[16] Methods (b) and (c) have been most commonly used. In these cases, it is found that the observed time delays depend not only on the temperature and velocity of the igniting gas but also upon its chemical constitution, particularly on the amount of oxygen it contains. The presence of oxygen shortens the time to ignition as evidenced by the appearance of luminosity. Gun propellants are usually oxygen deficient and oxygen in the igniter gases should promote the combustion reactions. One would expect differences in ignition time also when different inert gases are used because the heat transfer coefficients for both conductive and convective transfer are functions of the chemical constitution.

Much of the recent work on ignition, both theoretical and experimental, has been done on composite propellants designed for use in rockets. In rocket propellants, the fuel and oxidizer are usually separate substances mixed more or less intimately. In gun propellants, the constituents cannot be classified separately as fuel and oxygen supplying elements. Each constituent carries its own oxygen which forms part of the molecular structure. The present discussion is concerned primarily with gun propellants. Reports of further work on composite propellants are to be found in the publication cited in Reference 16.

In most of the laboratory investigations, correlations have been made between the observed ignition delay times and the heat transfer, for different propellant samples, igniter gas composition and temperature, heating times and other pertinent parameters. Although these correlations often lead to quantitative relations between ignition times and such quantities as heat input rates or total heat input, it cannot be said, as yet, that any complete and generally agreed upon understanding of the ignition process has been arrived at. The quantitative results are specific to the experimental method and procedures adopted and to the nature of the propellant sample investigated.

In general, it is observed that if heat is applied to the surface of a propellant at a fixed rate and under steady conditions of pressure and other controllable experimental parameters, the propellant will eventually ignite and the sample will be consumed. If the pressure is low enough and the ignition is not too vigorous or if the heat is supplied by a fast moving hot gas, the sample may fizz burn only. If the pressure is an atmosphere or more and the ignition is not too brief or gentle, the flame will appear and what is considered to be effective ignition and normal combustion is observed. In many experiments, it is possible to observe the onset of the fizz reaction and the flame reaction as separate and nonsimultaneous events.[14]

If the time interval over which the heat is supplied is shortened sufficiently, the ignition may or may not go to completion. There seems to be a threshold condition, determined by the manner of heating the surface, below which the propellant will not ignite or above which it always ignites. In the threshold region, the ignition is unstable and effective ignition may or may not take place. If it does take place, it does so after a variable time delay.

5-2.3 Theories of Ignition

Attempts have been made to formulate general theories of ignition based on thermal and chemical considerations. Although the result of these theories can be brought into rough correlation with certain aspects of the ignition process as revealed by observation, they are by no means complete or adequate for quantitative prediction of the ignition characteristics of a given propellant or as guides for the development of ignition systems for guns. In formulating a theory of ignition, one must of necessity assume a much simplified model of the process.

The purely thermal theory due to Hicks[17] will serve to illustrate one approach. It is assumed that the ignition and burning of the propellant is dependent on the flow of heat in it and is a function only of its temperature. The propellant is assumed to occupy the half space defined by the coordinate x for $x > 0$. It is heated uniformly over its surface

at $x = 0$ by gas at temperature, T_g, and heat is generated within it by a chemical reaction at a rate dependent on the temperature.

The partial differential equation describing the heat flow in such a model is

$$c' \frac{\partial T}{\partial t} = K \frac{\partial^2 T}{\partial x^2} + Q; \quad x \geqq 0, \quad t > 0, \tag{5-8}$$

where

T is the temperature at any point in the propellant
t the time
x the space coordinate as defined above
c' the heat capacity of the propellant per unit volume
K the thermal conductivity of the propellant and
Q the heat evolution per unit volume

The evolution of heat due to the reaction is assumed to be of the form

$$Q = qf e^{-E/RT} \tag{5-9}$$

where

q is the heat of reaction per unit volume
f the frequency factor
E the activation energy for the reaction and
R the gas constant

At the surface, the boundary condition is

$$-K \frac{\partial T}{\partial x} = h(T_g - T); \quad x = 0, \quad t > 0, \tag{5-10}$$

where h is the heat transfer coefficient.

At an infinite distance, it is assumed that the heat flow vanishes so that the second boundary condition is

$$\frac{\partial T}{dx} = 0; \quad x \to \infty, \quad t > 0 \tag{5-11}$$

Initially, the temperature of the propellant is assumed to be a constant and independent of x so that

$$T = T^{(0)}; \quad x \geqq 0, \quad t = 0. \tag{5-12}$$

It is assumed also that at $t = 0$ the hot igniter gas at temperature, T_g, is suddenly brought in contact with the propellant surface and continues to transfer heat to the surface at a constant rate until $t = t_0$ (the heating time) when the heat transfer effectively ceases. This is taken account of in the mathematical solution by assuming that T_g has a constant value $T_g^{(0)}$ until $t = t_0$ when it suddenly drops to a much lower constant value $T_g^{(1)}$ or

$$\begin{aligned} T_g &= T_g^{(0)}; \quad 0 < t \leqq t_0 \\ T_g &= T_g^{(1)}; \quad t > t_0 \end{aligned} \tag{5-13}$$

The mathematical problem is now defined. The solution yields values of the temperature as a function of x and t. The assumption is then made that if the temperature reaches a certain value, T_i, called the ignition temperature, the propellant will ignite. It is further assumed that when the surface reaches the ignition temperature effective ignition occurs.

Because of the exponential form assumed for the dependence of Q on T (Equation 5-9), the temperature in a sample of propellant obeying Equation 5-8 will always eventually reach the ignition temperature at some value of x. The time taken for this to happen when no heat is supplied to the surface is called by Hicks the adiabatic ignition time. This time will, obviously, be dependent on the initial temperature of the propellant. When heat is supplied from the outside, the propellant will, according to the theory, ignite sooner.

The equations are such that the solution can only be given numerically. Hicks solved the problem in the dimensionless variables U, τ and ξ, defined by

$$U = \frac{R}{E} T \tag{5-14}$$

$$\tau = \frac{Rqf}{c'E} t \tag{5-15}$$

$$\xi = \left(\frac{Rqf}{KE}\right)^{1/2} x \tag{5-16}$$

He also expressed h in the reduced form

$$H = \left(\frac{E}{RKqf}\right)^{1/2} h \tag{5-17}$$

The approximate range of the different parameters occurring in the theory is given in Table 5-5.

The nature of the solution at the surface ($\xi = 0$) is shown in Figure 5-3 for the indicated values of $U^{(0)}$, $U_g^{(0)}$ and $U_g^{(1)}$. The graph shows that under the influence of external heating the temperature of the surface rises monotonically. If the external heating is continued long enough, the surface reaches the ignition temperature ($U_i = 0.046$) at a time τ_{im}, the minimum ignition time. If the heating is stopped at a heating time τ_0 which is less than τ_{im} the surface temperature will then decline at first but will reach a minimum and then increase again and continue to rise until the ignition temperature is reached at an ignition time τ_i greater than τ_{im}.

TABLE 5-5. APPROXIMATE RANGE OF VALUES OF THE VARIABLES AND PARAMETERS USED IN HICKS' THERMAL THEORY OF IGNITION.*

	Dimensional	*Dimensionless*
Depth to which reaction penetrates	$\Delta x - 10^{-6} - 10^{3}$ cm	$\Delta\xi - 10^{2} - 10^{10}$
Time intervals	$\Delta t - 10^{7}$ sec	$\Delta\tau - 10^{3} - 10^{20}$
Heating time	$t_0 - 10^{-6} - 10^{3}$ sec	$\tau_0 - 10^{1} - 10^{16}$
Temperature	$T - 200° - 600°K$	$U - 0.010 - 0.050$
Gas temperature (hot)	$T_g^{(0)} - 1500° - 3000°K$	$U_g^{(0)} - 0.18, 0.20$
Gas temperature (cooled)†	$T_g^{(1)} - 300° - 600°K$	$U_g^{(1)} - 0.021$
Initial propellant temperature	$T^{(0)} - 200° - 400°K$	$U^{(0)} - 0.010 - 0.034$
Ignition temperature	$T_i - 675° - 1250°K$	$U_i - 0.045, 0.059$
Heat transfer coefficient	$h - 10^{-6} - 3 \times 10^{-2}$ cal/cm²-sec-°K	$H - 10^{-10} - 2 \times 10^{-6}$
Heat capacity/unit volume	$c' - 0.5 - 0.8$ cal/cm³-°C	
Thermal conductivity	$K - 10^{-5} - 10^{-2}$ cal/cm-sec-°C	
Heat of reaction/unit volume‡	$q - 10^{2} - 10^{3}$ cal/cm³	
Frequency factor	$f - 10^{13} - 10^{16}$ sec^{-1}	
Activation energy	$E - 3.0 - 5.0 \times 10^{4}$ cal/mole	
Gas constant	$R - 1.989$ cal/mole-°K	

* The values in the second column are, for the most part, those encountered in practice. The values in the third column are those used in the numerical work for the present report.

† Cf. Chapter 2 for significance of $T_g^{(1)}$.

‡ In our treatment, q and f do not enter separately and only the product, qf appears, which has the range $10^{15} - 10^{19}$ cal/cm³-sec.

The graph also shows the adiabatic ignition time τ_{i_a} and the effect of the surface heating in decreasing the ignition time from the adiabatic value is evident. As τ_0 is increased, τ_0 and τ_i become equal to one another and also to τ_{i_m}.

If τ_0 is decreased below τ_{i_m}, τ_i increases very rapidly. If $U_g^{(1)} \leqq U(0, \tau)$, $\tau > \tau_0$ (that is, at $\tau = \tau_0$ the igniter gas temperature falls to or below the surface temperature) then for a sufficiently short heating time τ_0, τ_i, defined as the time for the surface to reach the ignition temperature, becomes greater than the adiabatic ignition time. Under these conditions the maximum temperature is not at the surface and the ignition temperature is reached first somewhere inside the solid propellant. The heating time for which $\tau_i = \tau_{i_a}$ is called by Hicks the critical heating time and designated as τ_{0_c}. It is shown in Figure 5-3 to be close to τ_{i_m}.

If $U_g^{(1)} \geqq U(0, \tau)$, $\tau > \tau_0$, the maximum temperature remains at the surface and there is no critical heating time. τ_i is then less than τ_{i_a}. This situation would be most likely to occur in practice because hot gases evolved from the propellant would tend to be hotter than the surface itself and tend to maintain the heating after the igniter ceased to operate.

It is difficult to check a theory, such as that of Hicks, by detailed quantitative correlation with the results of experiments. One would not expect any close agreement, quantitatively, both because numerical values of the pertinent parameters are not known for certain and also because the model assumed by the theory is too simple. The theory, however, does in a rough way, account for the critical nature of the ignition process leading to the existence of variable time delays when the ignition is not sufficiently vigorous and extended in time.

Hicks later extended his theoretical work to include chemical effects associated with the production of nitrous oxide.[18]

5-2.4 Ignition in Guns

In guns the charge is a bed of propellant grains contained in a tightly sealed chamber. Initially the spaces between the grains are filled with air at atmospheric pressure. As soon as any gas is generated either by the igniter itself or by combustion of the propellant, the pressure will rise. Ignition in guns, therefore, is always accompanied by an increasing pressure.

In its usual form the igniter produces hot gas which possibly contains hot solid particles. The igniter gas flows more or less freely through the propellant bed and heats the surface of the grains by conductive and convective heat transfer. The igniter gases do not reach all parts of the charge at the same time and may never reach some parts at all. They also cool as they flow through the charge. The grains near the igniter will ignite first. These will produce hot gas which will combine with the igniter gas and aid in the ignition of more remote parts of the charge. The ignition, therefore, will

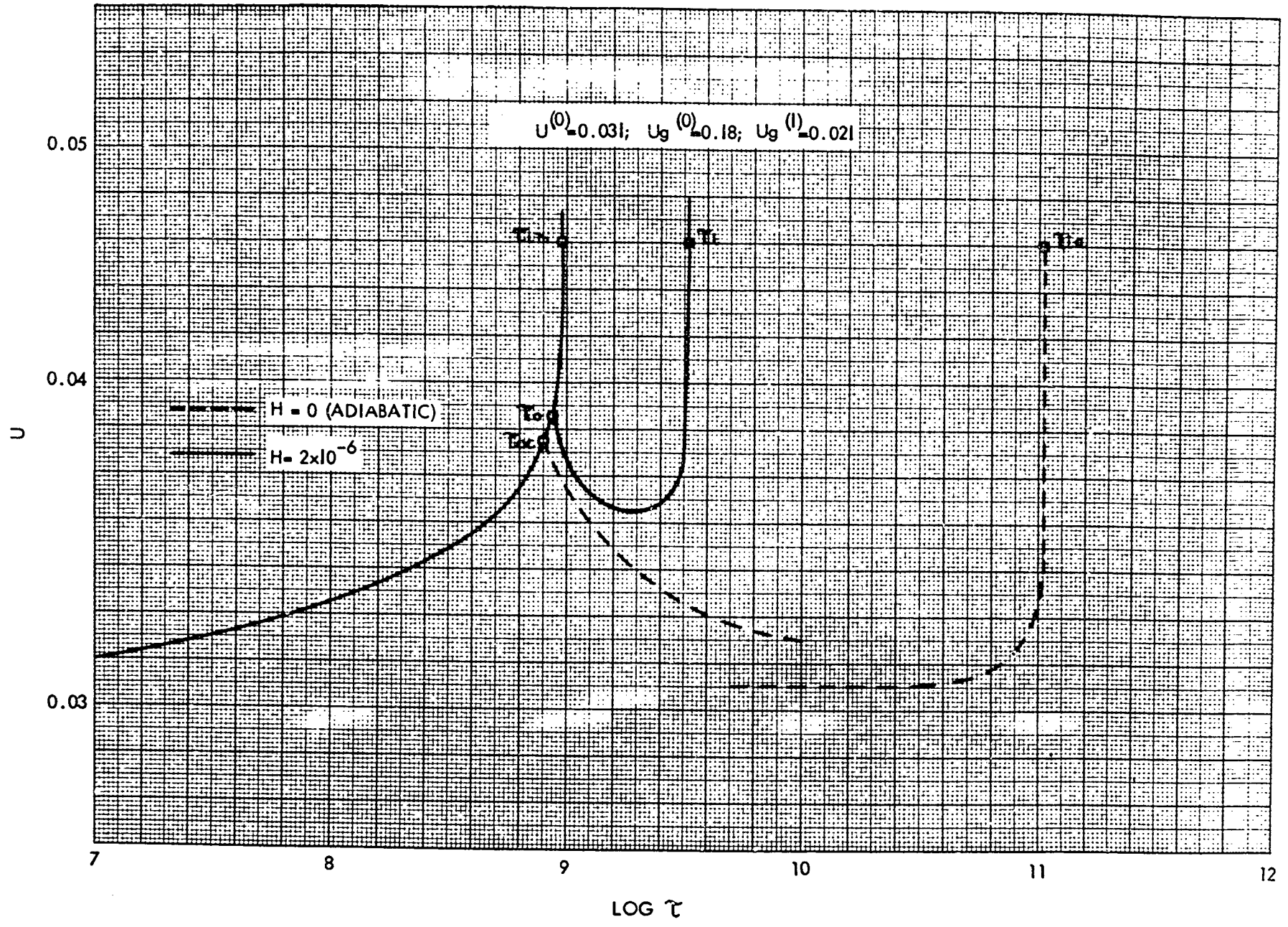


FIGURE 5-3. *Reduced Surface Temperature, U, Versus Logarithm of Reduced Time, τ*

spread through the charge even after the original igniter has ceased to function. The rise in pressure which accompanies this process tends to promote combustion and to make the ignition spread more effectively.

To start the combustion process effectively, the igniter gases must initiate the solid phase reaction and remain effective until the combustion process has been established. This requires that the igniter should be so designed as to initiate combustion simultaneously over as much of the surface of the entire charge as possible. If the initial region of ignition is too localized, it is possible for the more remote parts of the charge to be heated but not effectively ignited so that the solid phase reaction proceeds alone generating gases not completely reacted. These gases can accumulate and be subsequently ignited explosively, leading to sporadic surges of high pressure. Occasionally, the pressures so generated exceed the pressure for which the tube is designed, and it may be permanently distended or even ruptured completely. This sort of behavior is more probable when the ammunition is used at very low temperature because the igniter gases are cooled more rapidly in the cold propellant bed and become less effective in igniting the grains further away from the igniter.

Poor ignition in guns also results in less uniformity in muzzle velocity, pressure waves in the chamber which generate variations in burning rate and consequently rough pressure time curves. Poor ignition also results in variation in the length of the firing cycle of the gun. In rapid fire automatic weapons, this can cause difficulties because the firing rate of the gun should be uniform and properly related to the natural vibration rate of the mount.[19] In the development of any particular gun and ammunition system, therefore, the development of the ignition system is a matter of the greatest importance. Although general design principles have been formulated, the application of these principles is often complicated by the other aspects of the complete round under consideration, so that a certain amount of empiricism and experimentation is required.

5-2.5 Ignition Systems for Guns

The substance most commonly used to generate the igniter gas in guns is black powder,[20] although other materials have been and are being developed in an attempt to produce more effective ignition systems. The black powder is ignited by gases from a small charge of high explosive, which is initiated electrically or by percussion. The black powder charge, called the primer charge, is enclosed in a metal tube called a primer tube or in one or more cloth bags. The metal tube is used in cased ammunition and the cloth bags in separately loaded uncased ammunition. In cased ammunition the gas emerges from the primer tube through a system of holes or vents distributed along the length of the tube in various ways. The holes are closed by a paper liner in the tube. The paper liner ruptures when sufficient pressure develops inside the tube, to permit the efflux of the primer gases.

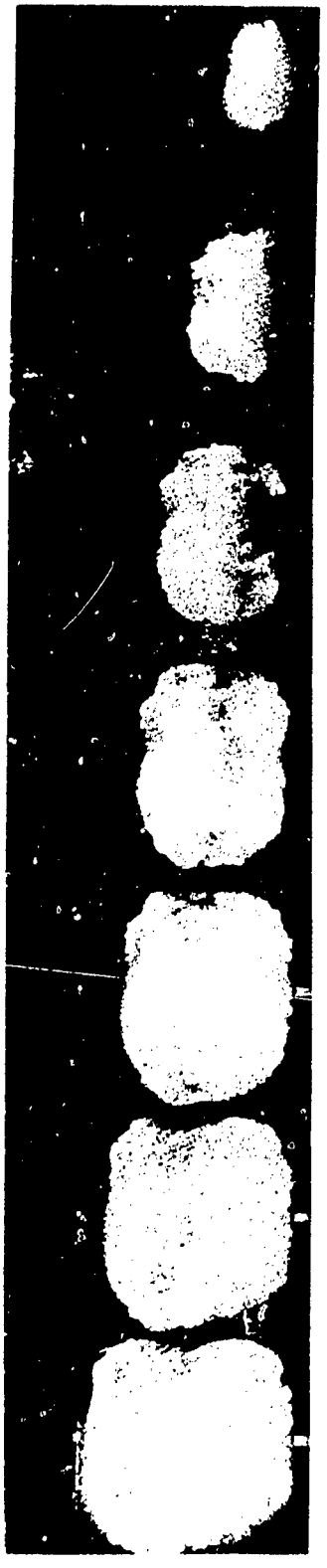
Factors affecting the design of artillery primers are discussed in Reference 21. Although a general guide for designing a primer can be deduced from experience and laboratory studies of ignition of propellants, the details of an effective design for any particular case are often specific to the case in question. A design feature which eliminates a certain difficulty in one case may not do so in another. The details of the behavior of a primer-propellant system are usually not known. The only criterion is whether satisfactory uniformity in pressure and muzzle velocity is obtained. Laboratory investigations of the functioning of standard artillery primers as well as experimental models designed to investigate the effect of certain specific design features have been conducted. The results of these experiments can be found in References 22 and 23. Further information on the development and evaluation of gun primers and igniters for separate loading ammunition may be found in References 24, 25, 26, 27 and 28.

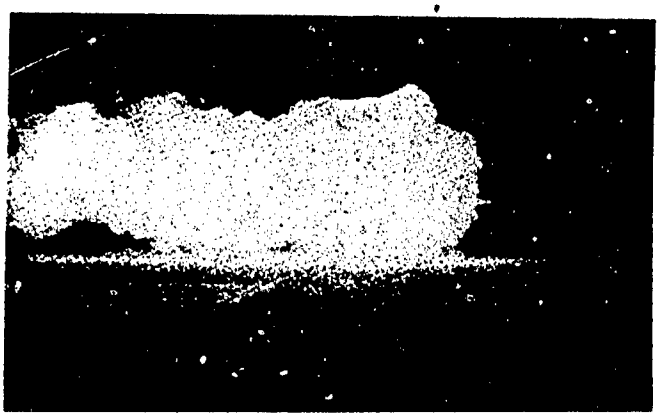
5-3 FLASH AND SMOKE

5-3.1 Flash

The gases issuing from the muzzle of a gun are usually hot enough to be luminous. The luminosity is frequently very intense and can be obvious even in broad daylight, and although it exists only momentarily as an intense flash of light, it is very effective in revealing the location of the weapon. It also may impair the vision of the gunner.

A study of the phenomenon reveals that there are three regions of luminosity;[29,30] (a) a rather small hemispherical region of low luminosity at the muzzle sometimes called the muzzle glow, (b) a region of high intensity, just beyond the muzzle and separated from the muzzle glow by a dark region, usually called the primary flash, and (c) a rather ill-defined region of high intensity, beyond but usually not well separated from the primary flash,





(a) Still Picture of Muzzle Flash.

(b) Motion Picture of Muzzle Flash, 1800 Frames/Second.

FIGURE 5-4. *Muzzle Flash from 57mm Gun.*

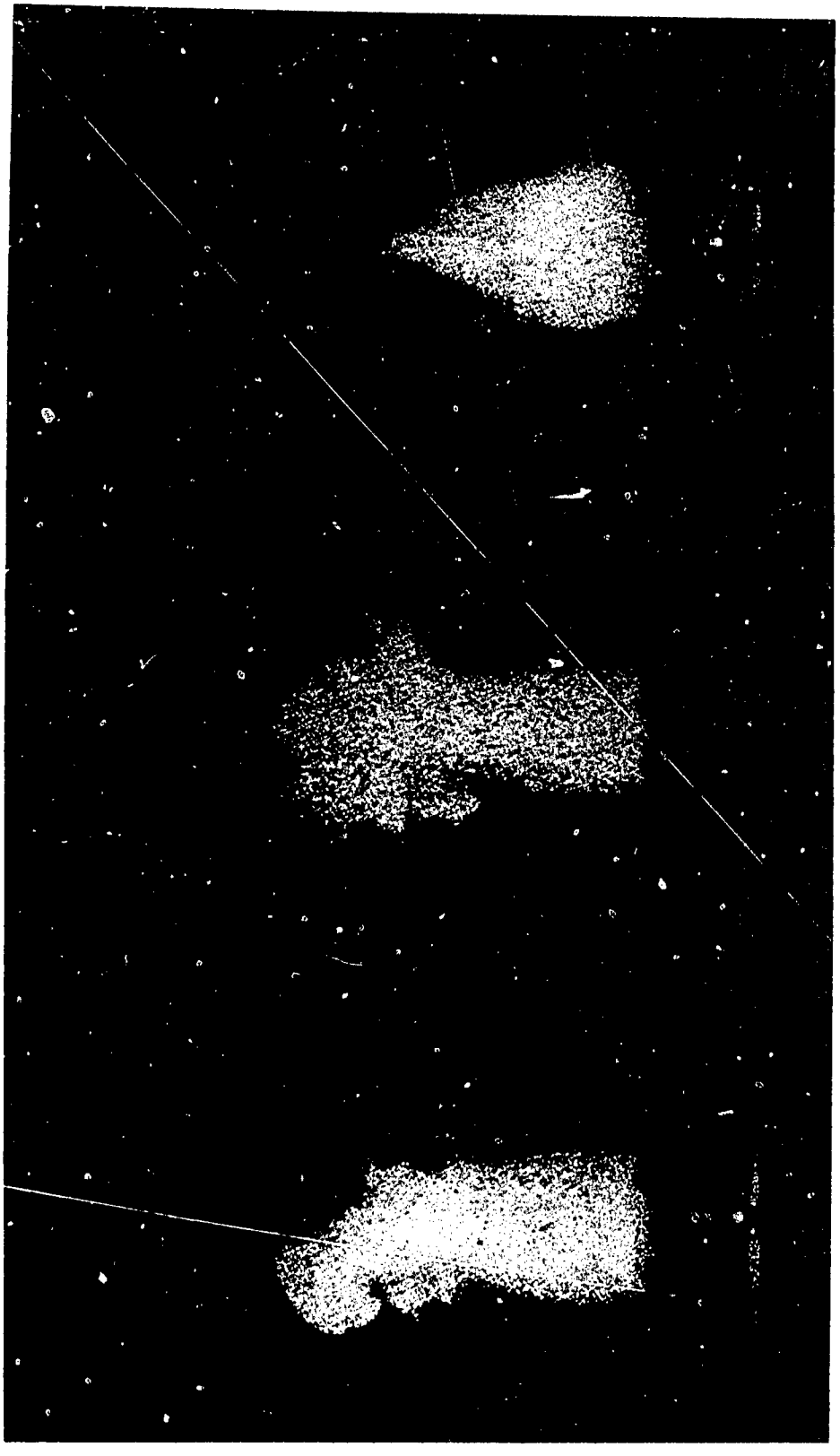


FIGURE 5-5. *Still Photograph of Caliber .30 Rifle with Shortened Barrel Fired in Air and Nitrogen.*

called the secondary flash.* The three luminous zones are most easily observed in small weapons. In medium and large artillery weapons the secondary flash can be very large and extend many feet beyond the muzzle and persist for relatively long times of the order of 0.1 second or more so that the primary flash is not obvious, Figure 5-4. If a small weapon such as a caliber .30 rifle is fired into an atmosphere of an inert gas such as nitrogen the secondary flash is suppressed and the appearance of the primary flash is clearly evident, Figure 5-5. The muzzle glow and primary flash, for a 37mm gun is shown in Figure 5-6.

While the phenomenon of muzzle flash is not understood in detail, the general view is that the gases as they leave the muzzle are hot enough to be self-luminous. Immediately after exit, they expand rapidly and cool so that the luminosity disappears forming the dark zone. At this point they are over expanded and subsequently are recompressed adiabatically through a shock. This recompression raises the temperature again almost to the muzzle temperature and the gases are again luminous and form the primary flash. In the meantime the gases have entrained air and a combustible mixture has been formed of the unburned hydrogen and carbon monoxide in the muzzle gases; and if the recompression has raised the temperature above the ignition temperature of this mixture, it will ignite and burn as a diffusion flame forming the secondary flash. Some investigators have also postulated that excited chemical species play a part in the ignition of the secondary flash. The primary flash is small and persists for a very short time (a few milliseconds) and is not visible at great distances. The secondary flash because of its extent and longer duration has a high visibility especially for the larger weapons. A phenomenon similar to muzzle flash occurs in the gases issuing from the nozzles of recoilless guns.

An examination of the spectra of muzzle flashes reveals that most of the luminosity is due to the presence of metallic impurities in the propellant gases. The gases produced by pure propellant constituents are mainly H_2O, H_2, CO and CO_2 along with N_2 and NO. These gases are poor emitters of visible radiation. Except for a weak background of continuous radiation, the spectrum of the muzzle gases in the visible region reveals strong radiation from sodium, potassium and calcium and the oxides of calcium and copper. The radiation from sodium is the source of the yellow tint of the flash. Sodium, potassium and calcium will be present as they are always present in the materials used in propellant manufacture. Copper comes predominantly from the rotating bands.

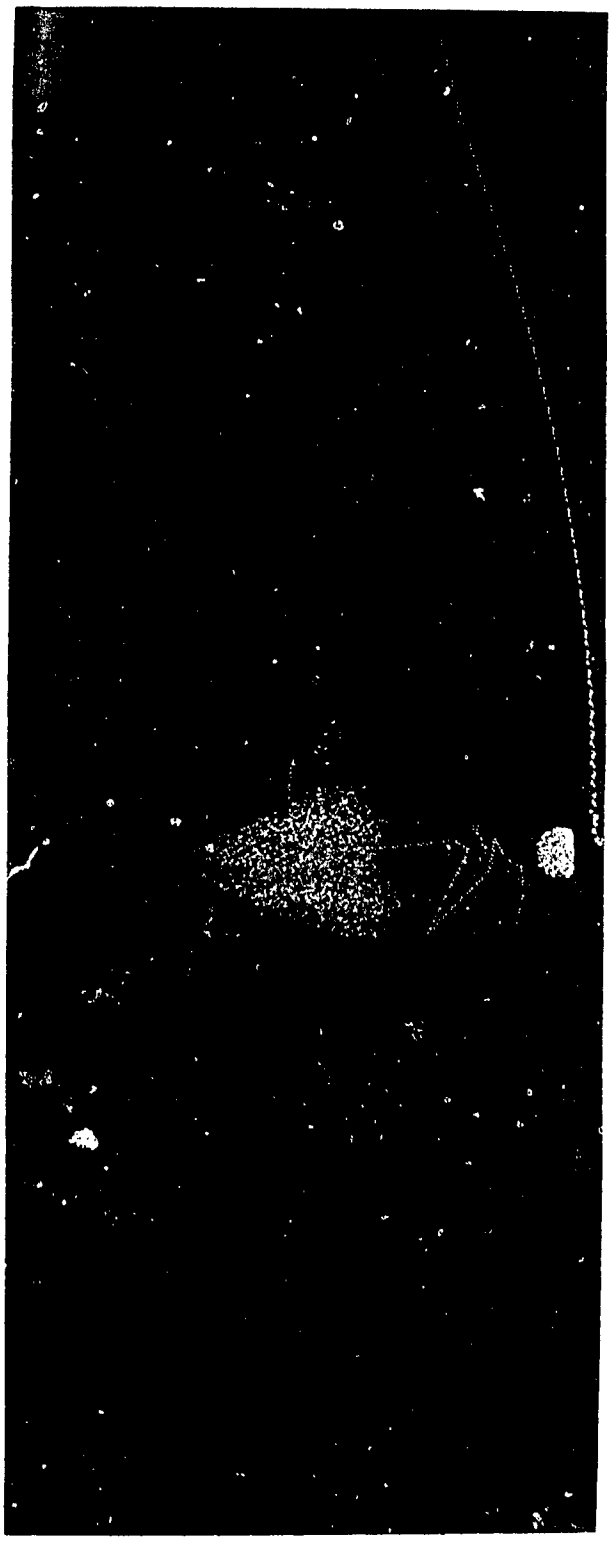


FIGURE 5-6. *Primary Flash and Muzzle Glow From 37mm Gun.*

* The nomenclature is not standardized. The three regions are also called primary, intermediate and secondary flash. Other nomenclature also exists in the literature.

5-3.2 Flash Suppression

The tendency of a weapon to flash depends in a complicated way on the design of the weapon and its interior ballistics as well as on the chemistry of the propellant. One would expect that anything which reduced the temperature and probably the pressure of the gases issuing from the muzzle would tend to reduce the tendency to flash. This is illustrated by the following example.

After the troops had complained of bright flashes accompanied by loud noise and strong blast in the 8-inch Howitzer, the High Explosive Projectile M106 was fired with experimental charges. Single perforated M1 propellant with a web thickness of 0.0161 inch was used for Zones 1 to 5, producing muzzle velocities from 820 to 1380 feet per second. Multiperforated M1 propellant with a web thickness of 0.0414 inch was used for Zones 5 to 7, producing muzzle velocities from 1380 to 1950 feet per second. With the single perforated grains, there was little flash and blast; but with the multiperforated grains, there was considerably more flash and blast, especially in Zone 5. Although a combination of black powder and potassium sulfate reduced the flash in Zones 5 and 6, it produced an intolerable amount of smoke.

In order to explain these phenomena, interior ballistic calculations were made for Zones 5 and 6 of the 8-inch Howitzer. The results are summarized in Table 5-6. The distance to burnout is greatest and the pressure at burnout lowest for the multiperforated propellant in Zone 5. The muzzle pressure with the multiperforated propellant is 50 percent higher than with the single perforated prepellant in the same zone. The temperature of the gas at the muzzle is highest with the multiperforated grains in Zone 5. This combination of high pressure and temperature at the muzzle was probably the cause of the flash and blast.

TABLE 5-6. INTERIOR BALLISTIC DATA FOR 8-INCH HOWITZER FIRING HE PROJECTILE M106

Zone	5	5	6
Web, in	.0161*	.0414†	.0414†
Charge weight, lb	13.0	16.6	21.8
Velocity, fps	1380	1380	1640
Length of Travel, in	173.83	173.83	173.83
Approximate Distance to Burnout, in	10	120	90
Copper Pressure, psi	27,000	12,900	19,800
Approximate Pressure at Point of Burnout, psi	21,600	6,400	11,600
Muzzle Pressure, psi	2700	4100	5500
Temperature of Gases at Muzzle, °F	1340	1580	1505

* Single perforated.
† Multiperforated.

Pressure-time traces of the standard charges showed that the base-ignited Zone 7 charge did not ignite properly, and that the point of burnout was closer to the muzzle than the calculations indicate. To improve the ignition, a long, thin, segmented igniter bag was inclosed in a tube located longitudinally through the center of the charge and an igniter pad assembled to the base of the charge. Also, dual granulation was adopted in order to increase the maximum pressure in the intermediate zones and thus reduce the distance to burnout. This eliminated most of the flash.

Although it has been proposed and investigated experimentally, it does not seem possible to eliminate flash by eliminating the impurities responsible for the luminosity. It has been discovered, largely by trial and error, that the secondary flash can be greatly reduced and often practically eliminated by two methods, namely; by adding certain chemical substances to the propellant, or by attaching a mechanical device to the muzzle. It is not known exactly in any particular case why either of these methods work.

a. Chemical Flash Suppressors. Numerous chemical compounds when added to the propellant will tend to reduce the tendency to flash. The most studied have been salts of the alkali metals. Research done in Japan during World War II showed that, for the alkali halides, the effectiveness in terms of the relative amount of material necessary to suppress the flash increased with both the atomic number of the alkali and the halide so that cesium iodide was the most effective compound. The tests were made in small weapons, a 60mm mortar, a 25mm rifle and a 7.7mm rifle. The results might not hold in larger or different weapons.

Most commonly used in practice are the salts of potassium. The Japanese workers found that some of the most effective compounds were:

Potassium iodide (KI)
Potassium bromide (KBr)
Potassium oxalate ($K_2C_2O_4 \cdot H_2O$)
Potassium acid oxalate ($KHC_2O_4 \cdot 1/2H_2O$)
Potassium sulfate (K_2SO_4).

The number of potassium atoms in the molecule had no appreciable effect on the effectiveness of the compound. In American practice the most com-

monly used compound is potassium sulfate. Chemical suppressors do not suppress the primary flash; the primary flash, being due to the adiabatic recompression of the gases, is not influenced by relatively small changes in their chemical constitution.

b. Mechanical Flash Suppressors. The earliest mechanical flash suppressor was in the form of a cone- or funnel-shaped device attached to the muzzle. There seems to be some doubt as to whether this device was originally intended to hide the flash from the enemy or to shield the eyes of the gunner so that his vision was not impaired. In any case it appeared to reduce the flash. This is probably because it reduced the amount of over-expansion of the gas by causing it to expand more slowly and smoothly and so eliminated or reduced the tendency for a shock to form in the flowing gases with a consequent sudden increase in luminosity.

In investigating this form of suppressor slits were cut in the cone to permit observation of the luminosity inside. It was found that these slits not only permitted observation but also had a favorable effect on the flash. Further study revealed that the conical shape could be eliminated entirely and a more effective suppressor designed by using a system of rods or bars arranged around the muzzle and parallel to the tube in such a way that they formed effectively a cylinder with wide longitudinal slots cut in it.

It is not known in detail why this device is effective but it is believed that the gas expands through the slots which breaks up the continuity of the flow and so prevents shock formation. Mechanical suppressors, therefore, suppress the primary flash as well as the secondary flash.

Mechanical flash suppressors are not used on larger caliber weapons. For the larger weapons dependence is on chemical methods. Potassium salt added to the propellant greatly increases the amount of smoke produced. An excessive amount will reduce the efficiency of the weapon and change its interior ballistics. The use of a chemical suppressor will also result in changes in the interior ballistics of the weapon and may require changes in the chemical composition of the propellant. An extensive treatment of the problem of gun flash and its suppression is given in the classified Reference 31.

REFERENCES

1. A. E. H. Love and F. B. Pidduck, "The Lagrange Ballistic Problem", Phil. Trans. Roy. Soc. **222**, 167 (1921).
2. J. Corner, *The Theory of the Interior Ballistics of Guns*, John Wiley & Sons, N. Y. 1950.
3. F. B. Pidduck, J. Appl. Phys. **8**, 144 (1937).
4. R. H. Kent, "Some Special Solutions for the Motion of the Powder Gas", Physics **7**, No. 9, 319 (1936); **8**, 144 (1937); **9**, 734 (1938).
5. J. P. Vinti and Sidney Kravitz, *Table for the Pidduck-Kent Special Solutions for the Motion of the Powder Gas in a Gun*, BRL Report No. 693, 1949.
6. P. de Haller, "Une Solution Graphique du Problem de Lagrange en Ballistique Interieure", Bull. Tech. de la Suisse Romande **1**, 1 (1948).
7. W. Heybey, *A Solution of Lagrange's Problem of Interior Ballistics by Means of Its Characteristic Lines*, Naval Ordnance Laboratory Report No. M-10819, 1950.
8. M. Farber and J. Lorell, Jet Propulsion Laboratory, California Institute of Technology, Progress Report No. 17-3, 1950.
9. A. E. Seigel, *An Experimental Solution of the Lagrange Ballistic Problem*, Naval Ordnance Laboratory Report No. 2693, 1952.
10. W. B. Stephenson, *Theoretical Light Gas Gun Performance*, Arnold Engineering Development Center Technical Report No. 61-1, 1961.
11. B. L. Crawford, Jr., C. Hugget and J. J. McBrady, "The Mechanism of the Burning of Double Base Propellants", J. Phys. Chem. **54**, 854 (1950). See also other authors in the same volume, pp. 885, 929.
12. M. L. Wolfram et al, "The Controlled Decomposition of Cellulose Nitrate", Part I, J. Am. Chem. Soc. **77**, 6573 (1955); Part II, **78**, 2719 (1956).
13. D. Altman and A. F. Grant, Jr., "Thermal Theory of Solid Propellant Ignition by Hot Wires", *Fourth Symposium on Combustion*, Williams and Wilkins Co., Baltimore, 1953.
14. H. G. Brickford and G. P. Wachtell, *Investigation of Propellant Ignition*, The Franklin Institute, Philadelphia, Pa., Final Report No. F-2411, 1955.
15. S. W. Churchill, R. W. Kruggel and J. C. Brier, "Ignition of Solid Propellants by Forced Convection", J. Am. Inst. Chem. Engrs. **2**, 568 (1956).
16. R. B. Beyer and Norman Fishman, "Solid Propellant Ignition Studies With High Flux Radiant Energy as a Thermal Source", *Solid Propellant Rocket Research*, Vol. I, Academic Press, N. Y., 1960.
17. B. L. Hicks, J. W. Kelso and J. Davis, *Mathematical Theory of the Ignition Process Considered as a Thermal Reaction*, BRL Report No. 756, 1951. Also in J. Chem. Phys. **22**, 414 (1953).
18. B. L. Hicks, *A Unified Theory of the Ignition and Burning of Propellants*, BRL Memorandum Report No. 666, 1953.
19. AMCP 706-252, Engineering Design Handbook, *Gun Tubes*.
20. AMCP 706-175, Engineering Design Handbook, *Solid Propellants, Part One*.
21. R. J. Sherwood, *Some Factors Affecting the Design of Artillery Primers*, Picatinny Arsenal Research and Development Lecture No. 14, 1954.
22. D. C. Vest et al, *On the Performance of Primers for Artillery Weapons* (U), BRL Report No. 852, 1953. (Confidential)
23. E. E. Ekstedt et al, *Pressure Studies of Artillery Primers Fired Statically* (U), BRL Report No. 938, 1955. (Confidential)
24. H. Hassman, *Ignition Studies of Igniter Design for Davy Crockett (XM 28) System*, Picatinny Arsenal Technical Note No. 35, 1959.
25. E. T. Smith, *An Adiabatic Self-Heating Apparatus for Determining the Kinetic Parameter of the Rocket Propellant Decomposition Process*, Picatinny Arsenal Technical Note No. 36, 1961.
26. E. Daniels and I. Nadel, *Combustible Igniter Types for Charge, Propelling, M-51 and XM-115 for Cannon, Howitzer, 155mm, T-255 and T-258*, Picatinny Arsenal Technical Report No. 3052, 1963.
27. T. Zimmerman, *Combustible Primers for Use in Combustible Cartridge Cases*, Picatinny Arsenal Technical Report No. 2522, 1958.
28. H. Hassman, *Initial Evaluation of Low Energy Detonating Cord to Ignite Metal Oxidant Type*

Powders in Artillery Primers, Picatinny Arsenal Technical Report No. 2460, 1957.
29. R. Ladenburg, *Report on Muzzle Flash*, BRL Report No. 426, 1943.
30. R. Ladenburg, *Studies of the Muzzle Flash and Its Suppression*, BRL Report No. 618, 1947.
31. P. P. Carfagno, *Handbook on Gun Flash* (U), The Franklin Institute, Philadelphia, Pa. Prepared for Ammunition Branch, Office Chief of Ordnance, U. S. Army, 1961. (Confidential)

* U. S. GOVERNMENT PRINTING OFFICE: 1970 O - 430-502-PO-5396A

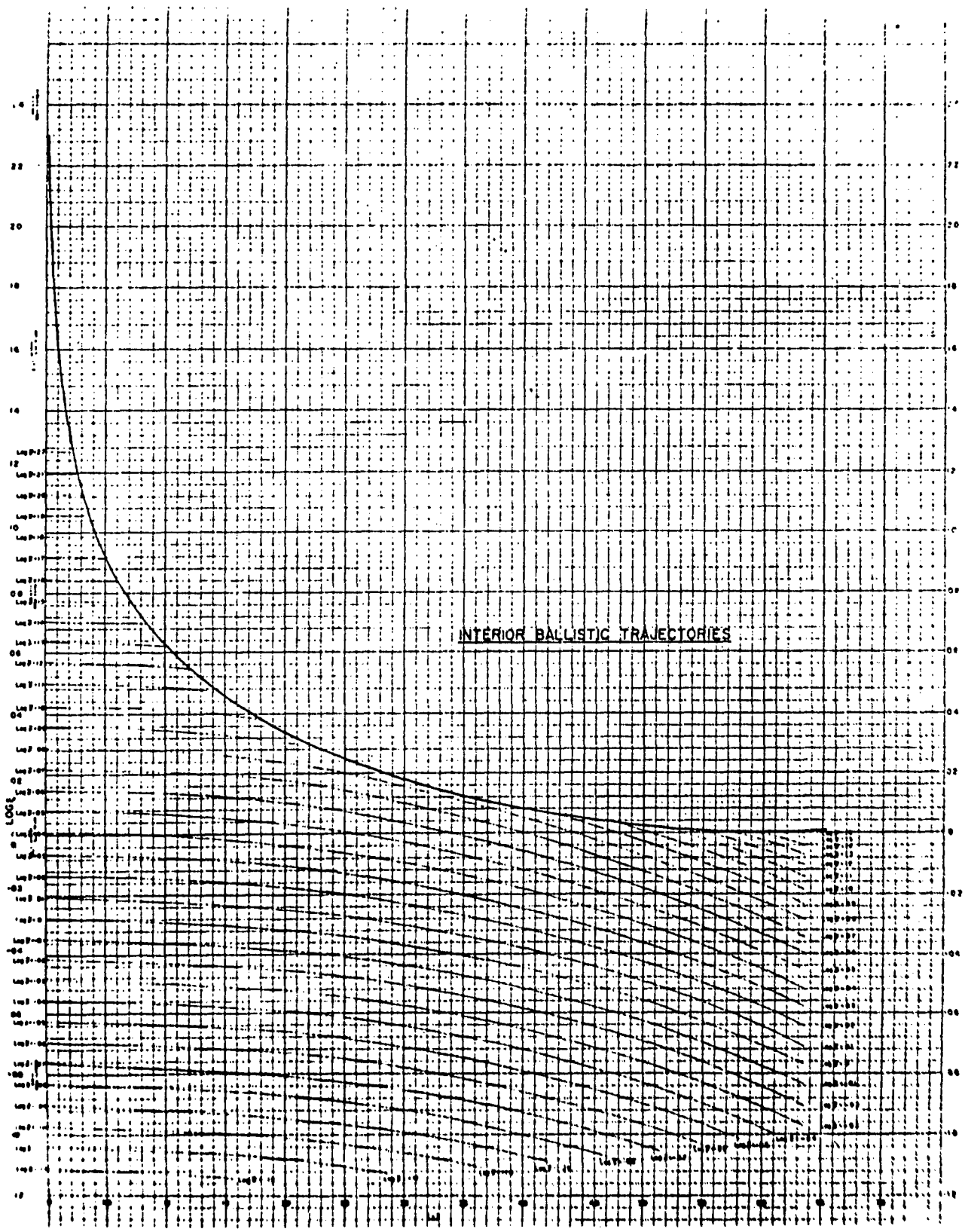


CHART 2-2v. *Interior Ballistics Trajectories*

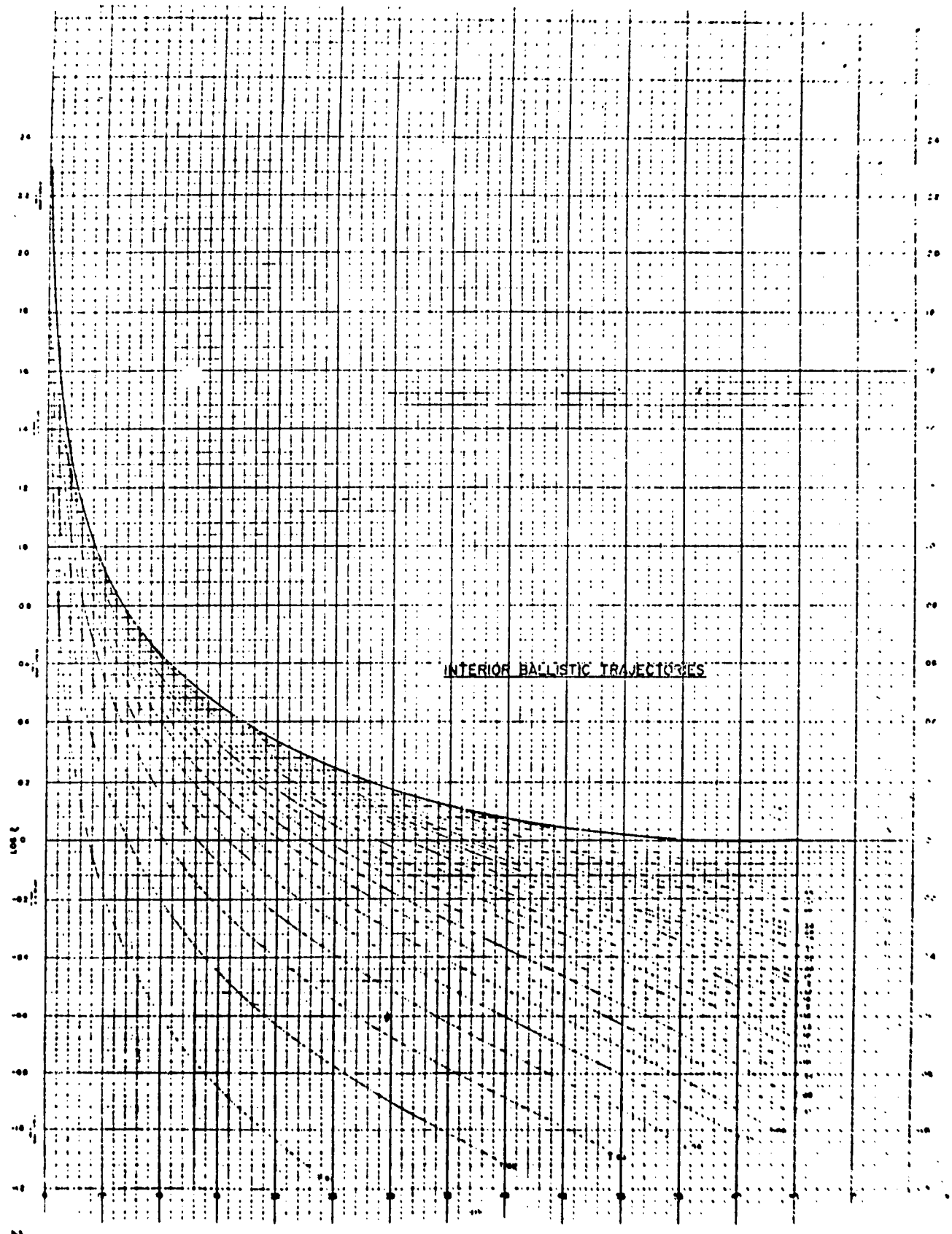


CHART 2-2b. *Interior Ballistics Trajectories*

TABLE 1-1 CALCULATED THERMOCHEMICAL VALUES FOR STANDARD PROPELLANTS (INCLUDING RESIDUAL VOLATILES)

Use	Artillery								Recoilless				Mortar			Small Arms		
Propellant	M1	M2	M5	M6	M14	M15	M17	T20	M10	T18	T25	M26	M7	M8	M9	IMR	M12	M18
Specification	JAN-P-309	JAN-P-323	JAN-P-323	JAN-P-309	JAN-P-309	PA-PD-26	PA-PD-26		PA-PD-123	PA-PD-329	PA-PD-329	PA-PD-329	JAN-P-659	JAN-P-381	MIL-P-20306	JAN-P-733	JAN-P-528	FA-PD-26A
Nitrocellulose	85.0	77.45	81.95	87.0	90.0	20.0	22.0	20.0	98.0	72.0	73.25	67.25	54.6	52.15	57.75	100.0	97.7	80.0
% Nitration	13.15	13.25	13.25	13.15	13.15	13.15	13.15	13.15	13.15	13.15	13.15	13.15	13.15	13.25	13.15	13.15	13.15	13.15
Nitroglycerin	...	19.50	15.00	...	...	19.0	21.5	13.0	...	10.75	20.00	25.00	35.5	43.00	40.00	...	...	10.0
Barium nitrate	...	1.40	1.40	...	...	...	...	...	...	0.75	0.75	0.75	...	...	...	...	..	...
Potassium nitrate	...	0.75	0.75	...	...	...	...	...	...	0.70	0.70	0.70	...	1.25	1.50	...	...	...
Potassium perchlorate	...	...	...	...	...	...	...	...	...	...	...	...	7.80	...	...	...	...	...
Nitroguanidine	...	...	...	...	...	54.7	54.7	60.0	...	...	...	...	...	...	...	...	...	...
Dinitrotoluene	10.0	...	...	10.0	8.0	...	...	...	...	...	...	...	...	...	...	...	...	...
Dibutylphthalate	5.0	...	...	3.0	2.0	...	...	5.0	...	...	...	...	...	...	...	8.0‡	...	...
Diethylphthalate	...	...	..	...	...	...	...	...	...	...	...	...	...	...	...	...	...	9.0
Potassium sulfate	...	...	...	...	...	...	...	...	1.0	...	...	...	...	3.00	...	...	...	...
Tin	...	..	...	...	...	...	...	...	...	...	...	...	...	...	...	1.0*	0.75	...
Diphenylamine	1.0*	..	...	1.0*	1.0*	...	...	...	...	...	...	...	...	...	...	...	0.75	...
Ethyl centralite	...	0.60	0.60	...	...	6.0	1.5	2.0	1.0	...	...	...	...	...	0.75	0.7*	0.80	1.0
Graphite	...	0.30	0.30	...	...	...	0.1†	...	...	6.50	5.00	6.00	0.90	0.60	...	...	...	...
Carbon black	...	..	...	...	...	...	...	...	0.10†	0.30	0.30	0.30	...	...	...	...	...	...
Cryolite	...	...	...	...	...	...	...	...	...	...	...	...	1.20	...	...	...	..	...
Ethyl alcohol (Residual)	0.75	2.30	2.30	0.90	1.00	0.3	0.3	...	...	...	...	...	...	...	...	...	...	...
Water (Residual)	0.70	0.70	0.70	0.50	0.25	0.30	0.30	0.30	1.50	1.20	1.20	1.20	0.80	0.40	0.50	0.60	1.00	0.50
Lead carbonate	...	..	...	...	...	0.00	0.00	0.00	0.50	0.30	0.30	0.30	0.00	0.00	0.00	1.00	1.00	0.00
						...	...	1.0*	...	...	...	...	...	...	...	...	...	...
Isochoric flame temp, °K	2417	3319	3245	2570	2710	2394	3017	2388	3000	2938	3071	3081	3734	3605	3709	2827	2996	2577
Force, ft-lb/lb × 10^{-3}	305	360	355	317	327	336	364	314	339	346	353	356	368	382	382	325	336	319
Uncombined carbon, %	8.6	0	0	6.8	5	9.5	3.9	11.6	4	3.4	1.8	2.2	0	0	0	1.9	6	6.8
Combustibles, %	65.3	47.2	47.4	62.4	58.9	51.0	38.7	53.1	54.5	59.1	...	...	33.4	37.2	32.8	59.2	53.66	66.6
Heat of explosion, cal/gm	700	1080	1047	758	800	796	962	712	936	910	962	966	1255	1244	1295	866	933	772
Gas volume, moles/gm	0.04533	0.03900	0.03935	0.04432	0.04338	0.04645	0.04336	0.04704	0.04068	0.04219	0.04133	0.04157	0.03543	0.03711	0.03618	0.04137	0.04037	0.0445
Ratio of specific heats	1.2593	1.2238	1.2253	1.2543	1.2496	1.2557	1.2402	1.2501	1.2342	1.2421	1.2373	1.2383	1.2100	1.2148	1.2102	1.2400	1.2326	1.2523
Isobaric flame temp, °K	1919	2712	2647	2030	2168	2066	2433	1807	2431	2365	2482	2488	3085	3042	3139	2280	2431	2056
Density, lb/in³	0.0507	0.0507	0.0506	0.0571	0.0582	0.0000	0.0003	...	0.0602	1.0588	0.0585	0.0585	...	...	...	...	...	...
Covolume, in³/lb	30.57	27.91	27.52	29.92	29.54	31.17	29.50	30.41	27.76	29.13	28.06	28.77	...	26.63	25.97	28.87	27.91	29.24

*Added †Glazed ‡Coating Added

REPRODUCED AT GOVERNMENT EXPENSE

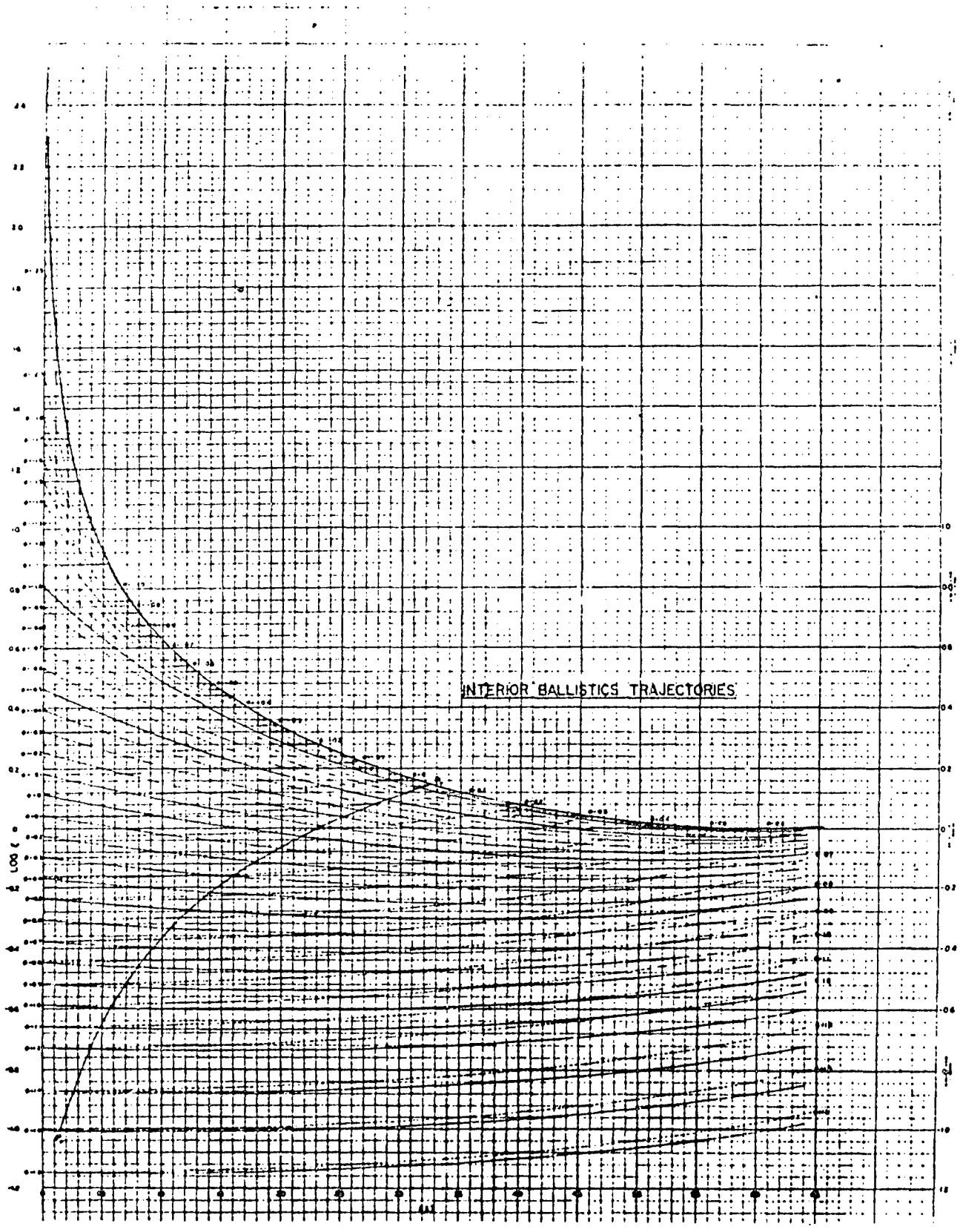


CHART 2-2a. *Interior Ballistics Trajectories*

TABLE OF CONTENTS

Paragraph		*Page*
	PREFACE	i
	LIST OF ILLUSTRATIONS	vii
	LIST OF CHARTS	x
	LIST OF TABLES	x

CHAPTER 1

DISCUSSION OF THE PROBLEM

	LIST OF SYMBOLS	1-1
1-1	Introduction	1-2
1-2	Guns	1-3
1-2.1	Definition	1-3
1-2.2	Classification	1-3
1-2.3	Action Inside the Gun	1-3
1-3	Projectiles	1-4
1-4	Distribution of Energy	1-4
1-5	Pressure-Travel Curves	1-4
1-6	Control of Interior Ballistic Performance	1-5
1-7	Effects of Propellant Grain Characteristics	1-6
1-7.1	Grain Configuration	1-6
1-7.2	Grain Size	1-6
1-7.3	Density of Loading	1-7
1-8	Black Powder	1-7
1-9	Gun Propellants	1-8
1-9.1	Present Gun Propellants	1-8
1-9.2	Burning Time	1-8
1-9.3	Burning Action	1-9
1-9.4	Degressive Burning	1-9
1-9.5	Neutral Burning	1-9
1-9.6	Progressive Burning	1-10
1-9.7	Single-Base Propellants	1-10
1-9.8	Double-Base Propellants	1-10
1-9.9	Nitroguanidine (Triple-Base) Propellants	1-11
1-9.10	Solvent Emulsion Propellant (Ball Powder)	1-11
1-9.11	Characteristics of Standard Propellants	1-11
1-9.12	The Rate of Burning	1-11
1-9.13	Energy of Propellants	1-15
	REFERENCES	1-17

Preceding page blank

TABLE OF CONTENTS—(continued)

CHAPTER 2

THEORY AND PRACTICE OF INTERIOR BALLISTICS

Paragraph		*Page*
	LIST OF SYMBOLS	2-1
2-1	Introduction	2-3
2-2	Statement of the Equations	2-3
2-2.1	The Energy Equation	2-3
2-2.2	The Equation of Motion	2-5
2-2.3	The Burning Rate Equation	2-6
2-2.4	Elimination of Variables	2-6
2-3	Solution of the Equations	2-7
2-3.1	Reduction to Normal Form	2-7
2-3.2	Numerical Integration of the Normal Form	2-8
2-3.3	Interior Ballistic Trajectories During Burning	2-9
2-3.4	Reduced Variables	2-9
2-3.5	Pressure Ratio Chart	2-10
2-3.6	Interior Ballistic Trajectory Charts	2-10
2-3.7	Conditions After Burnt	2-19
2-3.8	Time, Pressure and Travel Functions	2-19
2-3.9	Examples	2-21
2-3.10	Dual Granulation Charges	2-24
2-3.11	Example for Dual Granulation Charges	2-26
2-4	The Hirschfelder System	2-27
2-5	"Simple" Interior Ballistic Systems	2-27
2-5.1	General	2-27
2-5.2	The Mayer and Hart System	2-27
2-6	The Efficiency of a Gun-Ammunition System	2-28
2-7	Comparison With Experiment	2-29
2-7.1	General Considerations	2-29
2-7.2	Experimental Evaluation of the Parameters	2-29
2-8	Similarity and Scaling	2-34
2-9	Effects of Changes in the Parameters	2-35
2-10	Simple Graphical Methods	2-36
2-11	Empirical Methods	2-41
2-12	The Attainment of Higher Velocities	2-41
2-12.1	General	2-41
2-12.2	The Optimum Gun	2-41
2-12.3	The Conventional Procedure to Attain Higher Velocities	2-46
2-12.4	Unconventional High Velocity Guns	2-46
2-12.5	Extension of Interior Ballistic Theory to High Velocity Weapons	2-47
2-13	The High-Low Pressure Gun	2-47
2-14	Recoilless Rifles	2-47
2-14.1	Theory of Efflux of Gas through Nozzles	2-47
2-14.2	Application to Recoilless Rifles	2-49
2-14.3	Graphical Methods for Recoilless Rifles	2-53
2-15	Smooth Bore Mortars and Worn Guns	2-53
2-16	The Use of High Speed Computing Machines	2-54
	REFERENCES	2-55

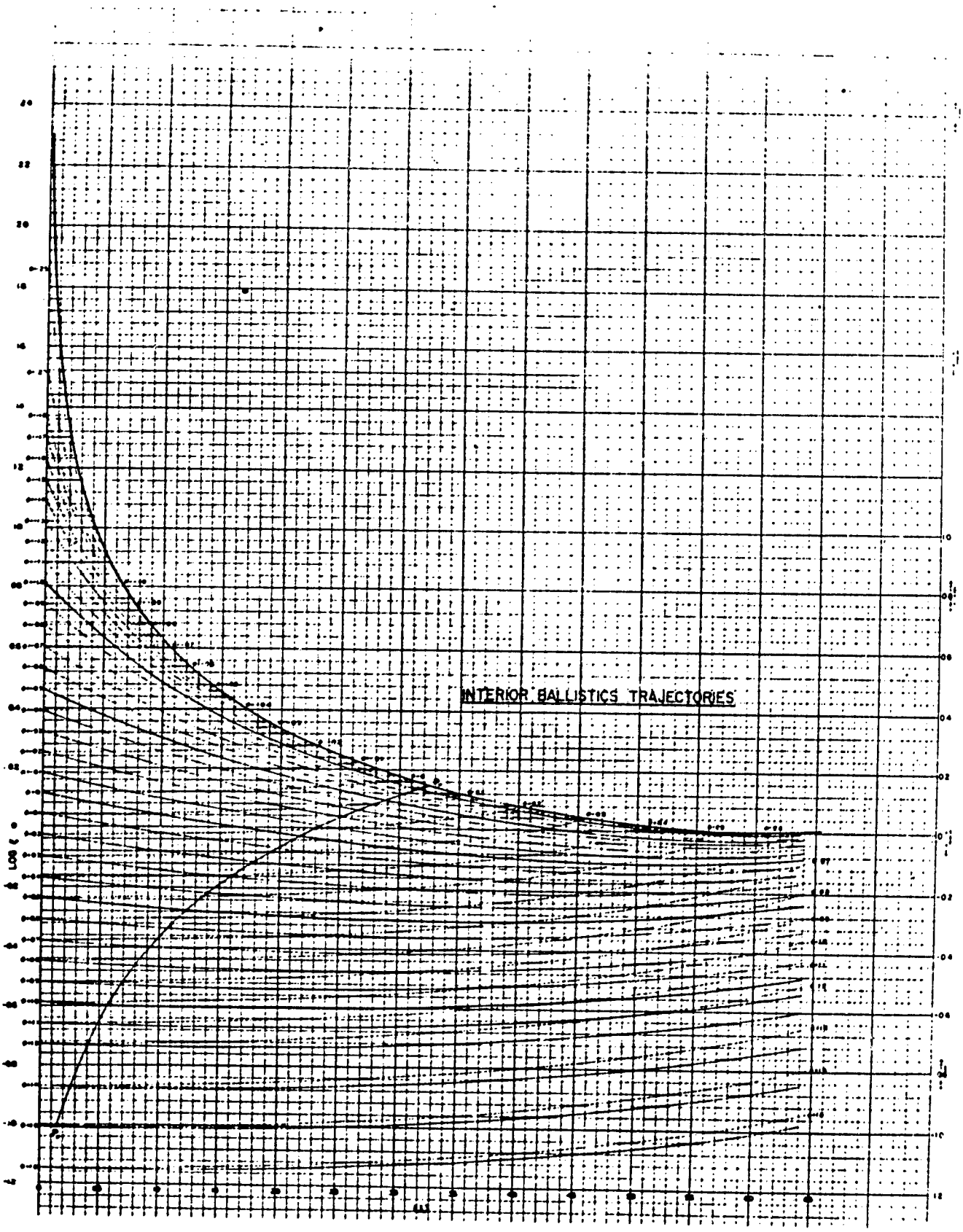


CHART 2-2a. *Interior Ballistics Trajectories*

TABLE 1-1 CALCULATED THERMOCHEMICAL VALUES FOR STANDARD PROPELLANTS (INCLUDING RESIDUAL VOLATILES)

Use	Artillery								Recoilless				Mortar			Small Arms		
Propellant	M1	M2	M5	M6	M14	M15	M17	T20	M10	T18	T25	M26	M7	M8	M9	IMR	M12	M18
Specification	JAN-P-309	JAN-P-323	JAN-P-323	JAN-P-309	JAN-P-309	PA-PD-26	PA-PD-20		PA-PD-123	PA-PD-329	PA-PD-329	PA-PD-329	JAN-P-650	JAN-P-381	MIL-P-20906	JAN-P-733	JAN-P-528	PA-PD-26A
Nitrocellulose	85.0	77.45	81.95	87.0	90.0	20.0	22.0	20.0	98.0	72.0	73.25	67.25	54.6	52.15	57.75	100.0	97.7	80.0
% Nitration	13.15	13.25	13.25	13.15	13.15	13.15	13.15	13.15	13.15	13.15	13.15	13.15	13.15	13.25	13.15	13.15	13.15	13.15
Nitroglycerin	...	19.50	15.00	...	...	19.0	21.5	13.0	...	19.75	20.00	25.00	35.5	43.00	40.00	...	...	10.0
Barium nitrate	...	1.40	1.40	...	...	...	...	...	...	0.75	0.75	0.75	...	...	...	...	...	...
Potassium nitrate	...	0.75	0.75	...	...	...	...	...	...	0.70	0.70	0.70	...	1.25	1.50	...	...	...
Potassium perchlorate	...	...	...	...	...	...	...	...	...	...	...	...	7.80	...	...	...	...	...
Nitroguanidine	...	...	...	...	...	54.7	54.7	60.0	...	...	...	...	...	...	...	...	...	...
Dinitrotoluene	10.0	...	...	10.0	8.0	...	...	...	...	...	...	...	...	...	...	...	...	...
Dibutylphthalate	5.0	...	...	3.0	2.0	...	...	5.0	...	...	...	...	...	...	...	8.0‡	...	...
Diethylphthalate	...	...	...	...	...	...	...	...	...	...	...	...	...	3.00	...	...	...	9.0
Potassium sulfate	...	...	...	...	...	...	...	...	1.0	...	...	...	...	...	...	1.0*	0.75	...
Tin	...	...	...	...	...	...	...	...	...	...	...	...	...	...	...	...	0.75	...
Diphenylamine	1.0*	...	...	1.0*	1.0*	...	...	...	1.0	...	...	...	...	...	0.75	0.7*	0.80	1.0
Ethyl centralite	...	0.60	0.60	...	...	6.0	1.5	2.0	...	6.50	5.00	6.00	0.90	0.60	...	...	...	...
Graphite	...	0.30	0.30	...	...	...	0.1†	...	0.10†	0.30	0.30	0.30	...	...	...	...	...	...
Carbon black	...	...	...	...	...	...	...	...	...	...	...	...	1.20	...	...	...	...	...
Cryolite	...	...	...	...	...	0.3	0.3	...	...	...	...	...	...	...	...	...	...	...
Ethyl alcohol (Residual)	0.75	2.30	2.30	0.90	1.00	0.30	0.30	0.30	1.50	1.20	1.20	1.20	0.80	0.40	0.50	0.60	1.50	0.50
Water (Residual)	0.50	0.70	0.70	0.50	0.25	0.00	0.00	0.00	0.50	0.30	0.30	0.30	0.00	0.00	0.00	1.00	1.00	0.00
Lead carbonate	...	...	...	...	...	...	...	1.0*	...	...	...	...	...	...	...	...	...	...
Isobaric flame temp, °K	2417	3319	3245	2570	2710	2394	3017	2388	3000	2938	3071	3081	3734	3695	3709	2827	2996	2577
Force, ft-lbs/lb × 10^{-3}	305	360	355	317	327	336	364	314	339	346	353	356	368	382	382	325	336	319
Uncombined carbon, %	8.6	0	0	6.8	5	9.5	3.9	11.6	4	3.4	1.8	2.2	0	0	0	1.9	6	6.8
Combustibles, %	65.3	47.2	47.4	62.4	58.0	51.0	38.7	53.1	54.5	49.1	...	...	33.4	37.2	32.8	59.2	53.66	66.6
Heat of explosion, cal/gm	700	1080	1047	758	809	796	992	712	936	910	962	966	1255	1244	1295	866	933	772
Gas volume, moles/gm	0.04533	0.03900	0.03935	0.04432	0.04338	0.04645	0.04336	0.04794	0.04068	0.04219	0.04133	0.04157	0.03543	0.03711	0.03618	0.04137	0.04037	0.04457
Ratio of specific heats	1.2593	1.2238	1.2258	1.2513	1.2490	1.2557	1.2402	1.2501	1.2342	1.2421	1.2373	1.2383	1.2100	1.2148	1.2102	1.2400	1.2326	1.2523
Isobaric flame temp, °K	1919	2712	2647	2030	2168	2066	2433	1907	2431	2365	2482	2488	3065	3042	3139	2280	2431	2056
Density, lbs/in³	0.0567	0.0507	0.0596	0.0571	0.0582	0.0600	0.0603	...	0.0602	1.0688	0.0585	0.0585	...	...	...	...	...	...
Covolume, in³/lb	30.57	27.91	27.52	29.02	29.54	31.17	29.50	30.41	27.76	29.13	28.06	28.77	...	26.63	25.97	28.87	27.91	30.24

*Added †Glazed ‡Coating Added

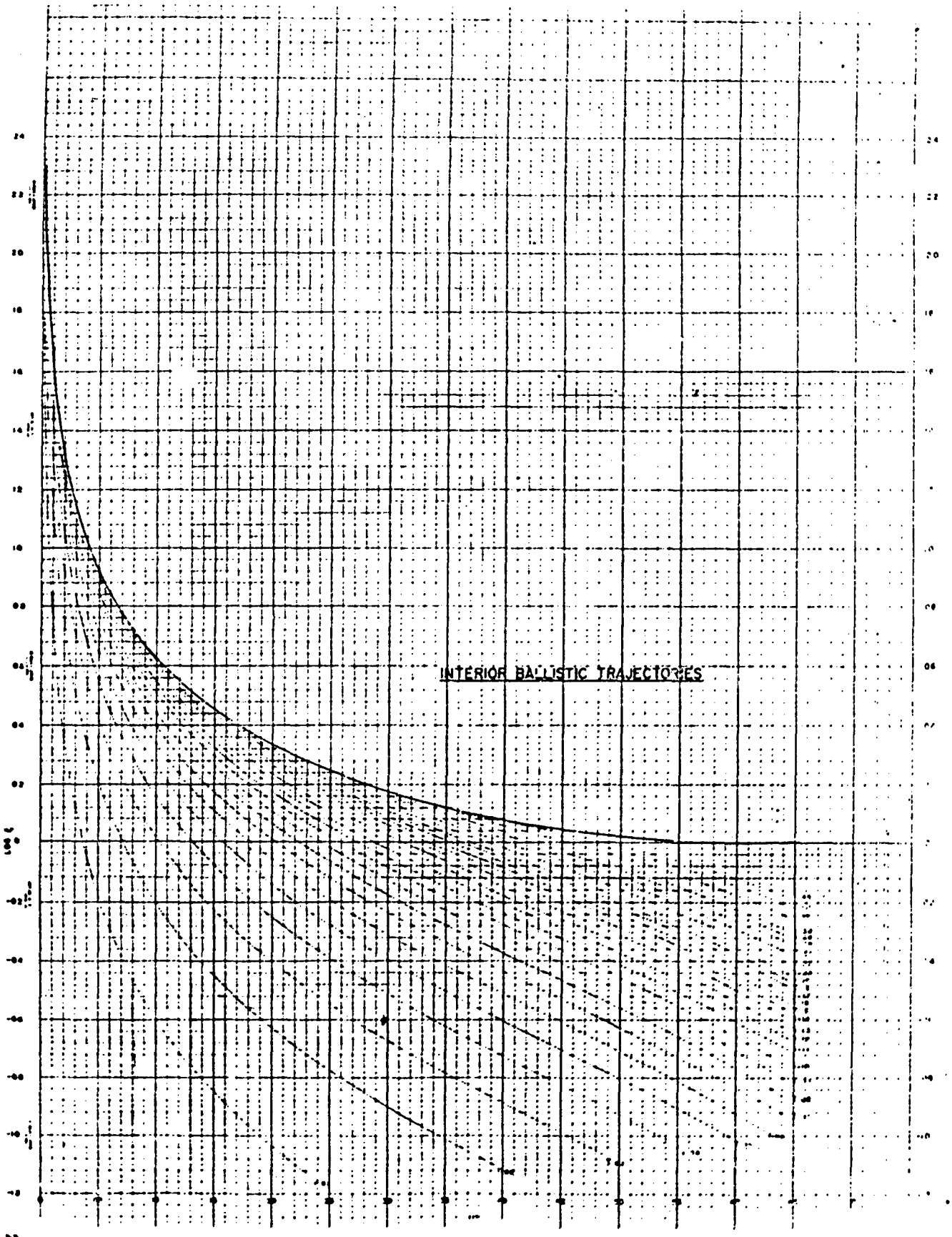


CHART 2-2b. *Interior Ballistics Trajectories*

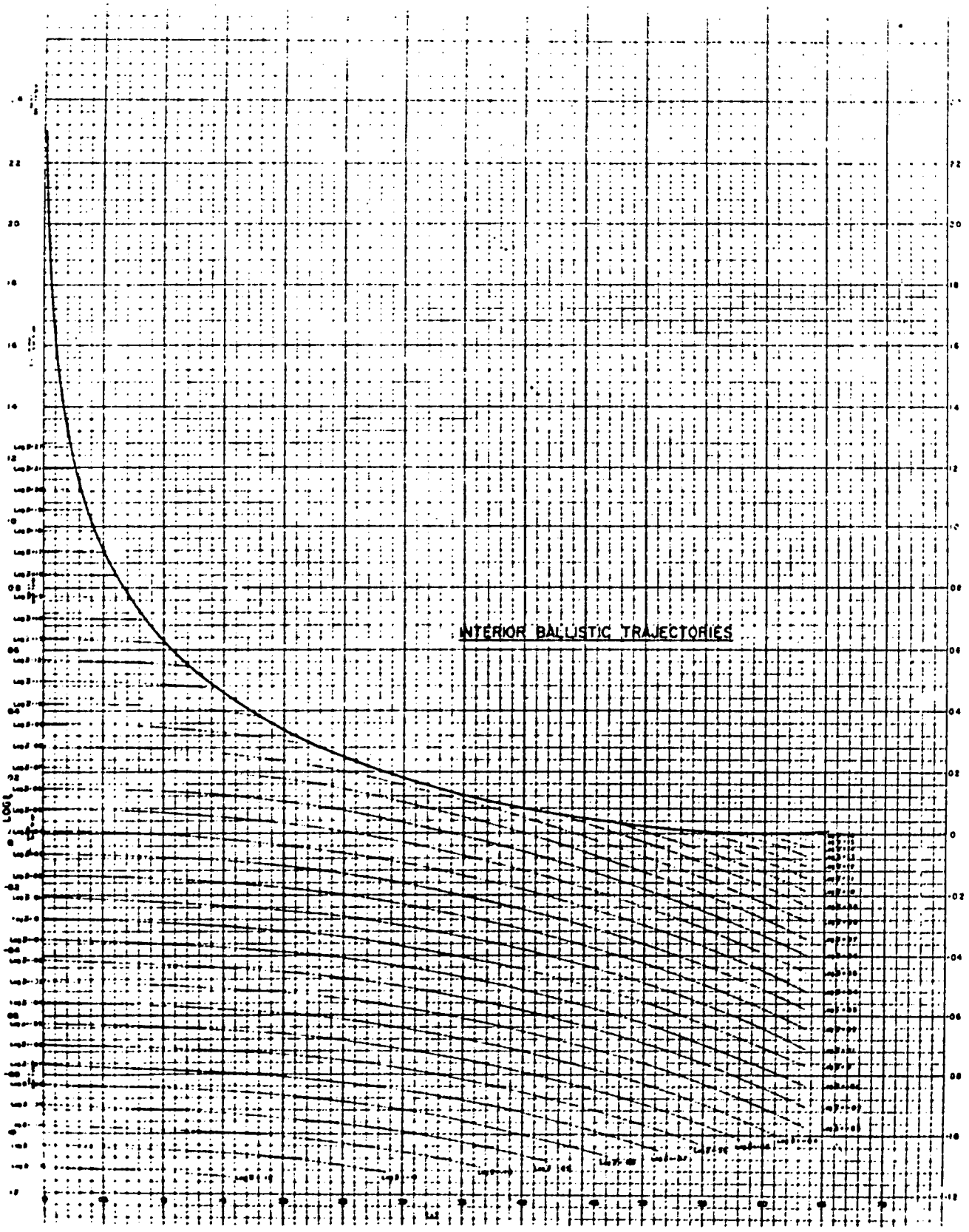


CHART 2-2c. *Interior Ballistics Trajectories*

ENGINEERING DESIGN HANDBOOK SERIES

Listed below are the Handbooks which have been published or submitted for publication. Handbooks with publication dates prior to 1 August 1962 were published as 20-series Ordnance Corps pamphlets. AMC Circular 310-38, 19 July 1963, redesignated those publications as 706-series AMC pamphlets (i.e., ORDP 20-138 was redesignated AMCP 706-138). All new, reprinted, or revised Handbooks are being published as 706-series AMC pamphlets.

General and Miscellaneous Subjects

Number	Title
106	Elements of Armament Engineering, Part One, Sources of Energy
107	Elements of Armament Engineering, Part Two, Ballistics
108	Elements of Armament Engineering, Part Three, Weapon Systems and Components
110	Experimental Statistics, Section 1, Basic Concepts and Analysis of Measurement Data
111	Experimental Statistics, Section 2, Analysis of Enumerative and Classificatory Data
112	Experimental Statistics, Section 3, Planning and Analysis of Comparative Experiments
113	Experimental Statistics, Section 4, Special Topics
114	Experimental Statistics, Section 5, Tables
121	Packaging and Pack Engineering
134	Maintenance Engineering Guide for Ordnance Design
135	Inventions, Patents, and Related Matters (Revised)
136	Servomechanisms, Section 1, Theory
137	Servomechanisms, Section 2, Measurement and Signal Converters
138	Servomechanisms, Section 3, Amplification
139	Servomechanisms, Section 4, Power Elements and System Design
170(C)	Armor and Its Application to Vehicles (U)
250	Guns--General (Guns Series)
252	Gun Tubes (Guns Series)
270	Propellant Actuated Devices
290(C)	Warheads--General (U)
331	Compensating Elements (Fire Control Series)
355	The Automotive Assembly (Automotive Series)

Ammunition and Explosives Series

175	Solid Propellants, Part One
176(C)	Solid Propellants, Part Two (U)
177	Properties of Explosives of Military Interest, Section 1
178(C)	Properties of Explosives of Military Interest, Section 2 (U)
210	Fuzes, General and Mechanical
211(C)	Fuzes, Proximity, Electrical, Part One (U)
212(S)	Fuzes, Proximity, Electrical, Part Two (U)
213(S)	Fuzes, Proximity, Electrical, Part Three (U)
214(S)	Fuzes, Proximity, Electrical, Part Four (U)
215(C)	Fuzes, Proximity, Electrical, Part Five (U)
244	Section 1, Artillery Ammunition--General, with Table of Contents, Glossary and Index for Series
245(C)	Section 2, Design for Terminal Effects (U)
246	Section 3, Design for Control of Flight Characteristics
247	Section 4, Design for Projection
248	Section 5, Inspection Aspects of Artillery Ammunition Design
249	Section 6, Manufacture of Metallic Components of Artillery Ammunition

Ballistic Missile Series

Number	Title
281(S-RD)	Weapon System Effectiveness (U)
282	Propulsion and Propellants
284(C)	Trajectories (U)
286	Structures

Ballistics Series

140	Trajectories, Differential Effects, and Data for Projectiles
150	Interior Ballistics of Guns
160(S)	Elements of Terminal Ballistics, Part One, Introduction, Kill Mechanisms, and Vulnerability (U)
161(S)	Elements of Terminal Ballistics, Part Two, Collection and Analysis of Data Concerning Targets (U)
162(S-RD)	Elements of Terminal Ballistics, Part Three, Application to Missile and Space Targets (U)

Carriages and Mounts Series

340	Carriages and Mounts--General
341	Cradles
342	Recoil Systems
343	Top Carriages
344	Bottom Carriages
345	Equilibrators
346	Elevating Mechanisms
347	Traversing Mechanisms

Materials Handbooks

301	Aluminum and Aluminum Alloys
302	Copper and Copper Alloys
303	Magnesium and Magnesium Alloys
305	Titanium and Titanium Alloys
308	Glass
309	Plastics
310	Rubber and Rubber-Like Materials

Military Pyrotechnics Series

186	Part Two, Safety, Procedures and Glossary
187	Part Three, Properties of Materials Used in Pyrotechnic Compositions

Surface-to-Air Missile Series

291	Part One, System Integration
292	Part Two, Weapon Control
293	Part Three, Computers
294(S)	Part Four, Missile Armament (U)
295(S)	Part Five, Countermeasures (U)
296	Part Six, Structures and Power Sources
297(S)	Part Seven, Sample Problem (U)